Characterising negative regulation of $CD8^+$ T cell function in tolerance and exhaustion

Mayura Vivek Wagle

June 2019

A thesis submitted for the degree of Doctor of Philosophy of The Australian National University

Australian National University

Declaration

This is to certify that

The thesis includes original research and works of the author, which have been published or submitted for publication at several scientific journals- the details of the publications are outlined on the next page.

The overall contributions of the author to each publication have been outlined and due acknowledgement has been made for each of the publications to other individuals who have helped and were not on the manuscript.

To the best of the author's knowledge, this work has not been used towards another award or degree from ANU or another university.

Mayura Vivek Wagle
June 2019

Statement of Contribution

This thesis is submitted as a Thesis by Compilation in accordance with https://policies.anu.edu.au/ppl/document/ANUP_003405

I declare that the research presented in this Thesis represents original work that I carried out during my candidature at the Australian National University, except for contributions to multi-author papers incorporated in the Thesis where my contributions are specified in this Statement of Contribution.

Title: FOXO3 is differentially required for $CD8^+$ T cell death during tolerance versus immunity.
Authors: Mayura V. Wagle and Ian A. Parish
Publication outlet: Immunology and Cell Biology
Current status of paper: Published
Contribution to paper: 75%
Senior author endorsement: Ian Parish

Title: The ubiquitin ligase adaptor NDFIP1 selectively enforces a $CD8^+$ T cell tolerance checkpoint to high dose antigen.
Authors: Mayura V. Wagle, Julia M. Marchingo, Jason Howitt, Seong-Seng Tan, Christopher C. Goodnow and Ian A. Parish
Publication outlet: Cell Reports
Current status of paper: Published
Contribution to paper: 90%
Senior author endorsement: Ian Parish

Title: The anergy-associated transcription factor EGR2 is re-purposed to promote terminal $CD8^+$ T cell exhaustion during chronic viral infection.
Authors: Mayura V. Wagle, Stephin J. Vervoort, Madison J. Kelly, Ben P. Martin, James R. Torpy, Deborah Roseingrave, Lisa A. Miosge, Renee Gloury, Sarah S.

Gabriel, Nenad Bartonicek, Jonathan D. Powell, Joseph A. Trapani, Ricky W. Johnstone, Axel Kallies, Christopher C. Goodnow, and Ian A. Parish

Publication outlet: N/A

Current status of paper: Not Yet Submitted

Contribution to paper: 80%

Senior author endorsement: Ian Parish

MAYURA VIVEK WAGLE	MVagli	20/06/2019
Candidate – Print Name	**Signature**	**Date**

Acknowledgements

Completing this PhD has been one of the most challenging yet highly rewarding experiences of my life. I could not have survived this rollercoaster of a journey with its highs and lows without the support and guidance of the following people.

I would firstly like to thank my supervisors Ian Parish and Chris Goodnow for their mentorship and for giving me the opportunity to undertake these projects at ANU. Thank you to Ian for introducing me to the complex fields of tolerance and exhaustion, for guiding me through the early daunting animal experiments and training me to be a thorough scientist. This thesis and the publications would not have been possible without the hard work, patience and commitment you provided as a supervisor. I would like to thank Chris for his support throughout this journey, for providing key guidance on the projects and sharing his scientific enthusiasm. Thank you also to my PhD panel members- David Tsharke and Ian Cockburn for their valuable advice throughout the PhD.

Next, I would like to thank the many amazing members of the Immunogenomics lab at JCSMR. Thank you to Debbie, Lisa, Yovina, Brigette and Sarp for helping me with my experiments and to other members including Michelle, Anselm, Kesuike, Mehmet, Manu, Yogesh, Jin, Zarah, Sofia and many others for your support and company. Thank you also to Immunogenomics lab at the Garvan Institute for welcoming me into the lab while I wrote my thesis. The experimental results included in this thesis would not have been possible without the great facilities at ANU. I would like to thank the wonderful staff at the flow cytometry unit at JCSMR- Mick and Harpreet, thank you for maintaining the machines so well, being very helpful and approachable with our FACS issues and for truly caring about our work. Also thank you to the APF staff, especially Barb and Christine who meticulously looked after all of the mice in the containment suites. Also a special mention to the administrative and support staff for the HDR students at ANU and JCSMR- thank you for all your prompt replies with our many queries throughout the degree and during the stressful submission time.

It was a pleasure working in the Immunology department at JCSMR; thank you to everyone past and present for the wonderful discussions at journal clubs, happy

hours and fun times at all the conferences. I would also like to thank the broader JCSMR community, especially to all the students in the building who helped set up JARs and participated in the activities; it was an incredible experience to undertake during my PhD. I would especially like to thank my JCSMR family- Sarp, Ilenia, Emilie, Mayank, Dandan and others for your friendship and support- all of you made those weekend experiments much more bearable with your company and our weekend road trips certainly brought timely relief from the thesis.

Next, I would like to thank all my friends in Canberra. To my housemates Sarah and Alice, for always checking in on me during the late nights spent in the lab and creating a warm home to come back to. Also thank you to Jason, Jin, Manab, Alex and Monique for your friendship and support at different times of this journey. Thank you also to my Canberra and Sydney friends- Nishthaa, Christine, Rushika, Angelica, Anna and many others for always making the time to meet and support me through these years. Thank you also to my Singapore friends- Kavita, Christina and Stephen for your constant motivation and encouragement with the thesis writing.

I would like to thank my parents and Mihir for always supporting my ambitions and looking out for me throughout this tough journey. Thank you for driving to Canberra several times with short notice, providing week-long meals and always ensuring I maintained balance during this period. Thank you also to my new family- Jean aunty, Sujith uncle and Gerry, thanks for your constant support and motivation throughout the thesis. Special thanks to the grandaunts Elizabeth and Mary, for always checking in on my thesis during our visits, your encouragement certainly kept me going.

Finally, I would like to thank my husband George, who endured the toughest parts of this journey with me over the last five and a half years. Thank you for being my mental support system through all of the downs, celebrating with me through all of the ups and for always believing in me. Thank you for tolerating the four years of long distance relationship, my thesis writing woes throughout our wedding planning and constantly encouraging me to complete the thesis as we set up a new life in Singapore. The incredible amount of patience and encouragement you have provided on a daily basis has been the most important factor in helping me get to the end of this road.

Abstract

$CD8^+$ T cells play a vital role in the immune system by clearing pathogen-infected tissues, however self-reactive $CD8^+$ T cells that escape thymic selection pose the danger of causing autoimmune disease. These self-reactive $CD8^+$ T cells are controlled in the periphery by tolerance mechanisms, which inhibit their function (anergy) or induce apoptosis (deletion). However, the specific molecular pathways crucial for negatively regulating self-reactive $CD8^+$ T cells are not well elucidated. A distinct form of negative regulation called "exhaustion" occurs within chronically stimulated effector $CD8^+$ T cells during cancer and chronic infection. Due to the phenotypical similarities between $CD8^+$ T cell tolerance and exhaustion, we aimed to understand if common underlying molecular pathways regulate these states.

The pro-apoptotic protein BIM is important in deletion of self-reactive $CD8^+$ T cells, however the transcriptional control of *Bim* induction has been unclear. In Chapter 2, we assessed the contribution of the transcription factor FOXO3 in deletion of self-reactive $CD8^+$ T cells given its role in *Bim* induction and cell death in effector and exhausted $CD8^+$ T cells. While FOXO3 protein underwent activatory dephosphorylation during tolerance, FOXO3-deficient $CD8^+$ T cells maintained the ability to induce BIM expression and undergo deletion. This result indicated that FOXO3 plays distinct roles in cell death of tolerant versus effector $CD8^+$ T cells.

To further characterise $CD8^+$ T cell tolerance pathways, in Chapter 3, we investigated whether the ubiquitin ligase adaptor NDFIP1, which is crucially required for $CD4^+$ T cell anergy, influences $CD8^+$ T cell tolerance. In a model of peptide-induced anergy, *Ndfip1*-deficient $CD8^+$ T cells aberrantly expanded and differentiated into effector cells against high dose exogenous antigen, likely driven by increases in TCR signaling. In contrast, NDFIP1 was dispensable for peripheral deletion to low-dose exogenous antigen, and had little impact upon effector responses to acute infection. These results showed the importance of NDFIP1 in regulating $CD8^+$ T cell tolerance and indicated that $CD8^+$ T cell deletion and anergy are molecularly separable checkpoints.

While $CD8^+$ T cell exhaustion appears distinct from tolerance, the transcriptional regulator EGR2 is commonly expressed between these states. In Chapter 4, we showed that exhausted $CD8^+$ T cells in chronic LCMV infection expressed elevated levels of EGR2 compared to functional effectors. Loss of *Egr2* severely disrupted terminal $CD8^+$ T cell exhaustion in a cell intrinsic manner, with RNA-Seq results indicating a global enrichment of the exhaustion "stem cell" gene set in *Egr2*-deficient cells. Strikingly, the genes regulated by *Egr2* during exhaustion appeared distinct from those controlled by *Egr2* during T cell tolerance, suggesting that EGR2 is repurposed during T cell exhaustion.

These findings indicate that while there is molecular overlap between $CD8^+$ T cell tolerance and exhaustion, shared proteins may differ in their mechanism of action. Such insight into the differences between tolerance and exhaustion checkpoints is important for refining future immunotherapies against cancer and autoimmune diseases.

Table of contents

List of figures

List of tables

Abbreviations

AIRE: Autoimmune Regulator

ANOVA: Analysis of variance

ANU: Australian National University

APC: Antigen Presenting Cell

APF: Australian Phenomics Facility

Arm: Armstrong

AxV: Annexin V

BATF: Basic Leucine Zipper transcription factor

Bcl2: B cell lymphoma 2

Bcl6: B cell lymphoma 6

BCR: B cell Receptor

BLIMP-1: B-lymphocyte-induced maturation protein 1

BM: Bone Marrow

BSA: Bovine Serum Albumin

CD: Cluster of Differentiation

c.f.u: colony forming units

ChIP: Chromatin Immunoprecipitation

cKO: conditional Knockout

Cl13: Clone 13

CNS: Central Nervous System

CTL: cytotoxic T lymphocyte

CTV: Cell trace Violet

CXCR5: Chemokine CXC motif receptor 5

DAG: Diacylglycerol

DC: Dendritic Cell

DGK: Diacylglycerol Kinase

DMEM: Dubelcco's Modified Eagle Media

DNA: Deoxyribonucleic Acid

DTR: Diptheria toxin receptor

EdU: 5-Ethynyl-2'-deoxyuridine

EGR2: Early growth response 2

EOMES: Eomesodermin

FACS: Fluoroscent activated cell sorting

FCS: Fetal calf serum

FOXO3a: Forkhead box O3

FOXP3: Forkhead box P3

GFP: Green fluorescent protein

GP: Glycoprotein

GZMB: Granzyme B

HA: Heamagglutinin

HEL: Hen Egg Lysozyme

HIV: Human Immunodeficiency Virus

ICAM-1: Intracellular Adhesion Molecule-1

IFN: Interferon

IL: Interleukin

IRF4: Interferon regulatory factor 4

i.p: intra peritoneal

IP_3: Inositol triphosphate

i.v: intra venous

ITIM: Immuno Tyrosine Inhibitory Motif

KLRG1: Killer Cell Lectin Like Receptor G1

LAG3: Lymphocyte activation gene 3

LCMV: Lymphocytic choriomeningitis virus

LM: Listeria monocytogenes

MFI: Mean fluorescence intensity

MHC I: Major Histocompatibility Complex Class I

MHC II: Major Histocompatibility Complex Class II

min: minutes

ml: milli litres

MS: Multiple Sclerosis

mTEC: medullary Thymic Epithelial Cells

mTOR: mammalian Target of Rapamycin

Ndfip1: NEDD4 family interacting protein 1

NEDD4: Neural precursor cell Expressed, Developmentally and Down-

regulated protein 4

NFAT: Nuclear Factor of Activated T cells

OVA: Ovalbumin

PAMPs: Pathogen Associated Molecular Patterns

PBS: Phosphate Buffered Saline

PD-1: Programmed Death 1

p.f.u: plaque forming units

PGE_2: Prostaglandin E_2

PIP_3: Phosphatidylinositol (3,4,5)-triphosphate

PI3K: Phosphoinositide-3 Kinase

PLN: Pancreatic Lymph node

PRRs: Pathogen Recognition Receptors

RA: Rheumatoid Arthritis

RIP: Rat insulin promoter

RNA: Ribonucleic acid

RPMI 1640: Roswell Park Memorial Institute 1640

SCID: Severe Combined Immunodeficiency

SLE: Systemic Lupus Erythematosus

SIV: Simian Immunodeficiency Virus

T1D: Type I Diabetes

TCR: T cell receptor

TF: Transcription Factor

Th: T helper

TIM3: T cell immunoglobulin and mucin-domain containing-3

TLR: toll like receptors

TNFα: Tumour necrosis factor alpha

TRAs: Tissue Restricted Antigens

Treg: regulatory T cells

µg: micro gram

µl: micro litre

µM: micro Molar

WT: Wild-type

CHAPTER 1: INTRODUCTION

1.1: $CD8^+$ T cell biology

1.1.1: Overview of the immune system

Living organisms have evolved to thrive in challenging external environments. A key factor for survival is the ability to protect oneself against pathogens or harmful microorganisms. Defense mechanisms collectively known as the organism's immune system have been evolving from the beginning of life. For successful protection, the immune system must be able to detect potential pathogens in the environment and mount an appropriate response against the pathogen.

The immune response of multicellular animals is multilayered and broadly classified into two arms - the innate and the adaptive immune systems. Each system consists of a network of cell types, which coordinate to recognise and combat pathogens. At the molecular level, immune cells express receptors to recognise conserved pathogen-associated molecular structures, as well as molecular moieties called antigens. When activated against a pathogenic antigen, the immune system generates an effective response to eliminate the pathogen through diverse cytotoxic and neutralizing mechanisms.

The immune system, however, can often be a double-edged sword, as dysregulated responses generated downstream of infection can also harm host tissues. Hence, regulation of immune responses through molecular checkpoints is crucial to generate a balanced and optimal response against the pathogen whilst limiting damage to host tissues due to excessive inflammation or inappropriate host-directed responses. If the response is unrestrained, this can harm the host in the form of immunopathology and autoimmune disease. On the other hand, excessive or prolonged dampening of the response can allow persistence of chronic infections and cancers. Therefore, understanding the molecular checkpoints that control this balancing act is important for the development of better therapeutics against immune-mediated diseases.

The innate immune system

In most organisms, the first line of defense includes physical barriers such as the skin and mucosal membranes, which limit entry of pathogens into the body. Upon breach of these barriers, multiple cell types forming the "innate immune system" such as the epithelium and phagocytes can be immediately activated due to their strategic location near these physical barriers. The innate immune system is crucial for rapid pathogen recognition and limiting pathogen spread. Phagocytes of the innate immune system comprise Dendritic Cells (DCs), macrophages and granulocytes, including neutrophils, eosinophils, and basophils. These cells are equipped with pattern recognition receptors (PRRs) to detect conserved pathogen-associated molecular patterns (PAMPs) such as bacterial cell wall components and viral nucleic acids (1). Activation of the PRRs leads to the generation of effector functions in the innate immune cells, such as the production of cytokines, degranulation of toxic molecules and phagocytosis. The latter allows the innate immune cells to ingest pathogens or infected cells with the aim to degrade the pathogen. This also enables "presentation" of pathogenic antigens on the surface of certain innate immune cells, which are classified as antigen presenting cells (APCs) (2). APCs are equipped with the task of processing pathogen-associated proteins in the phagosome and “present” pathogen-derived peptide fragments on their cell surface for recognition by cells of the adaptive immune system. Hence the innate immune system is vital for both quick responses to infection, and activation of the adaptive immune system through the production of cytokines and the presentation of antigen by APCs. However, it has multiple drawbacks, which necessitate the requirement for the adaptive immune system.

First, while PRRs comprise of multiple receptor families recognizing many classes of pathogens, they cannot distinguish between the various strains of viruses, bacteria or parasites (1). This poses a disadvantage in the defense mechanisms as a similar response is generated against potentially diverse types of infections caused by different pathogen strains. The lack of specificity in the functioning of the innate immune system creates the need for a more sophisticated system of antigen recognition. The second drawback of the innate immune system lies in its limited ability to improve responses against previously encountered pathogens. While the rapid kinetics of the innate immune system is crucial in limiting the spread of the

infection, in most cases the level of response generated against previously encountered pathogens does not change. This is an evolutionary disadvantage in the arms race against rapidly evolving pathogens. These factors potentially contributed to the development of the adaptive immune system in vertebrates.

The adaptive immune system

The adaptive immune system responds to specific molecular antigens and, hence, can confer pathogen-specific life-long protection or "immunity". Greek philosopher Thucydides was the first to observe and record the features of adaptive immunity in the Athens plague of 430 B.C. In *The History of the Peloponnesian War*, he commented, "the same man was never attacked twice - never at least fatally" (3). The adaptive immune system consists of cells called lymphocytes that possess highly specialized antigen recognition capacity.

Macfarlane Burnet theorized about the nature of antigen recognition in lymphocytes in his clonal selection theory (4). He correctly hypothesized that lymphocytes carried highly varied receptors, allowing them to detect an unlimited range of antigen specificities. Each lymphocyte was proposed to be a unique "clone" that would carry a unique genetically encoded receptor sequence that could be inherited by all daughter cells of this clone. Burnet correctly postulated that the clones recognizing a certain antigen would be selected by specific antigen binding to undergo rapid proliferation and form a clonal army to combat that specific antigen. While the selection of the correct clone against an antigen requires many days due to the low frequency of lymphocyte receptors specific for a given antigen (5,6), the responses generated are highly specific towards the pathogen at hand. Furthermore, some of the activated lymphocyte clones have the ability to survive past pathogen clearance as memory cells that can reactivate rapidly upon reinfection, providing highly specific lifelong protection against the pathogen. Given these advantages, it is not surprising that the majority of pathogen infections that escape initial innate immune control are successfully eradicated by lymphocytes. The importance of these cells is highlighted in patients with Severe Combined Immunodeficiency (SCID) that lack lymphocytes and succumb to severe and persistent viral and bacterial infections (7). Hence, the adaptive immune system makes up for the drawbacks of the innate system through the highly specific and long lasting protection it endows on the host. However, this

specialised system has its own disadvantages.

The nature of antigen recognition by the variable lymphocyte receptors is dependent on the chemical bonds formed between the antigen and the receptor, which determine the “affinity” of the interaction (8,9). Unlike the PRRs on innate immune cells, lymphocyte antigen receptors do not inherently recognise fixed molecular structures from bacterial cell walls or viral nucleic acids. This is because the unique lymphocyte receptor sequences are generated through randomized gene recombination events (10) as opposed to PRRs, which have conserved sequences. However, the diversity of lymphocyte receptor specificities thus generated can recognise any molecular moiety of a certain affinity regardless of whether they are host- or pathogen-derived, posing a risk of generating responses against self-tissues. Why does the immune system allow for the stochastic formation of lymphocyte receptors if it implies that the system has an equal chance of harming the host it has evolved to protect? The answer likely lies in the evolutionary advantage of a highly variable structure. The vast repertoire that randomized gene recombination provides outweighs the risk of generating self-specificities. Furthermore, the immune system employs multiple safeguards to mitigate the risk posed by self-reactive cells. First, the majority of lymphocytes bearing "self" specific receptors are either deleted from the repertoire, or functionally inactivated, via multiple immune "tolerance" processes (11) (described in the next section). Second, activation of adaptive immune cells typically requires signals from innate immune cells that are only produced upon innate immune recognition of an active infection, thus preventing the activation of self-reactive adaptive immune cells that may otherwise occur in the absence of infection (1). Lastly, the activation of lymphocytes is a multi-step process with each step stringently controlled by molecular networks acting as checkpoints to ensure lymphocytes are only activated against infectious stimulus (12,13). In this way, the immune system is able to usually keep any rogue self-reactive cells under control and limit their damage to the host.

Lymphocyte subsets

Lymphocytes of the adaptive immune system can be divided into two main subsets called B cells and T cells, which are armored with rearranged B Cell Receptors (BCRs) and T Cell Receptors (TCRs) respectively. While B cells and T cells are both

subjected to self-tolerance processes, their activation pathways are distinct due to differences in the structures of their lymphocyte receptors and hence the nature of the antigen that they recognize. B cells develop in the bone marrow and recognise native extracellular antigenic structures through their BCRs, such as repeating carbohydrates or intact proteins. Upon activation during an infection, pathogen-specific B cells can secrete their BCR as soluble proteins, known as antibodies, which can bind to the pathogen and induce multiple downstream effector responses to promote pathogen clearance. Hence B cells are crucial in clearing pathogens from the host circulation, however they are less effective at targeting intracellular pathogens residing in the cytoplasm of infected cells.

T cells detect and control intracellular infections through recognition of their specific antigens: small peptide fragments derived from proteins within the cell. In the 1970s, Doherty and Zinkernagel discovered that the TCR was in fact restricted to recognise antigen presented by the Major Histocompatibility Complex (MHC) molecules (14). Following this discovery, it was established that T cells carried either a CD4 or CD8 co-receptor to stabilize their interactions with MHC Class II ("MHC II") and MHC Class I ("MHC I") molecules respectively (15,16). These MHC molecules differ in their expression patterns and the nature of the peptide antigen presented in their grove. MHC II is almost exclusively expressed on APCs and usually presents extracellular phagocytized peptide antigens of typically 10-12 amino acids (2). MHC I, on the other hand, is expressed on most of the body's cells and typically presents peptide antigens of 8-10 amino acids from intracellular pathogens or proteins (17). This dichotomy reflects the different functions of the responding $CD4^+$ and $CD8^+$ T cells. $CD4^+$ T cells, known as "helper T cells", are a highly variable subset, which regulate the function of B cells and $CD8^+$ T cells through secretion of cytokines and expression of immunoregulatory cell surface receptors. $CD8^+$ T cells, or "killer T cells", are the primary responders against intracellular infections and have the ability to directly kill pathogen-infected cells. As $CD8^+$ T cells comprise the subject of this thesis, the remainder of the introduction will focus on this cell type.

The function of $CD8^+$ T cells requires access to most body cell types that could be infected, and hence these cells have evolved to recognise the intracellular peptides presented on MHC I. MHC I constitutively presents peptides typically derived from

self and foreign proteins processed by the proteasome within the cell. Thus, the continuous presentation of peptides on MHC I allows $CD8^+$ T cells to survey the dynamic intracellular proteome within a target cell and scan for potential pathogen-derived peptides. Upon activation, $CD8^+$ T cells produce cytotoxic enzymes called granzymes and the pore-forming toxin perforin, which are both released upon antigen recognition on an infected target cell to initiate programmed cell death or apoptosis. This cytotoxic machinery, along with other factors such as cytokines and death receptors, allows the activated $CD8^+$ T cells to directly kill pathogen-infected cells. For this reason, activated $CD8^+$ T cells are known as Cytotoxic T lymphocytes (CTLs) (18).

While $CD8^+$ T cells are crucial in clearing intracellular pathogens, they can cause bystander tissue damage and also have the power to recognise endogenous self-antigens presented on MHC I. Thus, if inappropriately activated, $CD8^+$ T cells have the potential to cause high levels of damage to host tissue. For instance, self-reactive $CD8^+$ T cells can cause autoimmune disease by inappropriately targeting uninfected self-tissue independent of the presence of infection (19). Additionally, pathogen-specific $CD8^+$ T cells can fatally damage whole organs during widely disseminated infections if their activity is not restrained (20–22). Hence regulation of $CD8^+$ T cell activation by molecular checkpoints is vital to ensure optimal responses are generated against infection with minimal damage to the host. Exploring these molecular checkpoints in $CD8^+$ T cell biology is the central aim of this thesis. However, in order to understand the pathways that limit $CD8^+$ T cell immunity, it is important to first delineate the molecular pathways involved in the activation and differentiation of a functional CTL response.

1.1.2: $CD8^+$ T cell activation and differentiation

Prior to activation, the repertoire of $CD8^+$ T cell clones continuously circulates between the blood and lymphoid organs in a "naïve" state. In this state, the cells are non-proliferative, metabolically quiescent, lack immune effector functions and cannot migrate into peripheral tissues. Instead, naïve cells are restricted to trafficking to the lymphoid organs through the expression of specific homing molecules, such as L-Selectin (CD62L), which allows them to bind to the high endothelial venules in

lymphoid tissues (23). Naïve T cells receive homeostatic survival signals from frequent low avidity interactions with self-MHC and through the cytokine interleukin-7 (IL-7), which binds to the IL-7R expressed by naïve cells (24,25). Naïve $CD8^+$ T cells do not acquire effector functions by default, and in the case of an infection must be provided with the correct signals for their activation by innate immune cells. Complete activation of $CD8^+$ T cells requires extrinsic signals from the innate immune system, which are then integrated intrinsically within the T cells to enable effector cell differentiation.

T cell activation by DCs

Activation of naïve $CD8^+$ T cells first requires activation of innate immune cells by the invading pathogen. While B cells and macrophages can also act as APCs, it was shown in mixed leukocyte reactions that DCs are the most potent stimulators of T cell activation (26). Named after their characteristic dendrite-like projections, DCs are the key APC required for activation of naïve $CD8^+$ T cells, as they provide context-specific activation signals to $CD8^+$ T cells. To understand the specific role of DCs in contributing to the $CD8^+$ T cell response, many genetic models were created to deplete DC populations *in vivo*, either using mice lacking the Transcription Factor (TF) *Batf3* (27,28) or genetically expressing Diptheria toxin receptor (DTR) under the CD11c (29), CD205 (30) BDCA2 (31), and Clec9A (32) promoters whereby delivery of the Diptheria toxin would result in selective loss of DC subsets expressing the above genes. The resulting loss of DCs (or specific DC subsets) in the above models led to a defective CTL response to a variety of infection and immune challenge models (27–32). The reliance on DCs for $CD8^+$ T cell activation and effector differentiation is due to a number of reasons such as their efficient activation in most infections, the unique ability to “cross-present” antigen and acting as a non-redundant source of key cytokines such as interferons (IFN).

DCs are a heterogeneous population classified according to their ontogeny and function (33). DCs localize in the peripheral tissue and lymph nodes where they patrol for the presence of pathogens and hence have early access to invading pathogens within most body tissues. Tissue resident DCs constitutively sample antigen from their localised environment and migrate from the periphery to lymph nodes, thereby providing naïve T cells access to antigens derived from tissue-

restricted pathogens. This steady state migration is especially important given that naïve $CD8^+$ T cells do not have access to peripheral tissues.

An important feature of the immune response is the ability to mount an efficient response tailored to the pathogen at hand. Along with providing information on the antigens present within a tissue, DCs are also able to provide the T cell with information on the type of pathogenic infection occurring in the peripheral site. The signals from the specific pathogenic infection result in the activation of the DCs, facilitating their transition into an “immunogenic state” capable of supporting effector T cell differentiation during infection (34,35). Immunogenic DCs, increase their migration to the nearest lymph nodes to activate the adaptive immune system, upregulate co-stimulatory molecules and cytokine production as well as activating other innate immune cells during infection. Costimulatory receptors, such as CD80 and CD86 (36,37), are upregulated after PRR activation and these play important roles in sending positive differentiation signals to the T cells that they interact with. Along with PRR stimulation, inflammatory cytokines, such as Type I interferons (IFN), that are produced by other innate immune cells and infected tissues can also act on the DCs to further boost expression of co-stimulatory receptors (38). Depending on the type of infection and hence specific PRR activated, DCs produce cytokines that can inform the adaptive system about the infection at hand. In regards to intracellular pathogens, bacterial infections induce IL-12 production by DCs (39,40), while viral infections trigger production of IL-12 as well as IFNα/β (41) – both of these signals are crucial for appropriate $CD8^+$ T cell activation in these respective infections. The activation and signaling of PRRs also enhances sampling and endocytosis of pathogenic antigen by DCs, leading to more efficient antigen presentation on MHC molecules to the naive T cell pool (42–44). Hence, given their presence throughout tissues, rapid activation in infection, and ability to provide the correct activation signals to T cells, DCs serve as excellent activators of the immune system. However, they are specifically crucial for $CD8^+$ T cell activation due to their ability to “cross-present” antigens.

$CD8^+$ T cells need to access intracellular antigens presented on MHC I, meaning that DCs need to present foreign antigens on MHC I in order to activate a $CD8^+$ T cell response. However, if DCs are not directly infected with a pathogen and only

encounter pathogenic antigen by phagocytosis, they have no obvious way to present foreign antigen on MHC I and induce a response. To address this dilemma, certain subsets of DCs are uniquely endowed with the capacity to present exogenous antigen on MHC I in a process called “cross-presentation” (45). This deviation from the classical MHC presentation pathway is crucial for activation of $CD8^+$ T cells against infections and tumor antigens, which are not intracellularly expressed within DCs (45–47). All $CD8^+$ DCs with XCR1 expression (commonly referred to as the cDC1 cells) are able to cross-present antigen to $CD8^+$ T cells (48–50). This subset stems from a common lineage controlled by the TF BATF3, which is crucial for the differentiation of cross-presenting DCs (27,51). Deletion of BATF3 in mouse models led to the crippling of the CTL response due to loss of the entire cross-presenting DC lineage (27). To specifically test the role of cross-presentation in the activation of $CD8^+$ T cells, a recent study utilised mice with deficiency in the WDFY4 protein, a factor required for cross-presentation. In this model, despite the presence of the $BATF3^+$ DC populations, the $CD8^+$ T cell response to tumors and virus infection was defective due to the inability of DCs to cross-present antigen (52). Thus, DCs are uniquely specialised to license a naïve $CD8^+$ T cell for effector differentiation within secondary lymphoid organs.

A productive outcome of the DC-T cell cross talk in the lymph nodes requires both recognition of specific antigen by the TCR, and concomitant interactions with multiple cell surface receptors and cytokines (53). These interactions largely occur at an organized and polarized contact point between the DC and T cell known as the “immunological synapse” (54). DC-T cell cross talk is a complex process which occurs in multiple stages (55) and the stability and duration of the contact strongly determines downstream T cell activation (53,56). Studies using two-photon microscopy have shown the importance of adhesion molecules such as ICAM-1 (57) as well as the abundance of antigen presented on the DC (58) in contributing to synapse stability and T cell differentiation into functional effectors. After formation of a stable synapse, the nature of interactions between the T cell and DC determine the outcome of the crosstalk. Co-stimulatory receptors such as CD80 and CD86 on the DC bind to the CD28 ligand on the surface of T cells (59). While CD28 signaling is highly crucial *in vitro*, it is often not necessary *in vivo* as CD28-deficient mice were able to mount normal $CD8^+$ T cell effector responses to viral infection (60). Along with

the CD28-CD80/86 interaction, $CD8^+$ T cells are also activated by multiple redundant co-stimulatory pathways, such 4-1BB-41BBL (61) as well as CD27-CD70 (62). Thus, multiple redundant interactions are involved in $CD8^+$ T cell activation; this redundancy likely evolved as a way to reduce possible immune evasion mechanisms by pathogens. In addition to co-stimulatory molecules, inflammatory cytokines such as IL-12 (63) or Type I IFN (64) released from DCs or other cell types, in addition to autocrine or paracrine IL-2 produced by the nascent effector T cell response (65), can directly act on the responding cells to enhance effector differentiation. The combination of cytokine and co-stimulatory signals encountered ultimately sum to both trigger effector differentiation of naive $CD8^+$ T cells and determine the magnitude of the effector $CD8^+$ T cell response (66).

T cell signaling

Productive $CD8^+$ T cell activation ultimately hinges on the capacity of $CD8^+$ T cells to convert the extracellular signals received (antigen, cytokines and co-stimulatory signals) into intracellular signaling events that direct effector differentiation. For this reason, insights into the signaling events engaged during effector differentiation have played a crucial role in shaping our understanding of the differentiation process. The TCR-antigen interaction, costimulatory receptor engagement and cytokine signals all engage both overlapping and independent signaling cascades in the T cell that culminate in the activation of transcription factors. Depending on the signals received, the respective transcription factors work together to cause the global gene changes required for the transition of naïve $CD8^+$ T cells into functional CTLs appropriate for the infection context. While there are numerous complex signaling pathways involved in T cell activation, the most relevant ones, in addition to the broad principles underlying signaling in T cells, are discussed below and summarised in Figure 1.1.

Upon formation of a stable TCR-MHC complex interaction, the signaling events downstream of the TCR are initiated by phosphorylation of the proximal CD3ζ chains by the kinase LCK (67). These phosphate groups then serve as docking and activation sites for further kinases resulting in a cascade of phosphorylation, serving to amplify the initial signal. The TCR signaling cascade results in the hydrolysis of the membrane protein lipid Phosphatidylinositol-3 phosphate (PIP_3) to generate Inositol

triphosphate (IP_3) and Diacylglycerol (DAG) molecules (68). IP_3 induces calcium-signaling which activates the key transcription factor NFAT (69,70). Many in vitro experiments use calcium ionophores to activate NFAT in T cells (68,71,72), illustrating the dependence of this transcription factor on calcium signaling. DAG produced from PIP_3 hydrolysis is responsible for initiating numerous pathways, and its function varies depending on context. One of the key functions of DAG is to induce Ras activation (73) and, ultimately, phosphorylation of ERK, which is a hallmark of TCR signaling (74,75). Importantly, ERK signaling contributes to activation of the TF Fos, a key component of the AP-1 TF complex that plays important roles in T cell activation (76) (see below). Thus, antigen signaling from TCR results in the induction of NFAT and Fos activity, however these pathways alone are not sufficient to completely activate the T cells and turn on effector genes.

Co-stimulatory and cytokine signals are equally important in the activation of T cells. This is a key point of regulation, as it ensures that $CD8^+$ T cell activation will only optimally occur in the presence of an active infection. These signals critically contribute to T cell activation in a number of ways. Firstly, costimulatory signals, along with the TCR, are important for activating the JNK pathway, which is required for the activation of the JUN and FOS TFs that cooperatively make up AP-1 (77). AP-1, in collaboration with NFAT, is important for activating many key effector genes, including cytokines (78). Furthermore, co-stimulatory interactions induce the Phosphoinositide 3 Kinase (PI3K) pathway, which in turn activates the kinase Akt, and the mammalian Target of Rapamycin (mTOR) (79). The Akt/mTOR axis plays essential roles in enhancing the metabolism of the T cell by, for example, augmenting protein translation (80,81). This is a particularly important function of this pathway, as profound metabolic shifts are required to support T cell differentiation. To convert a $CD8^+$ T cell from its naïve resting state to an army of effector cells loaded with cytotoxic machinery requires drastic changes in $CD8^+$ T cell physiology and changes in cellular respiration (82). mTOR activation is crucial in enabling a metabolic switch in activated $CD8^+$ T cells from using oxidative phosphorylation to aerobic glycolysis - an oxygen independent process which allows for effector function in hypoxic tissue environments (83,84). Aerobic glycolysis involves production of glycolytic intermediates such as pyruvate, which are used to synthesise important molecules in anabolic reactions, such as amino acids, phospholipids and carbohydrates (85).

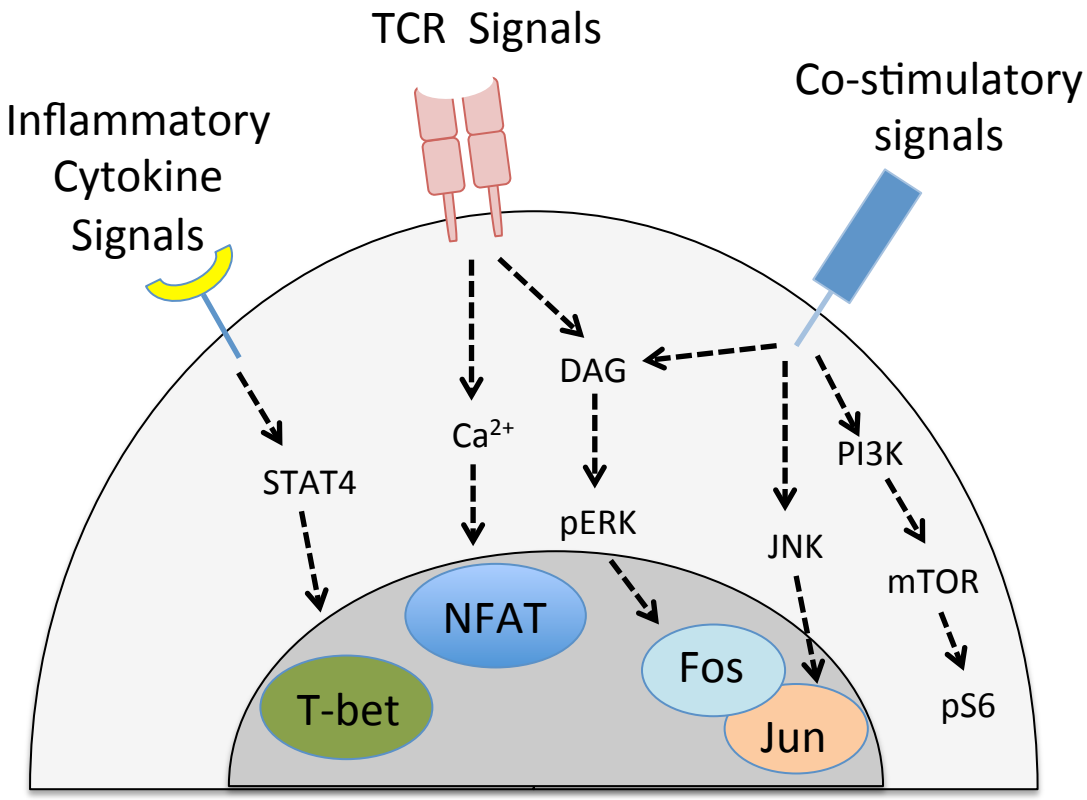

Figure 1.1: T cell signaling during effector differentiation: Productive activation of naïve $CD8^+$ T cells into effector cells requires TCR signals, cytokine signals and co-stimulatory signals from the immunogenic APC. This figure summarises the downstream pathways triggered by the different signals and the final transcription factors induced downstream of the signaling pathways.

These factors can then fuel synthesis of key effector proteins, as well as support growth and proliferation (86). Furthermore, mTOR signaling increases surface expression of glucose and amino acid transporters, which in turn allow greater nutrient uptake into the cell to compensate for inefficient energy generation by aerobic glycolysis (86,79,87,88).

While TCR and co-stimulatory signals are necessary for activation of naïve $CD8^+$ T cells, inflammatory cytokines secreted by the DC (and surrounding innate immune cells) further aid T cell differentiation into effector cells (89). The presence of IL-12 during infection can induce expression of the transcription factor T-BET in $CD8^+$ T cells by binding to the IL-12R and signaling through STAT4 (90,91). T-BET is an important transcription factor that contributes to the effector function of $CD8^+$ T cells(90,92) and is described in detail in the following sections. Additionally extracellular receptor interactions that likely occur during the T cell-DC interaction, such as Notch signaling, also affect acquisition of effector functions by $CD8^+$ T cells by controlling downstream transcription factors (93,94).

Thus, the signaling events triggered by the TCR, co-stimulatory, and cytokine pathways, in addition to other extracellular signals, converge to activate transcription factors, which in turn determine the fate of the T cell in a manner appropriate to the infection at hand. While most $CD8^+$ T cells receiving these signals during an infection will differentiate into effector cells, a sub-population of cells persists beyond the clearance of infection and differentiates into memory cells. The bifurcation of cell fate between effector and memory cells begins early during activation and is controlled by various molecular factors discussed below.

Effector and Memory $CD8^+$ T cell differentiation

The goal of the $CD8^+$ T cell response is to firstly produce sufficient numbers of robust effector cells to clear the pathogen at hand, and to secondly form long-term memory to combat future invasion by the same pathogen. The typical $CD8^+$ T cell response to an acute infection is categorized into three phases - expansion of effector cells, effector cell contraction and memory formation. The ideal features of effector cells include rapid expansion, the ability to produce cytotoxic molecules and the capacity to traffic to sites of infection. On the other hand, memory cells should ideally persist

and self-renew to maintain a stable population in the absence of antigen, and rapidly differentiate and re-expand upon pathogen re-encounter. Hence given that the cellular properties of effector and memory cells are distinct from each other, a highly regulated differentiation process ensures that the correct proportion of effector $CD8^+$ T cells either undergo terminal differentiation or persist as memory cells. This decision to either form a short-lived effector cell or persist as a memory cell begins early during effector differentiation (95,96) , and is controlled by a suite of extensively studied molecular cues. This section will cover the molecular pathways that control effector cell expansion and persistence through to memory.

Naïve $CD8^+$ T cells undergo rapid proliferation following activation, with expansion capacity reaching up to 1000-fold over the initial naïve precursor frequency. However, not all T cell clones expand to similar levels, and proliferation is controlled by multiple factors including precursor frequency of clones specific for the antigen and pMHC affinity (6,97–99), as well as pathways downstream of TCR and co-stimulatory receptors such as mTOR signaling, cytokine activation of STAT1/4 and potentially Notch signaling (100). Multiple TCRs can be specific for a given antigen at different affinities and, although $CD8^+$ T cells of lower avidities are recruited into the effector program, they undergo less proliferation due to competition with the high-affinity clones for the peptide-MHC complexes (101,102). This allows preferential expansion of the high-affinity TCR populations during effector differentiation in a process driven by the transcription factors IRF4 and BATF. IRF4 is induced downstream of NFAT and AP-1 activation in an antigen-dependent manner, with its expression directly proportional to the strength of TCR signaling (103). IRF4 enables high-affinity clones to undergo the metabolic switch to aerobic glycolysis and catabolic metabolism that is required to fuel effector cell expansion; this allows high affinity cells to become the dominant clonal population of effector cells (103). BATF is also induced downstream of TCR signalling, and it forms a complex with IRF4 and JUN proteins to initiate transcription of *T-bet*, *Eomes* and the cytokine receptor genes that control effector development (104).

Along with expansion, the CTL clones acquire the capacity to migrate into infected peripheral tissues (105,106), and this is controlled by multiple selectin and integrin molecules. In particular, primed effector cells downregulate CD62L and up-regulate

both inflammatory chemokine receptors and specific integrins to enable homing to inflamed and infected tissues (23,107,108). Once they reach infected sites, they are able to mobilise effector functions upon target cell recognition. Downregulation of CD62L is linked to PI3K-mTOR activity, and this serves as a checkpoint ensuring that a cell's migratory capacity and the metabolic changes required for effector function are acquired in parallel (109). PI3K-mTOR-dependent regulation of CD62L levels is achieved through PI3K dependent proteolytic shedding, and through suppression of the transcription factor KLF2. KLF2 induces expression of a number of receptors that promote recirculation (including CD62L), meaning that KLF2 inhibition facilitates $CD8^+$ T cell migration into the tissue (110–112).

In order to achieve rapid expansion, tissue migratory capacity and cytolytic function, effector $CD8^+$ T cells undergo a unique transcriptional and epigenetic differentiation program that results in global changes in gene expression (100,113–117). This differentiation program allows $CD8^+$ T cells to perform effector functions, including secretion of inflammatory cytokines such as Interferon γ (IFNγ), Tumour Necrosis Factor α (TNFα) and Interleukin-2 (IL-2) (118) . Effector cells also gain cytotoxic functions to enable target cell killing by apoptosis, including release of granzymes and perforin, and ligation of the FAS receptor on target cells via FASL (119,120). Many of these gene changes are initiated by transcription factors such as T-BET and EOMES, which induce the *Ifng*, *Gzmb* and *Prf1* genes (121,122). In order to reinforce and stabilize effector differentiation, certain TFs create positive feedback loops. T-BET provides an example of such a positive loop in effector $CD8^+$ T cells. The expression, and thus function, of T-BET is controlled by the amount of inflammatory signals in the environment, specifically IL-12 (90). T-BET acts as a rheostat: measuring inflammation and driving the terminal differentiation of effector cells accordingly in a threshold dependent manner (90). T-BET promotes effector differentiation by inducing other TFs that reinforce the effector gene program. T-BET promotes effector function, in part, by inducing the transcription factor ZEB2, which allows $CD8^+$ T cells to commit to the effector lineage and die after antigen clearance (123,124). T-BET also drives the expression of other TFs, such as BLIMP-1 (125), which prevents premature memory differentiation. BLIMP-1 contributes to transcription of Granzyme B (GZMB) in co-ordination with EOMES and T-BET (125). Finally, BLIMP-1 represses the transcriptional regulator ID3 (126), leading to

induction of a related factor, ID2 (127), and optimal expansion and effector differentiation. These examples illustrate how a single TF (T-BET) can trigger a cascade of positive feedback loops that reinforce CTL differentiation and expansion.

Effector cells become terminally differentiated if they excessively proliferate and differentiate. Terminally differentiated cells have a poor capacity to persist (90), and once the infection is cleared, 90-95% of the effector $CD8^+$ T cell population (predominantly comprising terminally differentiated cells) undergoes apoptotic cell death (128). The crucial factors responsible for cell death during contraction are the pro-apoptotic BH3-only Bcl2 family members BIM (129) and, to a lesser extent, PUMA (130). The pathways that trigger BIM-dependent death are still being characterised. Many studies have suggested that transcriptional induction of BIM expression by the transcription factor FOXO3 plays an important role in BIM-dependent contraction. FOXO transcription factors are excluded from the nucleus and degraded upon phosphorylation by Akt (131). Conversely, upon loss of cytokine signaling, FOXO3 is dephosphorylated, leading to protein accumulation, nuclear translocation and access to target genes. *In vitro* experiments in several B and T cell lines (132,133) have indicated that FOXO3 directly binds to the *Bim* promoter, where it then induces expression of *Bim* mRNA (134) and subsequent death of the cells. *In vivo* models have confirmed a role for FOXO3 in contraction using mouse models with a T cell-intrinsic deficiency in FOXO3. These mice exhibited an accumulation of effector $CD8^+$ T cells due to reduced apoptosis, and diminished *Bim* expression, during the T cell contraction phase in both LCMV and LM-OVA infections (135,136). However, it remains unclear whether FOXO3 directly controls Bim expression *in vivo*. Recent studies have presented contrasting evidence about the binding of FOXO3 to the BIM promoter (137), as mutation of the FOXO3 binding sites within the Bim promoter did not hinder BIM expression or apoptosis. Hence, other pathways, such as loss of Erk-mediated repression of BIM expression and protein levels (138–140,75) upon pathogen clearance, could also contribute to BIM-dependent death during T cell contraction.

Not all T cells undergo death during the contraction phase, with survival of $CD8^+$ T cells beyond contraction linked to the degree of terminal differentiation that occurs during infection. The surface markers Killer-like Lectin Receptor G1 (KLRG1)

(141,142) and IL-7R (95,143) can help to identify these early populations of short-lived effector cells and memory precursors, and these markers have enabled tracking of these populations in several infection models. While there are multiple hypotheses explaining how these T cell populations arise (100), the “decreasing potential” model is backed by multiple lines of evidence. The decreasing potential model claims that the differentiation of naïve $CD8^+$ T cells into either effector or memory precursors is dependent on the balance in their expression of effector versus memory associated transcription factors. This model suggests that the more effector cells differentiate, the more they lose memory potential (100). This is postulated to occur due to increased expression of effector-specific TFs that specifically silence competing memory-associated TFs. However, the changes in TF expression are also compatible with other models of memory differentiation, such as binary fate determination by asymmetric cell division. There is likely a stochastic component to this differentiation process, with the small fraction of cells that are, by chance, exposed to less of the factors that promote terminal differentiation (such as inflammatory cytokines) retaining more memory potential. For example, $CD8^+$ T cells exposed to high levels of IL-12 will up-regulate *T-bet* expression, while those clones that encounter less IL-12 will maintain expression of the opposing transcription factor, *Eomes*, aiding subsequent persistence and differentiation into memory cells (144). Multiple transcription factor pairs oppose each other to promote either a memory or short-lived effector fate. These pairs include *Id2* and *Id3* (126,127,145), *Zeb1* and *Zeb2* (123,124,146), *T-bet* and *Eomes* (144,147–149), *Stat4* and *Stat3* (150–152), and *Blimp-1* and *Bcl6* (125,150,153–157), with the former molecule involved in effector development and the latter in memory differentiation. The process of short-lived effector and memory commitment is also controlled at the epigenetic level, with the memory genes being shut down in effector cells as they commit to that lineage (158). On the other hand, memory cells do not repress the effector genes but have bivalent modifications on the associated histones, allowing the cells to differentiate back into effector cells for subsequent infections (158,159). Hence the fate of effector and memory cells is tightly regulated by extrinsic factors, which control the intrinsic regulatory machinery.

Following the contraction phase, the remaining $CD8^+$ T cells form part of the memory compartment. Memory cells have unique properties that differentiate them from their

effector cell counterparts. First, they do not rely on antigen for their survival (160), but instead depend upon the homeostatic cytokines IL-7 (143,161) and IL-15 (162) for survival and self-renewal. Second, they produce greater amounts of IL-2 (163), and can rapidly give rise to effector cells upon antigen reencounter. In particular, memory cells undergo epigenetic changes that facilitate rapid re-expression of effector genes (114,115,164,165). Memory cells exhibit heterogeneity, with specialised subsets such as long-lived central memory cells (T_{CM}), which reside in the lymphoid organs and exhibit greater proliferative capacity, and short-lived effector memory cells (T_{EM}), which patrol tissues and can launch immediate responses to pathogen reinfection, but are less proliferative upon restimulation (163,166). T_{CM} become enriched over time, likely largely due to preferential survival and homeostatic proliferation of the T_{CM} population (98,167,168). Recently, a new subset of memory cells called tissue resident memory cells (T_{RM}) was defined, with this subset restricted to the tissue site of primary infection; this subset plays non-redundant roles in protection against re-infection at a specific tissue site (169,170). Each of these subsets is characterised by a unique combination of transcription factors, which drives their differentiation and maintains their identity and "stemness". In general, long-lived circulating central memory $CD8^+$ T cells are characterised by expression of multiple transcriptional regulators, including *Eomes* (149), *Bcl6* (156), *Id3* (126,145), *Foxo1* (171,172), *Tcf7* (173) and *Zeb1* (146). In contrast, recent data indicate that T_{RM} appear to have a distinct transcriptional program from circulating memory cells (174–177). While decades of research have thoroughly characterised the network of transcription factors in effector-memory differentiation, the TF networks that dampen the $CD8^+$ T cell response to chronic antigen are less well characterised.

1.1.3: Negative regulation of $CD8^+$ T cells

While a highly coordinated effector and memory response is required to contain infection and prevent reinfection, a completely unrestrained $CD8^+$ T cell response poses danger to the host. Hence, there is a need for negative regulation and checkpoints in $CD8^+$ T cell activation. T cell clones that recognise self-antigen need to be suppressed to prevent inadvertent activation and acquisition of effector function. The regulation of self-reactive cells is collectively known as immunological tolerance, and this process is necessary to prevent autoimmune disease by self-

reactive cells. Second, negative regulatory mechanisms are required during infection to protect the host against fatal collateral tissue damage. The negative regulatory pathways engaged to limit such immunopathology typically dampen the inflammatory function of chronically stimulated effector cells in a process often called T cell “exhaustion”. These two states of $CD8^+$ T cell differentiation are driven by chronic antigen recognition, which induces negative regulatory pathways that suppress $CD8^+$ T cell function to limit damage to host tissues. The pathways downstream of chronic antigen that cause exhaustion and tolerance are poorly characterised, and it is unclear whether the same or different pathways are utilized in both cases. A major theme of this thesis is to better define whether common regulatory pathways are engaged by chronic antigen in the context of both tolerance and exhaustion.

1.2: $CD8^+$ T cell tolerance

The vast diversity of lymphocyte receptor specificities in the adaptive immune system means an almost unlimited spectrum of antigens can be recognised, however this implies that B and T cells can also recognise self-antigens. This introduces a dilemma in the functioning of the adaptive immune system, as there is a possibility of generating cytotoxic responses against host tissues. To mitigate this risk, multiple layers of regulation, collectively referred to as immunological tolerance mechanisms, have evolved to control self-reactive lymphocytes. These mechanisms act in an antigen-specific manner, such that typically only T cells specific to self and steady-state antigens are subjected to these tolerance processes. The tolerance mechanisms are usually subdivided into two main categories: central tolerance mechanisms, which purge self-reactive cells from the repertoire during lymphocyte development, and peripheral tolerance mechanisms, which restrain those self-reactive cells that escape central tolerance.

While tolerance processes are able to successfully control self-reactive B and T cells in the majority of individuals, roughly 5-7% of the population develops autoimmune diseases, indicating that these tolerance mechanisms can fail (178). Autoimmune diseases comprise of over 80 different conditions that are defined by the onset of immune responses against self-epitopes present in either specific organs, or expressed systemically throughout the body. Examples of organ-specific autoimmune diseases include Type I Diabetes (T1D), Multiple Sclerosis (MS), and Vitiligo; and systemic autoimmune conditions include Systemic Lupus Erythematosus (SLE) and Rheumatoid Arthritis (RA) (178). While determining the precise cause or triggers of autoimmune disease remains a holy grail in this research area, it is postulated that multiple genetic, environmental and cellular factors contribute to the eventual break in tolerance. Furthermore, current treatments for these diseases are limited to immunosuppressive drugs that non-specifically shut down all B and T cell responses, causing severe side effects that warrant the development of more specific treatments. Self-reactive $CD8^+$ T cells are implicated in multiple organ-specific autoimmune diseases, and can cause significant organ damage through their cytotoxic function (19). Thus, understanding the cellular and molecular tolerance pathways that act as checkpoints for self-reactive $CD8^+$ T cells is crucial, as these

pathways could become potential drug targets for the treatment of $CD8^+$ T cell-mediated autoimmune disease.

1.2.1: Central Tolerance

In his clonal selection theory, Macfarlane Burnet proposed that clones recognizing self-antigens would be purged from the repertoire before they entered the periphery (4). In subsequent decades, this hypothesis was validated with the identification of "central tolerance" pathways that delete self-reactive B cells and T cells during their development in bone marrow and thymus respectively. To ensure that the bulk of self-reactive cells are rapidly eliminated before they can pose a risk to the host, these pathways operate immediately after lymphocyte receptor rearrangement. In the case of T cells, TCR rearrangement occurs within the thymus after immature Pre-T cells formed in the bone marrow migrate to the thymus. Due to the stochastic nature of the TCR gene recombination process, a diverse lymphocyte receptor repertoire of up to 10^{15} unique specificities is predicted to be generated in the thymus (179,180). While random receptor recombination can generate self-reactive clones, it can also generate useless clones that cannot interact with MHC. Thus, to ensure the TCRs are both functional and not self-reactive, the final receptor products need to be selected for their ability to interact with self-MHC molecules, and selected against recognition of self-antigens. For this reason, two selection processes have evolved within central tolerance: one to ensure that only T cells with TCRs capable of binding to MHC are retained (positive selection), and one to actively eliminate cells that are self-reactive (negative selection) (181).

Positive and negative selection during thymic development is a two-step process, where selection is based on the affinity of the TCR for self-peptide-MHC complexes. Positive selection occurs in the outer cortex of the thymus, where the newly rearranged TCRs interact with the MHC II and MHC I molecules on cortical thymic epithelial cells (cTECs) (182). T cells that recognise MHC molecules with low affinity are provided with survival signals and proceed with thymic development. The selected T cells then undergo negative selection, where their TCRs are screened for affinity to self-antigens, and those exhibiting strong recognition of self-antigens are deleted from the repertoire. The APCs in the thymus responsible for inducing

negative selection include the medullary TECs (mTECs) and DCs, which present an array of self-antigens (183). While mTECs directly present self-antigens that they express, DCs have been shown to cross-present antigens to $CD8^+$ T cell precursors (184,185). Negative selection can occur in both the medulla and the cortex regions of the thymus, and is manifested in two “waves” of selection. The first wave deletes immature thymocytes that can strongly recognise self-antigens presented in the thymus, and the second wave is important in generation of Tregs from mature $CD4^+$ self-reactive thymocytes (186,187). While T cells are selected against ubiquitously expressed self-antigens within the thymus (188), it was initially hypothesized that T cells would not be tolerised against tissue restricted antigens (TRA) during thymic selection, and that peripheral tolerance mechanisms exclusively controlled T cells specific for TRAs. However, this dogma was challenged by multiple studies. Firstly, it was shown that DCs from the periphery could pick up antigen from peripheral tissues and migrate to the thymus for subsequent negative selection of TRA-specific $CD8^+$ T cells (189). Secondly, early studies indicated promiscuous mRNA expression of TRAs in thymic mTECs, such as insulin, alpha-fetoprotein and myelin proteins (190–192). The source of this promiscuous expression was eventually attributed to the transcription factor AIRE, which is responsible for a leaky expression system that turns on expression of different sets of tissue-restricted genes in each mTEC (193,194). While DCs do not express AIRE, they are able to cross-present AIRE-dependent TRAs derived from mTECs and thereby participate in negative selection (184,195). AIRE is likely not responsible for controlling all of the observed promiscuous TRA expression, and recently the transcription factor FEZF2 (196) was also shown to contribute to promiscuous TRA expression within mTECs. The importance of these transcription factors in thymic negative selection and immune tolerance has been highlighted in AIRE deficient mice and humans, which succumb to multi-organ autoimmune diseases (193,197–199).

The major goal of thymic negative selection is to purge cells reactive to TRAs and ubiquitous self-antigens from the T cell repertoire. This is achieved through induction of apoptosis in the self-reactive cells and is primarily mediated by the pro-apoptotic factor BIM. Loss *of Bim* resulted in defective thymic deletion, although the surviving self-reactive cells did not break tolerance as peripheral tolerance mechanisms appeared to keep these cells in check (200). Other apoptotic factors such as PUMA

also contribute to thymic deletion, as a lack of both *Bim* and *Puma* resulted in the onset of autoimmune disease, presumably by overwhelming peripheral tolerance processes (201).

Despite the comprehensive negative selection process in the thymus, negative selection is "leaky" and self-reactive $CD8^+$ T cells do escape into the periphery. Self-reactive T cells have been observed in the peripheral blood of healthy individuals at comparable levels to patients with autoimmune disease (202–206). More recently, tetramer enrichment of self-antigen specific T cells revealed that male antigen H-Y specific $CD8^+$ T cell numbers were present in both male and female adults despite the presence of H-Y as a self-antigen in males (207). The number of $tetramer^+$ cells present in males was a third of the number found in females, indicating that thymic selection only purged ~70% of the repertoire specific for H-Y antigen. This finding suggested that, at least in the case of the H-Y antigen, thymic selection was incapable of deleting all self-reactive T cells from the repertoire.

There are multiple reasons for the escape of potentially autoreactive T cells from the thymic selection process. First, the deletion of self-antigen specific TCRs during negative selection is biased towards high-affinity TCR-MHC interactions, and low avidity clones are often spared (208,209). Second, despite promiscuous TRA expression, not all peripheral tissue antigens are displayed on the mTECs and DCs during negative selection, allowing escape of T cells specific to those tissue antigens not presented in the thymus (210). Furthermore, expression of TRAs in the thymus does not necessarily guarantee deletion of the responding thymocytes (211). Third, and importantly, complete purging of self-specific T cells from the thymus would result in holes in the TCR repertoire. Self-antigen affinity of TCRs is a continuum, rather than an "all or nothing" process, and setting a too stringent threshold for selection would thus decrease repertoire diversity. This would be evolutionarily disadvantageous to the host, as it would leave the immune system vulnerable to evasion by pathogens mimicking the self-antigens against which T cells were excessively selected. Thus, as the threat of pathogenic infection is greater than the slow onset of autoimmune disease that may occur downstream of slightly leaky thymic selection, the escape of some self-reactive T cells into the periphery is likely tolerated by the immune system. Supporting this theory, the above-mentioned study

on tolerance of H-Y specific T cells in males also demonstrated the presence of unlimited TCR specificities in healthy controls against all possible mutagenic variations of a Hepatitis B viral peptide, emphasizing that a broad TCR repertoire was present in most individuals (207). Thus, to maintain this vast T cell repertoire in the periphery while simultaneously restraining the rogue self-reactive T cells that are an inevitable consequence of this diversity, the immune system has developed several "peripheral" tolerance mechanisms.

1.2.2: Peripheral tolerance

Peripheral tolerance mechanisms identify self-reactive T cells by selectively tolerising cells that recognise their cognate antigen in the steady state. This is based on the presumption that antigen encountered in the steady state (ie. in absence of inflammation or danger signals) is likely enriched for self-antigens, and hence any responding T cells are likely self-reactive. Furthermore, non-self antigens presented in the steady state are likely not harmful to the host, and an immune response against such steady-state persistent antigens could thus result in immunopathology and be detrimental to the host. As a result, antigen recognition by naïve peripheral $CD8^+$ T cells in a non-inflammatory context typically fails to result in effector differentiation, and even if the responding cells do acquire effector characteristics, their functions are greatly muted compared to those adopted during the response to an active infection. These regulatory outcomes are imposed on the self-reactive $CD8^+$ T cells through tolerogenic interactions with DCs, and suppression of activation by regulatory T cells (Tregs) (212,213). Similar peripheral tolerance mechanisms are responsible for limiting aberrant $CD8^+$ T cell responses to benign foreign antigens derived from food (214), gut bacteria (215) and a growing fetus (216).

Current understanding of tolerance mechanisms against peripheral self-antigens has stemmed from studies of transgenic animal models with tissue-restricted expression of model self-antigens. In particular, well-characterised model antigens derived from viral proteins such as Haemagglutinin (HA) from Influenza virus (217,218), Glycoprotein (GP) from the common mouse pathogen Lymphocytic Choriomeningitis Virus (LCMV) (219) or well defined animal proteins including chicken ovalbumin protein (OVA) (220–222) have been extensively used. These and other model

antigens were genetically engineered for transgenic expression under the control of tissue-specific promoters, such that they would be recognised by the immune system as surrogate “self-proteins” in their respective tissue of expression. The TCRs that recognised immunodominant epitopes within these model antigens were typically well characterised, with TCR transgenic mice often available for the specific model antigen of interest. These included $CD8^+$ TCR transgenic mice specific for well characterised MHC I peptides, such as “Clone 4 (CL4)” mice bearing $CD8^+$ T cells specific for the $HA_{533–541}$ peptide (223), “P14” mice with T cells specific for the GP_{33-41} peptide (224), and “OT-I” mice with cells specific for the $OVA_{257-264}$ peptide (225). The focus on peripheral, tissue-restricted antigens within these models was because many of these mouse strains were generated prior to the discovery of AIRE; as such, tolerance against tissue-restricted antigens was thought to occur solely in the periphery. The Rat Insulin Promoter (RIP) was used in many transgenic mice as it limited expression of the model antigen to the insulin-producing islet β cells of the pancreas (220,226,227). If the responding T cells mounted an effector response against the model antigen, it would result in destruction of the islet β cells and induction of diabetes, which was easily measured through high glucose levels in the urine (219,228,229). This was a useful model to study $CD8^+$ T cell tolerance in a disease-relevant context, as $CD8^+$ T cells are one of the major drivers of autoimmune diabetes (230). Multiple other models have utilised tissue promoters to study $CD8^+$ and $CD4^+$ T cell tolerance by limiting expression of model antigens to locations such as enterocytes in the intestinal tissue (221), lung parenchyma (218) and CNS (231,232), allowing study of self-tolerance mechanisms in relevant disease areas of intestinal bowel disease, lung inflammation and MS. However, not all tissue promoters were restricted to peripheral expression in the targeted tissue. Some promoters, including RIP, also elicited ectopic expression of antigen in the thymus, which led to central tolerance and thymic deletion of the endogenous antigen-specific T cells (220). Hence, depending on the model system used, endogenous T cells specific for the peripheral model antigen were either present in the mice and could be studied directly, or TCR transgenic T cells were adoptively transferred into the periphery to generate a population of model self-reactive T cells for further study. The multiple factors determining the presence or absence of endogenous T cells specific for the various model antigens within each model will be explained in later sections. While the different transgenic models utilised the same fundamental genetic tools,

the tissue-specific promoter, model antigen and strength of antigen expression varied between mouse strains. These differences translated into different experimental outcomes, with the above studies often observing one of three different $CD8^+$ T cell tolerance outcomes: ignorance, anergy or deletion (233,234). These tolerance outcomes are are largely guided by how T cells interact with steady-state DCs bearing self-antigen.

Regulation of peripheral tolerance by dendritic cells

Peripheral tolerance in $CD8^+$ T cells is typically induced by presentation of self-antigen by APCs in the absence of infection or pathology. In the steady state, DCs are in a quiescent state however they still continuously survey the environment for antigens. In particular, the $CD8\alpha^+$ subset of DCs actively captures apoptotic cells in the steady state and cross-presents captured proteins to self-reactive $CD8^+$ T cells in the lymph nodes (235–237). The role of DCs in antigen cross-presentation has also been highlighted in transgenic tolerance models such as RIP-mOVA and RIP-OVA^{hi}, where expression of membrane bound or soluble OVA respectively is limited to the pancreas, yet $CD8^+$ T cells specific for OVA peptide are able to recognise antigen in the draining pancreatic lymph nodes due to cross-presentation by the $CD8\alpha^+$ DC subset (238). DCs are extremely crucial to steady state tolerance induction in $CD8^+$ T cells, as several *in vivo* and *in vitro* experiments have shown loss of DCs through targeted depletion (239) or specific loss of cross-presentation capacity in the DCs results in loss of $CD8^+$ T cell tolerance (237). The importance of DCs in inducing tolerance was further illustrated by the Ins-HA transgenic model, where the model antigen Haemaglutinnin (HA) from the Influenza virus is expressed under the RIP locus. Infection of adult mice with Influenza did not result in diabetes induction (240), as all HA-specific $CD8^+$ T cells were tolerised by steady state DCs. However, when these experiments were carried out at 3 weeks of age, prior to the appearance of cross-presenting DCs within the pancreatic lymph nodes, Influenza infection led to diabetes induction due to the presence of endogenous HA specific $CD8^+$ T cells (241). This experiment highlighted the crucial role of cross-presenting DCs in inducing peripheral tolerance in $CD8^+$ T cells. Thus, DCs not only have the capacity to license T cells during infection, they also carry out the important process of inducing tolerance in naïve self-reactive T cells in the steady state.

How are DCs able to play critical roles in both peripheral tolerance and the priming of an effector T cell response to infection? This plasticity in DC function is due to the state, or "phenotype", of DCs in these two contexts. During an active infection, the presence of inflammatory cytokines, PRR activation and DC conditioning by activated $CD4^+$ T cells results in the transition of DCs into an immunogenic state, as described earlier. This state is characterised by upregulation of co-stimulatory receptors, cytokine production and, in the case of migratory DCs, enhanced migration to the lymph nodes for activation of $CD8^+$ T cells. In contrast, in the steady state, DCs sampling apoptotic tissues are not activated by PRR or inflammatory signals and assume a default "tolerogenic" state, where they lack expression of factors required to prime effector differentiation. Early experiments on tolerance induction by DCs correlated tolerogenicity with DC "maturity". Steady-state DCs often express lower levels of costimulation and MHC, which is termed an "immature" state, and PRR engagement triggers DC "maturation" through up-regulation of co-stimulation and MHC expression (35,242). Certain studies which showed that antigen targeted to immature DCs caused tolerance induction, lead to the assumption that the outcome of a DC-T cell interaction was linked to DC maturity (243,244). However, several publications have indicated that mature DCs are capable of tolerance induction (245,246), and recent transcriptomics studies found that an equal number of genes are differentially expressed after the maturation of both immunogenic and tolerogenic DCs *in vivo* (247). Upon "maturation", DCs in both immunogenic and tolerogenic states upregulate antigen presentation pathways, migrate to the draining lymph nodes while simultaneously down-regulating further antigen processing and phagocytosis pathways. Collectively, these data challenge the assumption that DC maturation predicts immunogenicity.

While the exact molecular features that define tolerogenic versus immunogenic DCs are still poorly characterised, there are a number of known features of a tolerogenic DC-T cell interaction. In particular, DC mediated tolerance induction is typically dependent on inhibitory receptors such as PD-1 and CTLA-4 (248–250). Expression of PD-L1 and other inhibitory receptors is not exclusive to the tolerogenic DCs, as immunogenic DCs likely upregulate these inhibitory receptors given their recently discovered roles in effector differentiation (251,252). However, it is likely the sum of the activatory and inhibitory interactions at the immunological synapse that determine

the outcome of interaction (66). Inhibitory receptors such as PD-1 and CTLA-4 induce negative outcomes through several mechanisms including inhibition of downstream signaling in T cells (covered in later section), and competing with other co-stimulatory receptors. While some reports have indicated a role for PD-1 and CTLA-4 in reducing the stable interaction time between the T cell and tolerogenic DC (249,250), which could lead to tolerance induction, another study indicated equal interaction times of the DC-T cell synapse formed in immunity and tolerance induction *in vivo* (253). Thus, there is conflicting evidence of the role of these receptors in reducing dwell time between the T cell and DC interaction. Therefore, while the precise molecular pathways are still unclear, the differentiation status of DCs, the nature of their interactions with naïve T cells and a number of other extrinsic factors (covered in later sections) cumulatively determines whether antigen recognition leads to tolerance or immunity. When $CD8^+$ T cells are tolerised, there are multiple differentiation paths that the responding self-reactive T cell can adopt, with the outcome primarily dependent on the amount of antigen presented by the tolerogenic DC.

1.2.3: $CD8^+$ T cell tolerance outcomes

$CD8^+$ T cell tolerance outcomes observed in most transgenic mouse models of tolerance can be classified into three groups – ignorance, anergy or deletion (Figure 1.2). As discussed below, a large body of evidence suggests that the choice between these outcomes is determined by the dose of self-antigen presented by the DC. T cell "ignorance" occurs when self-reactive T cells remain in a naïve state due to self-antigen presentation levels that lie below the activation threshold, while anergy and deletion occur when self-antigen is expressed at sufficient levels to provoke a response. When a response to tolerogenic self-antigen does occur, the self-reactive T cells undergo either anergy or deletion depending on whether high or low levels of self-antigen are encountered respectively. Examples of these three outcomes, their hallmarks and the experimental data supporting these conclusions are discussed below.

Ignorance of self-reactive CD8$^+$ T cells

"Ignorance" of self-reactive CD8$^+$ T cells was a concept derived from experiments indicating that CD8$^+$ T cells were not actively tolerised against their antigen in the steady state and, as a result, remained in a naïve or "ignorant" state. Ignorance was first observed in RIP-GP transgenic mice, which express LCMV GP as a neo-self-antigen within pancreatic islet β cells and soluble GP protein could be detected by histology of the pancreas (219). In RIP-GP mice, neither the endogenous GP-specific T cells, nor transferred CD8$^+$ MHC I-restricted TCR transgenic P14 cells, were tolerised against the GP antigen (219,254). Upon infection with LCMV, which lead to presentation of GP peptides in an inflammatory context, endogenously generated GP-specific effector CD8$^+$ T cells formed from the naïve GP-specific population of cells attacked the pancreatic tissues expressing the viral protein, resulting in induction of diabetes (219,229). Similarly, the ODC-OVA model expressing OVA in the oligodendrocytes resulted in ignorance of the responding OVA-specific CD4$^+$ and CD8$^+$ T cells (231), and hence bystander LCMV-OVA or LM-OVA infections resulted in CNS immunopathology (255). These early studies suggested that self-tolerance is maintained through an inability of T cells to access antigens sequestered in tissues.

Subsequent studies in other model systems challenged this paradigm. In particular, it was found that the model self-antigen OVA was constitutively presented to OVA-specific OT-I T cells in the draining pancreatic lymph node within RIP-mOVA mice, which express a transmembrane form of OVA (220). Transferred OT-I cells were subsequently found to be deleted after activation in the draining pancreatic lymph nodes of RIP-mOVA mice (256). Similar observations were made around the same time in transgenic mice expressing the model antigen Tag under control of RIP, and Tag-specific CD4$^+$ T cells were deleted within 2-3 weeks of activation (257). Thus, the results of these models were in stark contrast to that of the RIP-GP model. This discrepancy was subsequently explained through the study of two lines of RIP-OVA mice expressing different levels of soluble OVA antigen (258). The lines were named according to the levels of antigen expression, with RIP-OVA^{hi} mice expressing high OVA levels, and RIP-OVA^{lo} mice expression low OVA levels. Direct quantitation of OVA protein levels in the pancreatic tissue indicated at least a 33 fold difference in OVA expression between these two mouse lines, with RIP-OVA^{hi} mice expressing ~1ng OVA per µg pancreatic protein versus <0.03ng OVA/µg in RIP-OVA^{lo} mice.

While OT-I cells in the RIP-OVA^{hi} mice were activated in the pancreatic lymph nodes in the steady state and underwent deletion, OT-I cells in RIP-OVA^{lo} mice remained in a naïve or ignorant state (259). An important point to note is that, while OVA expression in RIP-OVA^{lo} mice was not sufficient for presentation in the draining LN, the protein expression level was sufficient to enable killing of islet cells and diabetes induction by *in vitro* activated OT-I CTL (259). As such, OVA expression in the pancreas of RIP-OVA^{lo} mice was at a physiologically relevant level to enable CTL-mediated autoimmunity, meaning that this model phenocopied the results obtained within the RIP-GP model. Thus, this result established the concept that antigen dose determines whether self-reactive CD8$^+$ T cells ignore self-antigen, or respond in a manner that leads to deletion or anergy.

Since ignorant cells are not anergised or deleted against their cognate antigen in the steady state, they can respond normally to their cognate antigen (or a foreign antigen that bears homology to their cognate antigen) if it is presented in an immunogenic context. While it possible that ignorant self-reactive cells are largely low affinity due to partial thymic selection, multiple studies have shown that low affinity self-reactive cells are capable of differentiating into pathogenic effector cells and have the potential to cause autoimmunity if they are inadvertently primed in the context of an infection (101,260). Therefore, self-reactive CD8$^+$ T cells that are ignorant likely pose a risk to the host, as inadvertent activation of these cells by pathogen molecular mimicry of self-antigens, or by recognition of their self-antigen in an immunogenic context, could lead to autoimmunity. Nevertheless, pathways such as anergy and deletion do exist to inactivate self-reactive cells in the periphery, and these processes likely prevent the majority of self-reactive cells from participating in future immune responses. These processes will be discussed in detail within the following sections.

Influence of antigen signals on tolerance outcomes within CD8$^+$ T cells

T cells that are actively tolerised in the periphery by antigen recognition on tolerogenic DCs undergo two different cell fates depending on the dose of antigen encountered. High doses of self-antigen result in “anergy”, whereby the responding CD8$^+$ T cells survive in a non-responsive state resistant to further stimulus. On the other hand, low doses of self-antigen result in apoptotic death of the responding T cells in a process termed “deletion”. While anergy and deletion have been observed

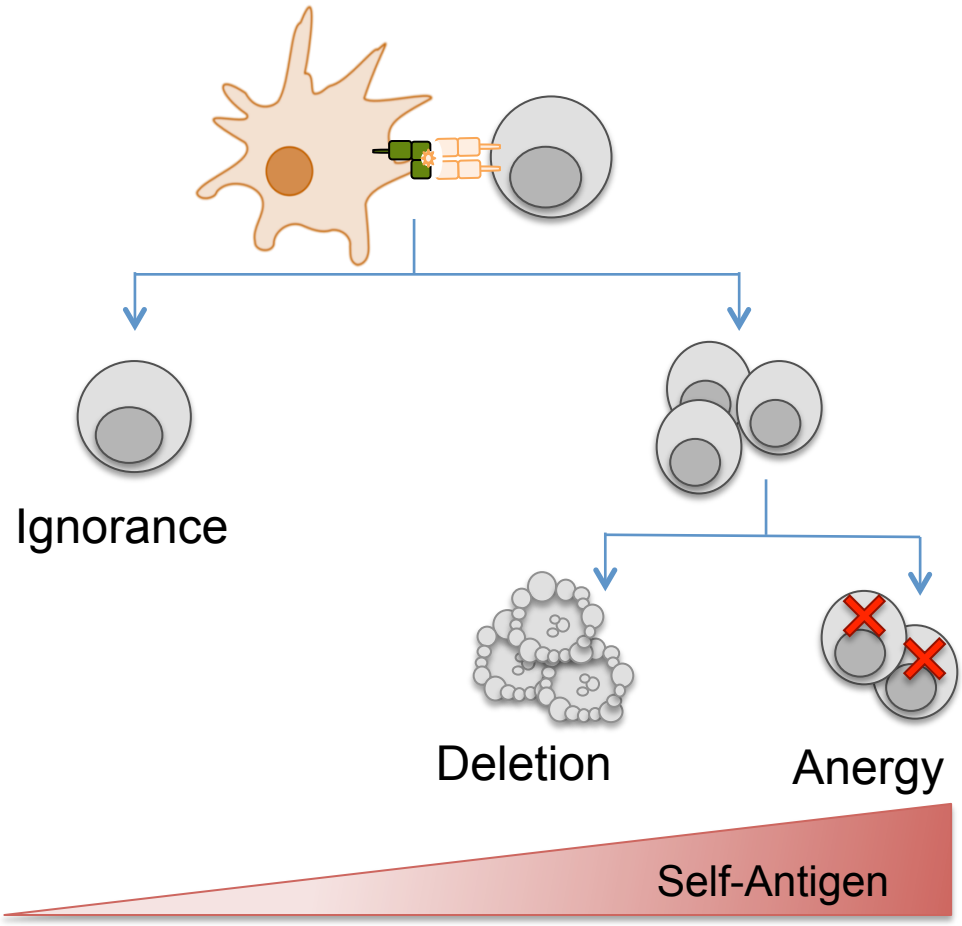

Figure 1.2: Multiple fates of CD8⁺ T cell tolerance: Steady state tolerogenic DCs present self-antigen to naïve self-reactive T cells. This interaction, depending on the dose of self-antigen presented, can result in different fates for the responding CD8⁺ T cells. If the dose of self-antigen presented is too low for T cell engagement, then ignorance occurs, where the self-reactive T cells remain in a naïve state. If the antigen dose is high enough to engage a response, the cells will proliferate, and then can either undergo deletion by BIM-mediated apoptosis, or can persist in an anergic state, where the cell's TCR signaling pathways become non-responsive to further stimulus. Deletion occurs when intermediate levels of self-antigen are presented, while anergy occurs when high antigen levels are encountered.

in multiple transgenic models, the importance of these processes in maintaining tolerance within endogenous self-reactive $CD8^+$ T cells remains largely unknown.

Antigen dose was initially shown to determine whether tolerance induction lead to anergy or deletion in early studies using transgenic $CD8^+$ T cells specific for H-Y antigen (261). The response of H-Y specific T cells was studied in irradiated bone marrow chimeras reconstituted with varying ratios of male and female cells, thus altering the amount of H-Y male antigen present in the mice (261). As the amount of male antigen was increased, there was a proportional increase in the percentage of anergic H-Y specific cells while the amount of deletion was inversely proportional to the percentage of male antigen. This dependence on antigen dose has been confirmed in models of peptide-induced tolerance, where delivery of self-peptide without adjuvant resulted in either anergy or deletion of the responding T cells depending on the dose of peptide injected (262,263). Similar results were found when the antigen dose was kept constant, but the affinity for antigen was varied; in this context low affinity interactions lead to deletion over anergy (263). Collectively, these data suggest that the TCR signal strength encountered during tolerance induction determines whether T cells persist in an anergic state or are deleted by apoptosis. It is important to note that anergy and deletion are not mutually exclusive as some amount of deletion of responding T cells does occur in anergy models (264).

Cells undergoing anergy and deletion share some hallmarks, including proliferation upon antigen recognition, a failure to acquire effector functions, and reliance on chronicity of self-antigen for optimal tolerance induction. Unlike their thymic counterparts, self-reactive T cells in the periphery typically undergo a few rounds of division within *in vivo* tolerance models before they undergo anergy or deletion (256,265). The level of proliferation is dependent on the amount of antigen encountered, although the number of cell divisions that a cell undergoes during tolerance induction does not affect the efficacy of the tolerance process (266,267). In both anergy and deletion, the proliferating cells fail to acquire effector functions. This occurs at the level of both cytokine production, where cells have a defect in their capacity to produce IFNγ upon restimulation (265), and cytotoxicity, where tolerant cells are unable to kill targets, likely due to a defect in GZMB up-regulation (265,268). Finally, cells undergoing anergy and deletion rely on continuous interactions with

presented self-antigen to maintain their tolerant states. After a period of rest in a host that lacks expression of their specific antigen, tolerised cells are able to regain function and proliferative capacity, meaning that continuous antigen presence is required to enforce the tolerant state. Adoptive transfer of anergic T cells into antigen-free hosts allowed these cells to be activated upon subsequent restimulation (269). Similar experiments conducted in the InsHA tolerance model showed that transfer of cells undergoing deletion into antigen-free hosts allowed the cells to both persist, and differentiate into effector cells upon infection with Influenza (270). Repeated injections of tolerogenic HA peptide antigen into the "antigen-free" recipients was required to achieve complete deletion of the transferred cells (270). Hence, tolerance is highly dependent on the chronicity of the antigen; this is likely an additional strategy for self/non-self discrimination, as a hallmark of a self-antigen will be sustained expression. Existence of tolerance processes in the steady-state imply that most self-reactive T cells present in the periphery would be tolerised against quiescent and chronic self-antigens before any potential bystander activation of these cells during a pathogenic infection. Thus, anergy and deletion likely play important roles in the maintenance of tolerance, and the features of these states are considered in more detail below.

Anergy

The classical definition of anergy was derived from *in vitro* experiments in the 1990's, where culture of $CD4^+$ T cells in the presence of anti-CD3 antibodies but without CD28 co-stimulatory signals resulted in the shut down of IL-2 production and proliferation upon restimulation due to the acquisition of specific deficiencies in ERK signaling (71,72,271,272). This traditional definition of anergy has been adapted over the years to describe non-responsiveness of $CD4^+$ and $CD8^+$ T cells in both *in vitro* and *in vivo* models (273). Early studies of $CD8^+$ T cell anergy *in vivo* involved delivery of cognate peptides in the absence of adjuvant. Efforts to vaccinate the mice with GP33 peptide without adjuvant resulted in a deficiency in the endogenous response to LCMV infection, suggesting that the endogenous repertoire had been tolerised (274). Other *in vivo* anergy models were pioneered using peptides from model antigens such as OVA and HA (262,275) or super antigens (276). *In vitro* and *in vivo* models of $CD8^+$ T cell anergy have also shown a "split anergy" phenotype, whereby cells are able to produce granzymes and perforin and kill targets, but lack cytokine

production capacity (221,277). One of the hallmark features of anergic self-reactive $CD8^+$ T cells is diminished ERK phosphorylation (pERK), which is possibly due to the multiple negative regulatory pathways that are activated in anergic cells (71,72,272). Another hallmark of anergy is long-term persistence of cells, with anergy maintenance dependent upon continuous antigen encounter. The molecular pathways responsible for the establishment and maintenance of anergy will be discussed in the next section.

Deletion

Deletion of self-reactive $CD8^+$ T cells was first documented in H-Y specific T cells in bone marrow chimera experiments expressing lower ratios of male bone marrow (261). Following this study, deletion of self-reactive $CD8^+$ T cells has been observed in multiple transgenic models, such as the InsHA (240), RIP-mOVA (256) and RIP-OVA^{hi} (259) models. Antigen specific transgenic T cells transferred into these models undergo proliferation in the draining lymph node after encountering antigen, and upregulate the activation markers CD44 and CD69 (256,265,268). However, as noted above, the tolerised $CD8^+$ T cells in RIP-mOVA and RIP-OVA^{hi} failed to differentiate into effector cells and underwent apoptosis through BIM upregulation (278). Cells undergoing deletion also do not have a block in TCR signaling unlike their anergic counterparts, and maintain pERK levels upon restimulation (262,268). Cells undergoing deletion up-regulate many of the genes linked to anergy induction (268). The functional relevance of these similarities is unclear, but it suggests that deletion and anergy maybe molecularly similar despite differences in outcome. It is thus unknown whether anergy and deletion can be molecularly separated as differentiation states, or whether they are essentially the same process, with the cells merely kept alive by antigen in anergy models.

1.2.4: Molecular regulation of $CD8^+$ T cell tolerance

Diverting $CD8^+$ T cells down the fates of anergy or deletion requires unique molecular changes that limit T cell function, prevent effector differentiation and (in some cases) induce death. Although the majority of the studies on the molecular circuitry of tolerised T cells have focused on $CD4^+$ T cell anergy, some of these pathways overlap with $CD8^+$ T cell tolerance. In the following sections, several aspects of

molecular regulation in T cell tolerance are highlighted and their role in $CD8^+$ T cell anergy and deletion discussed.

Cell extrinsic regulators of tolerance

Apart from DCs, which are crucial in the induction of tolerance in self-reactive $CD8^+$ T cells, several other factors in the steady state environment can also contribute to the induction and maintenance of tolerance in $CD8^+$ T cells. These include inhibitory receptor interactions, suppressive cytokines in the environment, lack of $CD4^+$ T cell help and involvement of regulatory T cells. All of these factors collectively contribute to inducing and maintaining suppression of self-reactive $CD8^+$ T cells.

Inhibitory receptors

The DC-T cell immunological synapse is dominated by inhibitory receptor interactions, which are important in inducing tolerance in the T cells. In particular, factors such as PD-1 (279,280), CTLA-4 (248,281), LAG3 (282) and TIM3 (283,284) have been implicated in T cell tolerance induction. PD-1 and CTLA-4 are both members of the B7 family of receptors, which includes CD28, however these receptors inhibit rather than activate T cells (285). Both CTLA-4 and PD-1 expression are induced on the T cell as part of a negative feedback circuit downstream of TCR signaling (286,287). While CTLA-4 inhibits activation by outcompeting CD28 for binding to CD80 and CD86 (288,289), PD-1 inhibits TCR and/or CD28 signaling upon binding separate ligands, PD-L1 (290) and PD-L2 (291), on the DCs and tissues (289,292). The importance of these pathways in the maintenance of self-tolerance has been observed in knockout mouse models; *Pdcd1-/-* (293,294) and *Ctla4-/-* (295) mice are characterised by severe widespread autoimmunity, inflammation and lupus-like disease. Subsequent studies have suggested that these pathways directly control $CD8^+$ T cell tolerance. OT-I cells lacking PD-1 were able to overcome deletional tolerance induction in RIP-OVA^{hi} mice, differentiate into effector cells and induce diabetes (279). However, PD-1 only appears to be involved in the induction but not maintenance of tolerance as anergic cells were resistant to PD-L1 blockade at later time points (296). CTLA-4 on the other hand has crucial functions in $CD4^+$ T cell tolerance (281,297) and Treg suppression (298,299), but was variably required in some $CD8^+$ T cell tolerance models *in vivo* (248) and not others (249,300).

LAG3 is a CD4-related molecule that binds to MHC II, and its expression is upregulated after T cell activation (301). $CD4^+$ T cells deficient in LAG3 exhibited reduced expansion to super antigen and peptide stimulation, although they displayed greater production of IL-2 and IFN-γ (302), indicating a regulatory role in T cell function. LAG3 deficient $CD8^+$ T cells accumulated in the C3-HA transgenic mice, which express HA as a self-antigen in the lungs, and caused inflammation in the lungs, indicating that LAG3 was crucial for maintaining tolerance in $CD8^+$ T cells in this model (282). TIM3 is important in regulating $CD4^+$ T cell tolerance (283,284) and has been postulated to bind multiple ligands such as GALECTIN-9 (303) and CEACAM-1 (304). However it's role in regulating $CD8^+$ T cell tolerance has not been investigated.

$CD4^+$ T cells

$CD4^+$ T cells play an important role in the activation of effector $CD8^+$ T cells through production of cytokines, and providing the "help" signal CD40L to "license" DCs for T cell activation (305,306). $CD4^+$ T cells themselves are activated by presentation of antigens on MHC II of professional APCs and require similar activation signals to those described above for $CD8^+$ T cell activation (307). Upon activation of $CD4^+$ T cells, they are able to produce high levels of cytokines, such as IL-2 and IFNγ, which can directly influence $CD8^+$ T cell activation (307). Importantly, though, $CD4^+$ T cells can provide signals to DCs, such as CD40L, which binds to CD40 on DCs that can support activation of the DC into an immunogenic state (308,309). $CD4^+$ T cell tolerance to self will mean that "help" for self-antigens is unlikely to normally occur. However, when $CD4^+$ "help" is provided in tolerance models, it is often sufficient to cause a breach in $CD8^+$ T cell tolerance. For example, provision of $CD4^+$ T cell help to RIP-OVA^{hi} mice led to a break in tolerance of OT-I cells and diabetes induction, which was partially mediated through CD40 signals (310). A similar break in $CD8^+$ T cell tolerance was observed in experiments supplementing iFABP-OVA mice with CD40 antibody, which mimics the DC "licensing" signal provided by $CD4^+$ T cells without the cytokine production (311). Hence, tolerance within the $CD4^+$ T cell compartment helps to maintain $CD8^+$ T cell self-tolerance.

Tregs, a regulatory lineage of $CD4^+$ T cells, play an equally important role in actively maintaining tolerance. Tregs enforce tolerance induction through a variety of

mechanisms, and the rapid autoimmune disease that ensues upon acute Treg depletion illustrates the importance of Tregs in the maintenance of self-tolerance (312–314). However, in terms of their role in $CD8^+$ T cell tolerance, Tregs perform the opposite role to conventional $CD4^+$ T cells by acting as a "sink" for IL-2. Through expression of the high affinity IL-2R, or CD25, Tregs "soak up" the IL-2 in the environment. Depletion of Tregs in the CD11c-OVA model, which constitutively expresses OVA in $CD11c^+$ DCs, resulted in an IL-2-dependent breach in $CD8^+$ T cell tolerance against self-antigen (315). Tregs also inhibit immune responses through actively inhibiting DC immunogenicity (316), and by producing inhibitory cytokines such as IL-10 and TGF-β (317–319). However, there is limited understanding of whether these mechanisms of immunosuppression directly contribute to the maintenance of $CD8^+$ T cell tolerance.

Cytokines

T cell homeostasis and phenotype is highly dependent on cytokines in the environment. Naïve T cells require IL-7 signals for their survival, however IL-7R is downregulated by cells undergoing anergy and deletion meaning that this cytokine can no longer sustain these populations (234,268). While there is a lack of inflammatory cytokines in steady state, the presence of these cytokines can reverse tolerance in a non-antigen specific manner. In particular, exogenous IL-2 treatment disrupts $CD8^+$ T cell tolerance and results in autoimmune disease (320). While a number of inhibitory cytokines exist, such as IL-10 and TGF-β, there is limited understanding of their roles in the $CD8^+$ T cell tolerance process.

Cell intrinsic regulators of tolerance

The above extrinsic factors influence the intrinsic changes within $CD8^+$ T cells, which ultimately affect the outcome of the immune response. This section considers the changes that occur within a T cell to enforce a tolerised state, including what is known about the similarity and differences between the intrinsic gene program triggered in deletion and anergy.

T cell signaling

A central characteristic of anergic cells is an inability to signal effectively via their TCR. While signaling deficiencies within *in vitro* anergy models are largely restricted

to blocks in pERK (71,72) and mTOR signaling (321,322) , the block in signaling appears more proximal and extensive within *in vivo* anergy models (262,323–325). These blocks in TCR signaling are achieved, at least in part, through up-regulation of phosphatases and ubiquitin ligases. Phosphatases are either transcriptionally up-regulated, or recruited through inhibitory receptor signaling, and dampen TCR signaling by dephosphorylating key signaling molecules. For example, PTPN2, a constitituvely active phosphatase crucial for dampening TCR signaling through dephosphorylation of LCK, and FYN, was shown to play an important role in maintaining $CD8^+$ T cells tolerance in the RIP-mOVA mice (326). Furthermore, inhibitory receptor signaling through PD-1 and CTLA-4, which is variably required to enforce tolerance as discussed above, results in recruitment of phosphatases such as SHP-1, SHP-2 and PP2A to the immunological synapse and further dampens the T cell signaling process (327–330). Apart from phosphatases, kinases such as DAG kinases (DGK α and ζ) were shown to be upregulated specifically in tolerance and their absence allowed the $CD4^+$ T cells to be resistant to anergy induction (331,332). DAG kinases phosphorylate DAG into phosphatic acid, which prevents induction of Ras signaling pathway and ERK phosphorylation downstream of TCR (332). As cells undergoing deletion maintain TCR signaling, it is also not clear what the potential role of *Dgkz* would be in deletional tolerance. While *Dgkz* was upregulated in $CD8^+$ T cells undergoing deletion, it's importance in the deletion process is unknown (268) and furthermore there has not been other studies confirming the role of this kinase in maintaining $CD8^+$ T cell anergy. However, it's role in other negatively regulated $CD8^+$ T cell contexts such as in tumour-sepcific T cell responses has been elucidated in multiple studies showing tumour specific $CD8^+$ T cells lacking DGK proteins resulted in enhanced tumour killing (333–335). Thus, DGK proteins have been defined as negative regulators of $CD8^+$ T cell function in other contexts. In summary, inhibition of TCR signaling through phosphatase and kinase-mediated pathways likely plays an important role in limiting $CD8^+$ T cell differentiation within tolerance models.

Another mechanism by which suppression of T cell signaling, and hence impaired effector differentiation, is maintained, is through active targeting of signaling components for degradation by the proteasome. A group of proteins called ubiquitin ligases carry out this process by targeting specific signaling molecules for ubiquitination, a process where ubiquitin molecules are covalently attached to

proteins to “tag” them for subsequent proteasomal degradation (336). The role of ubiquitin ligases in T cell tolerance was first revealed in microarray studies of anergic $CD4^+$ T cells, where increased levels of the ubiquitin ligase *Cbl-b*, *Itch* and *GRAIL* during anergy enforced hyporesponsiveness through degradation of PLC-γ, an important component of the TCR signaling pathway and subsequent poor immunological synapse formation (337). CBL-B has been shown to be crucial in limiting proliferation of self-reactive $CD8^+$ T cells *in vivo* against high dose self-antigen (338). Multiple other ubiquitin ligases have been revealed as playing a crucial role in $CD4^+$ T cell anergy and these include ITCH (339), GRAIL (340), and DELTEX (341). These factors degrade different signaling components downstream of TCR signaling, thus inhibiting further stimulation, however their role in $CD8^+$ T cell tolerance is less well characterised. Ubiquitin ligases also rely on other proteins called adaptors for their function. One such adaptor molecule called NDFIP1 was shown to bind and control the function of both NEDD4 and ITCH. Mice with mutations in NDFIP1 developed severe dermatitis due to aberrant expansion of $CD4^+$ T cells (342). *Ndfip1* deficient $CD4^+$ T cells are resistant to *in vitro* anergy (343), and, within *in vivo* tolerance models, failed to undergo cell cycle exit and aberrantly differentiated into Th2 cells (344). While extensive $CD8^+$ T cell activation is also seen in *Ndfip1* deficient mice, this phenotype appears cell extrinsic, and it is thus not known whether NDFIP1 also intrinsically contributes to $CD8^+$ T cell tolerance.

Transcriptional control of tolerance

While it was evident within *in vitro* anergy models that cells stably up-regulated factors that limited TCR signaling and differentiation, the transcriptional basis of this process was not well understood until a pioneering study demonstrating that the TF NFAT is critically required for *in vitro* anergy induction (345). In support of the critical role of NFAT in programming an anergic state, induction of calcium signaling alone by ionomycin treatment is sufficient to induce anergy (71,72,346). It was subsequently found that, in the absence of AP-1 activation downstream of MAPK signaling, NFAT adopts an inhibitory role and activates a unique gene network that leads to suppression of TCR signaling (337,345,347). In early efforts to characterise the molecular profile of cells undergoing anergy, *in vitro* generated anergic $CD4^+$ T cells were compared to *in vitro* generated effector $CD4^+$ T cells. The microarray

results revealed the presence of NFAT and upregulation of a unique transcriptional network driven by NFAT (337).

NFAT activation in the absence of AP-1 causes formation of NFAT homodimers that target different genes to suppress T cell function (345,347). NFAT interacts preferentially with AP-1 over itself, but in the absence of AP-1 forms inhibitory homodimers. While NFAT directly binds to the promoters of key anergy associated genes (345), much of the NFAT-mediated anergy program occurs indirectly, through induction of the TFs *Egr2* and *Egr3*. EGR2 and EGR3 have been described as master regulators of tolerance, with both *Egr2*$^{-/-}$ and *Egr3*$^{-/-}$ cells unable to become anergic, in part due to deficiencies in *Cblb* and *Dgka* expression (348,349). While the roles of *Egr2* and *Egr3* have not been directly validated in CD8^{+} T cell anergy or deletion, a microarray analysis of OT-I cells undergoing deletion in RIP-OVA^{hi} mice (268) revealed upregulation of both *Egr2* and *Egr3* along with its key target genes (*Cblb, Dgkz*) during deletional tolerance.

Survival and death

One of the key differences between CD8^{+} T cells undergoing anergy and deletion is differential survival, and it is unclear which pathways in these cells control the decision between survival and death. Key anergy-linked factors are up-regulated during deletion (268), and although there is some degree of contraction observed in cells undergoing anergy, most of them are able to persist for long periods of time while cells undergoing deletion undergo cell death. While the molecular basis of this differential survival is unclear, it is known that death during deletion is dependent on the pro-apoptotic protein BIM. *Bim* transcripts are induced to greater levels during tolerance relative to cells undergoing effector differentiation (268), and genetic loss of *Bim* in OT-I cells led to a block in cell deletion in RIP-mOVA and RIP-OVA^{hi} models of tolerance, although the cells did not cause diabetes suggesting that effector differentiation was not rescued (278). These data are consistent with results from CD4^{+} T cell tolerance models, in which blocking deletion lead to anergy within the surviving cells (350).

Given that death during both peripheral deletion and effector cell contraction is *Bim* dependent (129,278), it is unknown whether the pathways that induce *Bim*-

dependent death are similar or distinct in tolerance versus contracting effectors. While transcriptional induction of *Bim* occurs after OT-I cells receive tolerogenic signals in RIP-OVA^{hi} mice (268,278), it is not known which TFs are responsible for this gene induction process, and whether they differ from the factors required for BIM-dependent death of effector cells. More insight into the transcriptional pathways controlling *Bim* induction during deletion is required to understand why cells are either deleted or survive to persist as anergic cells. Furthermore, understanding the differences in death induction in tolerance versus immunity may provide therapeutic approaches to target self-reactive CD8$^+$ T cells without causing widespread immunosuppression by also affecting the effector-memory response to infection.

In summary, the current understanding of CD8$^+$ T cell tolerance has been built from studies in several transgenic animal models, whereby the cells can undergo different fates of ignorance, anergy or deletion. Further work is required to thoroughly characterise the molecular regulation of CD8$^+$ T cell tolerance and determine whether anergy and deletion are molecularly separable states.

1.3: CD8$^+$ T cell exhaustion

1.3.1: Overview of CD8$^+$ T cell exhaustion

As outlined in Section 1.1, the primary aim of the CD8$^+$ T cell response is to clear intracellular pathogens from host tissue. This is successfully achieved in most instances through differentiation of naïve pathogen specific CD8$^+$ T cells into potent cytotoxic effector cells, and formation of antigen-independent memory cells for combating future reinfection by the pathogen. However, the CD8$^+$ T cell response against chronic pathogenic infections or cancers does not follow the effector-memory differentiation pathway observed in response to acute infection. Persistence of antigen and inflammatory signals drive the CD8$^+$ T cell response to become "exhausted", a process characterised by a gradual loss of effector functions and defective antigen-independent memory cell formation. The blunted T cell responses triggered by chronic stimulation contribute to disease progression, and are thus an area of intense interest. Studies over the last few decades have thoroughly characterised the cellular and molecular features of exhaustion, revealing that exhaustion is a unique differentiation state governed by altered expression of surface receptors, and distinct transcriptional and epigenetic programs.

CD8$^+$ T cell exhaustion was first described in mice chronically infected with the natural mouse pathogen LCMV (351,352). The long-term viremia in chronically infected mice was accompanied by blunted responses within the effector CD8$^+$ T cells, which lost cytokine production capacity over time and were in some cases completely deleted from the repertoire (351–353). Subsequently, similar functional deficiencies in CD8$^+$ T cell responses were observed in several human chronic infections, such as during HIV (354,355), Hepatitis B (356) and C (357,358) viral infections, as well as within cancers (359–361). Research efforts to study the underlying molecular and cellular factors driving exhaustion have led to both a greater understanding of the exhaustion process, and the discovery of drug targets for reversing exhaustion, such as the inhibitory receptors PD-1 (20) and CTLA-4 (362). Blockade of PD-1 and CTLA-4 on exhausted CD8$^+$ T cells can rescue effector CD8$^+$ T cell function and reduce disease burden in both pre-clinical animal models of SIV (363) and HIV (364,365) infection, and within cancer patients in the clinic (366–

368). These results imply that exhausted cells do not irreversibly lose function, but instead can be revived by selectively targeting certain molecular pathways. Hence, a better understanding of the factors that contribute to exhaustion is critical to not only delineating the basic biology of this process, but also in the development of more efficacious therapeutic strategies for the treatment of cancer and chronic infection.

Much of the current molecular and cellular understanding of exhausted cells has been derived from studies in the chronic LCMV mouse model of infection, with validation often followed in human disease settings (369). Along with the benefits of animal work, a primary reason for the continued use of the LCMV infection model has been the ability to directly compare $CD8^+$ T cell exhaustion during infection with chronic strains of LCMV versus $CD8^+$ T cell effector and memory differentiation in mice infected with acute LCMV strains. Of the existing chronic and acute strains of LCMV, the most commonly used have been acute Armstrong (Arm) strain and chronic Clone 13 (Cl13) strain. The chronic Cl13 strain was isolated as a spontaneously arising genetic variant of the acute Arm strain (370). The Cl13 strain only differs from the Arm strain by two point mutations, which lead to single amino acid changes in the LCMV polymerase gene and the LCMV glycoprotein gene (371,372). These two amino acid changes allow Cl13 to sustain high viral titres over time and establish chronic infection (371–373). Fortunately, these amino acid changes do not affect the known T cell peptide epitopes within the virus (371–373), and hence $CD8^+$ T cell responses to the same viral antigens can be assessed in both chronic Cl13 and acute Arm infection. For this reason, the LCMV model has been extensively used to characterise the exhaustion process, as within this system the molecular and cellular features of the exhausted T cell response can be compared against effector cells from acute infection specific for the same viral antigen. This section of the introduction will describe the features of $CD8^+$ T cell exhaustion and the various factors that contribute to this differentiation state, with a primary focus on studies from the chronic LCMV model, and references to human conditions where appropriate.

1.3.2: Phenotype of exhausted CD8$^+$ T cells

Exhausted CD8$^+$ T cells display multiple unique hallmarks that distinguish them from other states of T cell differentiation. Notably, global gene expression profiling comparing virus-specific CD8$^+$ T cells from LCMV Cl13 infection to their effector-memory counterparts in LCMV Arm infection, revealed that multiple gene sets, including transcription factors, inhibitory receptors and metabolic factors, were uniquely regulated within exhausted cells (374). However, the alteration in cellular and molecular function of exhausted cells occurs in a slow, hierarchical manner over time and is driven by multiple factors. Hence, exhaustion is a progressive differentiation process in which cells lose function and become terminally exhausted as they differentiate. Some of the major features of exhaustion are described below and summarised in Figure 1.3.

Alterations in T cell function

Fully functional effector CD8$^+$ T cells co-produce multiple cytokines, and express cytotoxic molecules that can be mobilized to kill target cells. During exhaustion, cytokine function is lost in a hierarchical manner, with the cells first losing the ability to produce the cytokine IL-2, followed by losses in TNFα and IFNγ production respectively (353). Loss of inflammatory cytokine production is associated with a gain in production of the immunosuppressive cytokine IL-10, which can feedback and further inhibit the immune response (375). As cells differentiate further towards an exhausted state, they eventually die and are deleted from the repertoire (353). Along with loss of cytokine function, exhausted CD8$^+$ T cells can display deficiencies in *in vitro* cytotoxicity against target cells (352,353), although other groups have reported comparable *in vivo* cytotoxicity within exhausted cells relative to functional effectors (376), as well as stable expression of *Gzmb* and *Perforin* in exhausted CD8$^+$ T cells within tumours (377). This discrepancy may be due to differences between *in vitro* and *in vivo* killing assays, and could also be explained by the heterogeneous nature of the exhausted population as described later. Thus the ability to kill target cells is variably maintained in exhausted cells as opposed to their effector counterparts.

Expression of inhibitory receptors

A characteristic feature of exhausted cells is the expression of multiple inhibitory receptors, and elevated expression of these receptors plays a direct role in

dampening $CD8^+$ T cell function. As opposed to fully functional effector cells, which transiently express some of these receptors upon activation, exhausted cells exhibit sustained and elevated expression of multiple inhibitory receptors, which belong to different receptor families and hence likely act in a non-redundant manner (378). These receptors, including PD-1 (20,378–381), TIM3 (378,380–383), CTLA-4 (362,384), LAG3 (385,386), CD160 (378), 2B4 (378,387), TIGIT (388) and CD39(389–391), are frequently highly expressed on exhausted $CD8^+$ T cells from Cl13 infected mice, and HIV and cancer patients, and often actively inhibit effector function. Inhibitory receptors limit T cell function in exhaustion via a number of mechanisms, including competition with, and restriction of, co-stimulatory receptor interactions, recruitment of inhibitory signaling pathways and alteration of transcription factor biology (280,383,392–395). Several transcription factors and epigenetic regulators have been shown to induce the expression of certain receptors such as PD-1 (347,396–398) and TIM3 (399,400). However, the factors responsible for inducing the expression of most inhibitory receptors are not clear.

PD-1 is one of the most highly expressed and well-studied inhibitory receptors in exhaustion. PD-1 was identified as one of the most highly induced genes in a microarray screen of LCMV-derived exhausted versus effector $CD8^+$ T cells (20,374). PD-1 is a member of the B7 family of receptors consisting of CD28 and CTLA-4 (285) and contains an Immuno Tyrosine Inhibitory Motifs (ITIM) in its cytoplasmic domain. Upon binding to its ligands PD-L1 or PD-L2, PD-1 can signal to recruit phosphatases and dampen the TCR signaling cascade (328,330,401). However, these experiments were mostly performed *in vitro* with activated $CD8^+$ T cells and may not represent the signaling pathways utilised by PD-1 in exhausted cells *in vivo*. Indeed, recent *in vitro* biochemical and matching *in vivo* data indicate that PD-1 may predominantly operate by inhibiting CD28 co-stimulatory signaling rather than TCR signaling (394,395). Along with increased expression of PD-1 on $CD8^+$ T cells during exhaustion (20,378), the ligand PD-L1 is also upregulated on several cell types such as DCs, $CD4^+$ T cells and B cells as well as other infected cells (402,403) during chronic infection. Elevated PD-L1 expression during infection likely occurs as PD-L1 is induced on cells (including tumour cells) by IFNγ signaling (404), providing a mechanism by which inflammation may reinforce this regulatory circuit. Thus, elevated PD-1 and PD-L1 expression during chronic infection and within tumours is an important regulatory axis

during exhaustion. The importance of PD-1 signaling in exhaustion is best illustrated by studies where PD-1 function was blocked. PD-1 blockade during chronic LCMV infection leads to expansion of exhausted cells, restoration of their effector function, and enhanced viral control (20,379,402) and these findings extend to SIV (363), *in vitro* HIV cells (379,405,406), humanised mouse models of HIV (364,365) and cancer patients (366–368).

The number of inhibitory receptors co-expressed by exhausted cells is typically inversely associated with cytokine function (378). Although independent blockade of many inhibitory receptors has little influence on exhaustion, their combined suppressive effect is significant (378). Consistent with this idea, a number of studies have shown synergy with combined blockade of PD-1 and TIM3 (375), PD-1 and LAG3 (378) and blockade of PD-1 with activation of 4-1BB costimulatory receptor (407). Furthermore, combined blockade of PD-1 and CTLA4 in the clinic substantially boosts the efficacy of cancer immunotherapy (408). Hence, inhibitory receptors synergistically limited exhausted $CD8^+$ T cell function, although the complexities of receptor interactions are still being uncovered.

Altered metabolism

As described in Section 1, cellular metabolism is crucial for effector $CD8^+$ T cell function and memory formation (82). In exhausted cells, multiple studies have confirmed that the mTOR pathway is compromised, resulting in deficiencies in metabolic pathways and mitochondrial energetics (393,409,410). Much of the metabolic dysfunction in exhausted cells is driven by inhibitory receptors, such as PD-1 and CTLA-4, which limit mTOR signaling by restraining CD28 signaling (394,395,411). Limited mTOR signaling likely contributes to metabolic deficiencies through restraining activity of the transcription factor HIF1α. During normal effector differentiation, mTOR induces HIF1α, which subsequently induces genes that lead to the switch to anaerobic glycolysis required for growth and differentiation (412). Consistent with the idea that mTOR inhibition restrains HIF-mediated regulation of metabolism, Cl13 infection of mice lacking *Vhl1*, a negative regulator of HIF1α and HIF2α, results in both a gain of effector function, and induction of factors associated with glycolysis, in exhausted $CD8^+$ T cells within both chronic infection and cancer models (413). Beyond alterations in mTOR signaling, other factors contribute to

metabolic changes during exhaustion such as sustained and elevated expression of the transcription factor IRF4. While IRF4 promotes glycolytic metabolism of effector cells (103), in the context of exhaustion IRF4 instead promotes metabolic dysfunction of the $CD8^+$ T cells (396). As alluded to above, exhaustion is also associated with defects in mitochondrial metabolism, and rescuing these defects can rescue T cell function (409). Thus, metabolic deficiencies during exhaustion appear to contribute to diminished effector function, suggesting that therapeutic targeting of metabolism may have potential in immunotherapy.

Population homeostasis and response to cytokines

The long-lived memory $CD8^+$ T cells that develop after resolution of an infection depend on the homeostatic cytokines IL-7 and IL-15 for their maintenance in the circulation and tissues. In contrast, exhausted cells are not typically maintained by IL-15 and IL-7. Studies of viral specific $CD8^+$ T cells in Cl13 infection showed lack of IL-7R (CD127) expression, and antibody blockade of IL-7R signaling also did not affect survival of these cells (414), although treatment of Cl13 infected mice with supraphysiological levels of exogenous IL-7 increased T cell numbers, restored T cell function and led to viral control (415). Similarly, exhausted $CD8^+$ T cells do not rely on IL-15 signals for long term survival (414,416). Thus, exhausted $CD8^+$ T cells have distinct requirements for population homeostasis and maintenance in comparison to memory $CD8^+$ T cells. While homeostatic cytokines are dispensable for exhausted cell maintenance, exhausted cells do rely on the presence of chronic antigen for long term survival, and hence have often been called “antigen addicted” (414,417,418). Transfer of LCMV-derived exhausted $CD8^+$ T cells into recipients infected with a mutant virus lacking the immunodominant GP_{33-41} epitope (419) lead to maintenance deficiencies within GP_{33-41} specific $CD8^+$ T cells (414). Notably, the transferred cells failed to exhibit the extensive constitutive proliferation typically seen in exhausted cells, arguing that antigen engagement maintains exhausted cells in part through driving proliferation (414). As the transferred cells were still exposed to constitutive inflammation, this also argues that inflammation alone cannot sustain exhausted cells. Thus, chronic antigen plays a crucial role in exhausted cell maintenance.

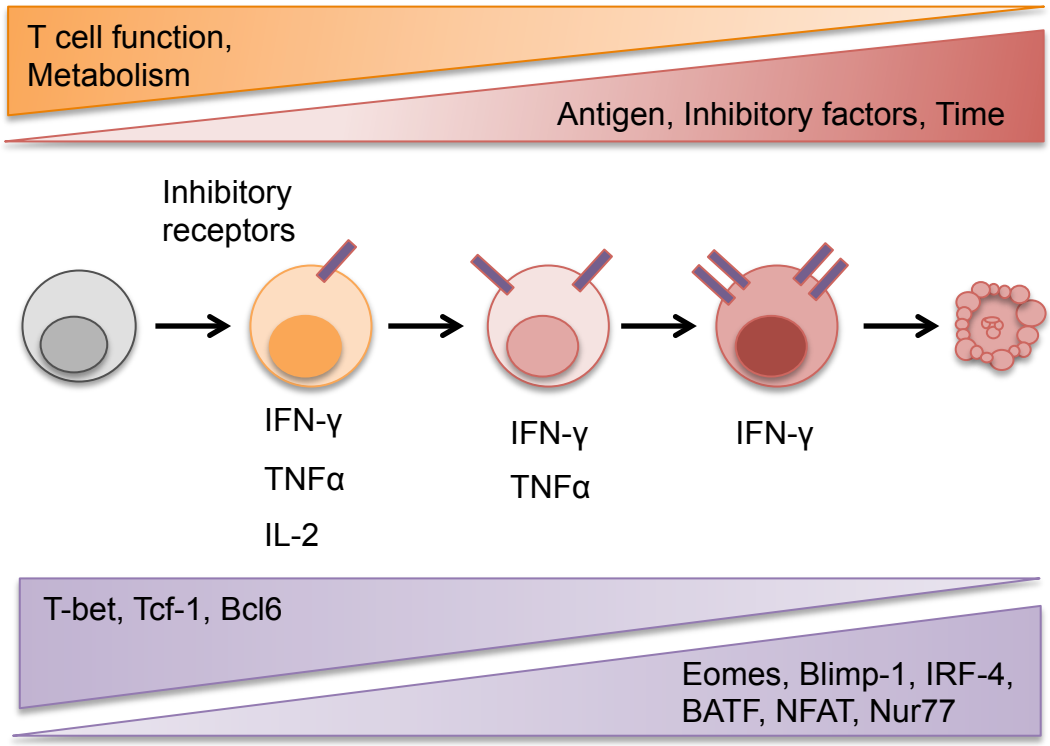

Figure 1.3: Progressive differentiation towards an exhausted state: $CD8^+$ T cells undergo exhaustion in chronic infection and cancer. Exhaustion is a slow and progressive differentiation process, characterised by a loss of effector functions, and alterations in metabolism. Exhaustion is programmed by chronic antigen engagement and various inhibitory factors (such as IL-10). The loss of cytokine production occurs in a hierarchical manner, with IL-2 loss occurring first, followed by loss of TNFα and then loss of IFN-γ before cells undergo apoptosis. There is a parallel increase in the expression of inhibitory receptors as cells progress through exhaustion. Multiple transcription factors drive the exhaustion process, and these are summarised in the graded boxes.

1.3.3: Evolutionary basis of exhaustion

Exhaustion most likely evolved as a mechanism to limit the potentially fatal immunopathology and organ damage that can be a natural consequence of a robust inflammatory T cell response. This has been best illustrated in the LCMV infection model, where infection of mice with an intermediate dose of virus that does not replicate to sufficient levels to induce exhaustion, but is also not cleared by the initial T cell response, can trigger fatal immunopathology (22). Mice that lack the inhibitory receptor PD-1 (20), and hence have deficiencies in the exhaustion process, similarly succumb to immunopathology. It is important point to note that "exhaustion" of $CD8^+$ T cells does not imply a complete abrogation of T cell function. Exhausted $CD8^+$ T cell still retain some function and this is crucial in containing infections and cancers. This was demonstrated through multiple studies where depletion of $CD8^+$ T cells from virally infected primate hosts led to an increase in viremia during chronic SIV infection (420,421). Hence, rather than complete eradication of infection, the immune system establishes a new equilibrium with the chronic pathogen by actively containing infection while limiting damage to the host.

1.3.4: Factors driving $CD8^+$ T cell exhaustion

Exhaustion of effector $CD8^+$ T cells is programmed by multiple extrinsic and intrinsic factors. While these factors can vary between infection types and cancers, there are still a number of conserved antigen and environment-derived signals that are crucial in driving the exhausted state.

Chronic Antigen

Persistence of antigen in chronic infection and cancers plays a prominent role in inducing exhaustion of responding $CD8^+$ T cells. The potential effect of antigen load on exhaustion was first observed when examining the immunodominance hierarchy in chronic versus acute LCMV infection. Some T cell specificities normally abundant in acute Arm infection are lost in the context of chronic Cl13 infection, while other specificities are either maintained or occasionally selectively expanded during Cl13 infection (353). These differences appeared to be associated with antigen load, with the degree of deletion or persistence correlating with the abundance of the specific antigen recognised. Consistent with this idea, vaccination strategies have proven to

be ineffective for chronic infection, as the cells are only further exhausted by additional antigen from the vaccine (422). Conversely, adoptive transfer of P14 cells from Cl13 infected mice into infection-matched Arm mice at early time points post infection resulted in rescue of effector function in the virus-free recipients (423). Furthermore, mice engineered to prevent $CD8^+$ T cell viral antigen recognition on non-haematopoeitic cells exhibited an early increase in cytokine function and a delayed development of exhaustion (424). Studies in chronic Influenza virus models have also confirmed that chronic antigen alone is sufficient to induce exhaustion (425). Finally, as noted earlier in this section, exhausted cells are addicted to antigen for their survival (414). Chronic antigen recognition drives numerous aspects of exhausted cell biology, including expression of inhibitory receptors and key transcriptional changes. In particular, loss of antigen recognition during chronic LCMV infection by epitope escape leads to loss of PD-1 expression selectively within the epitope specific $CD8^+$ T cell population (418). Chronic antigen recognition also engages a number of key transcriptional circuits responsible for programming the exhausted state, and these factors will be considered in detail in a later section.

Cellular and soluble mediators

Along with persistent antigen, the prolonged presence of chronic pathogen or cancer also has effects on other components of the immune system, which in turn affect the development of the $CD8^+$ T cell response and maintenance of exhaustion. APCs and $CD4^+$ T cells are the prime regulators of $CD8^+$ T cell exhaustion, although NK cells (426) and infected tissues (427) can also play an indirect role in contributing to the immunosuppressive environment (428). A number of key cytokines and soluble factors produced by these cells influence $CD8^+$ T cell exhaustion, although exhaustion can also be regulated by environmental factors such as cholesterol (429) and potassium levels (430).

DCs are the key APC cell type responsible for activation of naïve $CD8^+$ T cells against pathogens. However, during chronic infection with LCMV Cl13, DCs are more susceptible to direct viral infection, which alters their phenotype and function (431). Chronic infection can also alter the DC response to TLR stimulation (432). Notably, there is an inhibitory APC subset, which arises and expresses multiple inhibitory receptors along with IL-10 cytokine production (433). As IL-10 levels are increased in

chronic LCMV infection, and IL-10 aids in enforcement of the exhausted phenotype (434,435), DC-derived IL-10 may contribute to exhaustion. DCs also produce Type I IFN (436,437) throughout chronic infection, which can directly induce $CD8^+$ T cell exhaustion (438,439). Thus, DCs affect the T cell response by presentation of antigen, inhibitory receptor ligands and inhibitory cytokines. Other APCs, including MDSCs and inhibitory macrophages, also affect $CD8^+$ T cell exhaustion (438,440). Notably, recent work suggests that macrophages are a more important source of IL-10 than DCs (441). Additionally, T cell-derived TNFα can trigger production of immunosuppressive PGE_2 by macrophages, which can then feedback and inhibit exhausted T cell function (442).

Apart from APCs, $CD4^+$ T cells play a crucial role in maintenance of the exhausted CD8+ T cells response. Mice depleted of $CD4^+$ T cells were unable to clear Cl13 infection, resulting in lifelong viremia and severe exhaustion of viral-specific $CD8^+$ T cells (443). $CD4^+$ T are the primary *in vivo* source of cytokines IL-2 and IL-21, and either IL-21 loss (444–446), or inhibition of IL-2 signaling within exhausted $CD8^+$ T cells (447), compromises $CD8^+$ T cells maintenance and function during chronic infection. Conversely, supplementing Cl13 infected mice with recombinant IL-2 protein resulted in increased numbers of virus-specific $CD8^+$ T cells and reduced viral titres (448).

$CD4^+$ T cells also produce factors that limit exhausted $CD8^+$ T cell function. Chronic stimulation of virus-specific $CD4^+$ T cells leads to IL-10 production that plays important roles in limiting $CD8^+$ T cell function (441,449). Along with helper $CD4^+$ T cells, Tregs also influence the exhaustion process. Treg numbers increase in chronic infection and depletion of these cells at later time points of infection can restore the $CD8^+$ T cell function (450). Tregs can produce IL-10, TGF-β and IL-35, which can drive T cell exhaustion (451,452).

Population heterogeneity

Commitment to an exhausted fate is time and antigen dependent. Transfer of virus-specific $CD8^+$ T cells from Cl13 infected mice into antigen-free hosts at earlier time points post infection results in revival of effector function, but this recovery fails to

occur at later time points post infection. Thus, cells progressively, and ultimately irreversibly, commit to an exhausted fate (423,453).

A detailed examination of the exhausted T cell population at any given point in time reveals substantial heterogeneity that is likely reflective of cells at different points of the exhaustion differentiation program. One of the earliest examples of heterogeneity was variability in PD-1 expression, with evidence of PD-1 intermediate (PD-1^{int}) and PD-1 high (PD-1^{hi}) sub-populations. Notably, these sub-populations have different functional characteristics. In particular, while the PD-1^{int} population expands in the response to PD-1 blockade, the PD-1^{hi} population fails to respond (454). This suggests that PD-1^{hi} population is likely more irreversibly committed to an exhausted fate. Subsequent work using transcription factor deficient mice that lacked either of these subsets (see next section) illustrated that both of these subsets are required for optimal viral control (455). Thus, exhaustion triggers a continuum of differentiation states that cooperatively play important roles in infection control.

While equivalents of the PD-1^{int} and PD-1^{hi} subsets were found in several human disease models of HIV and cancer (361,405), subsequent studies revealed an alternative set of markers to identify less differentiated “stem cell-like”, and terminally differentiated exhausted sub-populations. A number of papers using the Cl13 model system, with validation studies in HIV infection, revealed that the transcription factor TCF1 marks the exhausted stem cell population (456–459). The $TCF1^{+}$ population also expressed CXCR5, which enabled the cells to reside in the follicular space in the lymphoid organs where there is less viral infection, and upon antigen encounter these cells proliferated and gave rise to terminally differentiated $TIM3^{+}$ and PD-1^{hi} progeny (456–459). As with the PD-1^{int} cells, the $TCF1^{+}$ cells are also the main exhausted cell sub-population that responds to PD-1 blockade (456–459). Thus, there are two main subsets of cells in exhaustion – a stem cell-like population, which is less differentiated and maintains proliferative potential, and the terminally differentiated progeny of these stem-like cells, which express more cytolytic granzymes, inhibitory markers and produce less cytokines. These subsets have been validated in human chronic infection and cancer (360,377,460,461), and so appear to be a conserved feature of the exhaustion process. Importantly, as with the PD-1^{int} and PD-1^{hi} subsets, both of these subsets appear important in infection and cancer

control (377). Understanding the differences in these subsets is crucial in guiding future immunotherapeutic strategies aimed at disrupting exhaustion, since the $TCF1^+$ subset is both crucial for maintenance of the exhausted population, and for the response to checkpoint blockade.

Transcriptional drivers

Transcriptional programs controlling effector and memory differentiation are crucial in determining the extent of cellular function and population numbers. $CD8^+$ T cell exhaustion is a unique differentiation state with a distinct transcriptional signature (374). The exhaustion process is governed by multiple transcription factors, which control the dynamics of exhausted sub-populations and the exhaustion differentiation process. TFs in exhaustion are differentially expressed in comparison to effector/memory differentiation and, in some cases, repurposed in their function in functional effector/memory differentiation (462). In particular, network analysis during exhaustion revealed vastly different TF interactions and networks in effector versus exhausted T cells (462). Multiple gene knockout studies have since been employed to understand the contribution of individual transcription factors to the exhaustion process.

The T-box transcription factors EOMES and T-BET play important roles in effector and memory differentiation, and are typically inversely expressed. Intriguingly, these TFs are also inversely expressed in exhaustion, but their roles in differentiation are swapped from that seen in their effector-memory counterparts. T-BET functions as a rheostat to IL-12 and inflammatory signals in effector cells during acute infection, and drives cells towards terminal differentiation (90). However in chronic infection, loss of T-BET led to increased viral titres, and augmented terminal differentiation of exhausted $CD8^+$ T cells in LCMV CL13 infection, with cells displaying increased levels of inhibitory receptors and reduced cytokine production (463,455). Furthermore, virus-specific cells were not able to persist in the absence of T-BET, and additional functional studies found that T-BET dampens PD-1 expression by direct binding to the PD-1 promoter (463). EOMES on the other hand is responsible for driving terminal differentiation of exhausted cells (399,455). The cell extrinsic factors that control expression of these two TFs remain unclear, however FOXO1 does appear to play a role in the induction of terminally exhausted $EOMES^{hi}$ $T\text{-}BET^{lo}$

cells (393). PD-1-mediated mTOR inhibition induces FOXO1 nuclear translocation, resulting in a positive feedback loop whereby FOXO1 induces further PD-1 expression and formation of the $EOMES^{hi}$ $T\text{-}BET^{lo}$ population (393).

The transcriptional repressor BLIMP-1 is another TF re-purposed to promote exhaustion. In the context of acute infection, BLIMP-1 promotes terminal differentiation of functional effector cells (125,155), while in the context of chronic infection BLIMP-1 appears to promote terminal exhaustion. Loss of BLIMP-1 in Cl13 infection led to increased numbers of virus-specific $CD8^+$ T cells (464), and also enhanced the expression of memory/stem-like markers (such as CD62L and CD127) while lowering the expression of inhibitory receptors (464). The cells also exhibited increased IL-2 production diminished GZMB expression. Overall, this suggested that BLIMP-1 deletion prevents terminal exhaustion. In the context of acute infection, BLIMP-1 in part limits memory potential and promotes terminal differentiation through antagonizing expression of BCL6. Given that BCL6 deletion during exhaustion also leads to loss of the $TCF1^+$ stem-cell like population (457) (ie. the opposite phenotype to that seen in BLIMP-1 deficient mice), it is likely that a similar mutually antagonistic gene program operates in exhaustion. Hence, there are some parallels in BLIMP-1 and BCL6 function between chronic and acute LCMV infection. Again, the extracellular signals that lead to BCL6 loss and BLIMP-1 induction during terminal differentiation remain unclear.

The transcription factor TCF1 is not merely a marker of stem cell-like exhausted cells, but also plays important functional roles in maintaining this population. In the context of acute infection, TCF1 is involved in the formation and maintenance of central memory $CD8^+$ T cells (173). In exhausted cells, TCF1 is important for the maintenance of the stem cell-like exhausted sub-population (456–459), which does bear some similarities to central memory cells. TCF1 functions by blocking IFN signals, suppressing expression of TIM3 and other exhaustion related genes, and also inducing BCL6 (400). Importantly, many studies in both animal models and patients have now confirmed that this population responds to PD-1 blockade in both chronic infection and cancer, and that TCF1 loss abrogates the response to therapy (360,377,456,458–461). Notably, the presence or absence of this $TCF1^+$ sub-population can predict melanoma patient responders to PD-1 blockade (360). Thus,

there is currently substantial interest in the role of TCF1 in exhaustion, although relatively little is known about the factors that trigger TCF1 down-regulation during the terminal exhaustion process.

As described in detail above, T cell exhaustion is driven by chronic antigen recognition. Multiple transcription factors downstream of the TCR are important in promoting the exhaustion gene program. Firstly, NFAT is activated in exhausted cells by chronic TCR signalling and promotes expression of PD-1, as well as a number of other key genes in the exhaustion gene signature (376). NFAT appears to function differently in exhaustion relative to functional effector cells by forming homodimers as in tolerance (347). These homodimers bind a unique set of exhaustion-associated genes (347), and induced a number of downstream TFs that reinforce the exhaustion process. BATF was originally identified in vitro as a gene induced by PD-1 ligation that limited T cell function in HIV samples (392), however subsequent studies identified BATF as an NFAT target (396). TCR-induced NFAT signaling also induces elevated expression of the TF IRF4 during exhaustion, and IRF4 appears to promote exhaustion by binding to the same gene loci as that of NFAT and BATF (396). Collectively, these results suggest that chronic NFAT engagement induces a transcriptional complex consisting of NFAT, IFR4 and BATF that promotes terminal exhaustion. NFAT was recently also shown to induce expression of the transcription factor NR4A1 and its family members (465,466), and deletion of these factors also abrogated exhaustion. Thus, antigen-induced NFAT triggers a positive feedback loop that promotes exhaustion via a range of mechanisms.

Epigenetic drivers

Epigenetic changes that influence DNA accessibility within chromatin are a crucial component of gene regulation and cellular differentiation. A number of studies have now indicated that epigenetic regulation plays an important role in programming the exhausted state. Early studies of the *Pdcd1* locus encoding the PD-1 inhibitory receptor revealed differential methylation of the *Pdcd1* gene regulatory regions in exhausted vs effector or memory cells (397). The *Pdcd1* locus was demethylated in effector cells during acute infection to promote chromatin accessibility and gene expression, however it was remethylated as cells transitioned to a memory phenotype (397). On the other hand, exhausted cells maintained the demethylation

of the *Pdcd1* locus even after antigen clearance or transfer of cells into antigen-free hosts. Additionally, a recent study also showed that there was a uniquely accessible enhancer region in exhausted cells, which was required for high PD-1 expression in exhausted cells (398). This result indicated that the epigenetic signature of exhausted cells was unique from effector cells. This study further compared the open chromatin regions of exhausted and functional effector cells in LCMV Cl13 and Arm infection and demonstrated that exhausted cells contained ~6000 unique accessible chromatin regions that were not present in their effector or memory cell counterparts (398). This result reinforces gene expression studies showing that exhausted cells are a unique lineage, distinct from functional effector or memory cells. A subsequent study conducted in tumours showed similar unique chromatin changes within exhausted tumour infiltrating $CD8^+$ T cells (467). The DNMT3 DNA methylase has been indicated as a crucial factor that regulates epigenetic state during exhaustion. Notably, DNMT3 deletion resulted in reversal of exhaustion-specific DNA methylation marks and a revival of cell function, particularly in response to PD-1 blockade therapy (468). As many of the exhaustion-specific chromatin changes are not fundamentally reversed by PD-1 blockade (469), it is likely that therapeutic targeting of epigenetic pathways in combination with PD-1 blockade will likely be needed for durable therapeutic disruption of exhaustion. Indeed, treating exhausted cells with a DNA demethylating agent augmented their response to PD-1 blockade (468).

Overall, these data collectively demonstrate that exhaustion is a unique differentiation state programmed by distinct transcriptional and epigenetic programs. A greater understanding of the pathways that regulate this differentiation processes is critical if we are to develop more efficacious immunotherapy approaches targeting exhaustion.

1.4: Comparing tolerance and exhaustion

$CD8^+$ T cell tolerance and exhaustion occur in different immune contexts, however both serve to limit the $CD8^+$ T cell response for the purpose of host protection. $CD8^+$ T cell tolerance pathways are enforced on self-reactive naïve T cells in steady state conditions (234), while exhaustion is a slow progressive process that targets pathogen-specific activated effector cells in chronic infection and cancer to reduce function (470).

The obvious major difference between tolerance and exhaustion is that exhaustion acts upon established effector cells later in the immune response, whereas tolerance acts upon cells that have undergone minimal or no effector differentiation (221,268). Nevertheless, several similarities are evident in the phenotypes, and pathways employed, during tolerance and exhaustion. $CD8^+$ T cells are increasingly being harnessed for immunotherapy in cancer, but autoimmune side effects are an emerging problem. While this could be because exhaustion is known to limit established autoimmune disease (471), this could additionally be because current therapies (PD-1 and CTLA4 blockade) target pathways that are also employed in peripheral tolerance induction (248,279). Refining immunotherapies to limit autoimmune side effects while retaining anti-tumour responses is thus not possible unless we better understand the similarities and differences between tolerance and exhaustion. The shared molecular pathways in tolerance and exhaustion are described below and summarised in Figure 1.4.

Loss of cytokine function

At a gross phenotypic level, both tolerant and exhausted $CD8^+$ T cells have similar deficiencies in effector function. For example, in both states, cells make transcripts for *Ifng*, but fail to make IFNγ protein due to a block in translation (265,268,472). Exhausted cells also have deficiencies in IL-2 and TNFα production (353), and similar deficiencies can be seen in tolerant $CD8^+$ T cells (I.A. Parish, unpublished observations). Interestingly, though, as discussed in the previous section exhausted cells retain expression of GZMB as well as cytotoxic capacity. This is in contrast to tolerant cells, which are often deficient in killing capacity and GZMB expression

(265,268), although tolerance models do exist where killing capacity is observed (221).

Chronic antigen

T cells undergoing tolerance generally recognise self- or non-dangerous antigen signals in the absence of infection/inflammation, leading to tolerance induction and deficiencies in effector function. However multiple studies have shown that different forms of tolerance, such as anergy and deletion, are dependent on persistent antigen recognition for their maintenance (270,273). Similarly, as discussed in the previous section, chronic antigen is a key driver of exhaustion (414,456). Notably, the key regulatory transcriptional pathways downstream of chronic antigen, such as NFAT-dependent pathways, are also shared between tolerance and exhaustion (345,347). In particular, key functionally important NFAT gene targets, such as NR4A family TFs (465,466) and the ubiquitin ligase CBLB (338,473), share similar roles in both tolerance and exhaustion. Additional NFAT induced TFs (347), such as *Egr2*, *Ikzf2* (encoding HELIOS) and *Tox*, are upregulated in both exhausted (374,462) and tolerant (268) $CD8^+$ T cells. Up-regulation of EGR2 in particular is notable as this TF is a master regulator of T cell anergy (348,349). This suggests that a common antigen-induced NFAT-dependent gene program operates in both exhaustion and tolerance. Consistent with this idea, there is a small but significant overlap in the gene expression profiles of tolerant and exhausted cells (268), with the degree of overlap more pronounced in some tolerance models (474). Nevertheless, certain functionally important NFAT-induced TFs, such as IRF4 and BATF (392,396), have not been investigated in tolerance, and there is only limited induction of these genes within some tolerance models (I.A. Parish, unpublished observations). Thus, further studies are needed to determine the degree to which antigen-induced negative regulatory pathways are shared in tolerance and exhaustion.

Inhibitory receptors

As described in earlier sections, certain inhibitory receptor interactions between T cells and DCs or other cell types can limit T cell function. Notably, a number of inhibitory receptors, such as PD-1, CTLA-4, TIM3 and LAG3, contribute to both tolerance (248,279,282,283) and exhaustion (378,470). While exhausted cells accumulate these receptors over time, where they constitutively limit function (378),

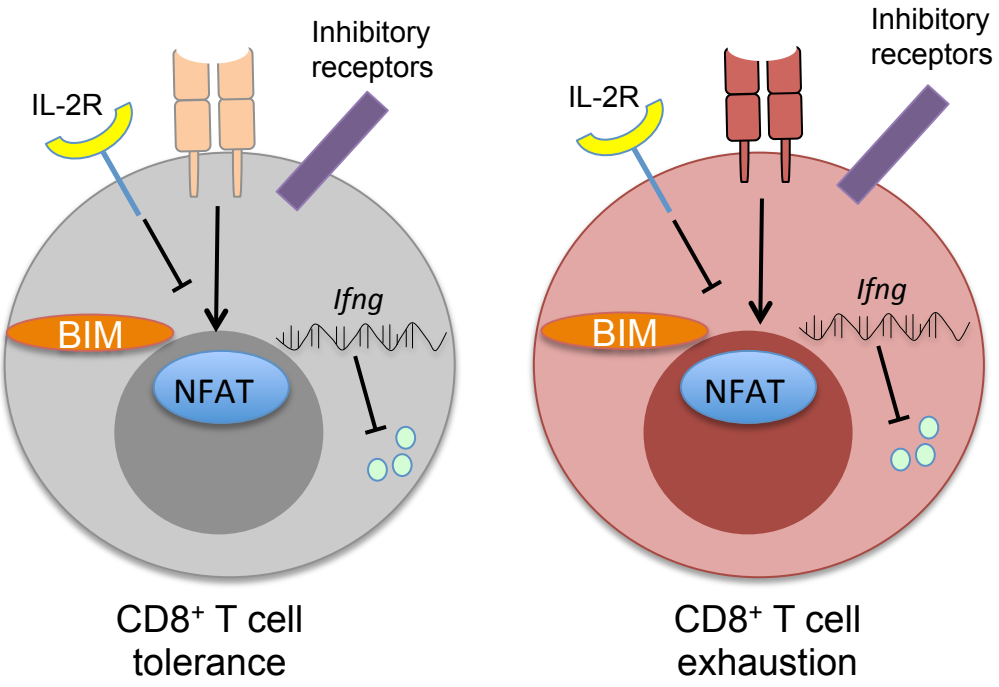

Figure 1.4: Comparison of molecular pathways in CD8⁺ T cell tolerance and exhaustion: CD8⁺ T cell tolerance and exhaustion are driven by chronic antigen signals and inhibitory receptors. Antigen engagement triggers the activity of the transcription factor NFAT in both tolerance and exhaustion, leading to induction of common downstream immunoregulatory factors such upregulation of inhibitory receptors. Signaling through IL-2R can result in rescue of tolerance and exhaustion, and cells in both states are chracterised by a block in cytokine translation and undergo BIM-dependent apoptotic death.

these receptors are often only required in the induction phase of tolerance (296,474). Relatively little is understood of the overlap and differences in the regulatory pathways engaged by these receptors in the context of exhaustion and tolerance. Further work on this topic is thus needed if refined immunotherapy approaches that spare peripheral tolerance are to be developed.

IL-2 signalling

As discussed in earlier sections, exogenous IL-2 treatment can rescue $CD8^+$ T cell function in both exhaustion (447,448) and tolerance (320). Thus, both differentiation states likely depend on development in an IL-2 depleted environment. In the case of tolerance, low levels of IL-2 are expected, as the lack of T cell activation in the steady-state means sparse amounts of free IL-2 will be available. This, coupled with deficiencies in expression of the high affinity IL-2 receptor CD25 (320), means that tolerant cells are normally starved of IL-2 signals. While abundant IL-2 is likely encountered by cells during chronic infection early during the immune response, IL-2 levels naturally drop as infection progresses due to loss of IL-2 producing capacity within chronically stimulated $CD4^+$ and $CD8^+$ T cells (353,423,475) It remains unclear, however, whether common pathways of IL-2-dependent immune activation are engaged in both tolerance and exhaustion.

Bim mediated death

Deletional tolerance and exhaustion both result in death of cells through apoptotic death. The apoptotic mechanisms responsible for cell death appear at least partially overlapping. While apoptotic death is almost completely BIM-dependent in the context of deletional tolerance, death of some exhausted $CD8^+$ T cell specificities is partially controlled by BIM (278,476). It is unknown whether similar transcriptional pathways upregulate BIM expression in tolerance and exhaustion, and/or if other overlapping apoptotic factors play a role in cell death.

Thus, given the overlapping phenotypic features of $CD8^+$ T cells undergoing tolerance and exhaustion, it is important to decipher whether these states are transcriptionally linked.

1.5: Research questions

The focus of this thesis was to expand the molecular understanding of $CD8^+$ T cell tolerance, and investigate any molecular overlap between $CD8^+$ T cell tolerance and exhaustion. Chapters 2 and 3 investigate the role of the TF FOXO3, and ubiquitin ligase adaptor NDFIP1, in $CD8^+$ T cell tolerance respectively. Chapter 4 investigates the role of the tolerance-associated TF EGR2 in $CD8^+$ T cell exhaustion. Collectively, these chapters address a number of key fundamental questions within the tolerance field, with each chapter focused on one of the following broad research questions.

1.5.1. Does the same transcription factor control BIM-dependent death in tolerant versus effector cells?

Tolerant $CD8^+$ T cells undergo BIM-mediated apoptosis, however it is not known whether similar transcriptional pathways trigger *Bim* expression in tolerance as during effector differentiation. FOXO3 has been postulated to trigger BIM dependent death in effector and exhausted cells (135,477). Chapter 2 investigates the role of the transcription factor FOXO3 in $CD8^+$ T cell deletion through use of the FOXO3 mutant mice and the RIP-OVA^{hi} model of tolerance. These data reveal that BIM induction pathways are likely distinct in effector versus tolerant cells.

1.5.2. Are similar molecular pathways engaged to enforce $CD8^+$ T cell anergy versus deletion?

During tolerance induction, cells either die by apoptosis or persist in a hypofunctional anergic state. It remains unclear whether similar pathways are employed to program both states. Chapter 3 explores the role of the ubiquitin ligase adaptor molecule NDFIP1, previously implicated in maintaining $CD4^+$ T cell anergy (344), within $CD8^+$ T cell tolerance models. By examining the effect of NDFIP1 deletion on $CD8^+$ T cell tolerance induction in a range of models, we reveal that $CD8^+$ T cell tolerance and anergy are molecularly separable.

1.5.3. Are the same transcriptional regulatory pathways engaged downstream of TCR signaling during tolerance and exhaustion?

Chronic antigen is a common signal responsible for induction of both tolerance and exhaustion, and common transcriptional pathways are induced downstream of TCR in both states. As noted above, the master transcriptional regulator of anergy, EGR2, is induced during exhaustion, but its role in the exhaustion process is unclear. In Chapter 4, we examine whether EGR2-dependent induction of the anergy gene program contributes to $CD8^+$ T cell exhaustion. Using conditional deletion of *Egr2*, and the chronic LCMV model of exhaustion, we find that EGR2 does promote terminal exhaustion, but appears to do so by engaging a fundamentally different gene program to that seen during anergy.

CHAPTER 2: FOXO3 is differentially required for $CD8^+$ T cell death during tolerance versus immunity

Wagle M V, Parish IA. FOXO3 is differentially required for CD8+ T-cell death during tolerance versus immunity. Immunol Cell Biol. 2016; 94 (9):895–9.

The online publication in *Immunology and Cell Biology* can be accessed through the following DOI: https://doi.org/10.1038/icb.2016.53

The following manuscript included in the thesis has been modified to fit the thesis layout and may differ from the original manuscript submitted to the journal in the following ways. In this version of the manuscript, the methods section is placed between the introduction and results sections. The result figures are incorporated into the results section 2.4 and the figure numbers have been modified to include the chapter number in the prefix, for example from Figure 1 to Figure 2.1.

2.1: Abstract

Peripheral tolerance mechanisms limit autoimmunity by constitutively eliminating self-reactive $CD8^+$ T cells from the periphery in a process called deletion. Previous work has demonstrated that this deletion process is mediated by BIM-dependent apoptotic death due to transcriptional induction of the *Bim* gene. Currently, the transcriptional pathways responsible for *Bim* induction during peripheral deletion remain unclear. We speculated that the transcriptional regulator FOXO3 may induce BIM-dependent death during peripheral deletion, as it has been implicated in *Bim* induction and cell death during effector $CD8^+$ T cell differentiation. Despite observing less Akt-dependent inactivation of FOXO transcription factors in tolerised cells relative to effector cells, we demonstrate that FOXO3 deficient $CD8^+$ T cells induce *Bim* and die normally during peripheral deletion. These data thus demonstrate that BIM-dependent death during $CD8^+$ T cell deletion is FOXO3 independent. Furthermore, these data provide the first evidence that the pathways responsible for *Bim* induction and cell death during effector differentiation versus tolerance of $CD8^+$ T cells are molecularly distinct.

2.2: Introduction

The random recombination events that give rise to T cell receptors inevitably generate self-reactive T cells. While the majority of self-reactive T cells are eliminated during thymic selection, this process is imperfect and rogue self-reactive cells escape into the periphery[1]. Peripheral tolerance mechanisms have thus evolved to restrain these self-reactive cells and prevent autoimmune disease. As peripheral tolerance mechanisms must be subverted in order for autoimmunity to occur, a better understanding of this process is essential for understanding autoimmune progression. In particular, there is a need to resolve the mechanisms guiding individual antigen-activated T cells into either functional effector cells that mediate immunity versus non-functional tolerised cells.

One of the main mechanisms responsible for peripheral T cell tolerance is peripheral deletion. Self-antigens expressed at low levels or in a tissue-specific manner are constitutively presented by tolerogenic dendritic cells (DCs) in the steady-state, and low level self-antigen recognition on such DCs results in the proliferation and apoptotic death of any responding self-reactive T cells[1-6]. Importantly, the responding T cells fail to develop into effectors prior to death[7], meaning that the proliferating self-reactive T cells are unable to cause pathology and are ultimately purged from the repertoire.

Apoptotic death during peripheral T cell deletion is dependent on transcriptional induction of the pro-apoptotic BH3-only protein BIM[8,9], however the transcriptional pathways responsible for *Bim* induction during peripheral deletion are not known. Interestingly, BIM is also responsible for effector T cell death at the cessation of an immune response to infection[10], but it remains unclear whether the same transcriptional pathways control BIM-dependent death during tolerance versus immunity.

FOXO3 is a member of the FOXO transcription factor family that regulates *Bim* induction upon growth factor withdrawal[11,12]. Importantly, FOXO3 regulates cell death and *Bim* induction within T cells *in vitro*[11, 12], and FOXO3 was recently shown to play roles in effector $CD8^+$ T cell death during expansion, contraction and/or memory cell formation *in vivo*[13-15]. Notably, enhanced survival of FOXO3-deficient effector $CD8^+$ T cells was associated with diminished BIM expression[14,15]. However, the role of FOXO3 in peripheral T cell deletion is not known.

The evidence above would predict that FOXO3 is responsible for elevated *Bim* induction during peripheral deletion relative to a productive immune response. One of the main pathways responsible for FOXO3 inactivation is the Akt pathway, as Akt phosphorylated FOXO3 is exported from the nucleus thereby inhibiting FOXO3 mediated gene induction[16]. IL-2 treatment and PD-1 blockade both disrupt peripheral deletion[17,18], and one of the main effects of both of these treatments is induction of Akt signaling. Thus, a more specific prediction is that a lack of Akt signaling during peripheral deletion causes *Bim* induction via accumulated nuclear (unphosphorylated) FOXO3. In contrast, effector cells will likely receive Akt-

dependent signals from infection-associated inflammation and IL-2 early during an immune response, leading to FOXO3 inactivation and diminished *Bim* expression relative to tolerance.

Consistent with this idea we observe more FOXO protein phosphorylation in $CD8^+$ T cell immunity compared to tolerance at early stages of the immune response. However, despite being partially resistant to contraction during a productive immune response, we find that FOXO3 deficient $CD8^+$ T cells exhibit normal BIM induction and cell death during peripheral deletion. Collectively these data suggest that molecularly distinct transcriptional pathways may regulate BIM induction and T cell death during tolerance compared to immunity.

2.3: Methods

2.3.1: Mice and mouse infection

C57BL/6, OT-I and B6.SJL-*PtprcaPep3b*/BoyJ (CD45.1) mice were purchased from the Australian Phenomics Facility, ANU, Australia. RIP-OVA^{hi} [19] and MommeR1[20] mice have been previously described. For *Listeria* infections, mice were infected with 5×10^4 c.f.u. LM-OVA[21] intravenously. All animals used in this study were cared for and used in accordance with protocols approved by the Australian National University Animal Experimentation Ethics Committee and the current guidelines from the Australian Code of Practice for the Care and Use of Animals for Scientific Purposes.

2.3.2: T cell preparation for adoptive transfer

Naïve $CD8^+$ $CD45.1^+$ OT-I cells were enriched from spleen and lymph nodes by generating single cell suspensions and incubating the cells with rat monoclonal Abs against Mac-1 (M1/70), macrophages (F4/80), red blood cells (Ter119), Gr1 (RB6-8C5), MHC class II (M5/114), CD44 (IM7) and CD4 (GK1.5) on ice for 30 min. The rat Ab-labelled cells were removed by anti-rat IgG-coupled magnetic beads (Polysciences Inc.). CTV labelling was performed by labelling cells in RPMI (Life

Technologies) containing 10% Foetal Calf Serum with 10 μM CTV (Invitrogen, CA, USA) at room temperature for 5 min.

2.3.3: Flow cytometric analysis

Single cell suspensions were stained in PBS containing 2.5% Foetal Calf Serum and 0.1% Azide. For surface staining, cells were stained for CD8, CD45.1 and CD45.2 (Biolegend). For intracellular BIM staining, cells were fixed with Fixation buffer (Biolegend) and permeabilised with Permeabilisation Buffer (BD Biosciences) according to manufacturer's instructions, and stained with unconjugated BIM antibody (Cell Signalling Technology) followed by a Goat anti-Rabbit A488 secondary antibody (Life Technologies).

Ex vivo phosphoflow analysis was conducted as described previously[22]. Briefly, spleens and LNs were dissociated into a single cell suspension within RPMI containing 1% paraformaldehyde (Sigma) upon harvest. Cells were counted, aliquoted into tubes and fixed in ice-cold methanol. Cells were then either treated with 1000U l-phosphatase (New England Biolabs) or left untreated in Tris Buffered Saline (TBS) at 37^{o}C for 15 min, and subsequently treated with FcBlock (BD Biosciences) in TBS containing 1% Bovine Serum Albumin (BSA) (Sigma) and 0.05% Azide. Cells were then stained for pFOXO1 (T24)/pFOXO3 (T32) using an unconjugated antibody (Cell Signalling Technology) followed by a Goat anti-Rabbit A488 secondary antibody (Life Technologies). Samples were collected on a BD LSRII or Fortessa flow cytometer (BD Biosciences), with data analysed using FlowJo Software (Tree Star).

2.3.4: Statistical analysis

Data analysis was conducted using Prism Software (GraphPad). Data were either analysed using a Two-way ANOVA with a Bonferroni post test (Figures 2.1b, 2.2a), or a One-way ANOVA with a Tukey's Multiple Comparison test (Figure 2.2d).

2.4: Results

2.4.1: Elevated phosphorylation of FOXO proteins within CD8$^+$ T cells in immunity versus tolerance

To test whether there is elevated Akt-dependent phosphorylation of FOXO proteins in CD8$^+$ T cells during immunity relative to tolerance, we examined *ex vivo* phosphorylation of FOXO proteins via flow cytometry. To track T cells during peripheral tolerance, the well-established RIP-OVA^{hi} tolerance model was employed. RIP-OVA^{hi} transgenic mice express soluble ovalbumin (OVA) selectively within insulin-producing pancreatic islet b-cells[19]. Transfer of OVA-specific OT-I CD8$^+$ T cell receptor transgenic cells into RIP-OVA^{hi} mice leads to proliferation in the draining pancreatic lymph nodes (PLNs) that triggers peripheral deletion by BIM-dependent death[8,23]. To track matched cohorts of T cells during an immune response that generates effector cells, OT-I cells were transferred into mice infected with OVA-transgenic *Listeria monocytogenes* (LM-OVA)[21]. In both cases, the transferred OT-I cells were labeled with the cell division dye Cell Trace Violet (CTV) to allow measurement of division-dependent changes in phosphorylation.

Elevated *Bim* expression is first evident within OT-I cells at sixty hours post-transfer into RIP-OVA^{hi} mice[9]. OT-I cells were thus isolated after sixty hours from the draining PLNs or spleen of RIP-OVA^{hi} or LM-OVA infected C57BL/6 (B6) mice respectively. Cells were immediately fixed upon isolation, and stained directly *ex vivo* using an antibody that recognises the Akt phosphorylated forms of FOXO1 and FOXO3. To control for background staining, cells that had been stripped of phosphorylated residues by phosphatase treatment were stained in parallel. Consistent with increased Akt-dependent signaling during immunity, OT-I cells from LM-OVA infected mice displayed elevated FOXO phosphorylation at later cell divisions relative to OT-I cells in RIP-OVA^{hi} mice (Figure 2.1a,b). Interestingly, lower levels of phosphorylation were observed in earlier cell divisions during LM-OVA infection, although the small number of cells recovered from these divisions means that these results may not be reliable. Thus, CD8$^+$ T cells in later cell divisions display less Akt-dependent FOXO inactivation during peripheral tolerance than during effector cell formation, at a timepoint when *Bim* expression is elevated during tolerance.

a

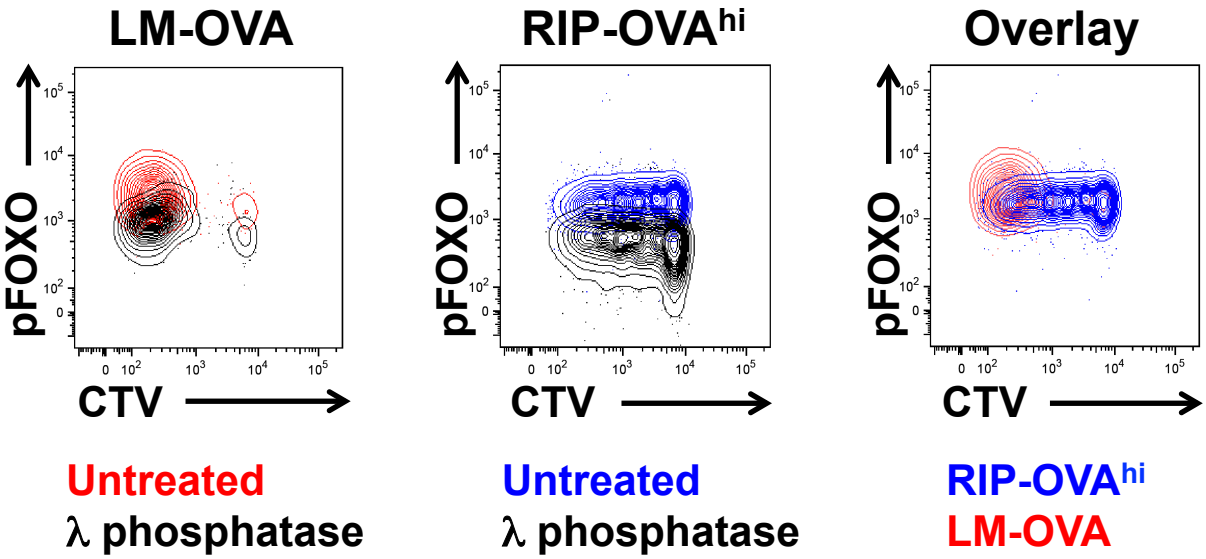
LM-OVA
RIP-OVAhi
Overlay
pFOXO
CTV
Untreated
λ phosphatase
Untreated
λ phosphatase
RIP-OVAhi
LM-OVA

b

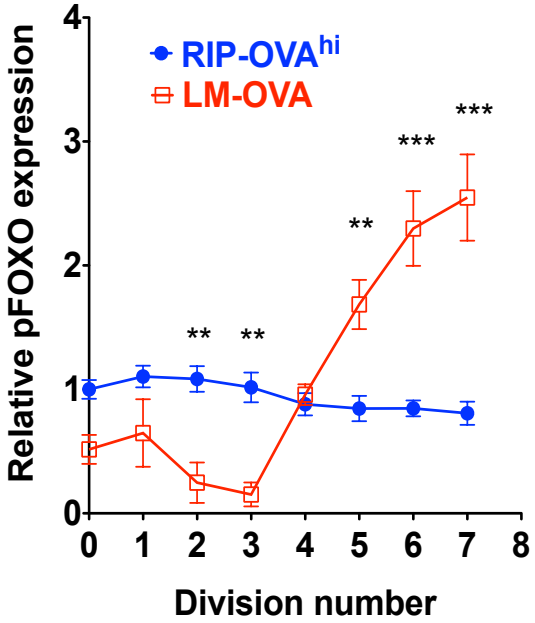
RIP-OVAhi
LM-OVA
Relative pFOXO expression
Division number
**
**
**
***
***

Figure 2.1. Akt-dependent FOXO phosphorylation is elevated in effector versus tolerised OT-I cells. 2×10^6 CTV labeled CD45.1$^+$ OT-I cells were transferred i.v. into either RIP-OVA^{hi} mice, or B6 mice simultaneously infected with LM-OVA. Sixty hours after transfer the spleen (LM-OVA) or PLNs (RIP-OVA^{hi}) were harvested and OT-I cells were analysed for *ex vivo* Akt-dependent FOXO phosphorylation (pFOXO). As a background staining control, cells were also stripped of phosphate by l-phosphatase treatment and analysed in parallel. (a) Representative flow cytometry contour plots showing OT-I pFOXO staining against cell division (CTV) for LM-OVA (red) or RIP-OVA^{hi} (blue) mice. Left and middle plot show staining relative to the relevant phosphatase background control (black), while right plot overlays OT-I cells from LM-OVA and RIP-OVA^{hi} mice. (b) Pooled quantified Mean Fluorescence data with phosphatase background MFI subtracted. Graph shows average MFI per OT-I division, with MFIs normalised to undivided cells during tolerance. Representative and pooled data from two independent experiments (n=7) are shown. Error bars represent SEM, ** = $p<0.01$, *** = $p<0.001$.

2.4.2: *Foxo3*$^{MmR1/MmR1}$ mutant effector OT-I cells are partially resistant to T cell contraction

We next tested whether a failure to inactivate FOXO proteins in CD8$^+$ T cells leads to FOXO3-dependent *Bim* induction. Using a previously reported mutant mouse strain (MommeR1), OT-I cells were generated that bore a homozygous inactivating mutation in the *Foxo3* gene[22]. We first confirmed that the MommeR1 mutant OT-I cells (OT-I.*Foxo3*$^{MmR1/MmR1}$) were able to phenocopy the resistance to contraction seen in OT-I.*Foxo3*$^{-/-}$ cells after LM-OVA infection[14]. Equal proportions of congenically marked OT-I.*Foxo3*$^{MmR1/+}$ or OT-I.*Foxo3*$^{MmR1/MmR1}$ were transferred into B6 mice that were subsequently infected with LM-OVA. The relative proportions of mutant and control OT-I cells were measured in the blood at day 8 and day 20 post-infection. The mutant OT-I cells almost exactly phenocopied the reported OT-I.*Foxo3*$^{-/-}$ phenotype[14], with OT-I proportions initial comparable at day 8 prior to an enrichment of mutant cells at day 20 (Figure 2.2a). Thus, OT-I.*Foxo3*$^{MmR1/MmR1}$ cells display a partial resistance to contraction after infection comparable to that seen in OT-I.*Foxo3*$^{-/-}$ cells.

2.4.3: FOXO3 is dispensable for BIM induction and cell death during peripheral CD8$^+$ T cell tolerance

To test whether FOXO3 mediates *Bim* induction during peripheral deletion, CTV-labelled OT-I.*Foxo3*$^{MmR1/MmR1}$ cells were transferred in RIP-OVA^{hi} mice. Sixty hours post-transfer, BIM protein induction was compared by flow cytometry between mutant cells and their wild-type counterparts. As a positive control for BIM down-regulation during a productive immune response, wild-type OT-I cells isolated from LM-OVA infected mice were also analysed for BIM expression. Consistent with previous results[9], effector OT-I cells displayed diminished BIM expression at later cell divisions (Figure 2.2b,c), with diminished BIM expression correlating with increased FOXO phosphorylation (Figure 2.1a,b). However, OT-I.*Foxo3*$^{MmR1/MmR1}$ cells displayed normal BIM induction in RIP-OVA^{hi} mice, suggesting that FOXO3 is dispensable for BIM induction during CD8$^+$ T cell peripheral deletion. OT-I.*Bim*$^{-/-}$ cells resist deletion in RIP-OVA^{hi} mice[8]. To further test whether *Foxo3* loss similarly protected cells from death during peripheral deletion, OT-I.*Foxo3*$^{MmR1/MmR1}$ or OT-I.*Foxo3*$^{MmR1/+}$ cells were

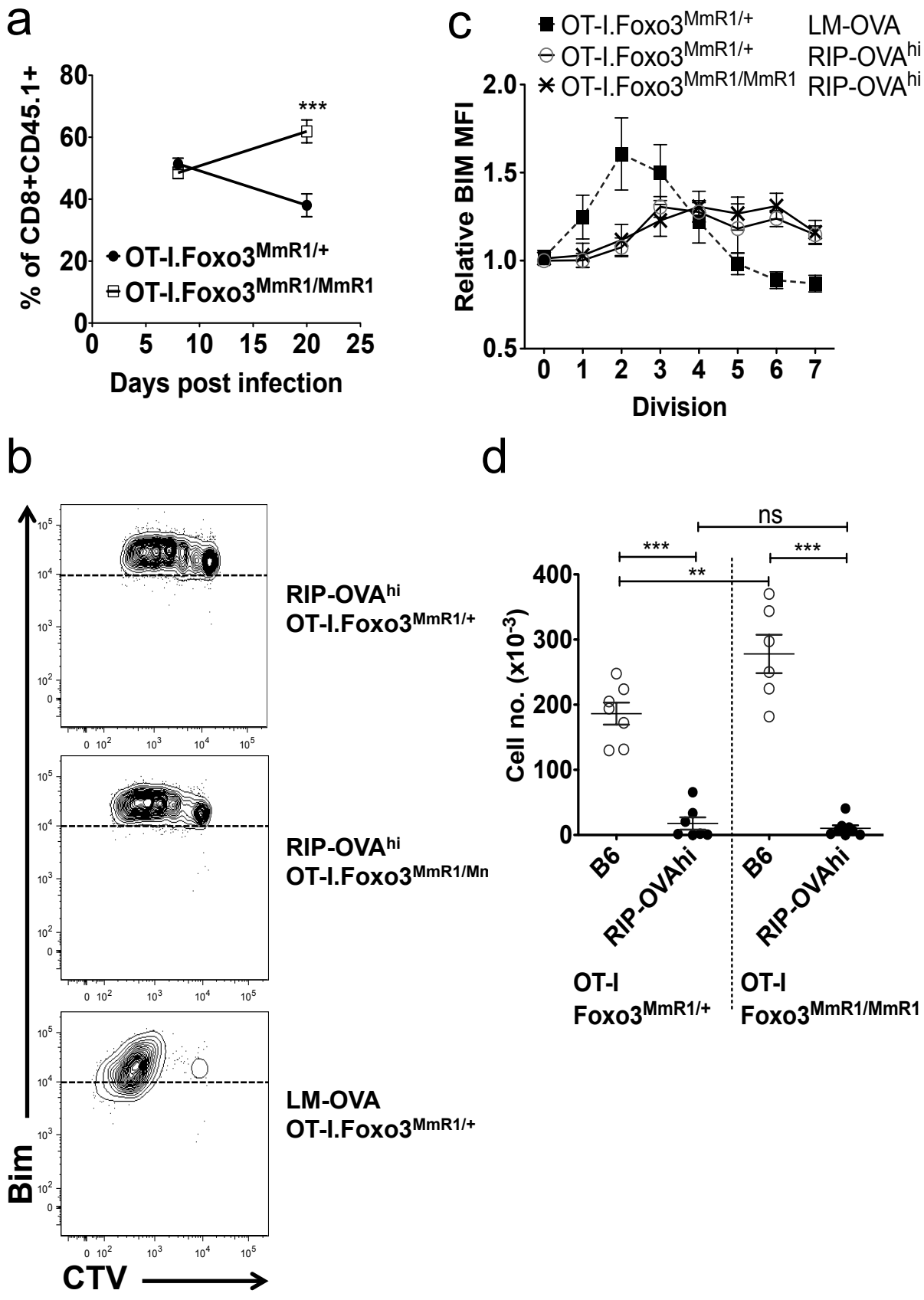
a
% of CD8+CD45.1+
80
60
40
20
0
***
OT-I.Foxo3MmR1/+
OT-I.Foxo3MmR1/MmR1
0 5 10 15 20 25
Days post infection
c
OT-I.Foxo3MmR1/+ LM-OVA
OT-I.Foxo3MmR1/+ RIP-OVAhi
OT-I.Foxo3MmR1/MmR1 RIP-OVAhi
Relative BIM MFI
2.0
1.5
1.0
0.5
0 1 2 3 4 5 6 7
Division
b
RIP-OVAhi
OT-I.Foxo3MmR1/+
RIP-OVAhi
OT-I.Foxo3MmR1/Mn
LM-OVA
OT-I.Foxo3MmR1/+
Bim
CTV
d
ns
***
***
**
Cell no. (x10-3)
400
300
200
100
0
B6
RIP-OVAhi
B6
RIP-OVAhi
OT-I
Foxo3MmR1/+
OT-I
Foxo3MmR1/MmR1

Figure 2.2. FOXO3 is dispensable for BIM induction and cell death during OT-I peripheral deletion. (a) 10^4 CD45.1/CD45.2 OT-I.*Foxo3*$^{MmR1/+}$ cells were mixed with 10^4 CD45.1/CD45.1 OT-I.*Foxo3*$^{MmR1/MmR1}$ cells, and injected i.v. into B6 mice subsequently infected with LM-OVA. The relative proportion of wild-type and mutant OT-I cells was assessed within the blood at days 8 and 20 post-infection. Graph depicts the percentages of wild-type (black circle) or mutant (open square) cells within the CD45.1$^+$CD8$^+$ population at each time-point. Pooled data from two independent experiments (n=9) are shown. (b,c) 2×10^6 CTV labeled CD45.1$^+$ OT-I.*Foxo3*$^{MmR1/+}$ or OT-I.*Foxo3*$^{MmR1/MmR1}$ cells were transferred i.v. into RIP-OVA^{hi} mice, with CD45.1$^+$ OT-I.*Foxo3*$^{MmR1/+}$ cells also transferred into LM-OVA infected B6 mice as a control. Sixty hours after transfer the spleen (LM-OVA) or PLNs (RIP-OVA^{hi}) were harvested and OT-I cells analysed for BIM expression. Both representative contour plots (b) and pooled data (c) are shown from 3 independent experiments (n=9-10). (d) 2×10^6 CTV labeled CD45.1$^+$ OT-I.*Foxo3*$^{MmR1/+}$ or OT-I.*Foxo3*$^{MmR1/MmR1}$ cells were transferred i.v. into RIP-OVA^{hi} mice or antigen-free B6 mice. The OT-I cells remaining were assessed 6 weeks post-transfer in either the B6 (white circles) or RIP-OVA^{hi} (black circles) mice. Pooled data from 2 independent experiments (n=6-8) are shown. Error bars represent SEM, ** = $p<0.01$, *** = $p<0.001$, ns = non-significant.

transferred into RIP-OVA^{hi} mice and then examined for survival at 6 weeks post-transfer. As a control for naïve OT-I survival in the absence of antigen, cells were also transferred into B6 mice. Interestingly, naïve OT-I.*Foxo3*$^{MmR1/MmR1}$ cells did exhibit slightly elevated survival within antigen-free B6 mice, however mutant cells were deleted normally in RIP-OVA^{hi} mice (Figure 2.2d). Thus, *Foxo3* loss fails to protect OT-I cells from death during peripheral deletion. Collectively, these data, coupled with previously published results[13-15], suggest that FOXO3 is differentially required for both BIM induction and cell death during CD8$^+$ T cell immunity versus tolerance.

2.5: Discussion

The experiments above reveal an unexpected separation between the pathways controlling cell death during CD8$^+$ T cell tolerance and immunity. Prior evidence that FOXO3 controls BIM induction in T cells[11-15] leads to the logical extrapolation that FOXO3 is responsible for BIM induction and cell death during peripheral T cell tolerance by deletion. This hypothesis was based upon the assumption that tolerant CD8$^+$ T cells that recognise antigen in the steady-state would lack the Akt-dependent survival signals typically received by effector cells during infection, leading to an accumulation of unphosphorylated, transcriptionally active FOXO3. Furthermore, treatments that activate the Akt signaling pathway (IL-2 treatment & PD-1 blockade) can break CD8$^+$ T cell tolerance in the RIP-OVA tolerance model[17,18]. Consistent with this idea, we found that tolerant CD8$^+$ T cells exhibited lower levels of Akt-phosphorylated FOXO3 than effector cells. However, despite enabling augmented effector cell survival during contraction, FOXO3 loss failed to alter both BIM induction and cell survival during peripheral deletion.

The reasons for differential FOXO3-dependent BIM regulation during tolerance and immunity remain unclear, however it is not due to lower FOXO3 expression during tolerance as our previous microarray studies indicated comparable high levels of FOXO3 expression during both CD8$^+$ T cell tolerance and immunity[9] (I.A.P., unpublished observations). One possibility is that other post-translational

modifications during tolerance inactivate FOXO3 function, as FOXO proteins are subject to a diverse array of modifications that differentially alter their function[24]. Alternatively, the FOXO3 binding sites within the *Bim* promoter may be packed into heterochromatin and inaccessible within tolerant cells. However, a more likely possibility is that FOXO3 does not directly induce *Bim* expression, with the elevated *Bim* expression seen in *Foxo3*$^{-/-}$ effector cells instead due to indirect effects of FOXO3. Mice in which the putative FOXO3 binding sites within the *Bim* promoter are mutated fail to phenocopy *Foxo3*$^{-/-}$ mice in terms of haematopoeitic cell survival[25].

Thus, the influence of FOXO3 on *Bim* expression and cell survival within effector cells may be by an indirect and potentially complex pathway that is not operable within tolerant cells. It should be noted that the *Foxo3*$^{-/-}$ CD8^{+} effector T cell phenotype is not as dramatic as the *Bim*$^{-/-}$ phenotype, suggesting that other pathways also contribute to BIM-dependent effector cell death. It should also be noted that we have not measured *Bim* mRNA levels during tolerance in the absence of FOXO3, which may be altered despite normal BIM protein induction. Nevertheless, the failure of FOXO3 deficiency to alter BIM protein induction and cell death during peripheral deletion provides the first evidence that the pathways controlling cell death during CD8^{+} T cell tolerance and immunity are molecularly separable.

2.6: Acknowledgements

We would like to kindly thank Ashraf Khalil for advice on phosphoflow, Christopher Goodnow for advice, feedback and support, and Carola Vinuesa for providing the MommeR1 mice. This work was supported by an Australian NHMRC Overseas Biomedical Postdoctoral Fellowship (I.A.P.), an Australian Government Australian Postgraduate Award (M.V.W.), and by NHMRC Program Grant 1016953 and NIH grant AI100627 to C. C. Goodnow.

2.7: Conflict of Interest

The authors declare no conflict of interest.

2.8: References

1. Parish IA, Heath WR. Too dangerous to ignore: self-tolerance and the control of ignorant autoreactive T cells. *Immunol Cell Biol* 2008; **86:** 146-52.

2. Kurts C, Heath WR, Carbone FR, Allison J, Miller JF, Kosaka H. Constitutive class I-restricted exogenous presentation of self antigens in vivo. *J Exp Med* 1996; **184:** 923-30.

3. Kurts C, Kosaka H, Carbone FR, Miller JF, Heath WR. Class I-restricted cross-presentation of exogenous self-antigens leads to deletion of autoreactive CD8(+) T cells. *J Exp Med* 1997; **186:** 239-45.

4. Morgan DJ, Kreuwel HT, Sherman LA. Antigen concentration and precursor frequency determine the rate of CD8+ T cell tolerance to peripherally expressed antigens. *J Immunol* 1999; **163:** 723-7.

5. Redmond WL, Marincek BC, Sherman LA. Distinct requirements for deletion versus anergy during CD8 T cell peripheral tolerance in vivo. *J Immunol* 2005; **174:** 2046-53.

6. Rocha B, Grandien A, Freitas AA. Anergy and exhaustion are independent mechanisms of peripheral T cell tolerance. *J Exp Med* 1995; **181:** 993-1003.

7. Hernandez J, Aung S, Redmond WL, Sherman LA. Phenotypic and functional analysis of CD8(+) T cells undergoing peripheral deletion in response to cross-presentation of self-antigen. *J Exp Med* 2001; **194:** 707-17.

8. Davey GM, Kurts C, Miller JF, Bouillet P, Strasser A, Brooks AG *et al.* Peripheral deletion of autoreactive CD8 T cells by cross presentation of self-antigen occurs by a Bcl-2-inhibitable pathway mediated by Bim. *J Exp Med* 2002; **196:** 947-55.

9. Parish IA, Rao S, Smyth GK, Juelich T, Denyer GS, Davey GM *et al.* The molecular signature of CD8+ T cells undergoing deletional tolerance. *Blood* 2009; **113:** 4575-4585.

10. Pellegrini M, Belz G, Bouillet P, Strasser A. Shutdown of an acute T cell immune response to viral infection is mediated by the proapoptotic Bcl-2 homology 3-only protein Bim. *Proc Natl Acad Sci U S A* 2003; **100:** 14175-80.

11. Dijkers PF, Medema RH, Lammers JW, Koenderman L, Coffer PJ. Expression of the pro-apoptotic Bcl-2 family member Bim is regulated by the forkhead transcription factor FKHR-L1. *Curr Biol* 2000; **10:** 1201-4.

12. Stahl M, Dijkers PF, Kops GJ, Lens SM, Coffer PJ, Burgering BM *et al.* The forkhead transcription factor FoxO regulates transcription of p27Kip1 and Bim in response to IL-2. *Journal of immunology* 2002; **168:** 5024-31.

13. Togher S, Larange A, Schoenberger SP, Feau S. FoxO3 is a negative regulator of primary CD8+ T-cell expansion but not of memory formation. *Immunology and cell biology* 2015; **93:** 120-5.

14. Tzelepis F, Joseph J, Haddad EK, Maclean S, Dudani R, Agenes F *et al.* Intrinsic role of FoxO3a in the development of CD8+ T cell memory. *Journal of immunology* 2013; **190:** 1066-75.

15. Sullivan JA, Kim EH, Plisch EH, Peng SL, Suresh M. FOXO3 regulates CD8 T cell memory by T cell-intrinsic mechanisms. *PLoS Pathog* 2012; **8:** e1002533.

16. Brunet A, Bonni A, Zigmond MJ, Lin MZ, Juo P, Hu LS *et al.* Akt promotes cell survival by phosphorylating and inhibiting a Forkhead transcription factor. *Cell* 1999; **96:** 857-68.

17. Keir ME, Freeman GJ, Sharpe AH. PD-1 regulates self-reactive CD8+ T cell responses to antigen in lymph nodes and tissues. *J Immunol* 2007; **179:** 5064-70.

18. Waithman J, Gebhardt T, Davey GM, Heath WR, Carbone FR. Cutting edge: Enhanced IL-2 signaling can convert self-specific T cell response from tolerance to autoimmunity. *J Immunol* 2008; **180:** 5789-93.

19. Kurts C, Miller JF, Subramaniam RM, Carbone FR, Heath WR. Major histocompatibility complex class I-restricted cross-presentation is biased towards high dose antigens and those released during cellular destruction. *J Exp Med* 1998; **188:** 409-14.

20. Youngson NA, Vickaryous N, van der Horst A, Epp T, Harten S, Fleming JS *et al.* A missense mutation in the transcription factor Foxo3a causes teratomas and oocyte abnormalities in mice. *Mamm Genome* 2011; **22:** 235-48.

21. Pope C, Kim SK, Marzo A, Masopust D, Williams K, Jiang J *et al.* Organ-specific regulation of the CD8 T cell response to Listeria monocytogenes infection. *J Immunol* 2001; **166:** 3402-9.

22. Khalil AM, Cambier JC, Shlomchik MJ. B cell receptor signal transduction in the GC is short-circuited by high phosphatase activity. *Science* 2012; **336:** 1178-81.

23. Kurts C, Sutherland RM, Davey G, Li M, Lew AM, Blanas E *et al.* CD8 T cell ignorance or tolerance to islet antigens depends on antigen dose. *Proc Natl Acad Sci U S A* 1999; **96:** 12703-7.

24. Hedrick SM, Hess Michelini R, Doedens AL, Goldrath AW, Stone EL. FOXO transcription factors throughout T cell biology. *Nature reviews. Immunology* 2012; **12:** 649-61.

25. Herold MJ, Rohrbeck L, Lang MJ, Grumont R, Gerondakis S, Tai L *et al.* Foxo-mediated Bim transcription is dispensable for the apoptosis of hematopoietic cells that is mediated by this BH3-only protein. *EMBO Rep* 2013; **14:** 992-8.

CHAPTER 3: The ubiquitin ligase adaptor NDFIP1 selectively enforces a CD8$^+$ T cell tolerance checkpoint to high dose antigen

Wagle M V., Marchingo JM, Howitt J, Tan SS, Goodnow CC, Parish IA. The Ubiquitin Ligase Adaptor NDFIP1 Selectively Enforces a CD8+T Cell Tolerance Checkpoint to High-Dose Antigen. Cell Rep. 2018;24(3):577–84.

The online publication in Cell Reports can be accessed through the following DOI: https://doi.org/10.1016/j.celrep.2018.06.060

The following manuscript included in the thesis has been modified to fit the thesis layout and may differ from the original manuscript submitted in the following ways. In this manuscript, the methods section is placed between the introduction and results sections, the methods included in the original manuscript and supplementary information are pooled together in section 3.3. The result figures are incorporated into the results section 3.4 and supplementary figures and tables are included after the references section 3.9. The figure numbers have been modified to include the chapter number in the prefix, for example from Figure 1 to Figure 3.1.

3.1: Abstract

Escape from peripheral tolerance checkpoints that control cytotoxic $CD8^+$ T cells is important for cancer immunotherapy and autoimmunity, but pathways enforcing these checkpoints are mostly uncharted. We reveal that the HECT-type ubiquitin ligase activator, NDFIP1, enforces a cell intrinsic $CD8^+$ T cell checkpoint that desensitises TCR signaling during *in vivo* exposure to high antigen levels. *Ndfip1*-deficient OT-I $CD8^+$ T cells responding to high exogenous tolerogenic antigen doses that normally induce anergy aberrantly expanded and differentiated into effector cells that could precipitate autoimmune diabetes in RIP-OVA^{hi} mice. In contrast, NDFIP1 was dispensable for peripheral deletion to low-dose exogenous or pancreatic islet-derived antigen, and had little impact upon effector responses to *Listeria* or acute LCMV infection. These data provide evidence that NDFIP1 mediates a $CD8^+$ T cell tolerance checkpoint, with a different mechanism to $CD4^+$ T cells, and indicate that $CD8^+$ T cell deletion and anergy are molecularly separable checkpoints.

3.2: Introduction

Activated $CD8^+$ T lymphocytes are key effector cells of the adaptive immune system that produce inflammatory cytokines and lytic granule proteins to kill infected or neoplastic cells. However, potentially pathogenic self-reactive $CD8^+$ T cells escape thymic selection, and peripheral tolerance checkpoints have thus evolved to control these cells and to enable tolerance to food, commensal microbiota, and fetal antigens. These peripheral checkpoints must respond to a wide range of antigen levels, due to variation in antigen amount released by different tissues. Malignant cancer cells can exploit these checkpoints to prevent immune recognition of mutated neo-antigens, and checkpoint inhibitors have emerged as a third pillar of cancer treatment alongside chemotherapy and radiotherapy.

Peripheral $CD8^+$ T cells undergo deletion or anergy when resting naïve T cells encounter antigen in the absence of infection or inflammation. In this context, the responding T cells do not become cytotoxic effectors and adopt a transcriptional

profile that is distinct from other differentiation states (Hernandez et al., 2001; Parish et al., 2009). $CD8^+$ T cell deletion occurs when cells undergo BIM-dependent apoptosis but largely retain T cell receptor (TCR) signaling capacity (Davey et al., 2002; Parish et al., 2009; Redmond et al., 2005; Wagle and Parish, 2016), whereas $CD8^+$ T cell anergy is characterised by persistence of cells with diminished TCR signaling, with tolerogenic antigen levels thought to determine outcome (Redmond et al., 2005). The molecular pathways that enforce $CD8^+$ T cell anergy *in vivo* are poorly defined, and it is unknown if anergy checkpoint disruption interferes with $CD8^+$ T cell deletion, or if the two processes are molecularly distinct.

NDFIP1, a Golgi and intracellular vesicle localized transmembrane protein, plays a selective checkpoint role within $CD4^+$ T cells (Altin et al., 2014; Oliver et al., 2006). NDFIP1 binds to and activates HECT-type E3 ubiquitin ligases (Mund and Pelham, 2009; Riling et al., 2015), thereby triggering ubiquitin-mediated degradation of key T cell differentiation regulators, including JUNB, RORgt and JAK1 (Layman et al., 2017b; O'Leary et al., 2016; Oliver et al., 2006). In T cells, NDFIP1 primarily recruits and activates the HECT-type E3 ligase ITCH (Oliver et al., 2006). *Ndfip1* deficient $CD4^+$ T cells resist both *in vitro* anti-CD3 induced anergy, and *in vivo* tolerance to low or high antigen levels, due to excessive IL-2 production, a failure to exit cell cycle and aberrant differentiation into Th2 or Th17 cells (Altin et al., 2014; Layman et al., 2017b; Oliver et al., 2006; Ramos-Hernandez et al., 2013). Mice lacking NDFIP1 develop a fatal T cell-mediated inflammatory disease associated with T cell activation, regulatory T cell dysfunction and Th2-mediated organ pathology (Altin et al., 2014; Beal et al., 2011; Layman et al., 2017a; Oliver et al., 2006). NDFIP1 likely plays similar roles in humans, as *NDFIP1* polymorphisms and *ITCH* deficiency are associated with inflammatory and autoimmune diseases (Ferreira et al., 2011; Franke et al., 2010; Hu et al., 2011; International Multiple Sclerosis Genetics et al., 2011; Lohr et al., 2010; Ramon et al., 2011).

Despite elevated activated effector $CD8^+$ T cells in *Ndfip1*$^{-/-}$ mice, and high *Ndfip1* expression in $CD8^+$ T cells (Altin et al., 2014), $CD8^+$ T cell activation in *Ndfip1*$^{-/-}$ mice is largely an indirect consequence of excessive IL-4 production by *Ndfip1*-mutant $CD4^+$ T cells (Altin et al., 2014; Kurzweil et al., 2014). However, excessive bystander inflammation in *Ndfip1*$^{-/-}$ mice may mask a $CD8^+$ T cell intrinsic role for NDFIP1. Here

we circumvent these complications by transferring *Ndfip1*-mutant and wild-type OT-I TCR transgenic $CD8^+$ T cells and tracing their response. We reveal that NDFIP1 is a critical checkpoint against $CD8^+$ T cell expansion and effector formation during chronic exposure to high tolerogenic antigen levels.

3.3: Experimental procedures

3.3.1: Mice

C57BL/6, OT-I, B6.129S7-*Rag1*^{tm1Mom}/J (*Rag1*$^{-/-}$) and B6.SJL-*PtprcaPep3b*/BoyJ (CD45.1) mice were purchased from the Australian Phenomics Facility, ANU, Australia. RIP-OVA^{hi} (Kurts et al., 1998), *Ndfip1*$^{kru/kru}$ (Altin et al., 2014), GzmB-cre (Jacob and Baltimore, 1999) and *Ndfip1*$^{f/f}$ (Howitt et al., 2012) mice have been previously described. All animal work was in accordance with protocols approved by the ANU Animal Experimentation Ethics Committee and current guidelines from the Australian Code of Practice for the Care and Use of Animals for Scientific Purposes.

3.3.2: Peptide injections, rapamycin treatment and mouse infection

SIINFEKL peptide (Biomolecular Resource Facility, ANU) was injected intravenously in PBS, while rapamycin was injected intraperitoneally at a dose of 600µg/kg (diluted in PBS from a concentrated stock in DMSO). For *Listeria* infections, mice were infected with 10^5 c.f.u. LM-OVA (Pope et al., 2001) intravenously. For LCMV-Armstrong infections, mice were injected intraperitoneally with $2x10^5$ p.f.u. of virus. Diabetes monitoring was conducted by urine glucose measurements using Diastix (Bayer).

3.3.3: T cell preparation for adoptive transfer

Naïve $CD8^+$ $CD45.1^+$ OT-I cells were enriched from spleen and lymph nodes by incubating single cell suspensions with rat monoclonal antibodies against Mac-1 (M1/70), macrophages (F4/80), red blood cells (Ter119), Gr1 (RB6-8C5), MHC class II (M5/114), CD44 (IM7) and CD4 (GK1.5) on ice for 30 min. The rat antibody-labelled cells were removed by anti-rat IgG-coupled magnetic beads (Polysciences

Inc.). Cells were CTV labelled in RPMI (Life Technologies) containing 10% Foetal Calf Serum with 10 μM CTV (Invitrogen) at room temperature for 5 min. Ratios of OT-I cells in the anergy group were normalised to the naïve ratio in the PBS treatment group by dividing the % population of each subset in anergy group by the % in PBS group. Cell enrichment after low OT-I cell number transfer experiments (Fig S2F,G) was conducted exactly as described previously (Hataye et al., 2006), except that a CD45.2-PE antibody was used to enrich the transferred cells.

3.3.4: EdU treatment and staining

Mice were injected i.p. with 0.25mg of EdU on days 4 and 5 of the experiment, after which splenocytes were stained using the indicated antibodies and the Click-iT EdU Alexa Fluor 647 Flow Cytometry Assay Kit (Life Technologies) followed according to manufacturer's instructions.

3.3.5: Flow cytometric analysis

Cell suspensions were stained in PBS containing 2.5% Foetal Calf Serum and 0.1% Azide. Intracellular staining was conducted using the Foxp3 Transcription Factor Staining Buffer Set (eBioscience) according to manufacturer's instructions. Samples were collected on a BD LSRII, Fortessa or X20 flow cytometer (BD Biosciences). The following antibodies/reagents were used for staining (purchased from Biolegend unless otherwise stated): CD8a (clone 53-6.7), CD44 (clone IM7), KLRG1 (clone 2F1), CD107a (clone 1D4B), IFN-g (clone XMG1.2), TNF-a (clone MP6-XT22), IL-2 (clone JES6-5H4), CD127 (clone A7R34), CD45.1 (clone A20), CD45.2 (clone 104), CD62L (clone MEL14), CD25 (clone PC61), GzmB (clone GB11; ThermoFisher Scientific), Ki67 (clone B56; BD Biosciences), JunB (clone C37F9; Cell Signaling Technology), Bim (Cat. No. 2819; Cell Signaling Technology), Bcl2 (3F11; BD Biosciences), ppErk1/2 (clone 197G2; Cell Signaling Technologies), pS6 (clone D57.2.2E; Cell Signaling Technologies), Annexin V, 7AAD and Zombie Aqua Fixable Viability Kit. Annexin V staining was conducted in Annexin V Binding Buffer (Biolegend). MHCI LCMV tetramers were purchased from the Biomolecular Resource Facility, JCSMR, ANU.

3.3.6: Phosphoflow and cytokine staining experiments

For phosphoflow analysis of OT-I cells, cells were restimulated with 0.1µg/ml SIINFEKL peptide for 15 minutes. Cells were then fixed and permeabilised using the BD Phosflow Fix Buffer I and Perm Buffer III according to manufacturer's instructions. Cells were stained with the appropriate surface and phosphoflow antibodies for 1 hour at room temperature in PBS containing 2.5% Foetal Calf Serum and 0.1% Azide. For cytokine staining, OT-I cells or LCMV-specific cells were restimulated with 0.1µg/ml OVA SIINFEKL, LCMV GP_{33-41} or LCMV $NP_{396-404}$ peptide in the presence of 3µg/ml Brefeldin A (eBioscience) and CD107a antibody for 5-6 hours, prior to surface staining then fixation with Biolegend Fixation Buffer, and intracellular cytokine staining in eBioscience Permeabilisation Buffer according to manufacturer's instructions. In order to normalize the MFI to the PBS group (or WT group in Figures 3.5 and 3.S5), the MFI in each of the subsets was divided by the MFI of the marker in the *Ndfip1*$^{+/+}$ OT-I cells in the PBS group, or corresponding cells from the WT group.

3.3.7:In vivo cytotoxicity assay

For the in vivo cytotoxicity assay (Oehen and Brduscha-Riem, 1998), pooled lymph nodes and spleens were harvested from CD45.1 mice, and red blood cells were lysed in 0.83% NH_4Cl. Cells were split in half, with half the cells pulsed in 0.3µg/ml SIINFEKL peptide at 37^{o}C for 1 hr, and the other half mock treated. Peptide pulsed cells were then labeled with a high concentration of CTV (5µM) while unpulsed cells were labeled with a low concentration of CTV (0.5µM) using the labeling protocol described above. Once labeled, cells were mixed together again, and 10^7 cells were injected per mouse. The ratios of CD45.1+ CTV^{hi} and CTV^{lo} cells were then assessed within the spleen by flow cytometry. % lysis was calculated as follows: [1 – (r unprimed/r primed)] x 100, where "r"= %CTV^{hi} / %CTV^{lo}.

3.3.8: Histology

H&E and GAF stains were performed on pancreata fixed in Neutral Buffered Formalin by the MCRF, JCSMR, ANU. Sections were visualised using a Olympus IX 71 microscope and DP 70 controller software (version 1.2.1.108).

3.3.9: Statistical analysis

Data analysis was conducted using Prism Software (GraphPad). Data were analysed using paired or unpaired T tests, or a Two-way ANOVA with a Bonferroni post-test (Fig. 3.S5A-C).

3.4: Results

3.4.1: Ndfip1 is dispensable for CD8$^+$ T cell deletional tolerance to a pancreatic self-antigen

Bystander CD8$^+$ T cell activation confounds analysis of any CD8$^+$ T cell intrinsic role of NDFIP1 in *Ndfip1*$^{kru/kru}$ mice homozygous for an NDFIP1-truncating null mutation (Altin et al., 2014). Activated/effector CD44^{hi} CD8$^+$ T cell accumulation was reduced in *Ndfip1*$^{kru/kru}$ mice bearing a rearranged TCR transgene encoding OT-I, an ovalbumin (OVA)-specific MHC I-restricted TCR, and was completely abolished in *Rag1*$^{-/-}$ OT-I *Ndfip1*$^{kru/kru}$ mice where no other TCRs can be expressed (Fig. 3.S1A). Thus *Rag1*$^{-/-}$ *Ndfip1*$^{kru/kru}$ OT-I mice provided a homogeneous source of naïve *Ndfip1*-deficient CD8$^+$ T cells.

We first tested a peripheral CD8$^+$ T cell deletion checkpoint triggered by low self-antigen from pancreatic islet b cells, as NDFIP1 loss disrupts a similar CD4$^+$ T cell checkpoint (Altin et al., 2014). A 50:50 mix of *Ndfip1*$^{kru/kru}$ (CD45.1/CD45.2) and *Ndfip1*$^{+/+}$ (CD45.1/CD45.1) *Rag1*$^{-/-}$ OT-I CD8$^+$ T cells was labeled with the cell division dye Cell Trace Violet (CTV). The cells were injected into CD45.2/CD45.2 *Ndfip1*$^{+/+}$ *Rag1*$^{+/+}$ recipients bearing the RIP-OVA^{hi} transgene, or non-transgenic (B6) controls (Fig. 3.S1B). In RIP-OVA^{hi} mice, soluble OVA expressed in insulin secreting pancreatic islet β cells is constitutively cross-presented by dendritic cells in the draining pancreatic lymph nodes. Transferred OT-I cells divide in response to cross-presented OVA, but do not form cytotoxic effector cells and undergo BIM-dependent apoptotic death (Davey et al., 2002; Parish et al., 2009; Wagle and Parish, 2016). However, co-transferred *Ndfip1*$^{kru/kru}$ and *Ndfip1*$^{+/+}$ OT-I cells proliferated comparably as assessed by cell ratios, numbers and CTV dilution (Fig. 3.S1C-E) and failed to

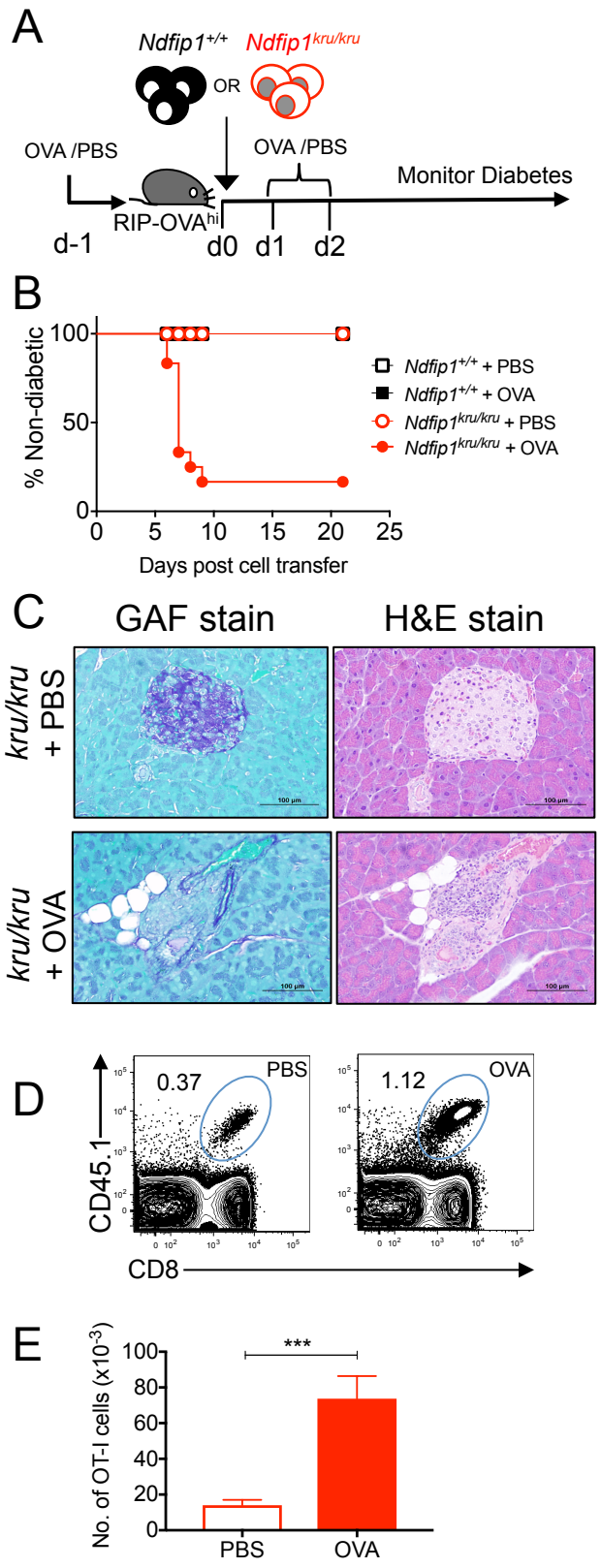
A
Ndfip1+/+
Ndfip1kru/kru
OR
OVA /PBS
OVA /PBS
Monitor Diabetes
RIP-OVAhi
d-1
d0
d1
d2
B
% Non-diabetic
100
50
0
0
5
10
15
20
25
Days post cell transfer
Ndfip1+/+ + PBS
Ndfip1+/+ + OVA
Ndfip1kru/kru + PBS
Ndfip1kru/kru + OVA
C
GAF stain
H&E stain
kru/kru + PBS
kru/kru + OVA
D
0.37
PBS
1.12
OVA
CD45.1
CD8
E
No. of OT-I cells (x10-3)
100
80
60
40
20
0
***
PBS
OVA

Figure 3.1. NDFIP1 limits autoimmune pathology after high antigen dose stimulation. 2x10^6 *Ndfip1*$^{+/+}$ or *Ndfip1*$^{kru/kru}$ OT-I cells were injected into RIP-OVA^{hi} mice that did or did not receive 10µg OVA peptide on days -1,1,2 as in (A). (B) Diabetes incidence in the treatment groups (n=17 mice/group from 2 experiments). (C) Representative day 9 islet histology sections from peptide or PBS treated RIP-OVA^{hi} mice in (B) that received *Ndfip1*$^{kru/kru}$ OT-I cells. (D,E) Representative (D) and pooled data (E; Error bars are SEM) showing *Ndfip1*$^{kru/kru}$ OT-I numbers at day 9 in the draining sacral and pancreatic lymph nodes of peptide treated RIP-OVA^{hi} versus PBS treated control mice (pooled B6 and RIP-OVA^{hi} mice) (n=7 mice/group from 2 experiments). *** = $p<0.001$

differentiate into effector cells (data not shown) in RIP-OVA^{hi} recipients. RIP-OVA^{hi} mice given either *Ndfip1*$^{kru/kru}$ or *Ndfip1*$^{+/+}$ OT-I cells also did not develop diabetes, with both wild-type and mutant cells deleted normally by 6 weeks post-transfer (Fig. 3.S1F-H). Thus, in contrast to CD4$^+$ T cells, *Ndfip1* is dispensable for a peripheral CD8$^+$ T cell deletion checkpoint to a tissue-restricted self-antigen.

3.4.2: Ndfip1-deficiency disrupts CD8$^+$ T cell tolerance to a pancreatic self-antigen in the context of higher antigen doses

Islet-specific *Ndfip1*-mutant CD4$^+$ T cells do not cause diabetes unless simultaneously exposed to a large, systemic bolus of tolerogenic antigen (Altin et al., 2014). To test if a similar NDFIP1-dependent checkpoint exists in CD8$^+$ T cells, RIP-OVA^{hi} mice injected with *Ndfip1* mutant or wild-type OT-I cells as in Fig. 3.S1F (day 0) were given either a high dose (10µg) of OVA-peptide (SIINFEKL) or saline (PBS) on days -1, 1 and 2 (Fig. 3.1A). As in Fig. 3.S1G, neither wild-type nor mutant cells caused diabetes without peptide treatment (Fig. 3.1B). Peptide treated wild-type OT-I cells also did not cause diabetes (Fig. 3.1B). However, 84% of RIP-OVA^{hi} mice given mutant OT-I cells and systemic OVA-peptide developed diabetes associated with pancreatic islet infiltration and destruction (Fig. 3.1B,C), with peptide treatment augmenting mutant cell numbers (Fig. 3.1D,E). Thus, NDFIP1 cell autonomously restrains effector CD8$^+$ T cell accumulation and target tissue cell destruction, but only in response to high systemic tolerogen levels.

3.4.3: Tolerogen concentration governs Ndfip1 restraint of CD8$^+$ T cell expansion and differentiation

Low tolerogen doses induce peripheral CD8$^+$ T cell deletion, whereas higher doses cause CD8$^+$ T cell persistence in an anergic state (Redmond et al., 2005). To test if NDFIP1 is important for the CD8$^+$ T cell anergy but not low dose deletion checkpoint, we co-transferred a 50:50 mix of CD45-marked *Ndfip1*$^{kru/kru}$ and *Ndfip1*$^{+/+}$ OT-I cells into wild-type B6 mice as before (day -1, Fig. 3.2A). Recipient mice were then given daily i.v. injections of either PBS or a low (1µg) or high (10µg) dose of OVA-peptide, on days 0, 1 and 2. The mutant and wild-type OT-I cell numbers increased comparably in the spleen by day 3 after the first peptide injection (Fig. 3.2B-D).

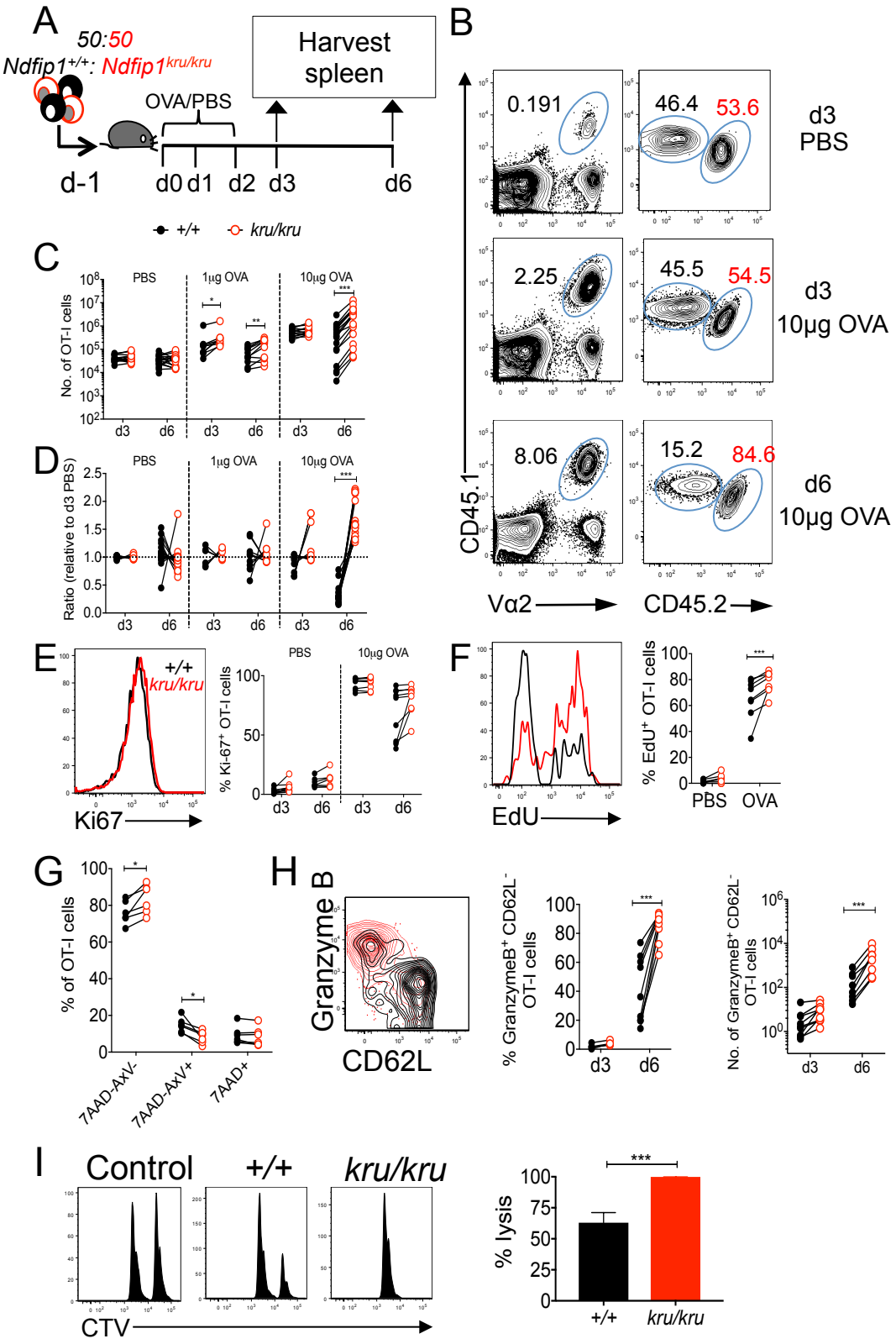
A
50:50
Ndfip1+/+: Ndfip1kru/kru
OVA/PBS
Harvest spleen
d-1
d0 d1 d2 d3
d6
+/+
kru/kru
B
0.191
46.4
53.6
d3 PBS
2.25
45.5
54.5
d3 10µg OVA
8.06
15.2
84.6
d6 10µg OVA
CD45.1
Vα2
CD45.2
C
PBS
1µg OVA
10µg OVA
No. of OT-I cells
d3
d6
D
Ratio (relative to d3 PBS)
E
+/+
kru/kru
Ki67
% Ki-67+ OT-I cells
F
EdU
% EdU+ OT-I cells
PBS
OVA
G
% of OT-I cells
7AAD-AxV-
7AAD-AxV+
7AAD+
H
Granzyme B
CD62L
% GranzymeB+ CD62L- OT-I cells
No. of GranzymeB+ CD62L- OT-I cells
I
Control
+/+
kru/kru
CTV
% lysis

Figure 3.2. *Ndfip1* mutant OT-I cells resist tolerance to high antigen doses. B6 mice were injected with 2x10^6 OT-I cells that were a 50:50 mix of *Ndfip1*$^{+/+}$ and *Ndfip1*$^{kru/kru}$ cells, then peptide treated and analysed as in (A). (B-D) Representative plots and pooled data showing the ratio (B,D) and number (C) of *Ndfip1*$^{+/+}$ (CD45.1/CD45.1) and *Ndfip1*$^{kru/kru}$ (CD45.1/CD45.2) OT-I cells after low and high dose OVA peptide treatment (n=6-19 mice/group from 3-5 experiments). (E) The % Ki67+ *Ndfip1*$^{+/+}$ and *Ndfip1*$^{kru/kru}$ OT-I cells after high dose peptide treatment on the indicated days (n=7-10 mice/group from 3-4 experiments). Histogram shows data at day 6. (F) EdU incorporation into *Ndfip1*$^{+/+}$ and *Ndfip1*$^{kru/kru}$ OT-I cells at day 6 after high dose peptide treatment (n=7-8 mice/group from 2 experiments). Histogram shows data at day 6. (G) The percent live (7AAD-AxV-), early apoptotic (7AAD-AxV+) and late apoptotic/necrotic (7AAD+) *Ndfip1*$^{+/+}$ and *Ndfip1*$^{kru/kru}$ OT-I cells at day 6 after high dose peptide (n=6 mice/group from 2 experiments). (H) The % and number of Granzyme B$^+$ CD62L$^+$ *Ndfip1*$^{+/+}$ and *Ndfip1*$^{kru/kru}$ OT-I cells at days 3 and 6 after high dose peptide (n=8-9 mice/group from 4 experiments). Contour plot shows data at day 6. (I) B6 mice given 2x10^6 *Ndfip1*$^{+/+}$ or *Ndfip1*$^{kru/kru}$ OT-I cells were treated with high dose OVA-peptide or PBS as in (A). At day 6, mice (including "Control" untreated B6 mice) were injected with a 50:50 mix of OVA-peptide coated CTV^{hi} and untreated CTV^{lo} CTL target cells, and splenic target cell lysis was measured after 4 hours. Representative histograms and the % lysis are shown (n=8 mice/group from 2 experiments, error bars are SEM). * = $p<0.05$, ** = $p<0.01$, *** = $p<0.001$

However, a striking increase in *Ndfip1*$^{kru/kru}$ relative to *Ndfip1*$^{+/+}$ OT-I cells occurred by day 6 after high dose peptide, with mutant cells making up 86% of cells (Fig. 3.2B-D). By contrast, mutant cell ratios and numbers exhibited little difference at day 6 after low dose peptide (Fig. 3.2C,D). Thus, NDFIP1 acts cell autonomously to inhibit CD8$^+$ T cell expansion to high systemic tolerogen levels.

In CD4$^+$ T cells, NDFIP1 promotes cell cycle exit as measured by Ki67 loss in T cells responding to low or high tolerising antigen doses (Altin et al., 2014). By contrast, the fraction of Ki67$^+$ OT-I cells induced by high dose peptide was comparable in mutant and wild-type cells (Fig. 3.2E). We next measured the replication rate of responding OT-I cells on days 4 and 5 through incorporation of the thymidine analogue 5-Ethynyl-2´-deoxyuridine (EdU), and a higher percentage of *Ndfip1*$^{kru/kru}$ OT-I cells had incorporated EdU by day 6 (Fig. 3.2F). By contrast, the pro-apoptotic protein BIM, which mediates CD8$^+$ T cell death in tolerance models (Davey et al., 2002), was comparably expressed in mutant and wild-type OT-I cells (Fig. 3.S2A). Paradoxically, the pro-survival BCL2 protein was down regulated in *Ndfip1*-mutant T cells (Fig. 3.S2B), but this likely reflects greater effector differentiation (see below). However, when mutant and wild-type OT-I cell death was analysed with the cell viability dye 7AAD and Annexin V (AxV), there was a small decrease in early apoptotic (AxV+7AAD-) mutant OT-I cells, with a corresponding increase in AxV-7AAD- live cells (and no change in late apoptotic/necrotic 7AAD+ cells) (Fig. 3.2G). Thus, NDFIP1 restrains both CD8$^+$ T cell replication rate and survival in response to high tolerogen doses.

We next tested if *Ndfip1*-mutant OT-I cells aberrantly became effectors, since CD8$^+$ T cell peripheral tolerance checkpoints normally inhibit cytotoxic effector cell differentiation by limiting cytolytic protease granzyme B (GzmB) expression and cytokine production (Hernandez et al., 2001; Parish et al., 2009). In response to high dose peptide, a higher percentage and number of GzmB$^+$ CD62L$^-$ *Ndfip1*-mutant OT-I cells were seen on day 6 (Fig. 3.2H). To assess if this translated into increased target killing by mutant cells, we conducted an in vivo cytotoxicity assay on day 6. After 4 hours, we observed significantly more killing by splenic mutant versus wild-type OT-I cells (Figure 3.2I). As the assay was saturated in the mutant condition (ie. all peptide-pulsed targets were killed), this likely underestimates mutant OT-I cell

killing. In contrast, mutant cells did not exhibit elevated cytokine production at any time point (Fig. 3.S2C). OT-I cells variably maintained the capacity to degranulate (as assessed by surface CD107a expression), but mutant and wild-type degranulation was similar (Fig. 3.S2D). Elevated GzmB$^+$ CD62L$^-$ *Ndfip1*-mutant OT-I cells were also seen at low peptide doses, although this was less pronounced than at high peptide doses (Fig. 3.S2E) and no GzmB$^+$ CD62L$^-$ mutant OT-I cells were seen in RIP-OVA^{hi} mice not treated with peptide (data not shown). Thus, in addition to increased expansion, NDFIP1-deficient CD8$^+$ T cells aberrantly form cytolytic effectors.

As naïve precursor frequency can affect CD8$^+$ T cell differentiation, we next examined if *Ndfip1*-mutant OT-I cells aberrantly expanded and differentiated at low precursor frequencies. While more variability was observed at lower precursor frequencies, we still observed augmented expansion and effector differentiation of mutant OT-I cells (Fig. 3.S2F,G) suggesting that the mutant phenotype is largely independent of precursor frequency.

3.4.4: Ndfip1 limits TCR signaling in anergic CD8$^+$ T cells

We next asked if exaggerated effector cell formation in *Ndfip1* deficient OT-I cells was via the same mechanism as in CD4$^+$ T cells. In *Ndfip1*$^{-/-}$ CD4$^+$ T cells, exaggerated Th2 differentiation is accompanied by greater levels of the Th2 transcription factor, JUNB, which is a direct target of ITCH (Altin et al., 2014; Oliver et al., 2006). *Ndfip1*$^{-/-}$ CD4$^+$ T cells also produce more IL-2 and express more of the high affinity IL-2 receptor (CD25) (Ramos-Hernandez et al., 2013). By contrast, there was no increase in IL-2, CD25 or JUNB in NDFIP1-deficient OT-I cells responding to high peptide doses (Fig. 3.S2C, Fig. 3.S3A,B). Thus, the NDFIP1-mediated CD8$^+$ T cell checkpoint is distinct from the checkpoint mechanism in CD4$^+$ T cells.

We next examined if NDFIP1 restrains TCR signaling in CD8$^+$ T cells, since the ITCH ubiquitin ligase inhibits TCR signaling during *in vitro* ionomycin-induced CD4$^+$ T cell anergy (Heissmeyer et al., 2004), and TCR-induced ERK phosphorylation is inhibited in CD8$^+$ T cells exposed to high tolerogen doses (Redmond et al., 2005). After *in vitro* peptide restimulation, 76% of control OT-I cells from PBS-treated mice

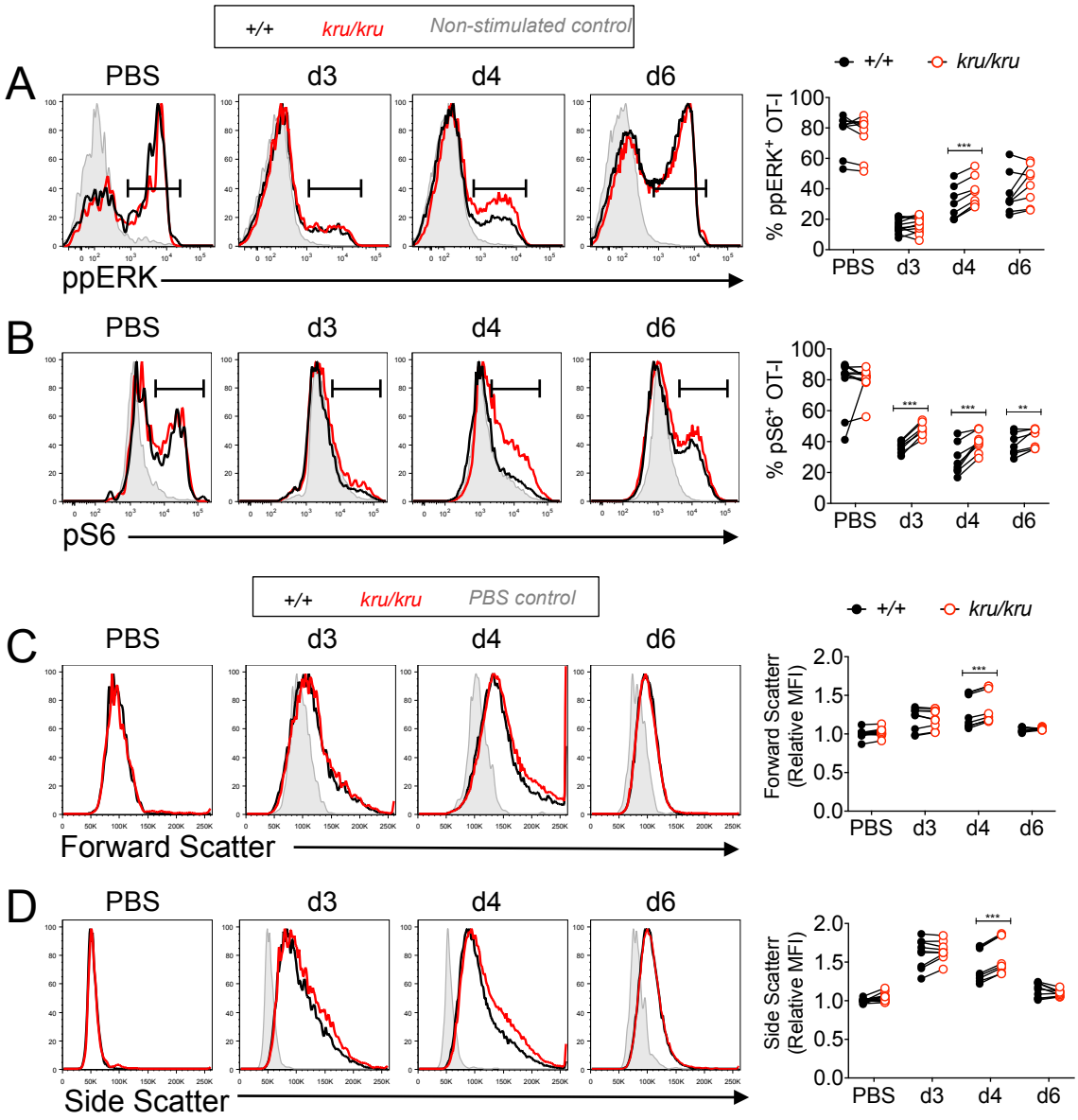

Figure 3.3. NDFIP1 restrains OT-I TCR signaling after high dose peptide treatment. OT-I cells subjected to high dose OVA peptide treatment in Fig. 3.2 were analysed for ppERK and pS6 upon 15 min *in vitro* peptide restimulation (A,B; n=7-11 mice/group from 3 experiments), or forward and side scatter (C,D; n=8-16 mice/group from 4 experiments), at the indicated time points. ** = p<0.01, *** = p<0.001

phosphorylated ERK (denoted ppERK; PBS group, Fig. 3.3A). By contrast, on day 3, only 15% of OT-I cells treated with high dose peptide were ppERK$^+$ after restimulation, regardless of *Ndfip1* genotype. However, on day 4, *in vitro* restimulation induced ppERK in 30% of OT-I cells, with a significantly more ppERK$^+$ *Ndfip1*-deficient versus wild-type cells (Fig. 3.3A). By day 6, ERK signaling in mutant and wild-type cells had recovered comparably. Recovery of function upon antigen withdrawal within peptide anergy models has been observed previously (Pape et al., 1998; Redmond et al., 2005).

TCR-induced mTOR signaling is impaired during CD4$^+$ T cell anergy (Zheng et al., 2007), and this was also seen in OT-I cells exposed to 10µg OVA peptide. 79% of restimulated OT-I cells from PBS-treated mice phosphorylated ribosomal protein S6 (pS6), an mTOR target, compared to only 37% of wild-type OT-I cells on day 3 (Fig. 3.3B). *Ndfip1*-deficient OT-I cells again had a partial rescue in signaling, with significantly greater pS6 responses at this timepoint and on days 4 and 6 (Fig. 3.3B).

Since ERK and mTOR signaling promote anabolic growth, we compared forward scatter as a measure of cell size in *Ndfip1*-deficient and wildtype OT-I cells before restimulation. Forward and side scatter were significantly increased in *Ndfip1* mutant versus wild-type OT-I cells on day 4 (Fig. 3.3C,D). Thus, an inability to fully dampen TCR signaling in *Ndfip1* mutant OT-I cells may explain their exaggerated expansion and effector differentiation.

To test if augmented mTOR signaling causes the *Ndfip1* mutant OT-I cell phenotype, mice containing peptide stimulated wild-type and mutant OT-I cells were treated with rapamycin from days 3-5 of the experiment. While rapamycin treatment reduced overall OT-I expansion and effector differentiation (Fig. 3.S3C,D), augmented expansion and differentiation of mutant relative to wild-type OT-I cells was still observed (Fig. 3.S3E,F). Thus, elevated mTOR signaling alone cannot explain the mutant phenotype.

3.4.5: Ndfip1 restrains CD8$^+$ T cell expansion and effector differentiation during continuous antigen exposure

NDFIP1-deficient CD8$^+$ T cells underwent exaggerated expansion and effector differentiation after the last peptide injection. We thus asked if NDFIP1 loss would disrupt this CD8$^+$ T cell checkpoint in the face of sustained antigen by continuing the high dose peptide injections for the duration of the experiment (Fig. 3.4A). *Ndfip1* mutant OT-I cells exposed to sustained antigen still expanded to much higher numbers than co-transferred wild-type cells (Fig. 3.4B) and formed more GzmB$^+$ CD62L$^-$ effector cells (Fig. 3.4C). As with transient peptide treatment, the NDFIP1-deficient cells retained higher TCR-induced ppERK and pS6 (Fig. 3.4D,E), and displayed an increase in forward and side scatter (Fig. 3.4F,G).

3.4.6: Ndfip1 does not limit CD8$^+$ T cell expansion and differentiation during infection

To test if NDFIP1 also repressed effector T cell expansion and differentiation during an acute infection, *Ndfip1* mutant or wild-type OT-I cells were transferred into B6 mice that were then infected with *Listeria monocytogenes,* using a strain that transgenically expresses OVA (Fig. 3.S4A). Wild-type and mutant OT-I cell expansion was similar at day 10 post-infection (Fig. 3.S4B). mTOR signaling promotes effector CD8$^+$ T cell terminal differentiation (Araki et al., 2009), but we did not see an increase in terminal effectors (KLRG1^{hi}CD127^{lo}) or loss of memory precursors (KLRG1^{lo}CD127^{hi}) in mutant cells, suggesting no functionally relevant increase in mTOR signaling (Fig. 3.S4C). Thus, *Ndfip1* loss does not influence effector CD8$^+$ T cell differentiation and expansion during *Listeria* infection.

To better delineate effector and memory differentiation of *Ndfip1*$^{-/-}$ CD8$^+$ T cells, we examined the response to acute lymphocytic choriomeningitis virus Armstrong strain (LCMV-Arm) infection. To avoid bystander autoimmunity in *Ndfip1*$^{kru/kru}$ mice, we used mice bearing a floxed *Ndfip1* allele (*Ndfip1*$^{f/f}$) and a GranzymeB-cre (GzmB-cre) transgene. GzmB-cre mice delete floxed alleles in activated effector CD8$^+$ T cells during LCMV infection, but only minimally flox genes in activated CD4$^+$ T cells (Rutishauser et al., 2009). Consistent with minimal gene deletion in CD4$^+$ T cells, no

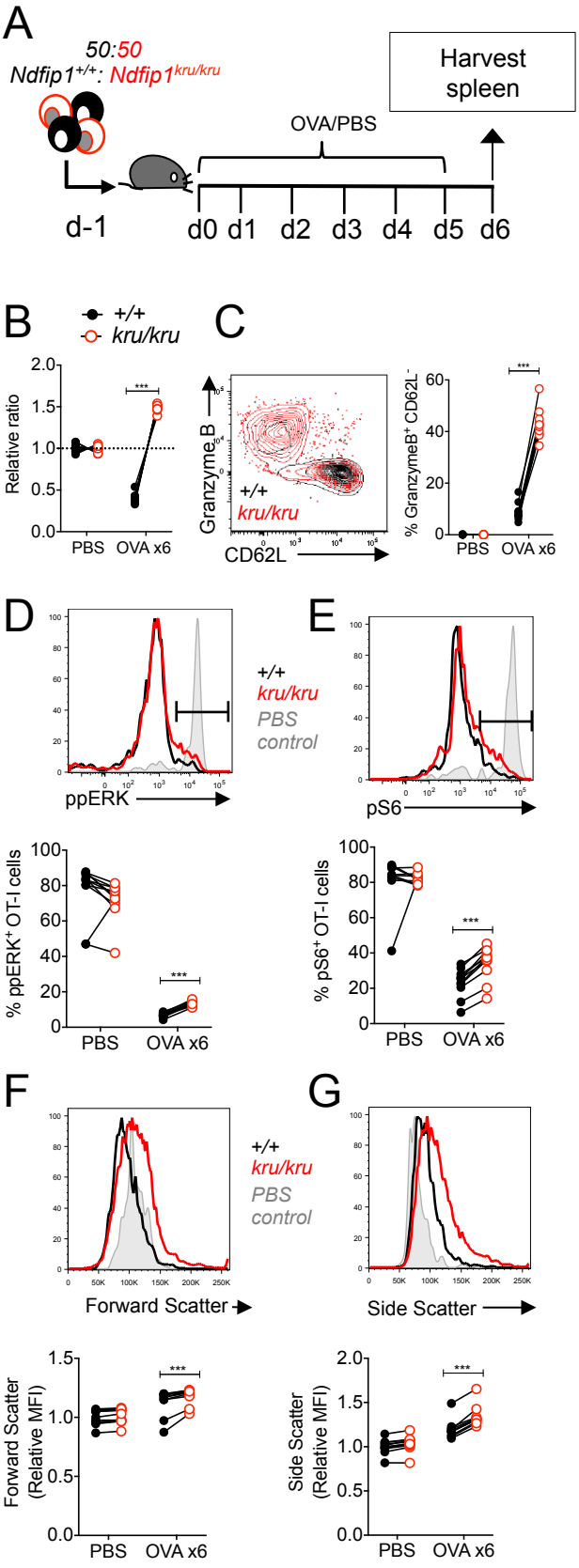
A
50:50
Ndfip1+/+: Ndfip1kru/kru
Harvest spleen
OVA/PBS
d-1
d0 d1 d2 d3 d4 d5 d6
B
+/+
kru/kru
Relative ratio
PBS OVA x6
C
Granzyme B
CD62L
+/+
kru/kru
% GranzymeB+ CD62L-
PBS OVA x6
D
ppERK
+/+
kru/kru
PBS
control
% ppERK+ OT-I cells
PBS OVA x6
E
pS6
% pS6+ OT-I cells
PBS OVA x6
F
Forward Scatter
Forward Scatter (Relative MFI)
PBS OVA x6
G
Side Scatter
Side Scatter (Relative MFI)
PBS OVA x6

Figure 3.4. NDFIP1 controls OT-I anergy to sustained antigen. A high dose peptide anergy experiment was conducted as in Fig. 3.2, except OVA peptide (or PBS) treatment was sustained as in (A). The ratio of wild-type to mutant cells (B), Granzyme B and CD62L expression (C), ppERK and pS6 after *in vitro* peptide restimulation (D,E) and forward and side scatter (F,G) are shown (n=10-11 mice/group from 2 experiments). *** = $p<0.001$

dermatitis or fatal autoimmune disease was seen in GzmB-cre^{+} *Ndfip1*$^{f/f}$ mice up to 3-4 months of age and, unlike *Ndfip1*$^{-/-}$ mice, there was no accumulation of activated T cells in the blood of 8 week old mice (data not shown). GzmB-cre^{+} *Ndfip1*$^{f/f}$ (conditional KO, or cKO) mice, or GzmB-cre^{+} *Ndfip1*$^{+/+}$ littermate (WT) controls, were infected with LCMV-Arm, and the CD8^{+} T cell response tracked in the blood to an early memory time-point (day 42) after which splenic memory T cell number, phenotype and function was assessed. There was no change in expansion, contraction and persistence of tetramer^{+} CD8^{+} T cells specific for the immunodominant LCMV GP_{33-41} or $NP_{396-404}$ peptides in cKO versus WT mice (Fig. 3.S5A,B). While the proportion of KLRG1^{hi} and KLRG1^{lo}CD127^{hi} cells was also unchanged at the peak of expansion (day 8), a significant decrease in KLRG1^{lo}CD127^{hi} cells was seen within GP_{33-41} and (to a lesser extent) $NP_{396-404}$-specific cells (Fig. 3.S5B and data not shown), although accumulation of CD62L^{hi} central memory cells was normal (Fig. 3.S5C). Similar trends were observed within splenic memory cells (Fig. 3.S5D-F). However, memory T cell function was unchanged. The same number of IFNγ-producing cells was recovered in WT and cKO mice (Fig. 3.S5G), with no alteration in IFNγ produced per cell or the proportions of IFNγ+TNFα+ and IFNγ+TNFα+IL-2+ cells (Fig. 3.S5H). Thus, *Ndfip1* loss minimally impacts the CD8^{+} T cell response to an acute systemic infection.

3.5: Discussion

In this study, we reveal a CD8^{+} T cell intrinsic, highly context dependent NDFIP1-mediated tolerance checkpoint. *Ndfip1*-deficiency dysregulates CD8^{+} T cells by a different mechanism than in CD4^{+} T cells. *Ndfip1*$^{-/-}$ CD4^{+} T cell hyper-proliferation is due to elevated IL-2 production and an inability to exit cell cycle (Altin et al., 2014; Ramos-Hernandez et al., 2013), and is accompanied by excessive IL-4 production and Th2 differentiation due to JUNB accumulation (Oliver et al., 2006). By contrast, IL-2 production and JUNB was not increased in *Ndfip1* deficient OT-I cells, and augmented expansion was via more rapid proliferation and diminished death rather than cell-cycle exit deficiencies. Elevated GzmB expression in *Ndfip1* deficient CD8^{+} T cells demonstrates that NDFIP1 can inhibit Type 1 immune responses, in contrast

to $CD4^+$ T cells where NDFIP1 loss has little effect on Th1 differentiation (Layman et al., 2017b; Oliver et al., 2006).

The primary biochemical effect of NDFIP1 deficiency in high-zone $CD8^+$ T cell tolerance was partial recovery of TCR signaling. Other mechanisms, such as the ubiquitin ligase CBLB (Heissmeyer et al., 2004; Jeon et al., 2004) or diacylglycerol kinase alpha (Olenchock et al., 2006), must also contribute to TCR desensitization, since signaling in NDFIP1-deficient $CD8^+$ T cells remained lower than non-tolerized control T cells. NDFIP1 may directly target mTOR signaling pathway components, and increased mTOR signaling was proposed to augment *Ndfip1*$^{-/-}$ Treg proliferation and differentiation (Layman et al., 2017a), however our data suggest that elevated mTOR signaling alone cannot explain the mutant $CD8^+$ T cell phenotype. Our data also do not rule out a role for pathways beyond partially rescued TCR signaling in the *Ndfip1* mutant cell phenotype, and further work is required to pinpoint the mechanism.

Current studies on $CD8^+$ T cell checkpoints largely focus on exhaustion, where established effector cells lose inflammatory function when chronically stimulated. By contrast, *in vivo* tolerance checkpoints that regulate initial $CD8^+$ T cell activation are poorly defined in molecular terms. Our findings provide evidence that molecularly distinct tolerance pathways operate in the context of high and low tolerogen doses. As high and low antigen doses favour anergy and deletion respectively (Redmond et al., 2005), and only high-zone tolerance depends on NDFIP1, these data imply that deletion and anergy are molecularly separable states. This difference may be due to the 6 day delay in *Ndfip1* mutant OT-I cell phenotype; responding cells may die in deletion models before a phenotype can manifest. Alternatively, as *Ndfip1* is TCR-induced, it may only enforce tolerance during strong TCR engagement. However, there may be a delay in the kinetics of peripheral deletion that was missed in our study. Moreover, as a hallmark of anergy is cell persistence, the long-term persistence of *Ndfip1* deficient anergic cells needs to be examined.

The NDFIP1-mediated tolerance checkpoint may maintain $CD8^+$ T cell tolerance to abundant environmental antigens (eg. commensal and food antigens), fetal antigens once the fetus has increased in mass, or abundant peripheral self-antigens not

efficiently expressed in the thymus. Thus, dysregulated $CD8^+$ T cell tolerance could contribute to the autoimmune and inflammatory diseases seen in patients with *NDFIP1* polymorphisms. NDFIP1 may also limit $CD8^+$ T cell priming against high burden tumours, and could have utility in cancer immunotherapy. Finally, although *Ndfip1* loss has little effect on the effector T cell response to acute infection, our data do not rule out a role for *Ndfip1* in effector $CD8^+$ T cell exhaustion during chronic stimulation within tumours or persistent viral infection. Future work is needed to evaluate these possibilities.

3.6: Acknowledgements

We thank Debbie Howard and Sarp Kaya for technical assistance. This work was funded by National Institutes of Health Grant U19-AI100627, by an Australian Government Research Training Program Domestic Scholarship (M.V.W.), by a Sydney Parker Smith Postdoctoral Research Fellowship from the Cancer Council of Victoria (J.M.M.), and by the National Health and Medical Research Council (NHMRC) through Program Grants 1016953, 1113904 & 1054925, Australia Fellowship 585490 (C.C.G.), Senior Principal Research Fellowship 1081858 (C.C.G.), CJ Martin Early Career Fellowship 585518 (I.A.P.) and Independent Research Institutes Infrastructure Support Scheme Grant 361646. Florey Institute of Neuroscience and Mental Health and WEHI acknowledge the strong support from the Victorian Government and in particular funding from the Operational Infrastructure Support Grant.

3.7: Author contributions

M.V.W., I.A.P. and J.M.M. conducted experiments, M.V.W., J.M.M., C.C.G. and I.A.P. designed experiments, J.H. and S.S.T. provided important experimental resources, M.V.W., C.C.G. and I.A.P. wrote the paper.

3.8: Declarations of Interests

The authors declare no competing interests.

3.9: References

Altin, J.A., Daley, S.R., Howitt, J., Rickards, H.J., Batkin, A.K., Horikawa, K., Prasad, S.J., Nelms, K.A., Kumar, S., Wu, L.C.*, et al.* (2014). Ndfip1 mediates peripheral tolerance to self and exogenous antigen by inducing cell cycle exit in responding CD4+ T cells. Proc Natl Acad Sci USA *111*, 2067-2074.

Araki, K., Turner, A.P., Shaffer, V.O., Gangappa, S., Keller, S.A., Bachmann, M.F., Larsen, C.P., and Ahmed, R. (2009). mTOR regulates memory CD8 T-cell differentiation. Nature *460*, 108-112.

Beal, A.M., Ramos-Hernandez, N., Riling, C.R., Nowelsky, E.A., and Oliver, P.M. (2011). TGF-beta induces the expression of the adaptor Ndfip1 to silence IL-4 production during iTreg cell differentiation. Nat Immunol *13*, 77-85.

Davey, G.M., Kurts, C., Miller, J.F., Bouillet, P., Strasser, A., Brooks, A.G., Carbone, F.R., and Heath, W.R. (2002). Peripheral deletion of autoreactive CD8 T cells by cross presentation of self-antigen occurs by a Bcl-2-inhibitable pathway mediated by Bim. J Exp Med *196*, 947-955.

Ferreira, M.A., Matheson, M.C., Duffy, D.L., Marks, G.B., Hui, J., Le Souef, P., Danoy, P., Baltic, S., Nyholt, D.R., Jenkins, M.*, et al.* (2011). Identification of IL6R and chromosome 11q13.5 as risk loci for asthma. Lancet *378*, 1006-1014.

Franke, A., McGovern, D.P., Barrett, J.C., Wang, K., Radford-Smith, G.L., Ahmad, T., Lees, C.W., Balschun, T., Lee, J., Roberts, R.*, et al.* (2010). Genome-wide meta-analysis increases to 71 the number of confirmed Crohn's disease susceptibility loci. Nat Genet *42*, 1118-1125.

Hataye, J., Moon, J.J., Khoruts, A., Reilly, C., and Jenkins, M.K. (2006). Naive and memory CD4+ T cell survival controlled by clonal abundance. Science *312*, 114-116.

Heissmeyer, V., Macian, F., Im, S.H., Varma, R., Feske, S., Venuprasad, K., Gu, H., Liu, Y.C., Dustin, M.L., and Rao, A. (2004). Calcineurin imposes T cell unresponsiveness through targeted proteolysis of signaling proteins. Nat Immunol *5*, 255-265.

Hernandez, J., Aung, S., Redmond, W.L., and Sherman, L.A. (2001). Phenotypic and functional analysis of CD8(+) T cells undergoing peripheral deletion in response to cross-presentation of self-antigen. J Exp Med *194*, 707-717.

Howitt, J., Lackovic, J., Low, L.H., Naguib, A., Macintyre, A., Goh, C.P., Callaway, J.K., Hammond, V., Thomas, T., Dixon, M.*, et al.* (2012). Ndfip1 regulates nuclear Pten import in vivo to promote neuronal survival following cerebral ischemia. J Cell Biol *196*, 29-36.

Hu, X., Kim, H., Stahl, E., Plenge, R., Daly, M., and Raychaudhuri, S. (2011). Integrating autoimmune risk loci with gene-expression data identifies specific pathogenic immune cell subsets. Am J Hum Genet *89*, 496-506.

International Multiple Sclerosis Genetics Consortium, Wellcome Trust Case Control Consortium, Sawcer, S., Hellenthal, G., Pirinen, M., Spencer, C.C., Patsopoulos, N.A., Moutsianas, L., Dilthey, A., Su, Z.*, et al.* (2011). Genetic risk and a primary role for cell-mediated immune mechanisms in multiple sclerosis. Nature *476*, 214-219.

Jacob, J., and Baltimore, D. (1999). Modelling T-cell memory by genetic marking of memory T cells in vivo. Nature *399*, 593-597.

Jeon, M.S., Atfield, A., Venuprasad, K., Krawczyk, C., Sarao, R., Elly, C., Yang, C., Arya, S., Bachmaier, K., Su, L.*, et al.* (2004). Essential role of the E3 ubiquitin ligase Cbl-b in T cell anergy induction. Immunity *21*, 167-177.

Kurts, C., Miller, J.F., Subramaniam, R.M., Carbone, F.R., and Heath, W.R. (1998). Major histocompatibility complex class I-restricted cross-presentation is biased towards high dose antigens and those released during cellular destruction. J Exp Med *188*, 409-414.

Kurzweil, V., LaRoche, A., and Oliver, P.M. (2014). Increased peripheral IL-4 leads to an expanded virtual memory CD8+ population. J Immunol *192*, 5643-5651.

Layman, A.A.K., Deng, G., O'Leary, C.E., Tadros, S., Thomas, R.M., Dybas, J.M., Moser, E.K., Wells, A.D., Doliba, N.M., and Oliver, P.M. (2017a). Ndfip1 restricts mTORC1 signalling and glycolysis in regulatory T cells to prevent autoinflammatory disease. Nat Commun *8*, 15677.

Layman, A.A.K., Sprout, S.L., Phillips, D., and Oliver, P.M. (2017b). Ndfip1 restricts Th17 cell potency by limiting lineage stability and proinflammatory cytokine production. Sci Rep *7*, 39649.

Lohr, N.J., Molleston, J.P., Strauss, K.A., Torres-Martinez, W., Sherman, E.A., Squires, R.H., Rider, N.L., Chikwava, K.R., Cummings, O.W., Morton, D.H.*, et al.* (2010). Human ITCH E3 ubiquitin ligase deficiency causes syndromic multisystem autoimmune disease. Am J Hum Genet *86*, 447-453.

Mund, T., and Pelham, H.R. (2009). Control of the activity of WW-HECT domain E3 ubiquitin ligases by NDFIP proteins. EMBO Rep *10*, 501-507.

Oehen, S., and Brduscha-Riem, K. (1998). Differentiation of naive CTL to effector and memory CTL: correlation of effector function with phenotype and cell division. J Immunol *161*, 5338-5346.

O'Leary, C.E., Riling, C.R., Spruce, L.A., Ding, H., Kumar, S., Deng, G., Liu, Y., Seeholzer, S.H., and Oliver, P.M. (2016). Ndfip-mediated degradation of Jak1 tunes cytokine signalling to limit expansion of CD4+ effector T cells. Nat Commun *7*, 11226.

Olenchock, B.A., Guo, R., Carpenter, J.H., Jordan, M., Topham, M.K., Koretzky, G.A., and Zhong, X.P. (2006). Disruption of diacylglycerol metabolism impairs the induction of T cell anergy. Nat Immunol *7*, 1174-1181.

Oliver, P.M., Cao, X., Worthen, G.S., Shi, P., Briones, N., MacLeod, M., White, J., Kirby, P., Kappler, J., Marrack, P.*, et al.* (2006). Ndfip1 protein promotes the function of itch ubiquitin ligase to prevent T cell activation and T helper 2 cell-mediated inflammation. Immunity *25*, 929-940.

Pape, K.A., Merica, R., Mondino, A., Khoruts, A., and Jenkins, M.K. (1998). Direct evidence that functionally impaired CD4+ T cells persist in vivo following induction of peripheral tolerance. J Immunol *160*, 4719-4729.

Parish, I.A., Rao, S., Smyth, G.K., Juelich, T., Denyer, G.S., Davey, G.M., Strasser, A., and Heath, W.R. (2009). The molecular signature of CD8+ T cells undergoing deletional tolerance. Blood *113*, 4575-4585.

Pope, C., Kim, S.K., Marzo, A., Masopust, D., Williams, K., Jiang, J., Shen, H., and Lefrancois, L. (2001). Organ-specific regulation of the CD8 T cell response to Listeria monocytogenes infection. J Immunol *166*, 3402-3409.

Ramon, H.E., Riling, C.R., Bradfield, J., Yang, B., Hakonarson, H., and Oliver, P.M. (2011). The ubiquitin ligase adaptor Ndfip1 regulates T cell-mediated gastrointestinal inflammation and inflammatory bowel disease susceptibility. Mucosal Immunol *4*, 314-324.

Ramos-Hernandez, N., Ramon, H.E., Beal, A.M., Laroche, A., Dekleva, E.A., and Oliver, P.M. (2013). Ndfip1 enforces a requirement for CD28 costimulation by limiting IL-2 production. J Immunol *191*, 1536-1546.

Redmond, W.L., Marincek, B.C., and Sherman, L.A. (2005). Distinct requirements for deletion versus anergy during CD8 T cell peripheral tolerance in vivo. J Immunol *174*, 2046-2053.

Riling, C., Kamadurai, H., Kumar, S., O'Leary, C.E., Wu, K.P., Manion, E.E., Ying, M., Schulman, B.A., and Oliver, P.M. (2015). Itch WW Domains Inhibit Its E3 Ubiquitin Ligase Activity by Blocking E2-E3 Ligase Trans-thiolation. J Biol Chem *290*, 23875-23887.

Rutishauser, R.L., Martins, G.A., Kalachikov, S., Chandele, A., Parish, I.A., Meffre, E., Jacob, J., Calame, K., and Kaech, S.M. (2009). Transcriptional repressor Blimp-1 promotes CD8(+) T cell terminal differentiation and represses the acquisition of central memory T cell properties. Immunity *31*, 296-308.

Wagle, M.V., and Parish, I.A. (2016). FOXO3 is differentially required for CD8+ T-cell death during tolerance versus immunity. Immunol Cell Biol *94*, 895-899.

Zheng, Y., Collins, S.L., Lutz, M.A., Allen, A.N., Kole, T.P., Zarek, P.E., and Powell, J.D. (2007). A role for mammalian target of rapamycin in regulating T cell activation versus anergy. J Immunol *178*, 2163-2170.

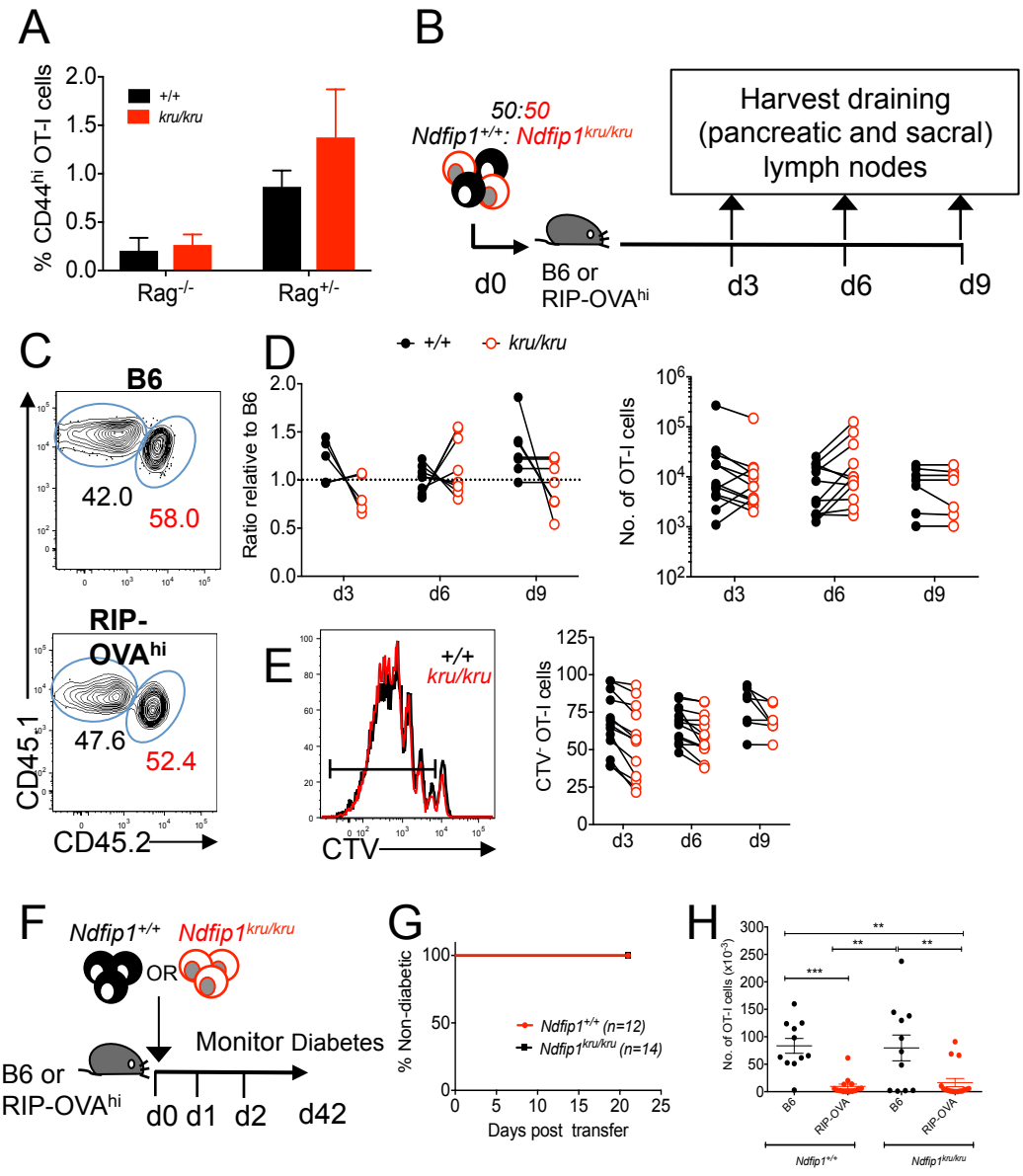
A
% CD44hi OT-I cells
+/+
kru/kru
Rag-/-
Rag+/-
B
50:50
Ndfip1+/+: Ndfip1kru/kru
Harvest draining (pancreatic and sacral) lymph nodes
d0
B6 or RIP-OVAhi
d3
d6
d9
C
B6
42.0
58.0
RIP-OVAhi
47.6
52.4
CD45.1
CD45.2
D
+/+
kru/kru
Ratio relative to B6
No. of OT-I cells
E
CTV
CTV- OT-I cells
F
Ndfip1+/+
OR
Ndfip1kru/kru
Monitor Diabetes
B6 or RIP-OVAhi
d0 d1 d2 d42
G
% Non-diabetic
Ndfip1+/+ (n=12)
Ndfip1kru/kru (n=14)
Days post transfer
H
No. of OT-I cells (x10-3)
B6
RIP-OVA
Ndfip1+/+
Ndfip1kru/kru

Figure 3.S1. *Ndfip1* is dispensable for peripheral tolerance in RIP-OVA^{hi} mice. Related to Figure 3.1. (A) The percentage of CD44^{hi} cells within *Ndfip1*$^{+/+}$ or *Ndfip1*$^{kru/kru}$ OT-I cells on either a *Rag1*$^{+/-}$ or *Rag1*$^{-/-}$ background (n=4-18 mice per group). Error bars depict SEM. (B) Experimental outline; CD45.2/CD45.2 *Ndfip1*$^{+/+}$ *Rag1*$^{+/+}$ B6 or RIP-OVA^{hi} mice were i.v. injected with 2x10^6 CTV labeled OT-I cells that were a 50:50 mix of *Ndfip1*$^{+/+}$ and *Ndfip1*$^{kru/kru}$ cells, and the cells within the draining sacral and pancreatic lymph nodes were analysed at the indicated time points post-injection. The ratio and numbers (C,D), and CTV dilution (E), of *Ndfip1*$^{+/+}$ (CD45.1/CD45.2) and *Ndfip1*$^{kru/kru}$ (CD45.1/CD45.1) OT-I cells at the indicated time points are shown (data is pooled with 5-13 mice per group from 3-5 independent experiments). Representative plots are from day 6 (C) and day 3 (E). (F-H) B6 or RIP-OVA^{hi} mice were i.v. injected with 2x10^6 *Ndfip1*$^{+/+}$ or *Ndfip1*$^{kru/kru}$ CD45.1$^+$ OT-I cells and monitored as illustrated in (F). (G) Diabetes incidence measured daily for 21 days within RIP-OVA^{hi} mice by urine glucose testing. (H) *Ndfip1*$^{+/+}$ or *Ndfip1*$^{kru/kru}$ OT-I cell numbers within B6 or RIP-OVA^{hi} mice 42 days after cell transfer. Pooled data with 11-16 mice per group from 5 independent experiments are shown, error bars depict SEM. ** = $p<0.01$, *** = $p<0.001$

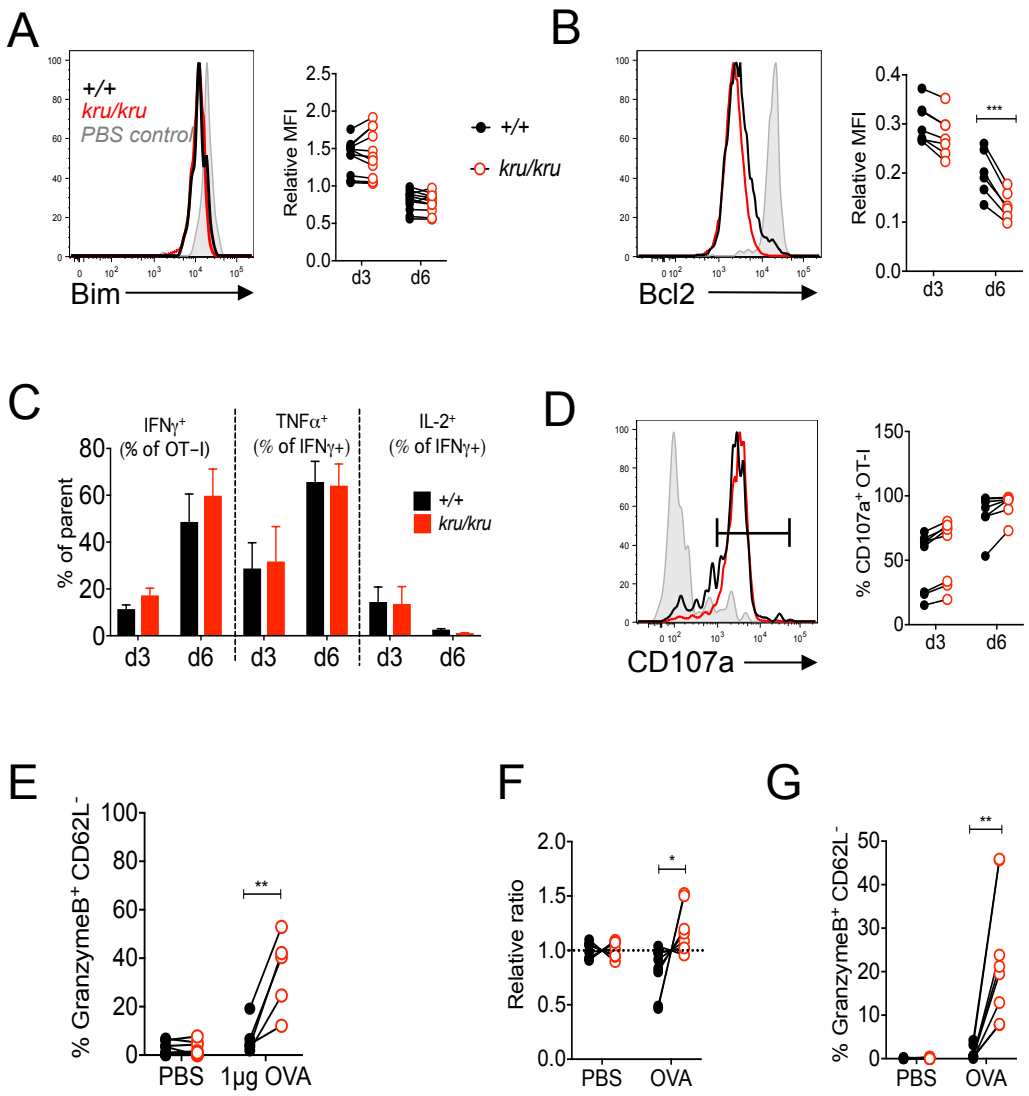
A
+/+
kru/kru
PBS control
Bim
Relative MFI
+/+
kru/kru
d3
d6
B
Bcl2
Relative MFI
***
C
IFNγ+ (% of OT-I)
TNFα+ (% of IFNγ+)
IL-2+ (% of IFNγ+)
% of parent
D
CD107a
% CD107a+ OT-I
E
% GranzymeB+ CD62L-
**
PBS
1μg OVA
F
Relative ratio
*
PBS
OVA
G
% GranzymeB+ CD62L-
**
PBS
OVA

Figure 3.S2: Expression of apoptosis regulators and cytokines by *Ndfip1* mutant OT-I cells. Related to Figure 3.2. The *Ndfip1*$^{+/+}$ and *Ndfip1*$^{kru/kru}$ OT-I cells treated with high dose (10µg) OVA-peptide from Figure 3.2 were analysed on the indicated days for Bim (A) and Bcl2 (B) expression, or cytokine production (C; error bars depict SEM) and degranulation (CD107a) (D) upon peptide restimulation, at the indicated time points. Representative plots are from day 6, and grey histograms indicate expression levels in PBS control naïve OT-I cells. Pooled data with 6-12 mice per group from 2-5 independent experiments are shown. (E) *Ndfip1*$^{+/+}$ and *Ndfip1*$^{kru/kru}$ OT-I cells treated with low dose (1µg) OVA-peptide as in Figure 3.2C,D were analysed for Granzyme B and CD62L expression at day 6. Pooled data with 5-11 mice per group from 3 independent experiments are shown. (F,G) CD45.1 B6 mice were injected with $5x10^4$ OT-I cells that were a 50:50 mix of *Ndfip1*$^{+/+}$ (CD45.2/CD45.2) and *Ndfip1*$^{kru/kru}$ (CD45.1/CD45.2) cells. Mice were then treated with PBS or a high dose (10µg) of OVA-peptide as in Figure 3.2A. At day 6, CD45.2+ cells were enriched from pooled lymph nodes and spleen of each mouse, and the ratio (F) and Granzyme B and CD62L expression (G) of wild-type and mutant cells was assessed. Pooled data with 8 mice per group from 2 independent experiments are shown. * = $p<0.05$, ** = $p<0.01$, *** = $p<0.001$

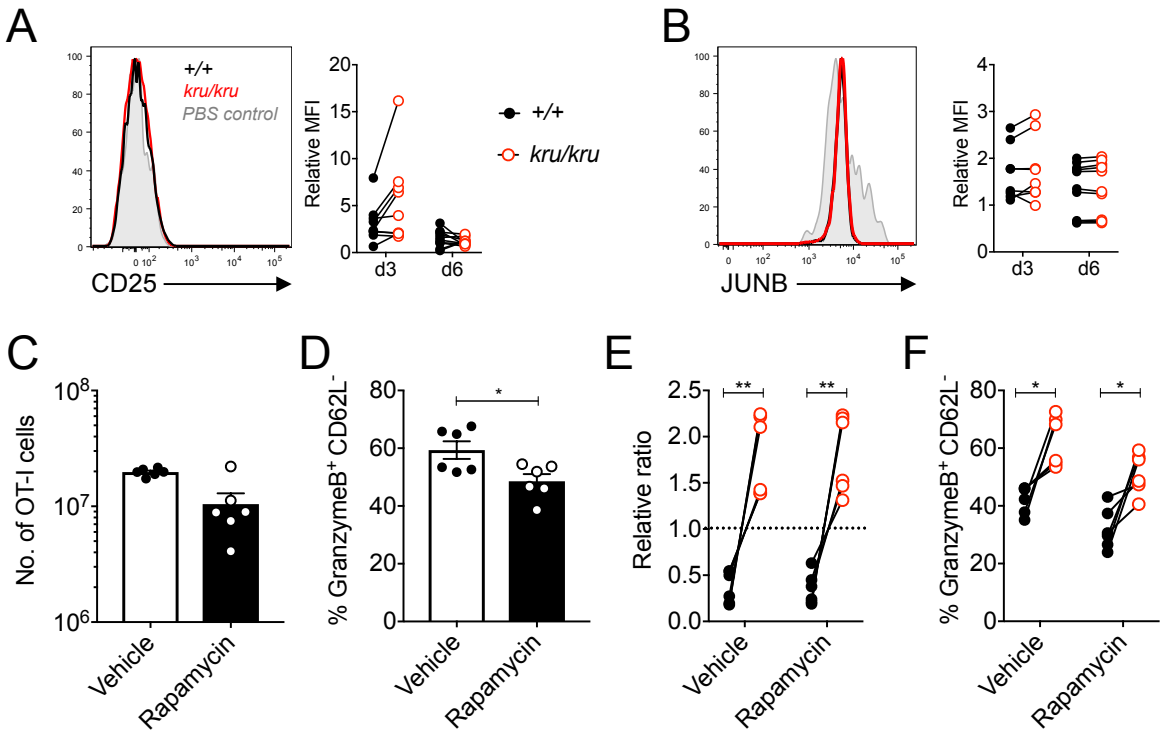

Figure 3.S3. JUNB and CD25 expression levels are unchanged by *Ndfip1* loss. Related to Figure 3.3. The *Ndfip1*$^{+/+}$ and *Ndfip1*$^{kru/kru}$ OT-I cells treated with high dose (10μg) OVA-peptide from Figure 3.2 were analysed on the indicated days for CD25 (A) and JUNB (B) expression. Representative plots are from day 6, and grey histograms indicate expression levels in PBS control naïve OT-I cells. Pooled data with 8-10 mice per group from 3 independent experiments are shown. (C-F) B6 mice given 2x10^6 OT-I cells that were a 50:50 mix of *Ndfip1*$^{+/+}$ and *Ndfip1*$^{kru/kru}$ cells were treated with high dose (10μg) OVA-peptide as in Figure 3.2A, except mice were then treated with 600μg/kg of rapamycin or vehicle from days 3-5 of the experiment. The total number of OT-I cells (ie. the combination of both genotypes) recovered as well as total Granzyme B and CD62L expression (C,D; error bars depict SEM), as well as the ratio (E) and Granzyme B and CD62L expression (F) of wild-type and mutant cells was assessed at day 6 of the experiment. Pooled data with 6 mice per group from 2 independent experiments are shown. * = p<0.05, ** = p<0.01

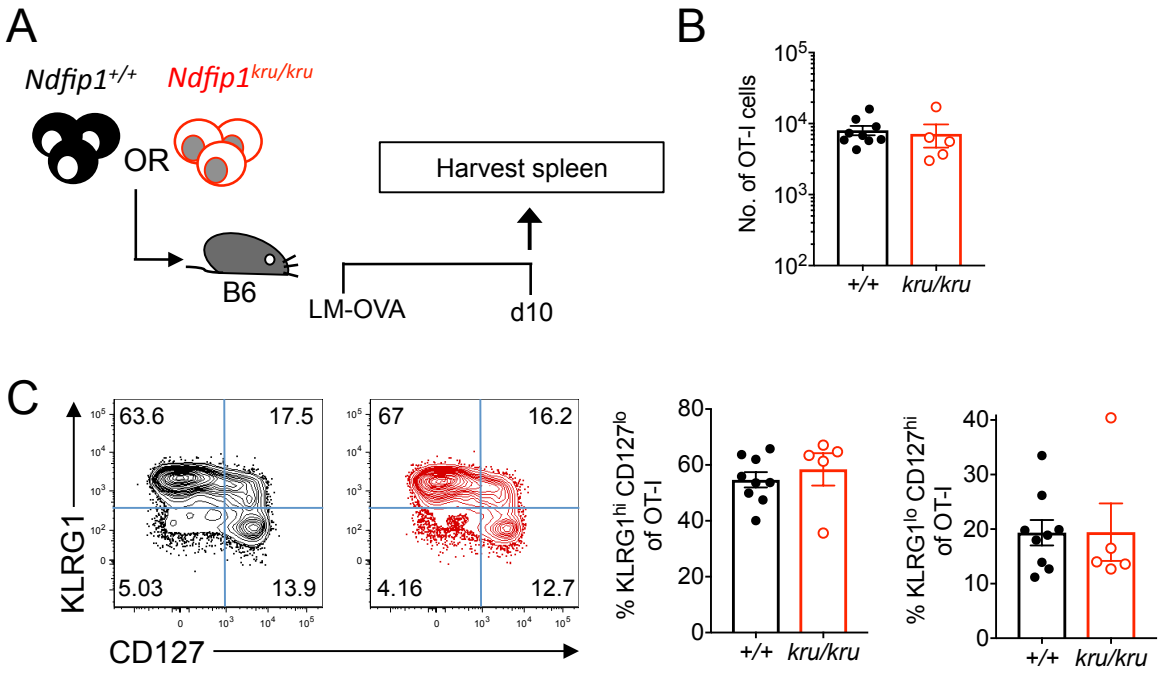

Figure 3.S4. *Ndfip1* loss does not affect OT-I expansion and differentiation during acute *Listeria* infection. Related to Figure 3.4. B6 mice were i.v. injected with 5x10^4 CD45.1$^+$ *Ndfip1*$^{+/+}$ or *Ndfip1*$^{kru/kru}$ OT-I cells and subsequently i.v. infected with 10^5 cfu of OVA transgenic *Listeria monocytogenes* (LM-OVA) as illustrated in (A). OT-I expansion (B) and terminal differentiation as assessed by KLRG1 and CD127 expression (C) was assessed at day 10 post-infection. Pooled data with 5-9 mice per group from 2 independent experiments are shown. Error bars depict SEM.

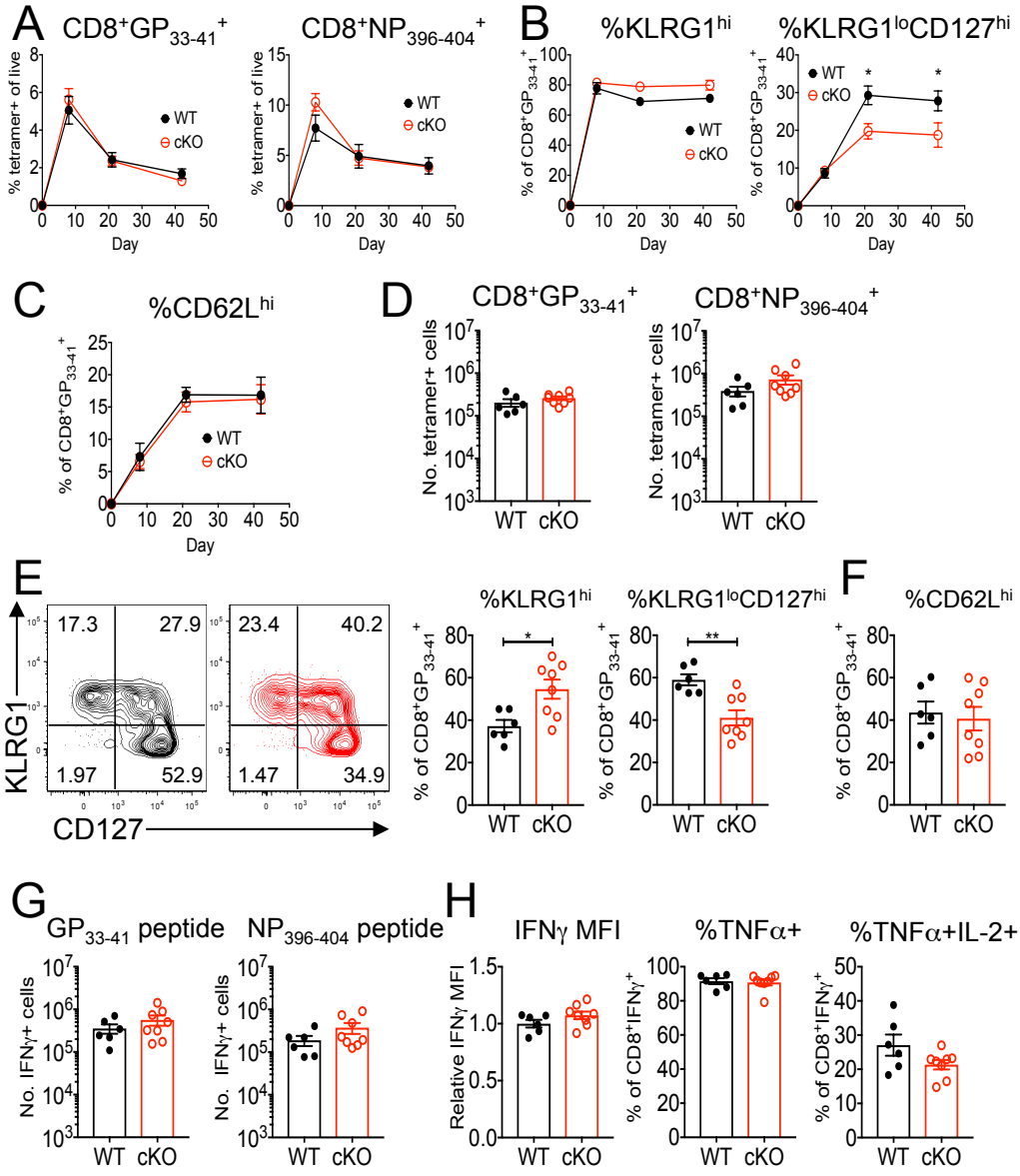
A
CD8+GP33-41+
CD8+NP396-404+
% tetramer+ of live
Day
WT
cKO
B
%KLRG1hi
%KLRG1loCD127hi
% of CD8+GP33-41+
C
%CD62Lhi
D
CD8+GP33-41+
CD8+NP396-404+
No. tetramer+ cells
E
KLRG1
CD127
17.3
27.9
1.97
52.9
23.4
40.2
1.47
34.9
F
%CD62Lhi
G
GP33-41 peptide
NP396-404 peptide
No. IFNγ+ cells
H
IFNγ MFI
Relative IFNγ MFI
%TNFα+
%TNFα+IL-2+
% of CD8+IFNγ+

Figure 3.S5. NDFIP1 loss has little effect on CD8$^+$ T cell effector and memory differentiation during acute LCMV infection. Related to Figure 3.4. GzmB-cre$^+$ *Ndfip1$^{f/f}$* (cKO) or GzmB-cre$^+$ *Ndfip1$^{+/+}$* (WT) mice were infected with LCMV-Arm, and the CD8$^+$ T cell response tracked in the blood (A-C) until day 42 post-infection when the splenic T cells were isolated and phenotyped (D-H). (A) The percentage of live WT or cKO blood cells that were CD8$^+$ and stained for the LCMV GP_{33-41} or $NP_{396-404}$ tetramers. (B,C) The percentage of KLRG1^{hi}, KLRG1^{lo}CD127^{hi} or CD62L^{hi} CD8$^+$$GP_{33-41}$$^+$ blood cells. (D) Number of splenic CD8$^+$$GP_{33-41}$$^+$ or CD8$^+$$NP_{396-404}$$^+$ cells. (E,F) The percentage of KLRG1^{hi}, KLRG1^{lo}CD127^{hi} or CD62L^{hi} CD8$^+$$GP_{33-41}$$^+$ splenocytes. (G) The number of CD8$^+$IFNγ$^+$ splenocytes after GP_{33-41} or $NP_{396-404}$ peptide restimulation. (H) IFNγ MFI, %TNFα+ and %TNFα+IL-2+ within CD8$^+$IFNγ$^+$ cells after GP_{33-41} peptide restimulation. n=6-8 mice per group from 2 experiments, error bars are SEM. * = $p<0.05$, ** = $p<0.01$

CHAPTER 4: The anergy-associated transcription factor EGR2 is re-purposed to promote terminal CD8$^+$ T cell exhaustion during chronic viral infection

Mayura V. Wagle[1], Stephin J. Vervoort[2,3], Madison J. Kelly[2], Ben P. Martin[2], James R. Torpy[4], Deborah Roseingrave[2], Lisa A. Miosge[1], Renee Gloury[5,6], Sarah S. Gabriel[5,6], Nenad Bartonicek[4], Jonathan D. Powell[7], Joseph A. Trapani[2,3], Ricky W. Johnstone[2,3], Axel Kallies[5,6], Christopher C. Goodnow[1,4,8,10], and Ian A. Parish[1,2,3,10]

[1]John Curtin School of Medical Research, Australian National University, ACT, Australia

[2]Peter MacCallum Cancer Centre, Melbourne, Victoria 3000, Australia

[3]Sir Peter MacCallum Department of Oncology, University of Melbourne, Melbourne, VIC, Australia.

[4]Garvan Institute of Medical Research, Darlinghurst, NSW 2010, Australia

[5]The Peter Doherty Institute for Infection and Immunity, University of Melbourne, Melbourne, VIC, Australia

[6]Department of Microbiology and Immunology, The University of Melbourne, Parkville, VIC, Australia

[7]Johns Hopkins University of Medicine, Baltimore, MD, USA

[8]Faculty of Medicine, University of New South Wales Sydney, Australia

[10]Senior author

The following manuscript included in the thesis has been modified to fit the thesis layout and may differ from the final manuscript to be submitted for publication. The result figures are incorporated into the results section 4.4 and supplementary figures and tables are included after the references section 4.8. The figure and table numbers have been modified to include the chapter number in the prefix, for example from Figure 1 to Figure 4.1 and Table S1 to Table 4.S1.

4.1: Abstract

Negative regulatory processes, such as anergy and exhaustion, cause active suppression of $CD8^+$ T cell effector functions. A longstanding question has been to what extent the same molecular pathways control exhaustion and anergy. We have addressed this question by examining the role of a transcriptional master regulator of anergy, EGR2, within the $CD8^+$ T cell exhaustion process. We demonstrate that EGR2 expression is elevated in an antigen-dependent manner within exhausted cells relative to functional effectors in the LCMV model of exhaustion. EGR2 loss triggered a block in terminal exhaustion, with evidence of direct EGR2-dependent regulation of key genes such as *Pdcd1*, *Tigit*, *Bcl6*, *Bach2* and *Tcf7*. Strikingly, the suite of genes directly regulated by EGR2 in the context of exhaustion minimally overlapped with previously characterised direct targets of EGR2 during anergy. Collectively, these data suggest that exhausted cells "re-purpose" a TCR-induced, anergy-associated transcription factor to promote terminal exhaustion.

4.2: Introduction

Chronic antigen encounter by $CD8^+$ T cells typically triggers diminished effector functions by engaging an array of regulatory pathways. Depending on the point during the T cell response at which persistent TCR signals are encountered, different outcomes can occur. Persistent stimulation of effector T cells during both chronic viral infection and tumour growth leads to a progressive loss of inflammatory cytokine production and survival capacity, in part due to up-regulation of inhibitory receptors that limit function (Wherry and Kurachi, 2015). This process is termed T cell exhaustion, and it represents a transcriptionally and epigenetically distinct differentiation state (Doering et al., 2012; Ghoneim et al., 2017; Man et al., 2017; Sen et al., 2016; Wherry et al., 2007). The regulatory pathways engaged within $CD8^+$ T cells during exhaustion impair immune control of tumours and infection, and thus rescuing the function of exhausted cells through inhibitory receptor blockade often demonstrates clinical efficacy in these contexts (Pauken and Wherry, 2015). Nevertheless, exhausted cells retain some inflammatory function and contribute to

immune control of infection (Jin et al., 1999; Schmitz et al., 1999), suggesting that exhaustion has evolved to enable T cells to contain an infection without causing deleterious immunopathology (Barber et al., 2006; Cornberg et al., 2013; Frebel et al., 2012). In contrast, persistent recognition of steady-state self-antigens by naïve T cells leads to peripheral tolerance induction (Redmond et al., 2003), a process that likely evolved to purge self-reactive T cells from the repertoire and thereby limit the risk of autoimmune disease (Parish and Heath, 2008; Walker and Abbas, 2002). Tolerant cells do not typically acquire effector functions (Hernandez et al., 2001), and are ultimately prevented from participating in future immune responses by either undergoing apoptotic death (Davey et al., 2002) or persisting in a hypofunctional state, termed anergy, which is characterised by TCR signaling deficiencies (Schwartz, 2003).

A longstanding and unresolved question within the field has been to what extent similar molecular pathways control anergy and exhaustion. While exhaustion, and peripheral tolerance processes such as anergy, occur at different points within the immune response, there are a number of similarities between these differentiation states. Both processes are programmed by persistent TCR signaling (Redmond et al., 2003; Shin et al., 2007), are maintained by the inhibitory receptor PD-1 (Barber et al., 2006; Goldberg et al., 2007; Keir et al., 2007; Probst et al., 2005; Tsushima et al., 2007), can be disrupted by IL-2 treatment (Blattman et al., 2003; Waithman et al., 2008), show deficiencies in TCR signaling (Schwartz, 2003; Staron et al., 2014), and both differentiation states exhibit a significant overlap in their gene expression profiles (Parish et al., 2009; Schietinger et al., 2016). These observations raise the possibility that the TCR-induced molecular pathways that limit effector functions during exhaustion and anergy are largely overlapping. Understanding whether these states are molecularly distinct has important clinical implications. Autoimmune adverse events are observed within a subset of cancer patients downstream of immune checkpoint blockade (Postow et al., 2018). Therapies such as PD-1 blockade disrupt both peripheral tolerance and exhaustion, which likely contributes to these autoimmune side-effects. However, if the pathways enforcing peripheral tolerance and exhaustion can be molecularly separated, it may be possible to develop more refined therapies that disrupt exhaustion within tumour-specific effector cells while leaving the peripheral tolerance process intact.

A key regulator of T cell anergy is the transcription factor EGR2. EGR2 inhibits T cell function during anergy through direct induction of factors that diminish TCR signalling, such as *Cblb*, *Dgka* and *Dgkz* (Zheng et al., 2012; Zheng et al., 2013), and *Egr2*$^{-/-}$ T cells are resistant to anergy induction (Safford et al., 2005; Zheng et al., 2012). Previous gene expression profiling studies have demonstrated that *Egr2* is also selectively up-regulated during CD8^{+} T cell exhaustion (Doering et al., 2012), suggesting that the EGR2-induced anergy program could contribute to impaired TCR signaling and diminished T cell function during exhaustion. In support of this idea, key EGR2 gene targets during anergy, such as *Cblb* and *Lag3* (Zheng et al., 2012; Zheng et al., 2013), are also induced during exhaustion (Blackburn et al., 2009; Man et al., 2017), and both *Cblb* and *Lag3* functionally contribute to the exhausted state (Blackburn et al., 2009; Ou et al., 2008).

Here, we directly examined the role of EGR2 in the exhaustion process. We found that persistent antigen recognition drove higher EGR2 expression within CD8^{+} T cells during chronic relative to acute lymphocytic choriomeningitis virus (LCMV) infection. EGR2 was transiently expressed within the TCF1^{+} memory-like exhausted T cell population, and promoted terminal differentiation of these cells. RNA-seq analysis revealed a broad loss of the terminal exhaustion program in EGR2-deficient T cells, with ChIP-seq analysis indicating that EGR2 directly induced key exhaustion genes, such as *Pdcd1* and *Tigit*, while directly repressing genes associated with a less terminally exhausted state, such as *Bcl6* and *Bach2*. Strikingly, there was little overlap between the gene targets bound by EGR2 in the context of exhaustion and those previously identified during anergy. Collectively, these data suggest that exhausted CD8^{+} T cells repurpose the function of an antigen-induced tolerance regulator to promote terminal exhaustion rather than the anergy gene program.

4.3: Methods

4.3.1: Mouse strains, adoptive transfer and infections

C57BL/6 (B6), B6.129S7-*Rag1*^{tm1Mom}/J (*Rag1*$^{-/-}$) and B6.SJL-*PtprcaPep3b*/BoyJ (CD45.1) mice were purchased from the Australian Phenomics Facility, ANU,

Australia or the Walter and Eliza Hall Institute Kew Animal Facility, VIC, Australia. P14 transgenic (Pircher et al., 1989), Egr2-GFP (Williams et al., 2017) and C57BL/6 backcrossed CD4-cre^{+} *Egr2* floxed (Ramon et al., 2010) mice have all been described previously. Mice were infected with 2x10^{5} pfu LCMV-Arm virus by intraperitoneal (i.p.) injection, or with 2x10^{6} pfu LCMV-Cl13 or LCMV-Cl13-V35A (Puglielli et al., 2001) virus by intravenous (i.v.) injection. LCMV viral plaque assays were conducted as described previously (Ahmed et al., 1984). For CD4 depletion, mice were injected with 200µg GK1.5 antibody (BioXCell) on days -1 and +1 of the infection. For P14 transfer experiments, 2x10^{3} CD45.1^{+} P14 cells were transferred i.v. into CD45.2^{+} B6 mice one day prior to infection. All animal work was in accordance with protocols approved by the ANU and Peter MacCallum Cancer Centre Animal Experimentation Ethics Committees, and current guidelines from the Australian Code of Practice for the Care and Use of Animals for Scientific Purposes.

4.3.2: Bone marrow chimeras

Bone marrow was prepared by flushing the bone marrow cells out of mouse femurs using a 26G needle. *Rag1*$^{-/-}$ recipient mice were irradiated with 5 Gy, and reconstituted with 2x10^{6} bone marrow cells consisting of a 50:50 mixture of wild-type B6.CD45.1^{+} bone marrow and B6.CD45.2^{+} CD4-cre^{+} *Egr2*$^{f/f}$ or CD4-cre^{+} *Egr2*$^{+/+}$ bone marrow. Mice were allowed to reconstitute for at least 8 weeks prior to use. To account for reconstitution differences between mice, the %CD45.2^{+} cells in the tetramer+ CD8^{+} T cell subset measured after infection was divided by the %CD45.2^{+} cells in all CD8^{+} T cells measured in the same mouse bled before infection, and then multiplied by 100 and divided by 2 to set the pre-infection %CD45.2^{+} at 50%.

4.3.3: CTV labeling, flow cytometric analysis and cell sorting

Single cell suspensions were prepared from lymphoid organs for flow cytometry and CTV labeling by passing the cells through a 70µm cell strainer. Cells were CTV labelled in RPMI (Life Technologies) containing 10% Foetal Calf Serum with 10 µM CTV (Invitrogen) at room temperature for 5 min. For MHCII I-A^{b}GP$_{66\text{-}77}$ tetramer staining, cells were stained at 37^{o}C for 1.5h in RPMI prior to staining for other markers. For all other surface flow cytometric staining, cell suspensions were stained in PBS containing 2.5% Foetal Calf Serum and 0.1% Azide on ice for 30 min. For

CXCR5 staining, cells were stained with CXCR5 antibody for 45 min. at room temperature prior to staining on ice for other markers. To eliminate dead cells from the analysis, cells were also stained with Fixable Viability Stain 620 (BD Biosciences) or LIVE/DEAD Fixable Aqua Dead Cell Stain Kit (Life Technologies) according to manufacturer's instructions. For intracellular staining, cells were fixed, permeabilised and stained using the Foxp3 Transcription Factor Staining Buffer Set (eBioscience) according to manufacturer's instructions. Samples were collected on a BD LSRII, Fortessa, X20 or Symphony flow cytometer (BD Biosciences), with data analysed using FlowJo Software (Tree Star).

4.3.4: Phosphoflow and cytokine staining experiments

For phosphoflow analysis, splenocytes were restimulated with plate-bound anti-CD3 (clone 500A2, BD Biosciences; coated using 1µg/ml antibody in PBS) in a flat-bottomed 96 well plate for 30 min. Cells were then fixed and permeabilised using the BD Phosflow Fix Buffer I and Perm Buffer III according to manufacturer's instructions. Cells were stained with the appropriate surface and phosphoflow antibodies for 1h at room temperature in PBS containing 2.5% Foetal Calf Serum and 0.1% Azide. For cytokine staining, cells were restimulated with 0.1µg/ml of the appropriate synthesised viral peptide (Biomolecular Resource Facility, ANU) in the presence of 3µg/ml Brefeldin A (eBioscience) and CD107a antibody for 6h, prior to surface staining then fixation with Biolegend Fixation Buffer, and intracellular cytokine staining in eBioscience Permeabilisation Buffer according to manufacturer's instructions.

4.3.5: Antibodies and tetramers used for flow cytometric analysis

The following antibodies were used for staining (purchased from Biolegend unless otherwise stated): CD8a (clone 53-6.7), CD4 (clone RM4-5), CD44 (clone IM7), CD107a (clone 1D4B), IFNg (clone XMG1.2), TNFa (clone MP6-XT22), IL-2 (clone JES6-5H4), CD45.1 (clone A20), CD45.2 (clone 104), Ly6C (clone AL21; BD Biosciences), PSGL1 (clone 4RA10; BD Biosciences), PD-1 (clone RMP1-30), Tim3 (clone RMT3-23), 2B4 (clone 2B4; BD Biosciences), Lag3 (clone C9B7W), CD160 (clone 7H1), Egr2 (clone erongr2; eBioscience), TCF1 (clone C63D9; Cell Signaling Technologies), CXCR5 (clone 2G8; BD Biosciences), Eomes (clone Dan11mag,

eBioscience), T-bet (clone eBio4B10, eBioscience), ppErk1/2 (clone 197G2; Cell Signaling Technologies), and pS6 (clone D57.2.2E; Cell Signaling Technologies). MHCI LCMV tetramers were purchased from the Biomolecular Resource Facility, JCSMR, ANU. The MHCII I-A^bGP_{66-77} tetramer was obtained from the NIH tetramer core facility (Emory University, Atlanta, GA).

4.3.6: RNAseq analysis

CD4 depleted WT or cKO mice were infected with LCMV-Cl13 (~5 mice per genotype per sort). At day 20 p.i., $CD8^+CD44^{int\text{-}hi}$ H-$2D^bGP_{33-41}$-tetramer stained cells were isolated by fluorescence activated cell sorting, with 2 separate sorts conducted per genotype (ie. 4 samples in total), and ~$1x10^5$-$2x10^5$ cells recovered per sort. Total RNA was isolated using Trizol LS (Thermo Fisher Scientific) according to manufacturer's instructions, and RNA-seq libraries were prepared at the Molecular Genomics Core Facility, Peter MacCallum Cancer Centre, using the Illumina TruSeq Stranded mRNA Library Prep Kit. Samples were sequenced on an Illumina NextSeq500 instrument with 75bp single-end reads. All reads were aligned to the mouse genome reference (GRCm38/mm10) sequence using HiSat2 (Kim et al., 2015) with default parameters. Read counts were then generated for each gene in each sample using FeatureCounts from the Subread package (v1.5.0-p3) (Liao et al., 2014) by using annotated gene locations. Differential expression analysis was performed using LIMMA (v3.32.4). An adjusted p-value threshold of 0.05 was used to identify significantly differentially-regulated genes. Pheatmap (v1.0.8) and ggplot2 (v2.2.1) were used for generation of volcano plots and annotated heatmaps. Gene Set Enrichment Analysis (Subramanian et al., 2005) was conducted by searching the fold change ranked cKO versus WT RNA-seq dataset against the genes from a published LCMV exhaustion signature (Man et al., 2017) or published signature of $CXCR5^+$ T cells during chronic LCMV (Im et al., 2016). For the Man *et al* dataset, a published gene list was filtered to only include genes with a FC of either >2 or <0.5 in the following 4 comparisons of WT RNAseq datasets: d8 Chronic vs d8 Acute, d8 Chronic vs Naïve, d30 Chronic vs d30 Acute and d30 Chronic vs Naïve. The resulting gene list was then split into genes up or down at d30 Chronic vs d30 Acute for the respective Exhaustion Up and Down signatures. For the Im *et al* dataset, genes with

a logFC of >2 ($CXCR5^-$ signature) or <-2 ($CXCR5^+$ signature) in the $CXCR5^-$ vs $CXCR5^+$ comparison were included.

4.3.7: ChIP-seq analysis

B6 mice were infected with LCMV-Cl13, and at day 20 p.i. Spleen and lymph nodes were isolated from the mice and pooled. $CD8^+$ T cells were then isolated by MACS enrichment (Miltenyi) according to manufacturer's instructions to yield ~93% purity of $CD8^+$ T cells. Briefly, cells were labelled with CD8-PE antibody then enriched with anti-PE beads. Bulk $CD8^+$ T cells were used in this analysis as we had previously confirmed by flow cytometry that, within total $CD8^+$ T cells during LCMV-Cl13 infection, EGR2 protein is only expressed within PD-1^+ $CD44^{int\text{-}hi}$ exhausted $CD8^+$ T cells. After enrichment, ~$60x10^6$ $CD8^+$ T cells from ~8 mice were then used for subsequent ChIP-seq analysis. Cells were resuspended in PBS and crossed-linked with fresh formaldehyde solution (Table 4.S4; 1X final concentration) for 30 min at room temperature. Excess formaldehyde was quenched with 125mM Glycine for 5 min before cells were washed once with ice-cold PBS. Cells were incubated 3 times with nuclear extraction buffer (Table 4.S4) containing Roche cOmplete protease inhibitors (MERCK, 04693159001) on ice for 5 min. Nuclear extracts were resuspended in sonication buffer (Table 4.S4) containing protease and Pierce phosphatase inhibitors (ThermoFisher Scientific, A32957) and sonicated using the Covaris S220 Focused Ultrasonicator for 18 min. Sheared lysates were diluted with 1 volume of ChIP dilution buffer (Table 4.S4) containing protease and phosphatase inhibitors. Protein A and Protein G Dynabeads (ThermoFisher Scientific, 10002D and 10004D) were mixed 1:1 (50µl total per IP) and washed in blocking buffer (Table 4.S4) containing protease inhibitors at 4^oC. Protein A/G beads were resuspended in ChIP IP buffer (Table 4.S4; ~0.5mL/IP) containing protease and phosphatase inhibitors and added to diluted lysates with 20µg of a previously validated polyclonal anti-EGR2 ChIP antibody (ab43020, Abcam) (Jang et al., 2010) and 0.45% bovine serum albumin (BSA). IP samples were incubated overnight at 4^oC while tumbling. Protein A/G beads were washed twice with ChIP IP buffer on ice, before washing once with ChIP Wash Buffer 1 and Wash Buffer 2 (Table 4.S4), each containing protease and phosphatase inhibitors, and washing twice with Tris-EDTA buffer (10mM Tris-HCl pH 7.5, 1mM EDTA). Washed beads were incubated with Reverse

Crosslinking Buffer (Table 4.S4) containing 45μg Proteinase K at 55°C for 1h and the supernatant was then isolated and incubated at 65°C overnight. DNA was isolated using the ChIP DNA Clean & Concentrator Kit (Zymo Research, D5205). Indexed libraries were prepared using KAPA Hyper Prep Kit for Illumina platforms (Kapa Biosystems) and the SeqCap Adapter Kit (Roche) following vendor's instructions. Library QC and quantification was performed using D1000 high-sensitivity screen tape with a 4200 TapeStation Instrument (Agilent Technologies) and size selected for between 200 bp and 500 bp using a Pippin Prep system (Sage Science). Libraries were pooled and sequenced with 75 bp single-end sequencing to a depth of 15–20x10^6 reads per sample on a NextSeq500 (Illumina). bcl2fastq (v2.17.1.14) was used for de-multiplexing. The Fastq files were then aligned to the mouse reference genome (GRCm38/mm10) using bowtie2 (v2.3.3). Samtools (v1.4.1) was used for manipulation of SAM and BAM files. MACS (v2.1.1) was used for peak-calling, and significant peaks (FDR<0.05) were then associated with the closest gene TSS using Bedtools (v2.26). Motif analysis was performed with Homer (v4.8). Browser viewable TDF files were generated using IGVTools (v2.3.95) and ChIP-Seq tracks were visualized using IGV (v2.3.55). Graphics were generated using deeptools (v2.5.3).

4.3.8: Statistical analysis

Data analysis was conducted using Prism Software (Version 7.0, GraphPad software). P values were calculated using a 2-tailed unpaired T test or a 2-tailed Mann–Whitney test when data failed normality tests. Where indicated in the text, a Chi-square test with Yate's correction or Fisher's Exact test was used to calculate enrichment P values.

4.4: Results

4.4.1: EGR2 expression is elevated in chronic relative to acute LCMV infection

During mouse infection with chronic LCMV Clone 13 (Cl13), virus-specific $CD8^+$ T cells adopt an exhausted state and fail to rapidly clear infection. In contrast, antigen-

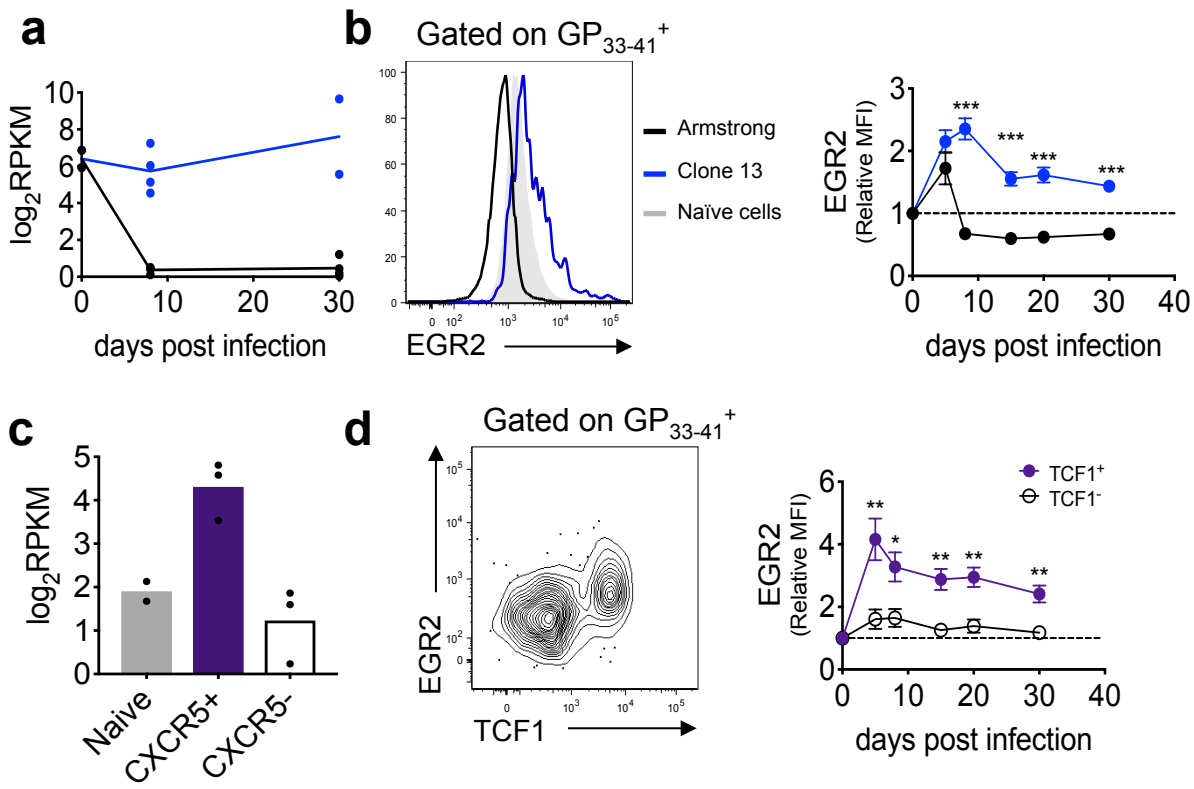
a
log2RPKM
days post infection
b
Gated on GP33-41+
EGR2
Armstrong
Clone 13
Naïve cells
EGR2 (Relative MFI)
days post infection
c
log2RPKM
Naive
CXCR5+
CXCR5-
d
Gated on GP33-41+
EGR2
TCF1
TCF1+
TCF1-
EGR2 (Relative MFI)
days post infection

Figure 4.1. EGR2 expression is elevated within TCF1$^+$ memory-like exhausted cells. (A) Expression levels of *Egr2* transcript within virus-specific CD8$^+$ T cells during chronic (blue) versus acute (black) LCMV infection extracted from RNAseq data from a published dataset (Man et al., 2017). n=2-4 replicates per time point. (B) EGR2 protein levels assessed by flow cytometry within splenic H2-D^{b}GP$_{33-41}$ tetramer stained CD8$^+$ T cells from B6 mice infected with LCMV-Arm (black) or Cl13 (blue) for the indicated times. Representative histogram (left) shows data from day 8 p.i., with naïve T cell staining included from polyclonal CD44^{lo}CD8$^+$ T cells from uninfected B6 mice. Right graph shows EGR2 expression relative to naïve levels (as defined above). n=11-15 mice per group per time point from 2-3 independent experiments. (C) Expression levels of *Egr2* transcript within CXCR5+ and CXCR5- virus-specific CD8$^+$ T cells during chronic LCMV infection, or within naïve CD8$^+$ T cells, extracted from RNAseq data from a published dataset (Leong et al., 2016). n=2-3 replicates per condition. (D) EGR2 protein levels assessed as in (B) within TCF1$^+$ and TCF1$^-$ tetramer-stained CD8$^+$ T cells from B6 mice infected with LCMV-Cl13 for the indicated times. Representative plot (left) shows data from day 20 p.i. Right graph shows EGR2 expression relative to naïve levels (as defined above). n=5-6 mice per group per time point from 2 independent experiments. Error bars depict SEM, * = $p<0.05$, ** = $p<0.01$, *** = $p<0.001$.

specific $CD8^+$ T cells during acute LCMV Armstrong (Arm) infection form non-exhausted effector cells that clear infection and differentiate into memory cells. Data obtained from a recent RNAseq analysis of virus-specific $CD8^+$ T cells during chronic relative to acute LCMV infection (Man et al., 2017) indicated that *Egr2* transcript levels are elevated during chronic versus acute LCMV infection at both day 8 and day 30 post-infection (p.i.) (Fig. 4.1A). To confirm that this translated to an increase in EGR2 protein levels, we examined EGR2 levels by flow cytometry within tetramer stained H-$2D^b$$GP_{33-41}$-specific $CD8^+$ T cells isolated from the spleens of C57BL/6 (B6) mice infected with either LCMV-Cl13 or Arm. During acute LCMV-Arm infection, EGR2 levels initially spiked above naïve $CD8^+$ T cell levels at day 5 p.i. before dropping below naïve levels from day 8 p.i. onwards (Fig. 4.1B). In contrast, EGR2 remained elevated in antigen-specific $CD8^+$ T cells compared to naïve cells at all time points measured during chronic LCMV-Cl13 infection, and was significantly higher than in LCMV-Arm infection from day 8 p.i. onwards. Thus, EGR2 expression is elevated in antigen-specific $CD8^+$ T cells in chronic relative to acute LCMV infection.

4.4.2: EGR2 is selectively expressed within $TCF1^+$ memory-like exhausted T cells

We next examined the dynamics of EGR2 expression during the exhaustion differentiation process. A small population of exhausted T cells with memory characteristics maintains $CD8^+$ T cell responses during chronic stimulation. These "exhausted memory" cells, characterised by expression of the chemokine receptor CXCR5 and diminished expression of TIM3, self-renew and continuously give rise to terminally exhausted progeny (He et al., 2016; Im et al., 2016; Leong et al., 2016; Wu et al., 2016). Results extracted from previously published RNAseq data (Leong et al., 2016) indicated that *Egr2* transcript expression was restricted to this less differentiated $CXCR5^+$ exhausted $CD8^+$ T cell population (Fig. 4.1C). Exhausted memory cells express the transcription factor TCF1, which is required for the maintenance of this population (Im et al., 2016; Leong et al., 2016; Utzschneider et al., 2016; Wu et al., 2016). Notably, among antigen-specific $CD8^+$ T cells, EGR2 expression was limited to the $TCF1^+$ population at all time-points examined p.i. (Fig. 4.1D). Thus, EGR2 expression is enriched within less differentiated $TCF1^+$ exhausted cells.

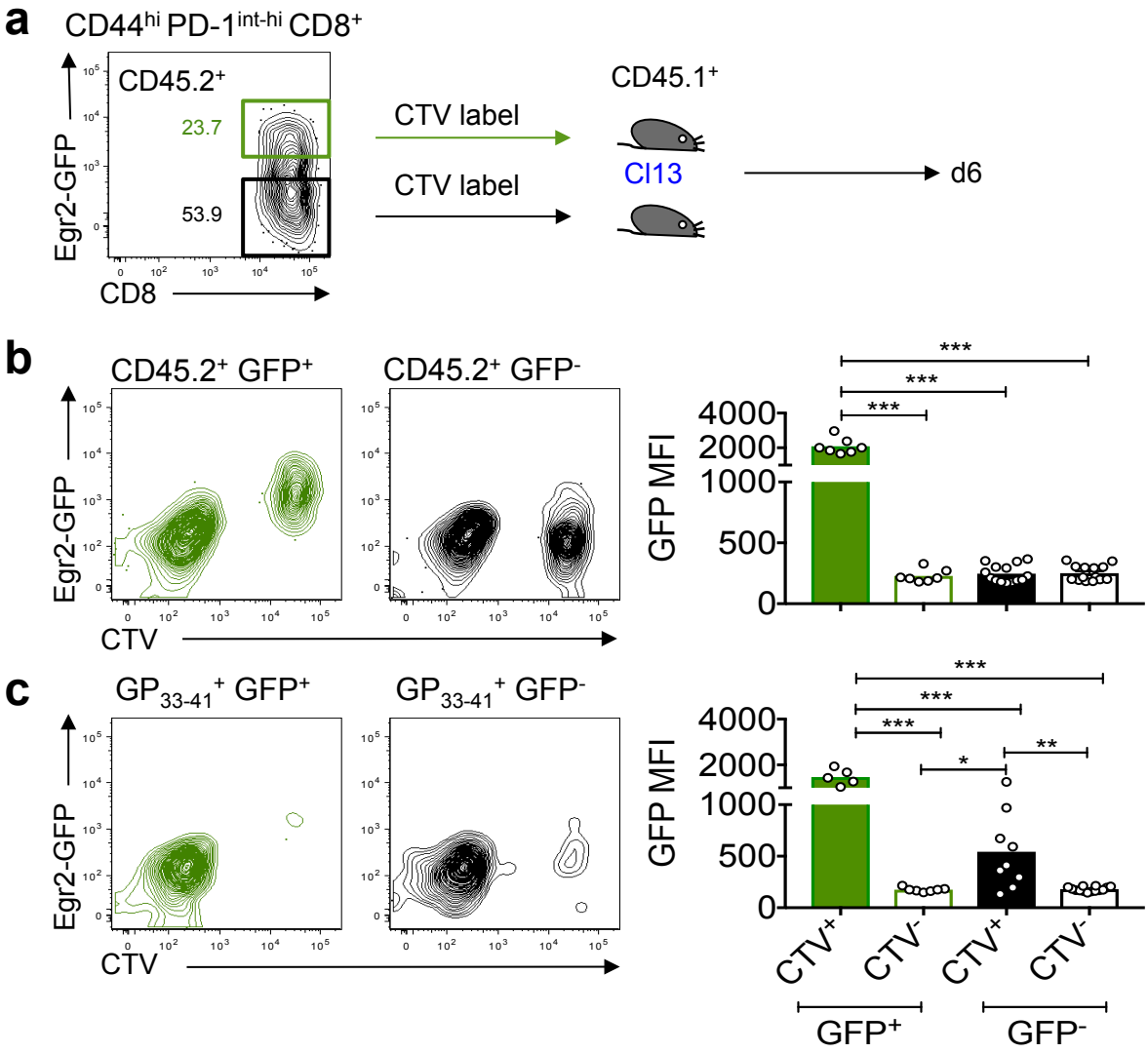

Figure 4.2. *Egr2* expression is lost as cells undergo terminal exhaustion. (A) Experimental outline. Egr2-GFP reporter mice were infected with LCMV-Cl13, and at day 20 p.i. spleens were isolated and CTV labeled splenocytes, transferred into infection-matched CD45.1$^+$ hosts (5x10^5 cells per mouse), and CD45.2$^+$ cells were analysed at day 6 post transfer. (B,C) CTV and GFP expression within total CD8$^+$ CD45.2$^+$ cells (B) or H2-D^{b}GP$_{33-41}$ tetramer-stained CD8$^+$CD45.2$^+$ cells (C). Left plots show representative profiles from mice that received GFP+ or GFP- cells, right graph shows pooled data from GFP MFI within undivided (CTV$^+$) or divided (CTV$^-$) populations. n=5-14 mice per group from 2 independent experiments. * = p<0.05, ** = p<0.01, *** = p<0.001.

The absence of EGR2 expression within TCF1$^-$ cells suggests that EGR2 expression is lost as cells differentiate during exhaustion. To formally test this idea, we conducted lineage-tracing experiments using GFP knock-in *Egr2* reporter (Egr2-GFP) mice (Williams et al., 2017). Egr2-GFP mice were infected with LCMV-Cl13, and at day 20 p.i. *Egr2* expressing GFP+ and *Egr2* non-expressing GFP- polyclonal exhausted (CD44^{hi}PD-1^{int-hi}) CD8$^+$ T cells were sorted into Egr2/GFP+ and GFP- populations and labeled with the Cell Trace Violet (CTV) division dye. 5x10^5 CTV labeled GFP+ or GFP- cells were then transferred into infection-matched congenically marked CD45.1$^+$ mice. 6 days later, proliferation and GFP expression was assessed both within the total transferred CD45.2$^+$ CD8$^+$ T cells, as well as in H-2D^{b}GP$_{33-41}$-specific cells within this transferred population (Fig. 4.2A). After adoptive transfer, both polyclonal and GP$_{33-41}$ tetramer$^+$ GFP+ cells that hadn't divided retained GFP expression, while GFP+ cells that diluted CTV and divided lost GFP expression (Fig. 4.2B,C). In contrast, GFP- cells remained GFP- after division (Fig. 2B,C). Collectively, these data support a model whereby TCF1$^+$ cells transiently express EGR2 prior to terminal exhaustion.

4.4.3: EGR2 expression is maintained by chronic antigen encounter

During anergy induction, EGR2 is directly induced downstream of TCR signaling via the transcription factor NFAT (Martinez et al., 2015). We thus speculated that EGR2 expression is maintained within exhausted CD8$^+$ T cells by chronic antigen encounter. To test this idea, 2x10^3 CD45.1$^+$ H-2D^{b}GP$_{33-41}$-specific CD8$^+$ TCR transgenic (P14) T cells were transferred into B6 mice that were subsequently infected with LCMV-Cl13 or LCMV-Arm. At day 8 p.i., when differential EGR2 expression is first observed between chronic and acute LCMV (Fig. 4.1A,B), 5x10^5 splenic CD45.1$^+$ P14 cells were isolated from these mice and transferred into either LCMV-Arm or LCMV-Cl13 infected-matched B6 recipients. As LCMV-Arm infected mice clear virus by day 8 p.i., this meant that the P14 cells were effectively transferred into mice that did or didn't contain virus. 7 days later (day 15 p.i.), EGR2 expression was assessed within the transferred CD45.1$^+$ P14 cells (Fig. 4.3A). Transfer of P14 cells from LCMV-Arm infection into LCMV-Cl13 infected hosts lead to increased EGR2 expression relative to P14 cells transferred into control LCMV-Arm infected mice (Fig. 4.3B). In the reciprocal experiment, transfer of P14 cells from

LCMV-Cl13 infection into LCMV-Arm infected hosts caused loss of EGR2 expression relative to cells transferred into control LCMV-Cl13 infected mice (Fig. 4.3C). Thus, active infection is required to maintain EGR2 expression.

Active infection could maintain EGR2 expression via antigen or inflammatory signals. To discriminate between these possibilities, the above experiment was repeated, except that P14 cells derived from LCMV-Cl13 infection were transferred into infection-matched recipients given either LCMV-Cl13, or a mutant form of Cl13 bearing a single point mutation (V35A) within the GP_{33-41} epitope that abolishes peptide binding to H-2D^b, thereby depriving P14 cells of antigen (Fig. 4.3D) (Puglielli et al., 2001). Transfer of P14 cells into V35A infected recipients lead to loss of EGR2 expression relative to cells transferred into Cl13 infected control mice, despite persistent infection in both hosts. Thus, persistent antigen engagement is required to sustain EGR2 expression during chronic LCMV infection.

4.4.4: EGR2 ablation cell intrinsically disrupts CD8$^+$ T cell exhaustion

To assess the role of *Egr2* in the CD8$^+$ T cell exhaustion process, we utilised *Egr2* floxed mice crossed to a CD4-cre transgene to delete the *Egr2* gene within all T cells (Ramon et al., 2010). CD4-cre$^+$ *Egr2*$^{f/f}$ mice (cKO), or CD4-cre$^+$ *Egr2*$^{+/+}$ littermates (WT), were infected with LCMV-Cl13 and the response to infection was assessed. The number of virus-specific cells, as assessed by both tetramer staining and by enumerating IFNγ$^+$ cells after peptide restimulation, was similar between WT and cKO mice across the course of infection (Fig. 4.S1A and data not shown). Dysregulated T cell responses during LCMV-Cl13 increase morbidity due to immunopathology, but there was no increase in morbidity within cKO mice as assessed by weight loss during infection (Fig. 4.S1B) and viral control was similar to WT controls (Fig. 4.S1C,D). However, GP_{33-41} and, to a lesser extent, $GP_{276-286}$-specific IFNγ$^+$CD8$^+$ T cells exhibited elevated IL-2 production at day 20 p.i. onwards that was not accompanied by a significant increase in TNFα production (Fig. 4.S1E,F). Inhibitory receptor expression was largely unchanged within tetramer+ CD8$^+$ T cells (data not shown), but diminished expression of the exhaustion-associated transcription factor EOMES (Paley et al., 2012) was observed within cKO

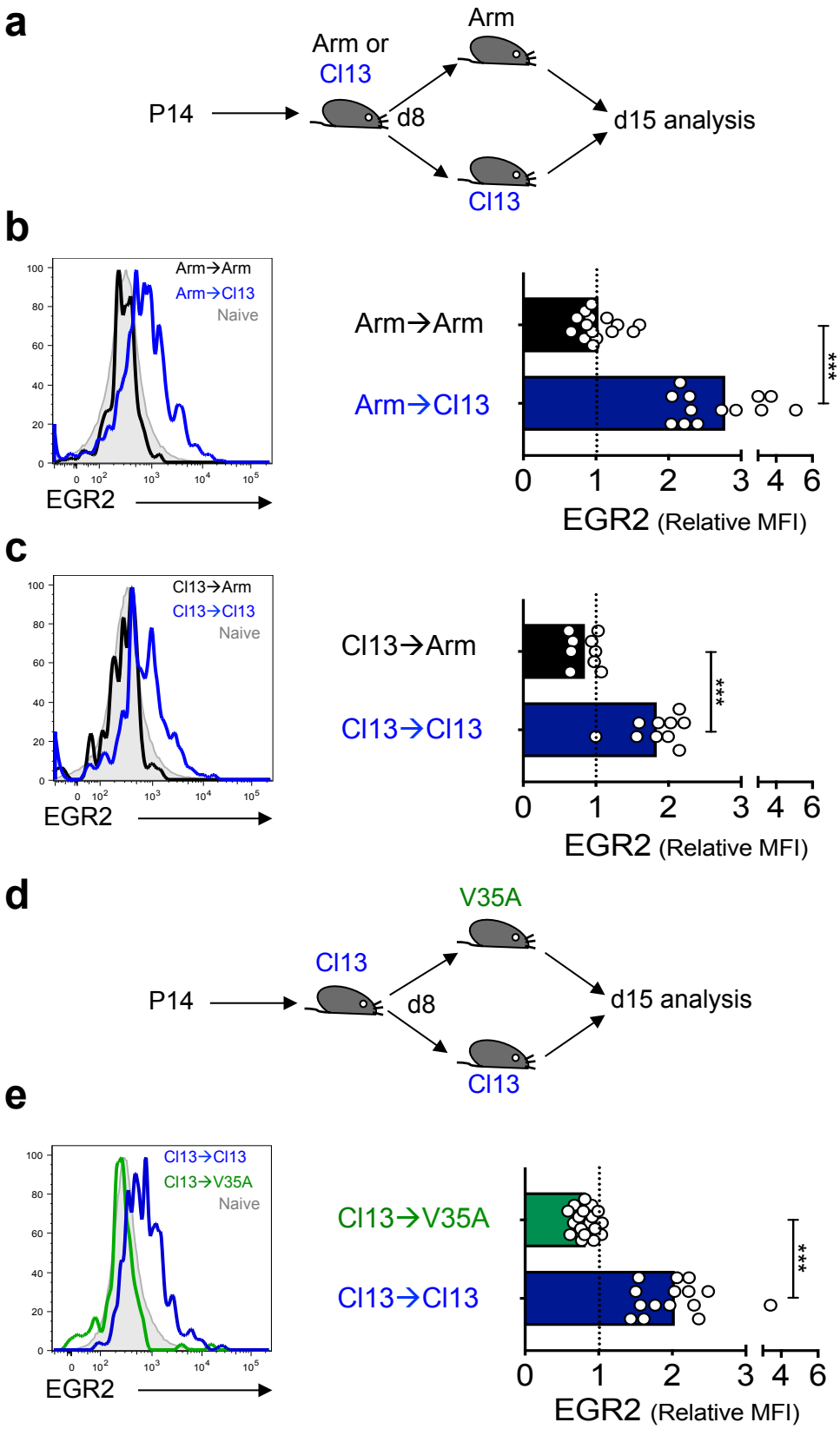
a
Arm
Arm or
Cl13
P14
d8
d15 analysis
Cl13
b
Arm→Arm
Arm→Cl13
Naive
EGR2
Arm→Arm
Arm→Cl13
***
0 1 2 3 4 6
EGR2 (Relative MFI)
c
Cl13→Arm
Cl13→Cl13
Naive
EGR2
Cl13→Arm
Cl13→Cl13
***
0 1 2 3 4 6
EGR2 (Relative MFI)
d
V35A
Cl13
P14
d8
d15 analysis
Cl13
e
Cl13→Cl13
Cl13→V35A
Naive
EGR2
Cl13→V35A
Cl13→Cl13
***
0 1 2 3 4 6
EGR2 (Relative MFI)

Figure 4.3. EGR2 expression is maintained by chronic antigen. (A) Experiment outline for (B,C). $2x10^3$ $CD45.1^+$ P14 cells were transferred into B6 mice subsequently infected with LCMV-Arm or LCMV-Cl13. At day 8 p.i., splenocytes were isolated and the equivalent of $5x10^5$ P14 cells were transferred into LCMV-Cl13 or LCMV-Arm infection matched B6 mice. 7 days later (day 15 p.i.), EGR2 protein levels were assessed within the transferred P14 cells. (B,C) EGR2 levels within cells transferred from LCMV-Arm (B) or LCMV-Cl13 (C) donors into Arm or Cl13 infected recipients. Left histograms show representative plots, with naïve $CD44^{lo}PD\text{-}1^{lo}$ cells from Cl13 infected mice also shown in grey. Right graphs show EGR2 MFI relative to the above naïve population. n=9-15 mice per group from 2-3 independent experiments. (D) Experiment outline for (E). Experiment was conducted as in (A) except that P14 cells derived from Cl13 infected donors were transferred into recipients infected with wild-type Cl13 or GP V35A mutant Cl13. (E) EGR2 levels within cells transferred from Cl13 donors into Cl13 or V35A recipients. Plots and data representation is as in (B,C). n=15-18 mice per group from 3 independent experiments. *** = $p<0.001$.

cells at day 20 p.i. (Fig. 4.S1G, data not shown). This was not associated with an increase in expression of markers associated with a memory-like exhausted state, with no alteration in the proportions of $CXCR5^{+}TIM3^{-}$ or $CXCR5^{-}TIM3^{+}$ cells, and no change in expression of T-BET and TCF1 (Fig. 4.S1H, and data not shown). Collectively, these data suggest that EGR2 deletion alters exhausted $CD8^{+}$ T cells differentiation during chronic infection. This phenotype appeared restricted to $CD8^{+}$ T cells, with virus-specific $CD4^{+}$ T cell numbers, differentiation into Th1 ($PSGL1^{hi}Ly6C^{hi}$) and Tfh ($PSGL1^{lo}$) subsets (Marshall et al., 2011; Parish et al., 2014), and cytokine function largely unaltered in cKO mice (Fig. 4.S2).

To determine whether the observed phenotypes were $CD8^{+}$ T cell intrinsic, an irradiation mixed bone marrow (BM) chimera approach was employed. Lethally irradiated *Rag1*$^{-/-}$ mice were reconstituted with a 50:50 mix of $CD45.1^{+}$ BM and $CD45.2^{+}$ WT or cKO BM, and subsequently infected with LCMV-Cl13. We failed to observe any consistent change in the proportion of cKO derived $tetramer^{+}$ cells within the blood or spleen over the course of infection, suggesting that EGR2 does not intrinsically influence $tetramer^{+}$ cell numbers (Fig. 4.S3A,B). However, a cell intrinsic decrease was observed in EOMES levels within $tetramer^{+}$ cKO cells, consistent with observations in cKO mice (Fig. 4.S3C). Furthermore, in the competitive environment of a mixed BM chimera, cKO cells also displayed decreased PD-1 levels (Fig. 4.S3D) although TIM3 levels were unchanged (Fig. 4.S3E). Similar to observations in cKO mice, cKO cells within mixed BM chimeras had unaltered levels of TCF1 (data not shown). Collectively, these results suggest that EGR2 loss causes a cell intrinsic defect in differentiation during exhaustion that is exacerbated in a competitive environment.

4.4.5: EGR2 controls inhibitory receptor expression and terminal exhaustion

The mixed BM chimera experiments above suggested that the differentiation block upon EGR2 loss could be exacerbated when cKO cells were further challenged. As depletion of $CD4^{+}$ T cells from mice prior to LCMV-Cl13 infection exacerbates exhaustion (Zajac et al., 1998), we next asked whether CD4-depleted cKO mice would exhibit a more pronounced phenotype. CD4-depleted WT or cKO mice were thus LCMV-Cl13 infected and the $CD8^{+}$ T cell response to infection was monitored.

Similar to infection of non-depleted cKO mice, there was little alteration in the number of virus-specific $CD8^+$ T cells in cKO mice aside from a slight ~2 fold decrease in GP_{33-41} and $GP_{276-286}$-specific cells at day 20 p.i. (Fig. 4.S4A). However, in the absence of CD4 help, EGR2 loss diminished expression of multiple inhibitory receptors (PD-1, 2B4 and TIM3) within tetramer+ $CD8^+$ T cells over the course of infection, although CD160 and LAG3 were either unchanged or even elevated in expression within cKO cells (Fig. 4.4A). This lead to a reduced overall load of inhibitory receptor expression, with a significant reduction in the proportion of cKO cells with 5 or more inhibitory receptors, and a corresponding expansion in cells with 2-3 inhibitory receptors (Fig. 4.4B). While we again observed a trend towards increased IL-2 production within virus-specific $CD8^+$ T cells, coupled with no alteration in TNFα production, the increase in IL-2 was more variable and not significant in this more severe model of exhaustion (Fig. 4.S4B,C), and viral control was again unchanged in this model (Fig. 4.4C). However, we did observe a pronounced block in differentiation in CD4-depleted cKO mice. EOMES was diminished in expression within cKO tetramer+ $CD8^+$ T cells at every time-point examined, and this was coupled with an increase in the proportion of $TCF1^+TIM3^-$ cells from day 20 p.i. onwards (Fig. 4.4D,E). This was coupled with elevated expression of the memory cell marker CD127 from day 20 p.i. onwards (Fig. 4.4F). Interestingly, other aspects of terminal exhaustion remained intact. CXCR5 down-regulation still occurred in cKO cells, with overall CXCR5 expression actually lower than in WT cells (Fig. 4.S4D,E). Thus, EGR2 plays a prominent non-redundant role in promoting terminal exhaustion in a more severe exhaustion model.

4.4.6: EGR2 broadly controls the terminal exhaustion gene program

To more broadly assess how EGR2 impacts upon the exhaustion gene program, RNAseq analysis was performed at day 20 p.i. on sorted, splenic $H\text{-}2D^bGP_{33-41}$-specific $CD8^+$ T cells isolated from CD4-depleted, LCMV-Cl13 infected WT or cKO mice. 415 differentially expressed genes were identified (Table 4.S1; FDR<0.05), with diminished expression of a number of key genes associated with terminal exhaustion evident (*Eomes*, *Pdcd1*, *Tigit*, *Batf*, *Tox*, *Tox2*, *Cd200r1*, *Cd200r4*), coupled with an increase in memory-like cell associated genes (*Bcl6*, *Satb1*, *Bach2*, *Fos*, *Il7r*) (Fig. 4.5A). Indeed, a previously published exhaustion signature (Man et al.,

2017) was depleted from cKO cells as assessed by Gene Set Enrichment Analysis (GSEA), with a concurrent increase in genes associated with acute infection (Fig. 4.5B,D). Similarly, cKO cells exhibited an enrichment of a published $CXCR5^+$ memory-like cell signature (Im et al., 2016), and a corresponding loss of a $CXCR5^-$ signature (Fig. 4.5C,D). However, consistent with our data suggesting an arrest at an intermediate differentiation state, a few gene changes opposed this trend, including diminished expression of *Cxcr5* and increased expression of the exhaustion promoting transcription factors *Nr4a1* and *Nr4a3* (Fig. 4.5A) (Chen et al., 2019; Liu et al., 2019). Nevertheless, collectively, our RNAseq data were reflective of a less differentiated state and suggest that EGR2 globally controls the $CD8^+$ T cell exhaustion differentiation process.

4.4.7: EGR2 is re-routed away from anergy gene targets during T cell exhaustion to directly regulate exhaustion-associated genes

To identify genes directly controlled by EGR2, we next conducted ChIP-seq analysis of EGR2 binding within exhausted $CD8^+$ T cells. $CD8^+$ T cells were enriched from LCMV-Cl13 infected B6 mice at day 20 p.i., and the genome-wide pattern of EGR2 binding was assessed. A total of 2259 EGR2 binding peaks were identified (FDR<0.05). To identify peaks associated with open chromatin regions within exhausted $CD8^+$ T cells, we cross-referenced our ChIPseq data with a previously published ATAC-seq dataset (Sen et al., 2016). Notably, 1983 peaks (87.8%, associated with 1643 genes) were found to localise to open chromatin regions, with EGR2 peak signal strength broadly correlating with binding site accessibility (Fig. 4.S5A). Unbiased *de novo* motif analysis identified a highly significant enrichment of an EGR2 motif within these ChIP-seq peaks (Table 4.S2), with the identified motif closely matching the consensus EGR2 motif (Fig. S5B). We observed a highly significant enrichment of promoters and 5'UTRs within the EGR2 binding sites ($p<0.0001$ for both, Chi-square test with Yate's correction)(Fig. S5C). 78 genes were bound by EGR2 and differentially expressed within cKO cells (Fig. 4.6A, Table 4.S3; 50 repressed and 28 induced by EGR2), which represents a significant enrichment over background ($p=0.035$, Fisher's exact test). In particular, binding peaks were observed in the open chromatin regions around key genes induced (*Pdcd1*, *Tigit*,

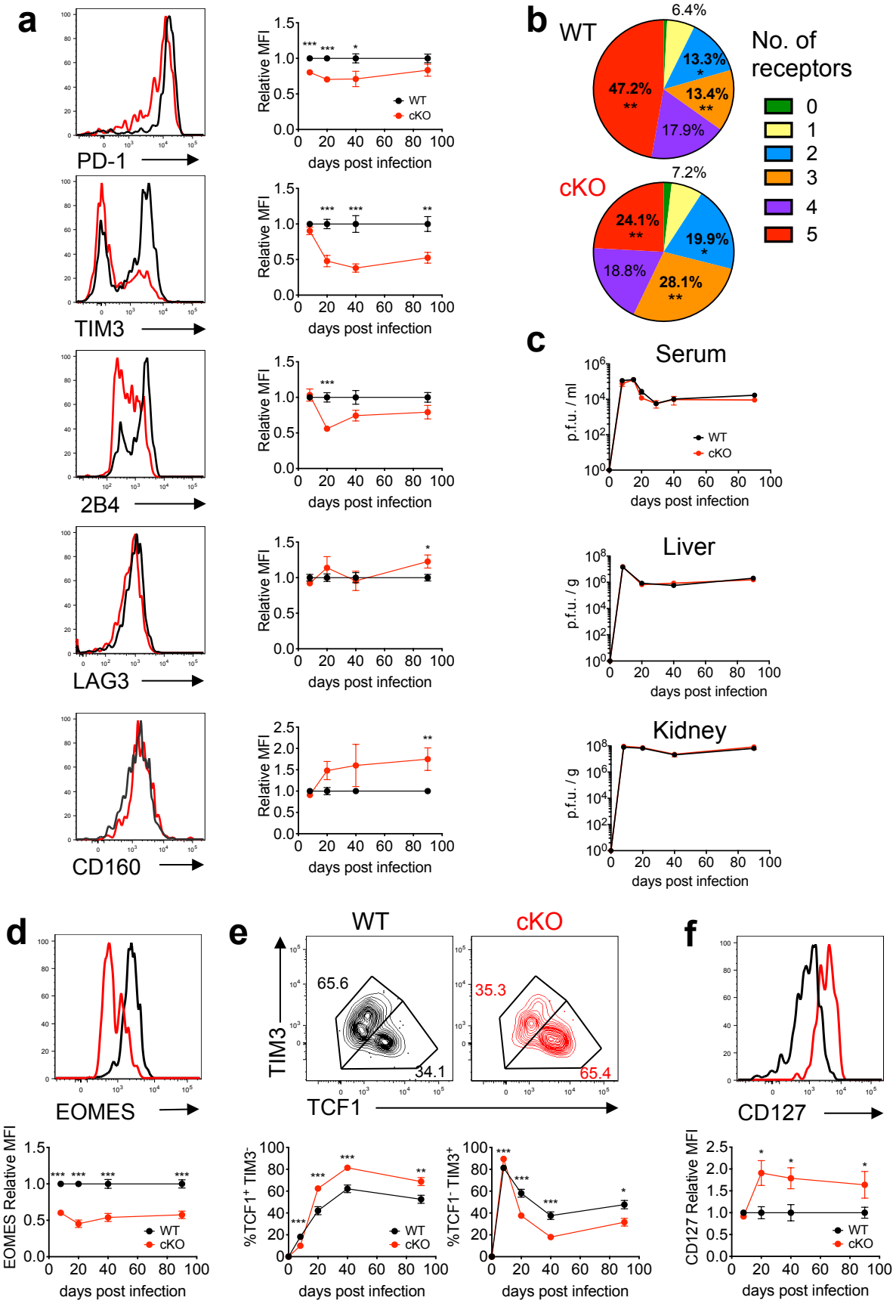
a
PD-1
TIM3
2B4
LAG3
CD160
Relative MFI
days post infection
WT
cKO
b
WT
cKO
6.4%
13.3%
13.4%
17.9%
47.2%
7.2%
19.9%
28.1%
18.8%
24.1%
No. of receptors
0
1
2
3
4
5
c
Serum
Liver
Kidney
p.f.u. / ml
p.f.u. / g
d
EOMES
EOMES Relative MFI
e
WT
cKO
TIM3
TCF1
65.6
34.1
35.3
65.4
%TCF1+ TIM3-
%TCF1- TIM3+
f
CD127
CD127 Relative MFI

Figure 4.4. *Egr2* loss blocks terminal exhaustion in the absence of $CD4^+$ T cell help. WT or cKO mice were depleted of $CD4^+$ T cells then infected with LCMV-Cl13 and the response tracked over time. (A) Inhibitory receptor MFI within H2-$D^b$$GP_{33-41}$ tetramer stained $CD8^+$ T cells over time (right; normalized to WT mean at each timepoint) with representative day 20 p.i. histograms (left). (B) Summary of data in (A) expressed as the proportion of cells expressing 0-5 of the listed inhibitory receptors at day 20 p.i. n=7-13 mice per group per time point from 2 independent experiments. (C) Viral titres in serum, liver and kidney over time. n=5-13 mice per group per time point from 2-3 independent experiments. (D) EOMES levels within tetramer+ cells over time (bottom; normalized to WT mean at each timepoint) with representative day 20 p.i. histogram (top). n=7-13 mice per group per time point from 2 independent experiments. (E) Representative (top; day 20 p.i.) and pooled (bottom) proportions of tetramer+ cells that were $TIM3^-TCF1^+$ or $TIM3^+TCF1^-$ over the course of infection. n=7-13 mice per group from 2 independent experiments. (F) CD127 levels within tetramer+ cells over time (bottom; normalized to WT mean at each timepoint) with representative day 20 p.i. histogram (top). n=7-13 mice per group per time point from 2 independent experiments. Error bars depict SEM, * = $p<0.05$, ** = $p<0.01$, *** = $p<0.001$.

Tox2) and repressed (*Bach2*, *Bcl6, Tcf7*) by EGR2 (Fig. 4.6B,C). Notably, the open chromatin region downstream of the *Pdcd1* gene bound by EGR2 has previously been shown to contribute to PD-1 expression (Sen et al., 2016).

Having defined the direct targets regulated by EGR2 during exhaustion, we were now able to directly examine the overlap between the genes directly regulated by EGR2 during exhaustion versus anergy. A high confidence set of 50 genes directly induced by EGR2 during anergy has previously been defined (Zheng et al., 2013). Strikingly, only 4 of these genes were shared direct targets during exhaustion (*Egr2*, *Bach2*, *Ryr1*, *Cd74*) (Fig. 4.6A). Moreover, with the exception of *Egr2* (which was deleted in both studies), the direction in which these genes were regulated in exhaustion versus anergy was opposing (*Bach2*, *Ryr1* and *Cd74* are induced by EGR2 in anergy, but repressed by EGR2 during exhaustion; Table 4.S3). Notably, functionally important genes that were identified as EGR2-induced anergy targets in other studies, including *Cblb*, *Dgka*, *Dtx1*, *Ndrg1*, *Rnf128, Tob1* and *Itch* (Oh et al., 2015; Zheng et al., 2012) were not differentially expressed within cKO cells, and none were EGR2 bound with the exception of *Cblb* (Fig. 4.S5D,E, and data not shown). Finally, we examined whether EGR2 is regulating the same fundamental processes in the context of exhaustion and anergy. In the context of anergy, EGR2 induces a set of genes that collectively inhibit TCR signaling (Zheng et al., 2012). As exhausted cells also have TCR signaling deficiencies, we assessed whether TCR signaling was rescued in exhausted cKO $CD8^+$ T cells. WT or cKO splenocytes isolated at day 20 p.i. from CD4-depleted LCMV-Cl13 infected mice were restimulated with anti-CD3 *in vitro* for 30 min, after which ERK1/2 phosphorylation (ppERK) and mTOR signaling (pS6) was assessed within $CD44^{hi}PD\text{-}1^{hi}$ $CD8^+$ T cells by flow cytometry. *Egr2* loss failed to rescue either the proportion of ppERK+ and pS6+ cells, or the degree of phosphorylation within the ppERK+ and pS6+ cells (as assessed by MFI) (Fig. 4.6D,E). Similar results were obtained from $CD8^+$ T cells isolated from LCMV-Cl13 infected CD4-replete mice (data not shown). Collectively, these data suggest that, although EGR2 promotes terminal exhaustion, it targets a fundamentally different gene program during exhaustion versus anergy.

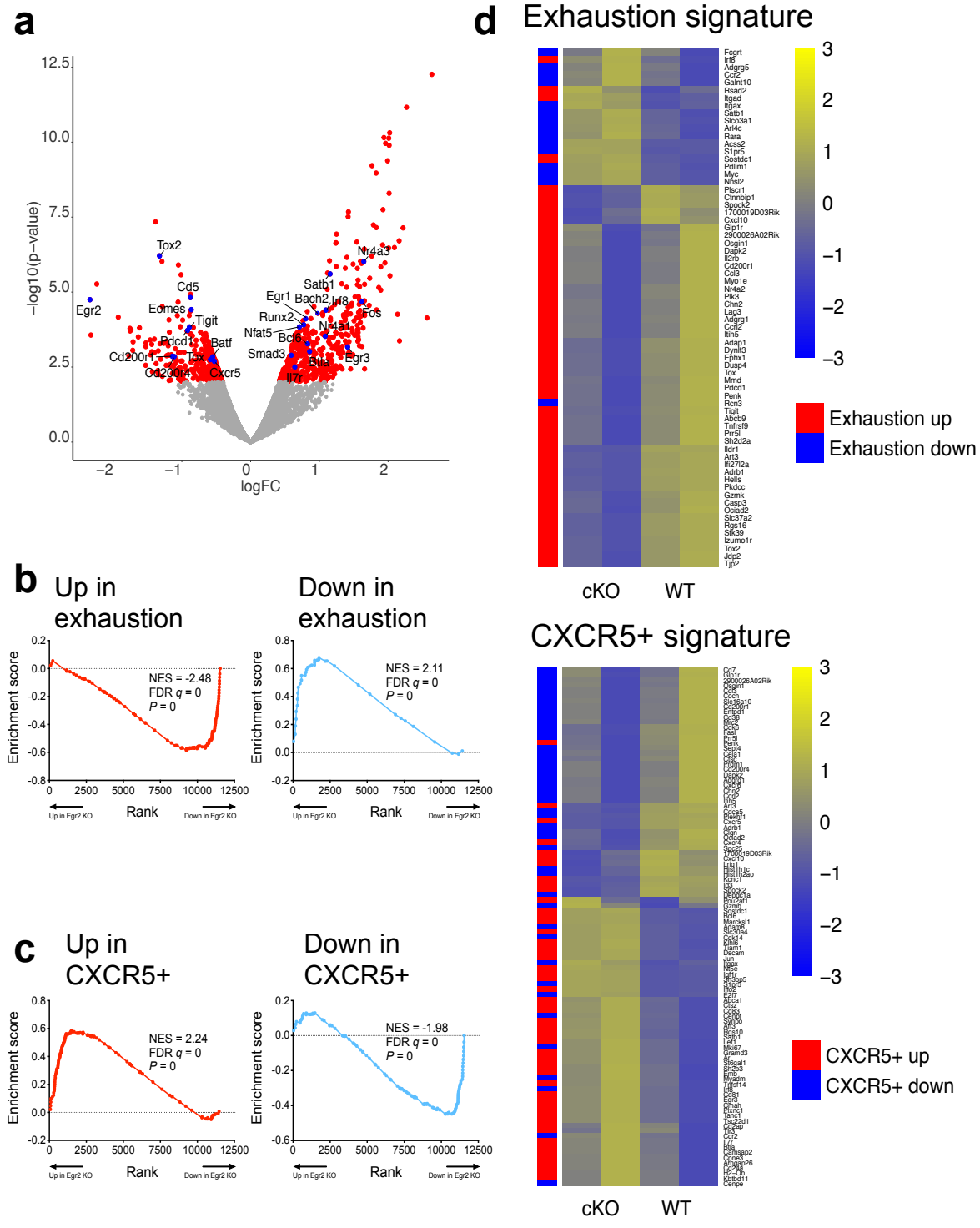
a
12.5
10.0
7.5
5.0
2.5
0.0
−log10(p−value)
−2
−1
0
1
2
logFC
Tox2
Cd5
Egr2
Eomes
Tigit
Pdcd1
Batf
Cd200r1
Tox
Cd200r4
Cxcr5
Nr4a3
Satb1
Egr1
Bach2
Irf8
Runx2
Tcf7
Nfat5
Nr4a1
Bcl6
Smad3
Egr3
Btla
Il7r
b
Up in exhaustion
Down in exhaustion
Enrichment score
NES = -2.48
FDR q = 0
P = 0
NES = 2.11
FDR q = 0
P = 0
0
2500
5000
7500
10000
12500
Rank
Up in Egr2 KO
Down in Egr2 KO
c
Up in CXCR5+
Down in CXCR5+
NES = 2.24
FDR q = 0
P = 0
NES = -1.98
FDR q = 0
P = 0
d
Exhaustion signature
3
2
1
0
−1
−2
−3
Exhaustion up
Exhaustion down
cKO
WT
CXCR5+ signature
CXCR5+ up
CXCR5+ down
cKO
WT

Figure 4.5. Global block in the terminal exhaustion gene program within EGR2 deficient cells. WT or cKO mice were depleted of $CD4^+$ T cells and infected with LCMV-Cl13, then H2-$D^b$$GP_{33-41}$ tetramer-stained $CD8^+$ T cells were sorted at day 20 p.i. and subjected to RNAseq analysis (n=2 per genotype). (A) Volcano plot denoting differentially expressed genes in cKO versus WT cells. (B-D) GSEA (B,C) and heatmap analysis (D) examining expression in cKO vs WT cells of a set of genes previously published to be selectively up or down within virus-specific $CD8^+$ T cells in chronic versus acute LCMV infection (Man et al., 2017) (B,D) or genes differentially expressed within CXCR5+ vs CXCR5- virus-specific $CD8^+$ T cells isolated from chronic LCMV infection (Im et al., 2016) (C,D). GSEA plots in (B) examine enrichment of genes selectively up (left; red) or down (right; blue) in exhaustion, while plots in (C) examine enrichment of published gene signatures associated with CXCR5+ (left; red) or CXCR5- (right; blue) cells. Heatmaps in (D) shows significantly differentially expressed genes ($p<0.05$) from these two signatures, with genes up or down in the respective gene sets indicated in red or blue in the left column.

4.5: Discussion

In this study, we investigated whether the negative regulatory pathways triggered by TCR engagement are conserved in the context of exhaustion and anergy. We demonstrate that expression of the anergy-associated transcription factor EGR2 is sustained in the context of T cell exhaustion in an antigen-dependent manner, and that EGR2 promotes terminal exhaustion by direct regulation of a number of key differentiation-linked genes. However, the genes directly regulated by EGR2 in the context of exhaustion differ fundamentally from those regulated by EGR2 during anergy. Thus, although a TCR-induced upstream negative regulator (EGR2) is similarly induced in the context of exhaustion and anergy, it triggers distinct differentiation outputs.

Our data identify EGR2 as a previously unappreciated regulator of exhaustion. During exhaustion, antigen-induced EGR2 expression peaks within $TCF1^+$ cells before being lost as cells proliferate and terminally differentiate. It is unclear why EGR2 expression is lost as cells terminally differentiate given that $TCF1^-$ cells will still encounter antigen, which is the trigger for *Egr2* expression during LCMV. It may either be related to diminishing TCR signal strength as terminally exhausted cells up-regulate inhibitory receptors, or increased access of $TCF1^-$ cells to inflammatory signals that are known to inhibit *Egr2* expression (Miao et al., 2017) within the red pulp of the spleen where there are higher viral loads (Im et al., 2016). Regardless, this wave of EGR2 expression plays an important role in promoting terminal exhaustion. Given that EGR2 expression is not maintained within $TCF1^-$ cells, we speculate that EGR2 plays roles in initiating the terminal differentiation process, but is unlikely to sustain this process once TCF1 down-regulation occurs. Additionally, only a subset of $TCF1^+$ cells expresses EGR2 (Fig. 4.1D), and we hypothesise that these cells have recently encountered differentiation signals and represent the subset of $TCF1^+$ cells *en route* to terminal exhaustion. EGR2 does not appear to control differentiation by initiating proliferation of $TCF1^+$ cells, as we saw no alteration in Ki67 expression within cKO vs WT cells (data not shown), and we failed to observe any change in cKO virus-specific $CD8^+$ T cell numbers. EGR2 likely operates in parallel to other NFAT-induced factors that promote exhaustion, such as IRF4, BATF

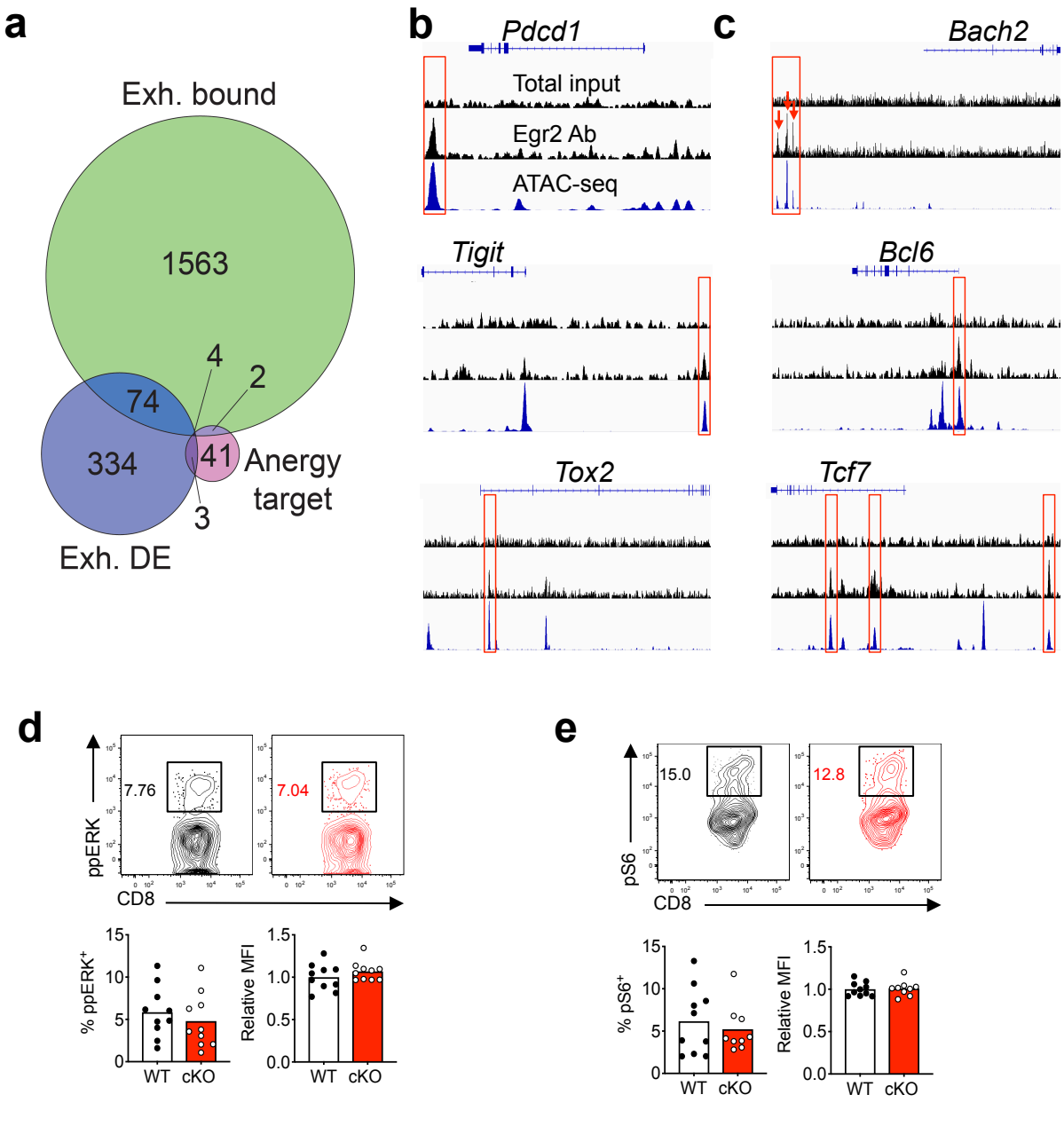
a
Exh. bound
1563
4
2
74
334
41
Anergy target
3
Exh. DE
b
Pdcd1
Total input
Egr2 Ab
ATAC-seq
Tigit
Tox2
c
Bach2
Bcl6
Tcf7
d
ppERK
CD8
7.76
7.04
% ppERK+
Relative MFI
WT
cKO
e
pS6
15.0
12.8
% pS6+

Figure 4.6. EGR2 directly regulates a non-overlapping set of genes in exhaustion versus anergy. $CD8^+$ T cells were isolated from B6 mice at day 20 p.i. with LCMV-Cl13 and subjected to EGR2 ChIP-seq analysis. (A) Venn diagram summarizing the overlap between genes identified as EGR2 bound by ChIP-seq within $CD8^+$ T cells isolated from LCMV-Cl13 infection (Exh. bound), genes differentially expressed within exhausted cKO vs WT cells from Fig. 4.5 (Exh. DE), and genes previously identified (Zheng et al., 2013) as directly induced by EGR2 during anergy (Anergy target). (B,C) Representative profiles of EGR2 ChIP-seq peaks within genes induced (B) or repressed (C) by EGR2 from Figs 4.4 and 4.5. Traces show EGR2 Ab signal, Total input signal, and published ATAC-seq accessibility within day 27 exhausted virus-specific $CD8^+$ T cells from LCMV-Cl13 infection (Sen et al., 2016). Red boxes (and arrows) denote significant peaks. (D,E) WT or cKO mice were depleted of $CD4^+$ T cells and infected with LCMV-Cl13, then splenocytes were isolated at day 20 p.i. and restimulated with anti-CD3 for 30 min. $CD44^{hi}PD\text{-}1^{hi}$ $CD8^+$ T cells were then analysed for ppERK and pS6 staining. n=9-10 mice per group from 2 independent experiments.

and the NR4A family (Chen et al., 2019; Liu et al., 2019; Man et al., 2017; Martinez et al., 2015; Quigley et al., 2010) . Compensatory induction of some of these factors in cKO cells, in particular *Nr4a1*Compensatory induction of some of these factors in cKO cells, in particular *Nr4a1* and *Nr4a3* (Fig. 4.5A), combined with elevated LAG3 and CD160 (Fig. 4.4A), could explain why the block in terminal exhaustion in cKO mice is only partial, and why EGR2 loss fails to durably rescue exhausted T cell function or impact upon cell persistence.

The dichotomy between EGR2 function in exhaustion and anergy logically aligns with the likely disparate roles of these differentiation states in immunoregulation. Peripheral tolerance processes such as anergy play important roles in completely inactivating self-reactive T cell clones so that they are unable to differentiate into productive effector cells. In contrast, exhaustion aids persistence of effector cells in a tempered state able to contain infection without causing immunopathology. We hypothesise that this is the reason why EGR2 is rerouted to a gene program aimed at promoting terminal differentiation during exhaustion, as opposed to simply preventing differentiation as it does during anergy. Interestingly, a few functionally important direct EGR2 anergy gene targets, namely *Lag3* and *Cblb*, are still induced during exhaustion and play roles in enforcing the exhausted state (Blackburn et al., 2009; Man et al., 2017; Ou et al., 2008). However, in the context of exhaustion, both genes are induced in an EGR2-independent manner, suggesting that the regulatory networks controlling expression of these genes in the context of exhaustion are distinct from those that operate during anergy. These data are in line with recent observations in tumour-infiltrating $CD8^+$ T cells, where *Lag3* expression early during the response was EGR2-dependent, but became EGR2-independent at later time-points (Williams et al., 2017). Overall, these data suggest that the pathways that induce key negative regulators to limit TCR signaling during exhaustion versus anergy are molecularly distinct.

Previous network analysis has suggested that other exhaustion-associated transcription factors, such as EOMES, are repurposed during exhaustion to target a distinct gene program (Doering et al., 2012) but our data provide direct evidence of this concept in the context of EGR2. This concept will now be important to revisit in

the context of other transcription factors. In particular, NR4A1, NR4A2 and NR4A3, another NFAT-induced transcription factor family, have recently been linked to both tolerance and exhaustion (Chen et al., 2019; Liu et al., 2019), and it will be important to determine whether they undergo similar context-dependent repurposing. The mechanism underlying this redirecting of EGR2 function is still unclear, but it does not appear due to exhaustion-associated chromatin accessibility changes. We have examined whether chromatin accessibility increases at exhaustion-specific EGR2 binding sites in naïve vs exhausted cells using a published dataset (Sen et al., 2016), but 73 of the 74 exhaustion-specific EGR2 gene targets showed no change in accessibility (the exception was *Tox2*). Thus, another mechanism, such as altered binding partners or cofactors, must underlie this shift in function. Finally, our finding that the TCR-induced negative regulatory circuitry may be differentially wired during exhaustion versus anergy could have practical applications. In particular, this finding may ultimately open avenues for designing more targeted immunotherapies that disrupt exhaustion while leaving peripheral tolerance intact, thereby limiting immune-related adverse events.

4.6: Acknowledgements

This work was funded by National Institutes of Health Grant U19-AI100627, and by the National Health and Medical Research Council (NHMRC) through Program Grants 1016953 & 1113904, Australia Fellowship 585490 (C.C.G.), Senior Principal Research Fellowship 1081858 (C.C.G.), and CJ Martin Early Career Fellowship 585518 (I.A.P.).

4.7: Author contributions

M.V.W., S.J.V., B.P.M., L.A.M., R.G., S.S.G. and I.A.P. conducted experiments, M.V.W., S.J.V., J.A.T., R.W.J., A.K., C.C.G. and I.A.P. designed experiments, S.J.V., M.J.K., J.R.T., N.B. designed and conducted bioinformatic analysis, J.D.P. provided important experimental resources, M.V.W., C.C.G. and I.A.P. wrote the paper.

4.8: References

Ahmed, R., Salmi, A., Butler, L.D., Chiller, J.M., and Oldstone, M.B. (1984). Selection of genetic variants of lymphocytic choriomeningitis virus in spleens of persistently infected mice. Role in suppression of cytotoxic T lymphocyte response and viral persistence. J Exp Med *160*, 521-540.

Barber, D.L., Wherry, E.J., Masopust, D., Zhu, B., Allison, J.P., Sharpe, A.H., Freeman, G.J., and Ahmed, R. (2006). Restoring function in exhausted CD8 T cells during chronic viral infection. Nature *439*, 682-687.

Blackburn, S.D., Shin, H., Haining, W.N., Zou, T., Workman, C.J., Polley, A., Betts, M.R., Freeman, G.J., Vignali, D.A., and Wherry, E.J. (2009). Coregulation of CD8+ T cell exhaustion by multiple inhibitory receptors during chronic viral infection. Nat Immunol *10*, 29-37.

Blattman, J.N., Grayson, J.M., Wherry, E.J., Kaech, S.M., Smith, K.A., and Ahmed, R. (2003). Therapeutic use of IL-2 to enhance antiviral T-cell responses in vivo. Nature medicine *9*, 540-547.

Chen, J., Lopez-Moyado, I.F., Seo, H., Lio, C.J., Hempleman, L.J., Sekiya, T., Yoshimura, A., Scott-Browne, J.P., and Rao, A. (2019). NR4A transcription factors limit CAR T cell function in solid tumours. Nature.

Cornberg, M., Kenney, L.L., Chen, A.T., Waggoner, S.N., Kim, S.K., Dienes, H.P., Welsh, R.M., and Selin, L.K. (2013). Clonal exhaustion as a mechanism to protect against severe immunopathology and death from an overwhelming CD8 T cell response. Front Immunol *4*, 475.

Davey, G.M., Kurts, C., Miller, J.F., Bouillet, P., Strasser, A., Brooks, A.G., Carbone, F.R., and Heath, W.R. (2002). Peripheral deletion of autoreactive CD8 T cells by cross presentation of self-antigen occurs by a Bcl-2-inhibitable pathway mediated by Bim. J Exp Med *196*, 947-955.

Doering, T.A., Crawford, A., Angelosanto, J.M., Paley, M.A., Ziegler, C.G., and Wherry, E.J. (2012). Network analysis reveals centrally connected genes and pathways involved in CD8+ T cell exhaustion versus memory. Immunity *37*, 1130-1144.

Frebel, H., Nindl, V., Schuepbach, R.A., Braunschweiler, T., Richter, K., Vogel, J., Wagner, C.A., Loffing-Cueni, D., Kurrer, M., Ludewig, B., and Oxenius, A. (2012). Programmed death 1 protects from fatal circulatory failure during systemic virus infection of mice. J Exp Med *209*, 2485-2499.

Ghoneim, H.E., Fan, Y., Moustaki, A., Abdelsamed, H.A., Dash, P., Dogra, P., Carter, R., Awad, W., Neale, G., Thomas, P.G., and Youngblood, B. (2017). De Novo Epigenetic Programs Inhibit PD-1 Blockade-Mediated T Cell Rejuvenation. Cell *170*, 142-157 e119.

Goldberg, M.V., Maris, C.H., Hipkiss, E.L., Flies, A.S., Zhen, L., Tuder, R.M., Grosso, J.F., Harris, T.J., Getnet, D., Whartenby, K.A.*, et al.* (2007). Role of PD-1 and its ligand, B7-H1, in early fate decisions of CD8 T cells. Blood *110*, 186-192.

He, R., Hou, S., Liu, C., Zhang, A., Bai, Q., Han, M., Yang, Y., Wei, G., Shen, T., Yang, X.*, et al.* (2016). Follicular CXCR5- expressing CD8(+) T cells curtail chronic viral infection. Nature *537*, 412-428.

Hernandez, J., Aung, S., Redmond, W.L., and Sherman, L.A. (2001). Phenotypic and functional analysis of CD8(+) T cells undergoing peripheral deletion in response to cross-presentation of self-antigen. J Exp Med *194*, 707-717.

Im, S.J., Hashimoto, M., Gerner, M.Y., Lee, J., Kissick, H.T., Burger, M.C., Shan, Q., Hale, J.S., Lee, J., Nasti, T.H.*, et al.* (2016). Defining CD8+ T cells that provide the proliferative burst after PD-1 therapy. Nature *537*, 417-421.

Jang, S.W., Srinivasan, R., Jones, E.A., Sun, G., Keles, S., Krueger, C., Chang, L.W., Nagarajan, R., and Svaren, J. (2010). Locus-wide identification of Egr2/Krox20 regulatory targets in myelin genes. J Neurochem *115*, 1409-1420.

Jin, X., Bauer, D.E., Tuttleton, S.E., Lewin, S., Gettie, A., Blanchard, J., Irwin, C.E., Safrit, J.T., Mittler, J., Weinberger, L.*, et al.* (1999). Dramatic rise in plasma viremia after CD8(+) T cell depletion in simian immunodeficiency virus-infected macaques. J Exp Med *189*, 991-998.

Keir, M.E., Freeman, G.J., and Sharpe, A.H. (2007). PD-1 regulates self-reactive CD8+ T cell responses to antigen in lymph nodes and tissues. J Immunol *179*, 5064-5070.

Kim, D., Langmead, B., and Salzberg, S.L. (2015). HISAT: a fast spliced aligner with low memory requirements. Nature methods *12*, 357-360.

Leong, Y.A., Chen, Y., Ong, H.S., Wu, D., Man, K., Deleage, C., Minnich, M., Meckiff, B.J., Wei, Y., Hou, Z.*, et al.* (2016). CXCR5(+) follicular cytotoxic T cells control viral infection in B cell follicles. Nat Immunol *17*, 1187-1196.

Liao, Y., Smyth, G.K., and Shi, W. (2014). featureCounts: an efficient general purpose program for assigning sequence reads to genomic features. Bioinformatics (Oxford, England) *30*, 923-930.

Liu, X., Wang, Y., Lu, H., Li, J., Yan, X., Xiao, M., Hao, J., Alekseev, A., Khong, H., Chen, T.*, et al.* (2019). Genome-wide analysis identifies NR4A1 as a key mediator of T cell dysfunction. Nature.

Man, K., Gabriel, S.S., Liao, Y., Gloury, R., Preston, S., Henstridge, D.C., Pellegrini, M., Zehn, D., Berberich-Siebelt, F., Febbraio, M.A.*, et al.* (2017). Transcription Factor IRF4 Promotes CD8(+) T Cell Exhaustion and Limits the Development of Memory-like T Cells during Chronic Infection. Immunity *47*, 1129-1141 e1125.

Marshall, H.D., Chandele, A., Jung, Y.W., Meng, H., Poholek, A.C., Parish, I.A., Rutishauser, R., Cui, W., Kleinstein, S.H., Craft, J., and Kaech, S.M. (2011). Differential expression of Ly6C and T-bet distinguish effector and memory Th1 CD4(+) cell properties during viral infection. Immunity *35*, 633-646.

Martinez, G.J., Pereira, R.M., Aijo, T., Kim, E.Y., Marangoni, F., Pipkin, M.E., Togher, S., Heissmeyer, V., Zhang, Y.C., Crotty, S.*, et al.* (2015). The transcription factor NFAT promotes exhaustion of activated CD8(+) T cells. Immunity *42*, 265-278.

Miao, T., Symonds, A.L.J., Singh, R., Symonds, J.D., Ogbe, A., Omodho, B., Zhu, B., Li, S., and Wang, P. (2017). Egr2 and 3 control adaptive immune responses by temporally uncoupling expansion from T cell differentiation. J Exp Med *214*, 1787-1808.

Oh, Y.M., Park, H.B., Shin, J.H., Lee, J.E., Park, H.Y., Kho, D.H., Lee, J.S., Choi, H., Okuda, T., Kokame, K.*, et al.* (2015). Ndrg1 is a T-cell clonal anergy factor negatively regulated by CD28 costimulation and interleukin-2. Nature Communications *6*.

Ou, R., Zhang, M., Huang, L., and Moskophidis, D. (2008). Control of virus-specific CD8+ T-cell exhaustion and immune-mediated pathology by E3 ubiquitin ligase Cbl-b during chronic viral infection. Journal of virology *82*, 3353-3368.

Paley, M.A., Kroy, D.C., Odorizzi, P.M., Johnnidis, J.B., Dolfi, D.V., Barnett, B.E., Bikoff, E.K., Robertson, E.J., Lauer, G.M., Reiner, S.L., and Wherry, E.J. (2012). Progenitor and terminal subsets of CD8+ T cells cooperate to contain chronic viral infection. Science *338*, 1220-1225.

Parish, I.A., and Heath, W.R. (2008). Too dangerous to ignore: self-tolerance and the control of ignorant autoreactive T cells. Immunol Cell Biol *86*, 146-152.

Parish, I.A., Marshall, H.D., Staron, M.M., Lang, P.A., Brustle, A., Chen, J.H., Cui, W., Tsui, Y.C., Perry, C., Laidlaw, B.J.*, et al.* (2014). Chronic viral infection promotes sustained Th1-derived immunoregulatory IL-10 via BLIMP-1. The Journal of clinical investigation *124*, 3455-3468.

Parish, I.A., Rao, S., Smyth, G.K., Juelich, T., Denyer, G.S., Davey, G.M., Strasser, A., and Heath, W.R. (2009). The molecular signature of CD8+ T cells undergoing deletional tolerance. Blood *113*, 4575-4585.

Pauken, K.E., and Wherry, E.J. (2015). Overcoming T cell exhaustion in infection and cancer. Trends in immunology *36*, 265-276.

Pircher, H., Burki, K., Lang, R., Hengartner, H., and Zinkernagel, R.M. (1989). Tolerance induction in double specific T-cell receptor transgenic mice varies with antigen. Nature *342*, 559-561.

Postow, M.A., Sidlow, R., and Hellmann, M.D. (2018). Immune-Related Adverse Events Associated with Immune Checkpoint Blockade. N Engl J Med *378*, 158-168.

Probst, H.C., McCoy, K., Okazaki, T., Honjo, T., and van den Broek, M. (2005). Resting dendritic cells induce peripheral CD8+ T cell tolerance through PD-1 and CTLA-4. Nat Immunol *6*, 280-286.

Puglielli, M.T., Zajac, A.J., van der Most, R.G., Dzuris, J.L., Sette, A., Altman, J.D., and Ahmed, R. (2001). In vivo selection of a lymphocytic choriomeningitis virus variant that affects recognition of the GP33-43 epitope by H-2Db but not H-2Kb. Journal of virology *75*, 5099-5107.

Quigley, M., Pereyra, F., Nilsson, B., Porichis, F., Fonseca, C., Eichbaum, Q., Julg, B., Jesneck, J.L., Brosnahan, K., Imam, S.*, et al.* (2010). Transcriptional analysis of HIV-specific CD8+ T cells shows that PD-1 inhibits T cell function by upregulating BATF. Nature medicine *16*, 1147-1151.

Ramon, H.E., Cejas, P.J., LaRosa, D., Rahman, A., Harris, J.E., Zhang, J., Hunter, C., Choi, Y., and Turka, L.A. (2010). EGR-2 is not required for in vivo CD4 T cell mediated immune responses. PLoS One *5*, e12904.

Redmond, W.L., Hernandez, J., and Sherman, L.A. (2003). Deletion of naive CD8 T cells requires persistent antigen and is not programmed by an initial signal from the tolerogenic APC. J Immunol *171*, 6349-6354.

Safford, M., Collins, S., Lutz, M.A., Allen, A., Huang, C.T., Kowalski, J., Blackford, A., Horton, M.R., Drake, C., Schwartz, R.H., and Powell, J.D. (2005). Egr-2 and Egr-3 are negative regulators of T cell activation. Nat Immunol *6*, 472-480.

Schietinger, A., Philip, M., Krisnawan, V.E., Chiu, E.Y., Delrow, J.J., Basom, R.S., Lauer, P., Brockstedt, D.G., Knoblaugh, S.E., Hammerling, G.J.*, et al.* (2016). Tumor-Specific T Cell Dysfunction Is a Dynamic Antigen-Driven Differentiation Program Initiated Early during Tumorigenesis. Immunity *45*, 389-401.

Schmitz, J.E., Kuroda, M.J., Santra, S., Sasseville, V.G., Simon, M.A., Lifton, M.A., Racz, P., Tenner-Racz, K., Dalesandro, M., Scallon, B.J.*, et al.* (1999). Control of viremia in simian immunodeficiency virus infection by CD8+ lymphocytes. Science *283*, 857-860.

Schwartz, R.H. (2003). T cell anergy. Annu Rev Immunol *21*, 305-334.

Sen, D.R., Kaminski, J., Barnitz, R.A., Kurachi, M., Gerdemann, U., Yates, K.B., Tsao, H.W., Godec, J., LaFleur, M.W., Brown, F.D.*, et al.* (2016). The epigenetic landscape of T cell exhaustion. Science *354*, 1165-1169.

Shin, H., Blackburn, S.D., Blattman, J.N., and Wherry, E.J. (2007). Viral antigen and extensive division maintain virus-specific CD8 T cells during chronic infection. J Exp Med *204*, 941-949.

Staron, M.M., Gray, S.M., Marshall, H.D., Parish, I.A., Chen, J.H., Perry, C.J., Cui, G., Li, M.O., and Kaech, S.M. (2014). The transcription factor FoxO1 sustains expression of the inhibitory receptor PD-1 and survival of antiviral CD8(+) T cells during chronic infection. Immunity *41*, 802-814.

Subramanian, A., Tamayo, P., Mootha, V.K., Mukherjee, S., Ebert, B.L., Gillette, M.A., Paulovich, A., Pomeroy, S.L., Golub, T.R., Lander, E.S., and Mesirov, J.P. (2005). Gene set enrichment analysis: a knowledge-based approach for interpreting genome-wide expression profiles. Proc Natl Acad Sci U S A *102*, 15545-15550.

Tsushima, F., Yao, S., Shin, T., Flies, A., Flies, S., Xu, H., Tamada, K., Pardoll, D.M., and Chen, L. (2007). Interaction between B7-H1 and PD-1 determines initiation and reversal of T-cell anergy. Blood *110*, 180-185.

Utzschneider, D.T., Charmoy, M., Chennupati, V., Pousse, L., Ferreira, D.P., Calderon-Copete, S., Danilo, M., Alfei, F., Hofmann, M., Wieland, D.*, et al.* (2016). T Cell Factor 1-Expressing Memory-like CD8(+) T Cells Sustain the Immune Response to Chronic Viral Infections. Immunity *45*, 415-427.

Waithman, J., Gebhardt, T., Davey, G.M., Heath, W.R., and Carbone, F.R. (2008). Cutting edge: Enhanced IL-2 signaling can convert self-specific T cell response from tolerance to autoimmunity. J Immunol *180*, 5789-5793.

Walker, L.S., and Abbas, A.K. (2002). The enemy within: keeping self-reactive T cells at bay in the periphery. Nat Rev Immunol *2*, 11-19.

Wherry, E.J., Ha, S.J., Kaech, S.M., Haining, W.N., Sarkar, S., Kalia, V., Subramaniam, S., Blattman, J.N., Barber, D.L., and Ahmed, R. (2007). Molecular signature of CD8+ T cell exhaustion during chronic viral infection. Immunity *27*, 670-684.

Wherry, E.J., and Kurachi, M. (2015). Molecular and cellular insights into T cell exhaustion. Nature reviews. Immunology *15*, 486-499.

Williams, J.B., Horton, B.L., Zheng, Y., Duan, Y., Powell, J.D., and Gajewski, T.F. (2017). The EGR2 targets LAG-3 and 4-1BB describe and regulate dysfunctional antigen-specific CD8+ T cells in the tumor microenvironment. J Exp Med *214*, 381-400.

Wu, T., Ji, Y., Moseman, E.A., Xu, H.C., Manglani, M., Kirby, M., Anderson, S.M., Handon, R., Kenyon, E., Elkahloun, A.*, et al.* (2016). The TCF1-Bcl6 axis counteracts type I interferon to repress exhaustion and maintain T cell stemness. Sci Immunol *1*.

Zajac, A.J., Blattman, J.N., Murali-Krishna, K., Sourdive, D.J., Suresh, M., Altman, J.D., and Ahmed, R. (1998). Viral immune evasion due to persistence of activated T cells without effector function. J Exp Med *188*, 2205-2213.

Zheng, Y., Zha, Y., Driessens, G., Locke, F., and Gajewski, T.F. (2012). Transcriptional regulator early growth response gene 2 (Egr2) is required for T cell anergy in vitro and in vivo. The Journal of experimental medicine *209*, 2157-2163.

Zheng, Y., Zha, Y., Spaapen, R.M., Mathew, R., Barr, K., Bendelac, A., and Gajewski, T.F. (2013). Egr2-dependent gene expression profiling and ChIP-Seq reveal novel biologic targets in T cell anergy. Mol Immunol *55*, 283-291.

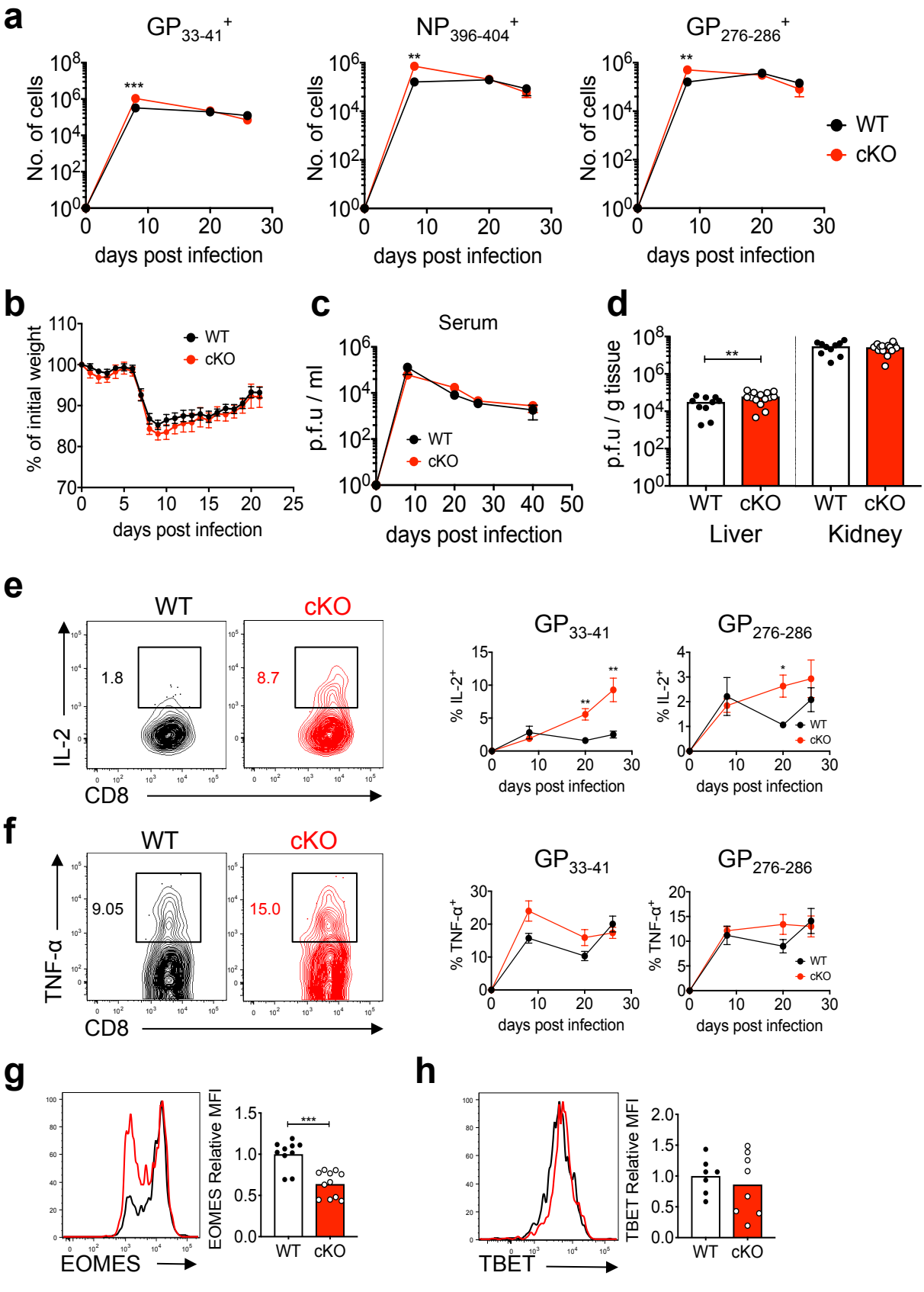
a
GP33-41+
NP396-404+
GP276-286+
No. of cells
days post infection
WT
cKO
b
% of initial weight
c
Serum
p.f.u / ml
d
p.f.u / g tissue
Liver
Kidney
e
WT
cKO
1.8
8.7
IL-2
CD8
% IL-2+
f
9.05
15.0
TNF-α
% TNF-α+
g
EOMES
EOMES Relative MFI
h
TBET
TBET Relative MFI

Figure 4.S1: CD8+ T cell phenotype in LCMV-Cl14 infected WT vs cKO mice. Related to Figure 4.4. WT or cKO mice were infected with LCMV-Cl13 and the response tracked over time. (A) The number of $CD8^+IFN\gamma^+$ T cells recovered over time upon stimulation of splenocytes with the indicated LCMV peptides. n=6-14 mice per group per time point from 2-4 independent experiments. (B) Weight loss over time, with weight expressed as % of starting weight pre-infection. n=4-16 mice per group per time point from 2-4 independent experiments. (C,D) Plaque forming units (p.f.u.) of virus determined by plaque assay in the serum over time (C) or at day 20 p.i. in the liver and kidney (D). n=4-15 mice per group per time point from 2-4 independent experiments. (E,F) IL-2 (E) and TNFα (F) production by $IFN\gamma^+CD8^+$ T cells upon restimulation with LCMV GP_{33-41} or $GP_{276-286}$ peptides. Representative plots (left, GP_{33-41} peptide) are shown from day 20 p.i. alongside pooled data over time (right). n=6-14 mice per group per time point from 2-4 independent experiments. (G,H) Representative (left) and pooled (right) EOMES (G) and T-BET (H) levels assessed by flow cytometry at day 20 p.i. within H2-D^bGP_{33-41} tetramer stained $CD8^+$ T cells. n=7-11 mice per group from 2-3 independent experiments. MFI data were normalized to the WT mean. All error bars depict SEM. * = $p<0.05$, ** = $p<0.01$, *** = $p<0.001$.

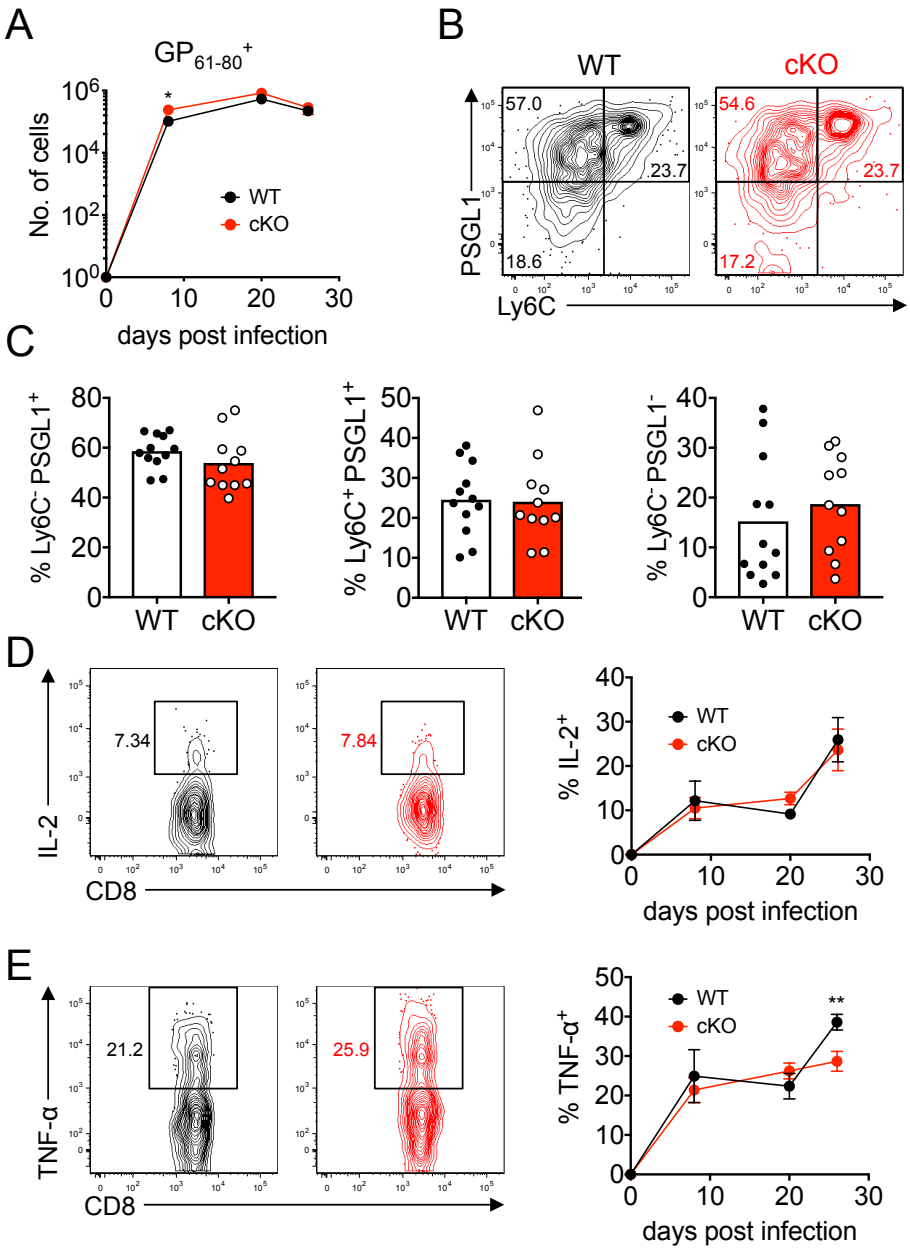

Figure 4.S2. The virus-specific CD4$^+$ T cell response within LCMV-Cl13 infected WT versus cKO mice. Related to Figure 4.4. In the experiment outlined in Figure 4.S1, the virus-specific CD4$^+$ T cell response was analysed. (A) The number of CD4$^+$IFNγ$^+$ T cells recovered over time upon splenocyte stimulation with the immunodominant CD4$^+$ T cell LCMV peptide GP_{61-80}. n=6-14 mice per group per time point from 2-3 independent experiments. (B,C) Representative (B) and pooled (C) proportions of PSGL1$^+$Ly6C$^+$, PSGL1$^+$Ly6C$^-$ and PSGL1$^-$Ly6C$^-$ MHCII I-A^bGP_{66-77} tetramer+ CD4$^+$ T cells at day 20 p.i. n=11-12 mice per group from 3 independent experiments. (D,E) Representative (left) and pooled (right) TNFα (E) and IL-2 (D) production within the CD4$^+$IFNγ$^+$ T cells from (A) over time. n=6-14 mice per group per time point from 2-3 independent experiments. All error bars depict SEM. * = p<0.05, ** = p<0.01.

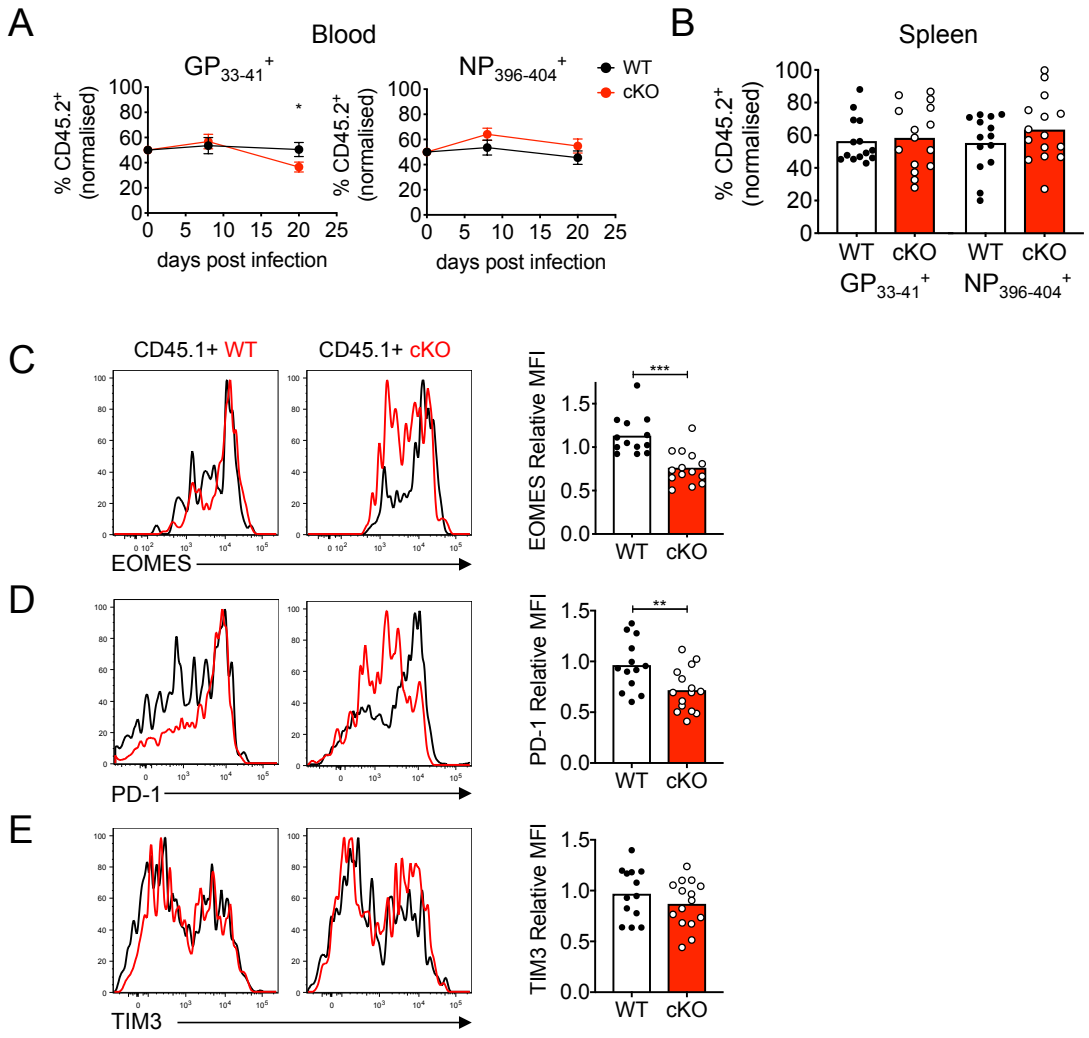

Figure 4.S3. Disruption of CD8$^+$ T cell exhaustion by *Egr2* loss is cell intrinsic. Related to Figure 4.4. Lethally irradiated *Rag1*$^{-/-}$ mice were reconstituted with a 50:50 mix of CD45.1$^+$ BM and CD45.2$^+$ WT or cKO BM, and allowed to reconstitute for 8 weeks prior to infection with LCMV-Cl13. (A,B) The percentage of CD45.2$^+$ cells within H2-D^{b}GP$_{33\text{-}41}$ tetramer stained blood (A) or splenic (B; day 20 p.i.) CD8$^+$ T cells in WT or cKO mixed BM chimeras. The % CD45.2$^+$ cells was normalized to the pre-infection % CD45.2$^+$ cells within blood CD8$^+$ T cells (with this starting percentage set to 50%). (C-E) Representative (left) and pooled (right) MFI values for EOMES (C), PD-1 (D) and TIM3 (E) within splenic H2-D^{b}GP$_{33\text{-}41}$ tetramer+ CD8$^+$ T cells at day 20 p.i. MFI values are expressed as relative to the MFI values of the CD45.1$^+$ tetramer$^+$ cells within the same mouse. n=13-15 mice per group per time point from 3 independent experiments. All error bars depict SEM. * = p<0.05, ** = p<0.01, *** = p<0.001.

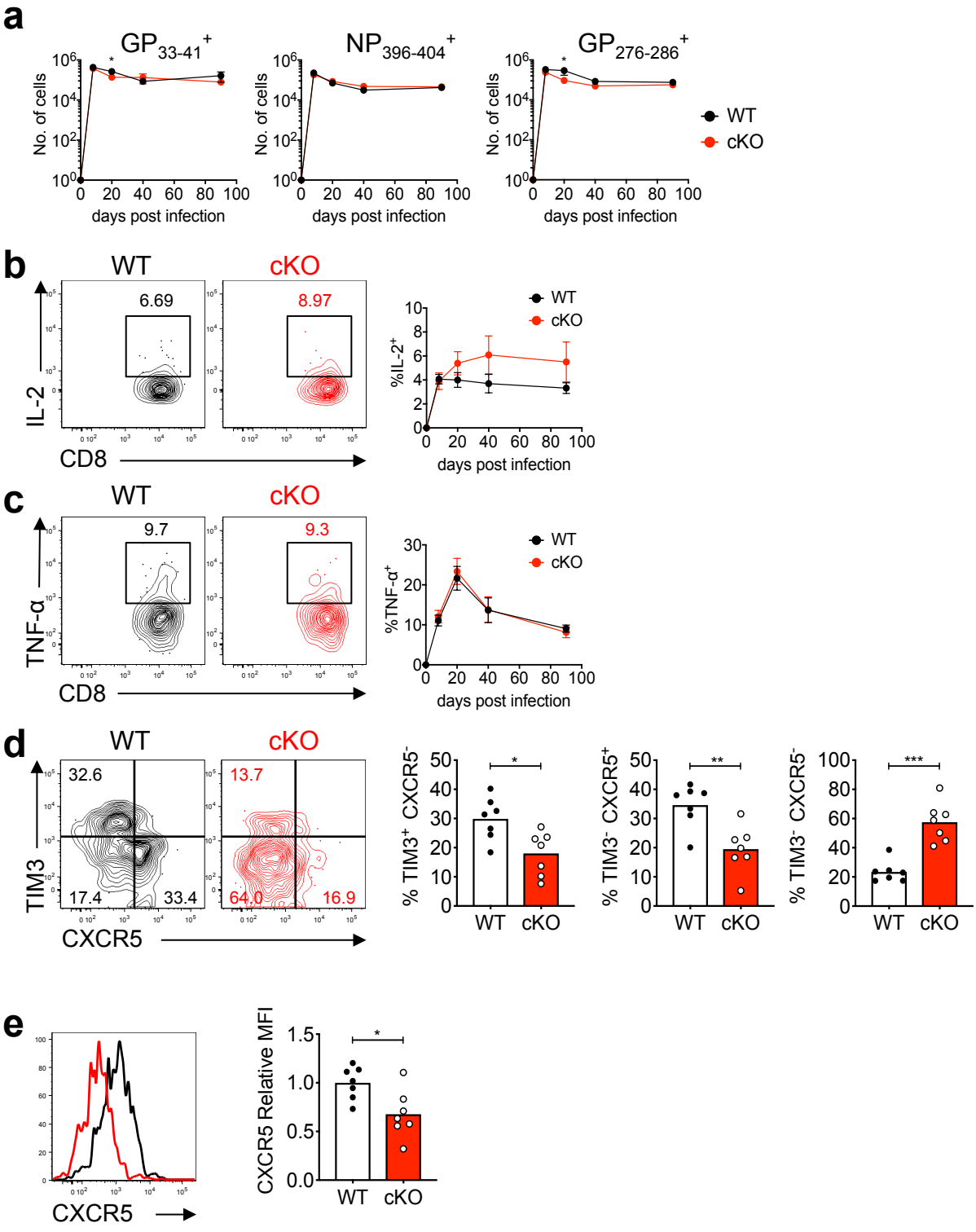
a
GP33-41+
NP396-404+
GP276-286+
No. of cells
days post infection
WT
cKO
b
WT
cKO
6.69
8.97
IL-2
CD8
%IL-2+
c
9.7
9.3
TNF-α
%TNF-α+
d
32.6
13.7
17.4
33.4
64.0
16.9
TIM3
CXCR5
% TIM3+ CXCR5-
% TIM3- CXCR5+
% TIM3- CXCR5-
e
CXCR5 Relative MFI

Figure 4.S4. $CD8^+$ T cell expansion and phenotype in CD4 depleted, LCMV-Cl13 infected WT vs cKO mice. Related to Figure 4.4. WT or cKO mice were depleted of $CD4^+$ T cells then infected with LCMV-Cl13 and the response tracked over time. (A) The number of $CD8^+IFN\gamma^+$ T cells recovered over time upon stimulation of splenocytes with the indicated LCMV peptides. n=7-13 mice per group per time point from 2-3 independent experiments. (B,C) Representative (left; day 20 p.i.) and pooled (right) TNFα (C) and IL-2 (B) production within the GP_{33-41} peptide-specific $CD8^+IFN\gamma^+$ T cells from (A) over time. (D,E) Representative (left) and pooled (right) data showing the proportions of $CXCR5^+TIM3^-$, $CXCR5^-TIM3^+$ and $CXCR5^-TIM3^-$ cells (D) and overall CXCR5 MFI (E) in tetramer+ cells from WT and cKO mice at day 40 p.i. n=7 mice per group from 2 independent experiments. All error bars depict SEM. * = $p<0.05$, ** = $p<0.01$, *** = $p<0.001$.

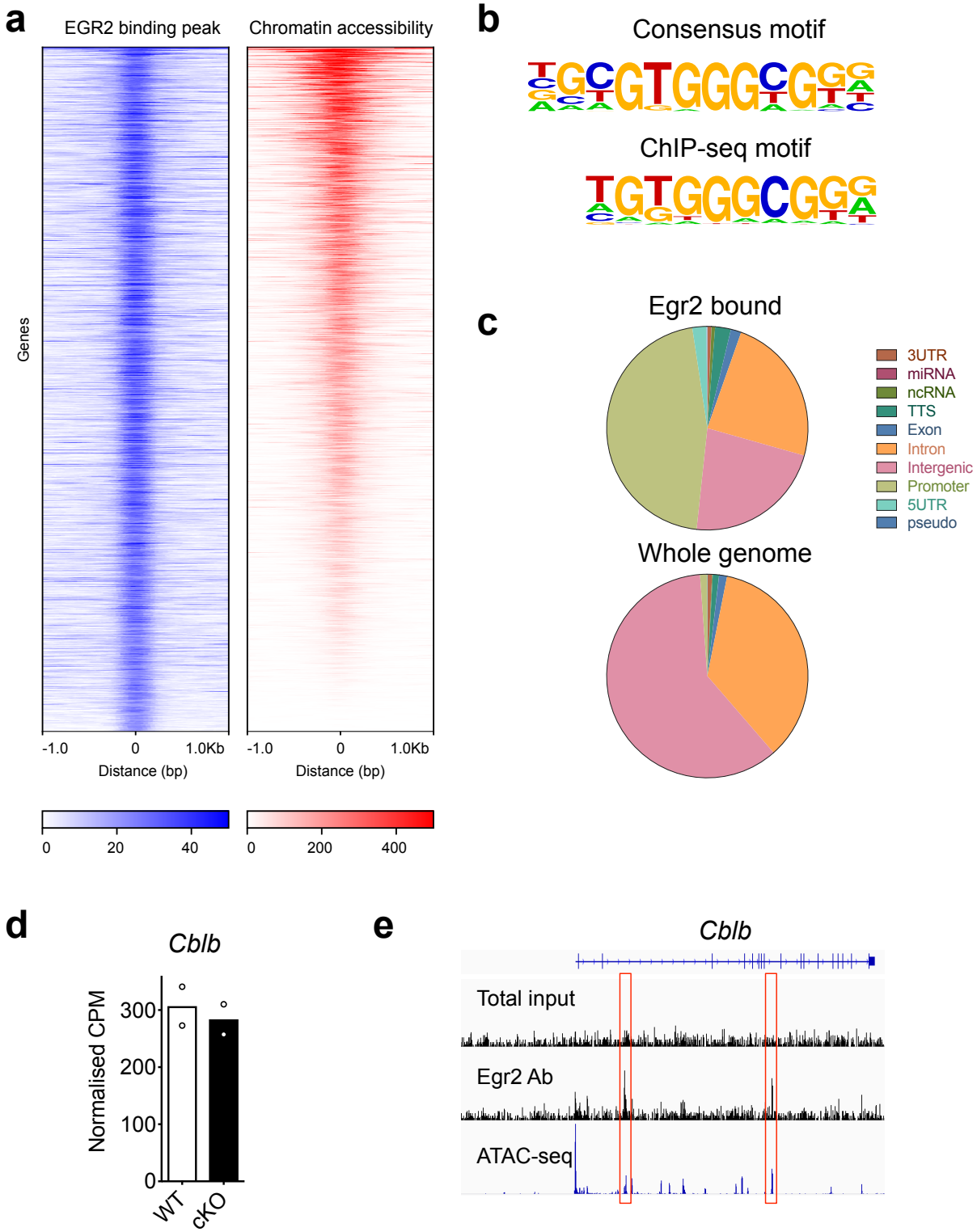
a
EGR2 binding peak
Chromatin accessibility
Genes
-1.0
0
1.0Kb
Distance (bp)
0
20
40
0
200
400
b
Consensus motif
ChIP-seq motif
c
Egr2 bound
Whole genome
3UTR
miRNA
ncRNA
TTS
Exon
Intron
Intergenic
Promoter
5UTR
pseudo
d
Cblb
Normalised CPM
300
200
100
0
WT
cKO
e
Cblb
Total input
Egr2 Ab
ATAC-seq

Figure 4.S5. EGR2 ChIP-seq analysis of CD8$^+$ T cells isolated from LCMV-Cl13 infection. Related to Figure 4.6. CD8$^+$ T cells were isolated from LCMV-Cl13 infected B6 mice at day 20 p.i. and subjected to ChIP-seq analysis. (A) Association between EGR2 peak signal (left) and chromatin accessibility at the binding site (right), ranked from most (top) to least (bottom) accessible EGR2 binding site. Each row represents a single gene, and the X-axis depicts signal strength in the genomic regions up to 1Kb either side of the centre of the binding site (labeled "0"). (B) Consensus EGR2 motif within the HOMER database (top), and the *de novo* EGR2 motif extracted from the ChIP-seq peaks (bottom). (C) Proportions of EGR2 binding within different genomic regions (top) relative to the proportion of those regions within the whole genome (bottom). (D,E) Expression levels of *Cblb* from the RNAseq data in Fig. 4.5 (D) and EGR2 binding peaks identified within the *Cblb* locus (E). Traces show EGR2 Ab signal, Total input signal, and published ATAC-seq accessibility within day 27 exhausted virus-specific CD8$^+$ T cells from LCMV-Cl13 infection as in Fig. 4.6. Red boxes denote significant peaks.

Table 4.S1- significantly differentially expressed genes within *Egr2* cKO CD8+ T cells relative to WT control cells (FDR<0.05)

Gene	logFC	AveExpr	t	P.Value	adj.P.Val	B
Gm11168	2.637	8.825	18.520	5.49E-13	5.30E-09	19.364
Ifitm1	2.566	3.127	5.146	7.25E-05	6.63E-03	1.665
Gm21738	2.269	11.449	15.914	6.86E-12	3.31E-08	17.208
Cadm1	2.218	4.395	8.811	7.22E-08	3.87E-05	8.130
Prex2	2.166	2.569	4.331	4.22E-04	2.01E-02	0.123
Itgae	2.161	4.940	8.221	1.95E-07	9.42E-05	7.376
Unc79	2.137	2.282	5.279	5.47E-05	5.68E-03	1.827
Clec9a	2.092	3.891	7.924	3.27E-07	1.26E-04	6.812
Mycl	2.028	3.571	6.743	2.87E-06	6.02E-04	4.672
Gm10717	2.024	9.587	14.120	4.87E-11	1.42E-07	15.407
Gm10718	2.016	7.106	13.306	1.27E-10	1.76E-07	14.437
Dnase1l3	2.015	5.940	10.528	5.06E-09	4.44E-06	10.908
Gm10719	2.011	7.597	13.765	7.37E-11	1.42E-07	14.982
Hrnr	2.009	4.809	7.901	3.40E-07	1.26E-04	6.807
Gm10721	1.993	6.518	12.354	4.17E-10	5.04E-07	13.277
Gm10801	1.964	9.909	13.433	1.09E-10	1.76E-07	14.659
Flt3	1.955	4.170	7.270	1.06E-06	2.93E-04	5.719
Gm10722	1.940	9.329	13.806	7.02E-11	1.42E-07	15.068
Plbd1	1.926	6.031	9.688	1.78E-08	1.43E-05	9.743
Adam23	1.921	4.573	8.038	2.68E-07	1.08E-04	7.024
Anpep	1.895	4.317	7.105	1.44E-06	3.48E-04	5.459
Zfp366	1.894	3.074	6.183	8.57E-06	1.45E-03	3.671
Shtn1	1.865	3.984	6.283	7.03E-06	1.23E-03	3.945
Reln	1.833	3.369	5.437	3.93E-05	4.78E-03	2.267
Gm10720	1.829	4.906	8.825	7.06E-08	3.87E-05	8.327
Ttn	1.827	6.926	11.637	1.07E-09	1.04E-06	12.472
Itgax	1.787	5.818	8.948	5.77E-08	3.48E-05	8.612
Gm10800	1.766	13.918	12.064	6.08E-10	6.52E-07	13.060
Xcr1	1.763	4.464	7.558	6.28E-07	2.09E-04	6.264
Tbc1d9	1.734	4.393	6.646	3.45E-06	7.09E-04	4.654
Dbn1	1.725	3.738	5.602	2.79E-05	3.74E-03	2.654
Notch4	1.661	3.693	5.238	5.97E-05	5.88E-03	1.960
Apol7c	1.659	4.025	6.407	5.50E-06	1.04E-03	4.182
Pbx1	1.658	3.601	5.307	5.16E-05	5.51E-03	2.068
Nav1	1.656	4.095	5.264	5.65E-05	5.80E-03	2.025
Cbfa2t3	1.656	4.185	5.775	1.96E-05	2.95E-03	3.012
Naaa	1.655	6.380	7.857	3.68E-07	1.32E-04	6.831
Nr4a3	1.647	4.700	7.328	9.56E-07	2.71E-04	5.866
Dnm3	1.638	3.288	4.786	1.57E-04	1.15E-02	1.042
Fnip2	1.634	4.211	5.711	2.23E-05	3.17E-03	2.894

Fos	1.621	3.988	5.736	2.12E-05	3.10E-03	2.919
Gm6377	1.621	4.217	4.133	6.51E-04	2.53E-02	-0.274
Cd74	1.614	10.164	7.252	1.10E-06	2.95E-04	5.721
Rab7b	1.609	3.670	5.218	6.22E-05	5.95E-03	1.934
Mroh2a	1.599	4.785	7.340	9.35E-07	2.71E-04	5.897
Hydin	1.598	3.503	4.985	1.02E-04	8.44E-03	1.446
Abca13	1.592	3.943	5.416	4.11E-05	4.84E-03	2.314
Trpm2	1.587	4.711	6.316	6.59E-06	1.20E-03	4.057
Cxcl9	1.584	3.906	5.808	1.83E-05	2.80E-03	3.075
Fbn1	1.582	2.796	4.160	6.13E-04	2.44E-02	-0.186
Il12rb2	1.579	3.616	5.158	7.08E-05	6.57E-03	1.792
Mpeg1	1.579	7.269	5.645	2.55E-05	3.52E-03	2.608
Sh3pxd2b	1.572	2.629	4.371	3.86E-04	1.89E-02	0.231
Kit	1.570	4.269	5.935	1.41E-05	2.31E-03	3.322
Fmnl2	1.570	3.812	5.343	4.79E-05	5.37E-03	2.178
Olfm1	1.567	3.537	4.744	1.72E-04	1.22E-02	0.992
Tlr3	1.565	3.922	4.626	2.22E-04	1.41E-02	0.727
Dnah7a	1.564	3.185	4.472	3.10E-04	1.62E-02	0.435
Duxf3	1.564	4.461	6.569	4.01E-06	8.07E-04	4.506
Lrp1b	1.559	3.118	4.317	4.35E-04	2.04E-02	0.130
Wdfy4	1.554	7.706	7.045	1.62E-06	3.72E-04	5.345
Sostdc1	1.554	4.395	6.390	5.69E-06	1.06E-03	4.175
Aif1	1.553	3.440	4.880	1.28E-04	1.03E-02	1.255
Lima1	1.551	3.312	4.716	1.82E-04	1.27E-02	0.920
Dnah10	1.549	3.351	4.596	2.37E-04	1.45E-02	0.685
Gpr55	1.546	6.212	8.167	2.14E-07	9.72E-05	7.360
Nav2	1.540	3.775	5.145	7.27E-05	6.63E-03	1.777
H2-Eb1	1.519	8.371	5.925	1.44E-05	2.32E-03	3.164
Plcb4	1.514	3.411	4.530	2.73E-04	1.50E-02	0.564
Ank2	1.505	3.703	5.040	9.10E-05	7.57E-03	1.570
Cst3	1.491	8.194	7.219	1.17E-06	3.05E-04	5.665
Astn1	1.487	2.751	3.852	1.21E-03	3.62E-02	-0.779
Igf1r	1.482	3.457	4.648	2.11E-04	1.39E-02	0.794
Treml4	1.475	3.894	4.760	1.66E-04	1.18E-02	1.025
H2-Ab1	1.474	9.070	5.675	2.40E-05	3.36E-03	2.652
Obscn	1.466	4.099	5.592	2.85E-05	3.77E-03	2.659
Dnah6	1.466	2.791	3.804	1.34E-03	3.75E-02	-0.868
Specc1	1.454	3.944	5.294	5.30E-05	5.57E-03	2.078
Fras1	1.433	3.336	4.303	4.48E-04	2.07E-02	0.115
Fam186a	1.432	3.129	3.845	1.23E-03	3.62E-02	-0.785
Myh2	1.428	2.980	3.923	1.03E-03	3.32E-02	-0.635
Hba-a2	1.423	8.964	9.581	2.11E-08	1.56E-05	9.624
Gm26992	1.423	3.747	4.527	2.75E-04	1.50E-02	0.539
Ciita	1.420	5.817	5.538	3.19E-05	4.05E-03	2.464
Hba-a1	1.419	9.013	9.343	3.06E-08	2.11E-05	9.259

Egr3	1.411	3.648	4.117	6.75E-04	2.59E-02	-0.259
Zbtb46	1.405	3.958	4.849	1.37E-04	1.07E-02	1.200
Csf2rb2	1.402	3.307	4.205	5.55E-04	2.34E-02	-0.077
Slc4a1	1.401	5.416	7.503	6.95E-07	2.24E-04	6.219
Asb2	1.397	4.643	6.290	6.93E-06	1.23E-03	4.008
Itga1	1.395	4.044	5.251	5.81E-05	5.85E-03	1.997
Pag1	1.394	5.021	5.364	4.58E-05	5.20E-03	2.185
Csf2rb	1.386	4.404	4.565	2.53E-04	1.46E-02	0.605
Tifab	1.379	4.061	4.786	1.57E-04	1.15E-02	1.071
Gcsam	1.379	3.868	5.106	7.90E-05	6.94E-03	1.712
Ccnd1	1.378	3.621	4.326	4.26E-04	2.02E-02	0.161
Gm2a	1.378	7.159	7.051	1.60E-06	3.72E-04	5.362
AW822073	1.375	4.089	5.054	8.81E-05	7.47E-03	1.611
Jaml	1.359	4.494	5.184	6.69E-05	6.34E-03	1.856
Ank3	1.352	4.249	4.845	1.38E-04	1.08E-02	1.185
H2-Aa	1.350	8.351	5.257	5.74E-05	5.83E-03	1.787
Dnah2	1.346	3.197	3.916	1.05E-03	3.35E-02	-0.647
Grk3	1.333	3.595	4.134	6.49E-04	2.53E-02	-0.224
Gm13698	1.333	3.720	4.496	2.94E-04	1.57E-02	0.499
Apobr	1.326	5.004	6.429	5.27E-06	1.04E-03	4.268
Wdfy3	1.326	3.831	4.542	2.66E-04	1.48E-02	0.590
Adgrv1	1.319	3.345	4.021	8.32E-04	2.92E-02	-0.440
Fam196b	1.314	4.032	4.553	2.60E-04	1.46E-02	0.600
Ryr1	1.314	4.178	4.971	1.05E-04	8.62E-03	1.441
Fat4	1.313	3.075	3.753	1.51E-03	4.03E-02	-0.965
Ccr2	1.312	5.590	4.761	1.66E-04	1.18E-02	0.863
Sbf2	1.291	3.317	3.882	1.13E-03	3.47E-02	-0.716
AC133103.1	1.282	4.845	5.740	2.10E-05	3.10E-03	2.943
Zfp600	1.280	3.450	4.072	7.44E-04	2.76E-02	-0.341
Atp8a2	1.279	3.291	3.894	1.10E-03	3.43E-02	-0.691
Vwf	1.279	3.354	3.956	9.62E-04	3.17E-02	-0.571
Nhsl2	1.275	3.666	4.286	4.65E-04	2.10E-02	0.080
Zan	1.264	3.651	4.179	5.89E-04	2.40E-02	-0.135
Spta1	1.252	3.786	4.585	2.42E-04	1.45E-02	0.673
Sfi1	1.250	7.427	8.523	1.17E-07	5.93E-05	7.947
Arhgef11	1.248	3.705	4.193	5.71E-04	2.36E-02	-0.110
Adam8	1.247	5.594	7.121	1.40E-06	3.47E-04	5.536
Mctp1	1.244	3.579	4.080	7.32E-04	2.74E-02	-0.335
Gm17535	1.243	7.449	8.133	2.27E-07	9.72E-05	7.292
Gm10715	1.240	7.332	8.122	2.31E-07	9.72E-05	7.273
Itgad	1.237	4.019	4.628	2.21E-04	1.41E-02	0.755
Tns3	1.236	4.583	4.047	7.87E-04	2.84E-02	-0.509
Trio	1.225	4.703	5.634	2.61E-05	3.55E-03	2.739
Ryr2	1.208	3.715	4.140	6.40E-04	2.51E-02	-0.217
Hs3st3b1	1.207	3.926	4.465	3.15E-04	1.63E-02	0.428

Itsn1	1.190	4.142	4.451	3.25E-04	1.66E-02	0.385
Pdzd2	1.189	3.684	4.072	7.45E-04	2.76E-02	-0.354
Snca	1.184	3.392	3.624	2.00E-03	4.82E-02	-1.235
Akap2	1.184	3.482	3.838	1.25E-03	3.63E-02	-0.813
Alas2	1.183	4.985	5.506	3.41E-05	4.27E-03	2.466
Sdc3	1.179	5.367	4.854	1.35E-04	1.07E-02	1.079
Tbc1d8	1.172	4.147	3.663	1.83E-03	4.63E-02	-1.262
Acss2	1.164	4.439	5.061	8.69E-05	7.42E-03	1.609
Plekho1	1.162	4.655	5.137	7.40E-05	6.67E-03	1.745
Satb1	1.157	6.482	6.819	2.48E-06	5.44E-04	4.938
Afdn	1.155	3.958	4.216	5.42E-04	2.32E-02	-0.082
Rxra	1.154	3.866	3.742	1.54E-03	4.07E-02	-1.048
Hbb-bt	1.149	8.160	7.359	9.02E-07	2.71E-04	5.922
Cd36	1.141	4.366	3.748	1.52E-03	4.03E-02	-1.103
Rasgrp3	1.138	4.210	4.449	3.26E-04	1.66E-02	0.372
March1	1.138	4.905	4.298	4.53E-04	2.08E-02	-0.030
Myo9a	1.136	5.071	5.428	4.01E-05	4.78E-03	2.296
5031410I06 Rik	1.133	3.517	3.699	1.70E-03	4.36E-02	-1.097
Rasa4	1.125	3.770	3.848	1.22E-03	3.62E-02	-0.817
Il18r1	1.120	6.992	6.854	2.32E-06	5.21E-04	4.994
Dst	1.116	5.316	6.212	8.09E-06	1.40E-03	3.835
Ryr3	1.101	4.355	4.685	1.95E-04	1.32E-02	0.845
Irf8	1.095	7.520	5.431	3.98E-05	4.78E-03	2.158
Gabbr1	1.090	4.701	4.617	2.26E-04	1.42E-02	0.658
Nr4a1	1.086	4.426	4.493	2.96E-04	1.57E-02	0.442
Slc8b1	1.080	4.501	4.559	2.56E-04	1.46E-02	0.549
Kctd12	1.067	4.782	4.537	2.69E-04	1.49E-02	0.486
Pkib	1.055	4.220	4.076	7.39E-04	2.75E-02	-0.402
Ppt1	1.052	7.418	5.329	4.93E-05	5.47E-03	1.949
Ece1	1.050	5.951	5.239	5.95E-05	5.88E-03	1.823
Psap	1.046	9.220	5.304	5.19E-05	5.51E-03	1.882
Med12l	1.045	3.646	3.608	2.07E-03	4.89E-02	-1.295
Slco3a1	1.044	4.516	4.576	2.47E-04	1.45E-02	0.597
Tmcc2	1.037	3.922	4.025	8.26E-04	2.92E-02	-0.509
Tanc1	1.035	4.273	3.837	1.25E-03	3.63E-02	-0.906
Marcksl1	1.022	4.050	3.986	9.00E-04	3.04E-02	-0.568
H2-DMb1	1.002	4.673	4.021	8.32E-04	2.92E-02	-0.586
Zbtb20	0.977	5.151	5.306	5.18E-05	5.51E-03	2.034
Rara	0.976	4.844	4.401	3.62E-04	1.81E-02	0.184
Bach2	0.975	5.179	5.314	5.09E-05	5.51E-03	2.047
Tsc22d1	0.954	4.208	3.613	2.05E-03	4.86E-02	-1.368
Ifi205	0.951	6.386	4.259	4.94E-04	2.19E-02	-0.300
Diaph2	0.949	4.192	3.883	1.13E-03	3.47E-02	-0.804
A530032D1	0.939	4.771	4.632	2.19E-04	1.41E-02	0.678

5Rik						
Galnt10	0.935	4.747	3.628	1.98E-03	4.80E-02	-1.435
Apol11b	0.926	4.167	3.894	1.10E-03	3.43E-02	-0.796
Ly6c2	0.922	7.552	5.557	3.06E-05	3.94E-03	2.417
Slc7a5	0.916	4.679	3.988	8.96E-04	3.04E-02	-0.662
Pld4	0.916	5.222	3.754	1.50E-03	4.03E-02	-1.252
St6gal1	0.916	5.094	4.255	4.98E-04	2.19E-02	-0.162
Cacna1e	0.912	4.908	4.163	6.09E-04	2.44E-02	-0.332
Rgs10	0.911	5.115	4.677	1.98E-04	1.32E-02	0.724
Jun	0.905	4.945	4.613	2.28E-04	1.42E-02	0.614
Hivep3	0.902	4.909	4.587	2.41E-04	1.45E-02	0.566
Fosl2	0.902	4.432	4.014	8.47E-04	2.94E-02	-0.570
Tiam1	0.887	5.018	4.610	2.29E-04	1.42E-02	0.597
Prkd3	0.878	5.578	5.124	7.59E-05	6.79E-03	1.609
Hbb-bs	0.867	8.250	4.312	4.40E-04	2.05E-02	-0.232
Btla	0.859	6.258	3.958	9.57E-04	3.16E-02	-0.950
Iqgap2	0.855	6.442	3.902	1.08E-03	3.41E-02	-1.085
Ctnna1	0.847	5.037	4.445	3.28E-04	1.67E-02	0.242
Alms1	0.840	5.115	4.574	2.48E-04	1.45E-02	0.505
Plcg2	0.839	5.812	4.014	8.46E-04	2.94E-02	-0.765
Plekhm3	0.838	4.872	4.213	5.46E-04	2.32E-02	-0.226
AC125149.1	0.835	4.609	3.604	2.09E-03	4.91E-02	-1.466
Ly6c1	0.829	5.875	4.852	1.36E-04	1.07E-02	1.004
Bcl6	0.828	4.864	4.230	5.26E-04	2.26E-02	-0.188
Mdn1	0.825	6.806	5.376	4.46E-05	5.13E-03	2.055
Kmt2d	0.823	8.786	4.736	1.75E-04	1.23E-02	0.679
Csprs	0.820	4.610	3.709	1.66E-03	4.30E-02	-1.243
Rab43	0.819	6.639	4.820	1.46E-04	1.10E-02	0.888
Lrrk2	0.818	5.542	4.161	6.13E-04	2.44E-02	-0.428
Atrn	0.807	4.594	3.617	2.03E-03	4.85E-02	-1.435
Aldh2	0.803	4.713	3.643	1.92E-03	4.71E-02	-1.410
Arrb1	0.803	4.983	4.048	7.85E-04	2.84E-02	-0.597
Egr1	0.802	6.069	5.117	7.71E-05	6.83E-03	1.548
Ptprs	0.798	4.684	3.720	1.62E-03	4.24E-02	-1.243
Vav2	0.797	4.741	3.814	1.31E-03	3.72E-02	-1.050
D1Ertd622e	0.797	5.371	4.581	2.44E-04	1.45E-02	0.483
Apoe	0.795	5.027	4.252	5.01E-04	2.19E-02	-0.168
Sipa1l3	0.793	5.303	4.407	3.57E-04	1.80E-02	0.122
Sh2b3	0.792	5.522	3.924	1.03E-03	3.32E-02	-0.943
Cln3	0.786	4.847	4.006	8.61E-04	2.98E-02	-0.663
Marcks	0.785	5.012	3.672	1.80E-03	4.57E-02	-1.404
Parp8	0.780	5.152	4.108	6.88E-04	2.62E-02	-0.496
Plxnc1	0.780	5.298	3.872	1.16E-03	3.52E-02	-1.021
Runx2	0.773	6.108	4.898	1.23E-04	1.00E-02	1.082
Zeb2	0.772	5.771	4.713	1.83E-04	1.27E-02	0.717

Atp8b4	0.764	6.622	4.406	3.58E-04	1.80E-02	-0.004
Il18rap	0.763	7.038	5.048	8.93E-05	7.50E-03	1.359
Gusb	0.748	5.599	4.172	5.98E-04	2.42E-02	-0.424
Cmah	0.747	5.694	4.034	8.10E-04	2.90E-02	-0.732
Unc93b1	0.744	6.929	4.087	7.21E-04	2.72E-02	-0.702
Vim	0.743	9.229	4.231	5.25E-04	2.26E-02	-0.413
Rreb1	0.740	5.114	3.882	1.13E-03	3.47E-02	-0.976
Tsc22d2	0.736	5.085	3.811	1.32E-03	3.73E-02	-1.121
Patj	0.722	5.374	4.200	5.62E-04	2.35E-02	-0.335
Ahnak	0.722	10.738	4.685	1.95E-04	1.32E-02	0.558
Tep1	0.715	5.384	3.973	9.25E-04	3.09E-02	-0.823
Stx16	0.712	5.172	3.941	9.95E-04	3.25E-02	-0.859
Jchain	0.710	6.119	4.119	6.71E-04	2.58E-02	-0.523
Nfat5	0.710	6.659	4.822	1.45E-04	1.10E-02	0.892
Kdm6b	0.709	5.682	3.887	1.12E-03	3.47E-02	-1.050
Prrc2c	0.708	9.111	4.258	4.95E-04	2.19E-02	-0.354
Grn	0.707	5.661	4.181	5.86E-04	2.40E-02	-0.413
Atp11a	0.704	5.101	3.858	1.19E-03	3.58E-02	-1.025
Utrn	0.703	8.854	4.381	3.78E-04	1.87E-02	-0.086
Ubn2	0.703	5.985	4.494	2.95E-04	1.57E-02	0.225
Klrd1	0.693	5.554	4.052	7.78E-04	2.83E-02	-0.677
Tmem131	0.683	6.394	4.601	2.34E-04	1.44E-02	0.424
Zbtb37	0.679	5.123	3.739	1.55E-03	4.08E-02	-1.282
Slc7a1	0.676	5.628	4.065	7.57E-04	2.79E-02	-0.661
Macf1	0.676	9.516	4.062	7.60E-04	2.79E-02	-0.780
Hectd4	0.675	6.658	4.614	2.27E-04	1.42E-02	0.443
Ifngr1	0.674	7.402	4.457	3.20E-04	1.65E-02	0.087
Huwe1	0.664	8.505	4.551	2.60E-04	1.46E-02	0.284
Smg1	0.654	8.264	4.188	5.77E-04	2.38E-02	-0.501
Gvin1	0.652	10.217	4.282	4.70E-04	2.11E-02	-0.310
Ssh2	0.650	6.993	4.135	6.48E-04	2.53E-02	-0.602
Kdm7a	0.647	6.355	4.353	4.02E-04	1.94E-02	-0.109
Ppp1r15a	0.646	5.685	3.607	2.08E-03	4.89E-02	-1.652
Gm4070	0.644	10.198	4.255	4.98E-04	2.19E-02	-0.368
Clcn3	0.641	5.879	3.887	1.12E-03	3.47E-02	-1.074
Rnf213	0.641	9.680	4.510	2.85E-04	1.54E-02	0.188
Zfp407	0.639	5.636	3.619	2.02E-03	4.85E-02	-1.620
Itpr1	0.635	6.788	3.867	1.17E-03	3.53E-02	-1.177
Mtmr4	0.635	5.626	3.748	1.52E-03	4.03E-02	-1.344
Kmt2a	0.633	8.311	4.330	4.23E-04	2.01E-02	-0.195
Sgk1	0.621	5.578	3.761	1.48E-03	3.98E-02	-1.308
Mki67	0.614	8.687	3.904	1.08E-03	3.40E-02	-1.118
Klrc2	0.614	6.048	3.751	1.51E-03	4.03E-02	-1.384
Cit	0.613	5.471	3.655	1.87E-03	4.68E-02	-1.523
Zfp36l1	0.612	7.401	3.871	1.16E-03	3.52E-02	-1.181

Dnajc15	0.610	5.860	3.800	1.36E-03	3.77E-02	-1.260
Ubr4	0.603	8.313	4.187	5.79E-04	2.38E-02	-0.504
Srrm2	0.600	9.453	4.097	7.04E-04	2.68E-02	-0.704
Map4k4	0.595	7.950	3.986	9.00E-04	3.04E-02	-0.937
Zfc3h1	0.593	6.511	3.655	1.87E-03	4.68E-02	-1.623
Smad3	0.592	6.042	3.827	1.28E-03	3.65E-02	-1.222
Plec	0.581	9.353	3.748	1.52E-03	4.03E-02	-1.458
Mib1	0.580	5.707	3.592	2.15E-03	4.99E-02	-1.688
Cad	0.570	6.049	3.719	1.62E-03	4.24E-02	-1.456
Dock5	0.565	6.793	3.799	1.36E-03	3.77E-02	-1.323
Klrk1	0.564	6.430	3.612	2.05E-03	4.86E-02	-1.714
Golgb1	0.560	6.611	3.686	1.74E-03	4.46E-02	-1.562
Fbxw7	0.554	6.117	3.650	1.89E-03	4.69E-02	-1.611
Birc6	0.549	8.673	3.698	1.70E-03	4.36E-02	-1.562
Luc7l2	0.546	7.870	3.644	1.91E-03	4.71E-02	-1.675
Mycbp2	0.543	8.169	3.649	1.89E-03	4.69E-02	-1.666
4932438A13Rik	0.538	7.883	3.633	1.96E-03	4.78E-02	-1.699
Sema4a	0.533	6.458	3.617	2.03E-03	4.85E-02	-1.704
Hist1h4d	-0.511	9.747	-3.642	1.92E-03	4.71E-02	-1.690
Hist1h2br	-0.512	9.512	-3.593	2.14E-03	4.99E-02	-1.794
Hist1h4b	-0.514	8.964	-3.638	1.94E-03	4.74E-02	-1.693
Hist1h2ak	-0.516	9.077	-3.632	1.96E-03	4.78E-02	-1.706
Sub1	-0.525	8.548	-3.701	1.69E-03	4.35E-02	-1.555
Hist1h2be	-0.525	8.578	-3.665	1.83E-03	4.63E-02	-1.633
Cxcr5	-0.527	6.578	-3.617	2.03E-03	4.85E-02	-1.717
Trim14	-0.535	7.357	-3.751	1.51E-03	4.03E-02	-1.444
Cox17	-0.540	6.482	-3.709	1.66E-03	4.30E-02	-1.516
Hist1h2bf	-0.544	8.452	-3.828	1.27E-03	3.65E-02	-1.280
Dnajc9	-0.547	6.981	-3.603	2.10E-03	4.91E-02	-1.759
Batf	-0.552	6.659	-3.772	1.44E-03	3.94E-02	-1.388
Hist1h4j	-0.552	8.678	-3.817	1.31E-03	3.71E-02	-1.306
Casp3	-0.553	6.659	-3.614	2.04E-03	4.86E-02	-1.727
Nab1	-0.558	7.457	-3.908	1.07E-03	3.38E-02	-1.104
Smpdl3a	-0.559	6.878	-3.808	1.33E-03	3.74E-02	-1.315
Hist1h4a	-0.562	8.991	-3.971	9.31E-04	3.10E-02	-0.974
Glipr1	-0.563	6.256	-3.797	1.36E-03	3.77E-02	-1.314
Pfdn5	-0.567	8.101	-3.787	1.40E-03	3.83E-02	-1.368
Hist1h4k	-0.576	9.079	-4.000	8.72E-04	2.99E-02	-0.911
Hist1h4i	-0.577	8.337	-4.027	8.22E-04	2.92E-02	-0.849
Hist1h4h	-0.578	9.378	-4.039	8.00E-04	2.87E-02	-0.829
Fcgr3	-0.581	6.348	-3.953	9.69E-04	3.18E-02	-0.983
Hist1h4m	-0.581	8.405	-3.984	9.04E-04	3.04E-02	-0.943
Gpr65	-0.583	6.391	-3.822	1.29E-03	3.68E-02	-1.267
Dhrs7	-0.583	5.487	-3.595	2.13E-03	4.99E-02	-1.682

Rab27a	-0.584	7.291	-4.051	7.79E-04	2.83E-02	-0.794
Tox	-0.585	8.526	-3.681	1.77E-03	4.50E-02	-1.599
Gm21987	-0.596	5.896	-3.844	1.23E-03	3.62E-02	-1.194
Hist1h4c	-0.597	8.739	-4.085	7.24E-04	2.72E-02	-0.726
Prkch	-0.597	8.442	-3.879	1.14E-03	3.48E-02	-1.170
1810009A15Rik	-0.599	5.642	-3.836	1.25E-03	3.63E-02	-1.186
Cd3d	-0.602	8.393	-3.796	1.37E-03	3.77E-02	-1.350
Tmem9b	-0.603	5.720	-3.648	1.90E-03	4.69E-02	-1.598
Zfp827	-0.604	6.136	-3.991	8.89E-04	3.03E-02	-0.888
Tma7	-0.606	7.225	-4.147	6.31E-04	2.49E-02	-0.586
Hist1h4f	-0.609	8.750	-4.287	4.64E-04	2.10E-02	-0.288
Hist1h4n	-0.611	8.442	-4.198	5.65E-04	2.35E-02	-0.480
Hist1h2bl	-0.618	8.389	-4.317	4.34E-04	2.04E-02	-0.221
Gm20388	-0.621	7.484	-3.913	1.06E-03	3.36E-02	-1.095
Adap1	-0.625	5.975	-3.764	1.47E-03	3.98E-02	-1.369
Dut	-0.625	6.544	-3.763	1.47E-03	3.98E-02	-1.401
Galnt2	-0.635	7.483	-4.015	8.45E-04	2.94E-02	-0.874
Iqcg	-0.638	5.760	-3.833	1.26E-03	3.65E-02	-1.203
Ddx3y	-0.641	5.617	-3.896	1.10E-03	3.43E-02	-1.041
S100a11	-0.644	6.954	-4.479	3.05E-04	1.61E-02	0.136
Cetn2	-0.651	5.677	-4.093	7.12E-04	2.69E-02	-0.637
Rgs1	-0.653	7.599	-4.582	2.44E-04	1.45E-02	0.353
Tecr	-0.654	6.052	-4.368	3.89E-04	1.90E-02	-0.071
Pglyrp1	-0.660	5.663	-4.154	6.21E-04	2.46E-02	-0.501
Tmem135	-0.664	6.058	-3.709	1.66E-03	4.30E-02	-1.492
Fasl	-0.665	6.721	-3.961	9.51E-04	3.16E-02	-0.980
Hist4h4	-0.669	7.187	-4.563	2.54E-04	1.46E-02	0.315
2410015M20Rik	-0.670	5.161	-3.846	1.23E-03	3.62E-02	-1.093
Ndufb4	-0.679	6.086	-4.294	4.57E-04	2.08E-02	-0.232
Vamp8	-0.690	6.068	-4.553	2.60E-04	1.46E-02	0.327
Ap1s2	-0.702	5.660	-4.380	3.79E-04	1.87E-02	-0.015
Ctsc	-0.708	7.055	-3.828	1.27E-03	3.65E-02	-1.274
Gimap7	-0.714	8.561	-4.031	8.16E-04	2.91E-02	-0.843
Hist3h2ba	-0.722	4.612	-3.658	1.85E-03	4.66E-02	-1.396
Pet100	-0.729	6.135	-4.636	2.17E-04	1.40E-02	0.502
Stard3nl	-0.747	5.097	-3.868	1.17E-03	3.53E-02	-1.033
Glmn	-0.788	4.355	-3.658	1.85E-03	4.66E-02	-1.339
Suox	-0.792	4.600	-3.861	1.18E-03	3.56E-02	-0.958
Eif2s3y	-0.793	5.080	-4.351	4.04E-04	1.94E-02	0.003
Rgs16	-0.796	4.813	-4.171	5.99E-04	2.42E-02	-0.338
Lgalsl	-0.817	4.960	-4.005	8.63E-04	2.98E-02	-0.717
Map2	-0.832	5.243	-4.802	1.51E-04	1.13E-02	0.941
Chn2	-0.843	6.048	-3.642	1.92E-03	4.71E-02	-1.635

Cyth3	-0.846	5.029	-4.508	2.86E-04	1.54E-02	0.346
Ift27	-0.857	4.539	-4.197	5.66E-04	2.35E-02	-0.236
Eomes	-0.863	7.782	-5.448	3.85E-05	4.76E-03	2.187
Smpdl3b	-0.866	4.794	-4.573	2.48E-04	1.45E-02	0.520
Sh2d1a	-0.873	6.671	-6.023	1.18E-05	1.97E-03	3.373
Cd5	-0.876	7.147	-5.899	1.52E-05	2.40E-03	3.116
Slc27a4	-0.877	6.064	-5.394	4.31E-05	5.01E-03	2.107
Mrpl10	-0.881	4.859	-4.575	2.47E-04	1.45E-02	0.515
Tigit	-0.888	6.965	-4.820	1.46E-04	1.10E-02	0.870
Cst7	-0.892	7.279	-5.233	6.03E-05	5.88E-03	1.741
Pdcd1	-0.917	8.138	-4.697	1.90E-04	1.30E-02	0.598
Ephx1	-0.924	5.491	-4.673	2.00E-04	1.32E-02	0.636
Gm28778	-0.966	3.979	-3.931	1.02E-03	3.29E-02	-0.700
Slc37a2	-0.988	4.812	-5.070	8.53E-05	7.36E-03	1.557
Lrig1	-0.995	3.881	-3.626	1.99E-03	4.82E-02	-1.319
Ctla2a	-1.012	7.422	-6.784	2.65E-06	5.69E-04	4.852
Rpa3	-1.013	3.819	-3.623	2.00E-03	4.82E-02	-1.310
Immp1l	-1.020	3.824	-3.931	1.02E-03	3.29E-02	-0.677
Abcb9	-1.022	5.867	-4.829	1.43E-04	1.10E-02	0.934
Insl6	-1.049	3.834	-3.916	1.05E-03	3.35E-02	-0.709
Cd6	-1.050	7.411	-7.183	1.25E-06	3.17E-04	5.600
Sec14l1	-1.054	6.687	-5.726	2.16E-05	3.11E-03	2.772
Mien1	-1.065	4.659	-5.229	6.09E-05	5.88E-03	1.905
Galm	-1.074	3.852	-3.653	1.88E-03	4.68E-02	-1.255
Adrb1	-1.095	3.600	-4.055	7.73E-04	2.83E-02	-0.409
Prmt2	-1.101	3.814	-3.765	1.46E-03	3.98E-02	-1.020
Borcs5	-1.106	3.509	-3.705	1.67E-03	4.33E-02	-1.100
Cd200r4	-1.111	5.094	-3.779	1.42E-03	3.88E-02	-1.219
Cd200r1	-1.138	5.108	-3.791	1.38E-03	3.81E-02	-1.198
Plekhf1	-1.151	3.337	-3.847	1.22E-03	3.62E-02	-0.802
Sept4	-1.181	5.116	-4.636	2.17E-04	1.40E-02	0.612
Nanos1	-1.186	3.314	-3.830	1.27E-03	3.65E-02	-0.828
Izumo1r	-1.188	4.273	-5.078	8.38E-05	7.29E-03	1.636
Vamp5	-1.198	3.243	-3.839	1.24E-03	3.63E-02	-0.809
Penk	-1.199	4.114	-4.159	6.14E-04	2.44E-02	-0.243
Polr2h	-1.222	3.354	-3.811	1.32E-03	3.73E-02	-0.870
Adgrg1	-1.227	6.959	-4.311	4.41E-04	2.05E-02	-0.225
Tbx1	-1.265	3.431	-4.244	5.11E-04	2.22E-02	-0.005
Tnfrsf9	-1.285	6.999	-5.561	3.04E-05	3.94E-03	2.427
Gzmk	-1.289	7.383	-7.331	9.50E-07	2.71E-04	5.872
Pak6	-1.309	2.940	-3.691	1.72E-03	4.41E-02	-1.089
Cisd3	-1.318	3.235	-4.231	5.25E-04	2.26E-02	-0.026
Tox2	-1.325	5.846	-7.565	6.20E-07	2.09E-04	6.317
Mob3c	-1.343	2.926	-3.981	9.10E-04	3.05E-02	-0.519
Itga9	-1.383	7.049	-9.097	4.53E-08	2.92E-05	8.875

Pfn2	-1.399	3.225	-3.923	1.03E-03	3.32E-02	-0.636
Gm15013	-1.399	3.561	-4.392	3.69E-04	1.84E-02	0.289
Ccrl2	-1.437	4.304	-3.950	9.74E-04	3.19E-02	-0.703
Rnf135	-1.438	3.043	-4.208	5.52E-04	2.34E-02	-0.073
Cela1	-1.456	4.148	-3.844	1.23E-03	3.62E-02	-0.893
Clgn	-1.461	3.426	-4.362	3.94E-04	1.91E-02	0.234
Uxt	-1.523	2.985	-4.259	4.93E-04	2.19E-02	0.025
Taco1	-1.525	2.789	-4.130	6.56E-04	2.53E-02	-0.238
Pcbd2	-1.616	3.101	-4.791	1.55E-04	1.15E-02	1.056
Gm4950	-1.634	2.827	-4.469	3.12E-04	1.63E-02	0.412
Prr7	-1.709	2.756	-4.296	4.55E-04	2.08E-02	0.090
Pcgf1	-1.714	2.609	-4.001	8.72E-04	2.99E-02	-0.498
Rpp25l	-1.739	2.910	-4.717	1.82E-04	1.27E-02	0.890
Snai3	-1.753	2.809	-4.680	1.97E-04	1.32E-02	0.813
Apobec2	-1.755	3.157	-4.771	1.62E-04	1.18E-02	1.022
Mrc2	-1.770	4.120	-3.804	1.34E-03	3.75E-02	-0.979
Sgpp2	-1.925	2.814	-5.174	6.84E-05	6.41E-03	1.712
Ociad2	-2.238	3.931	-6.418	5.39E-06	1.04E-03	4.175
P2ry10b	-2.324	2.282	-4.535	2.70E-04	1.49E-02	0.488
Egr2	-2.337	3.149	-5.818	1.79E-05	2.79E-03	2.975

Table 4.S2 - HOMER *de novo* TF binding motifs identified within EGR2 ChIP-seq binding peaks

P-value	% of Targets	% of Background	Best Match
1.00E-206	38.77%	11.80%	Etv2(ETS)
1.00E-92	17.21%	4.73%	RUNX1(Runt)
1.00E-65	**31.45%**	**15.87%**	**Egr2(Zf)**
1.00E-43	16.20%	6.97%	Atf1(bZIP)
1.00E-32	0.86%	0.01%	PB0099.1_Zfp691_1
1.00E-30	0.81%	0.01%	MF0009.1_TRP(MYB)_class
1.00E-30	0.81%	0.01%	ZBTB7B
1.00E-29	6.87%	2.20%	IRF2(IRF)
1.00E-28	1.11%	0.03%	KLF10(Zf)
1.00E-27	0.76%	0.01%	PB0117.1_Eomes_2
1.00E-27	4.39%	1.04%	GFX(?)
1.00E-25	0.76%	0.01%	PB0056.1_Rfxdc2_1
1.00E-22	0.56%	0.00%	HINFP
1.00E-21	18.02%	10.71%	NRF(NRF)
1.00E-20	0.50%	0.00%	GCM2
1.00E-20	0.50%	0.00%	CEBPA
1.00E-20	0.50%	0.00%	SP4
1.00E-19	0.56%	0.01%	PB0091.1_Zbtb3_1
1.00E-18	5.65%	2.14%	FOSL1
1.00E-17	0.45%	0.00%	Maz(Zf)
1.00E-17	7.47%	3.40%	NFY(CCAAT)
1.00E-17	0.71%	0.02%	EKLF(Zf)
1.00E-17	0.76%	0.03%	PB0022.1_Gata5_1
1.00E-16	8.68%	4.35%	Mef2c(MADS)
1.00E-15	6.51%	2.93%	NFY(CCAAT)
1.00E-15	0.40%	0.00%	CRX(Homeobox)
1.00E-15	0.81%	0.04%	PB0196.1_Zbtb7b_2
1.00E-14	5.50%	2.39%	NFAT(RHD)
1.00E-13	0.45%	0.01%	PH0017.1_Cux1_2
1.00E-10	4.09%	1.78%	PB0176.1_Sox5_2
1.00E-09	0.30%	0.01%	SPI1
1.00E-08	0.76%	0.10%	PB0179.1_Sp100_2
1.00E-05	4.90%	2.97%	YY2/MA0748.1
1.00E-03	1.41%	0.71%	Ap4(bHLH)

Table 4.S3 - Directly bound EGR2 targets during CD8$^+$ T cell exhaustion

Gene	Up or down in KO during exhaustion?	EGR2 anergy target?
Nr4a3	Up	No
Cd74	Up	Yes (down in KO in anergy)
Cst3	Up	No
Il18r1	Up	No
Satb1	Up	No
Cbfa2t3	Up	No
Ly6c2	Up	No
Irf8	Up	No
Bach2	Up	Yes (down in KO in anergy)
Il12rb2	Up	No
Ryr1	Up	Yes (down in KO in anergy)
Rab43	Up	No
Kmt2d	Up	No
Zeb2	Up	No
Ahnak	Up	No
Jun	Up	No
Hivep3	Up	No
D1Ertd622e	Up	No
Nr4a1	Up	No
Rara	Up	No
Utrn	Up	No
Kdm7a	Up	No
Kmt2a	Up	No
Gvin1	Up	No
Gm4070	Up	No
Bcl6	Up	No
Ubr4	Up	No
Ssh2	Up	No
Egr3	Up	No
Parp8	Up	No
Srrm2	Up	No
Btla	Up	No
Sh2b3	Up	No
Iqgap2	Up	No
Diaph2	Up	No
Zfp36l1	Up	No
Itpr1	Up	No
Smad3	Up	No
Dnah6	Up	No
Plec	Up	No
Mtmr4	Up	No
Birc6	Up	No

Marcks	Up	No
Fbxw7	Up	No
Mycbp2	Up	No
Luc7l2	Up	No
Atrn	Up	No
Klrk1	Up	No
Med12l	Up	No
Ppp1r15a	Up	No
Tox2	Down	No
Egr2	Down*	Yes (down in KO in anergy)*
Izumo1r	Down	No
Abcb9	Down	No
Tigit	Down	No
Pdcd1	Down	No
Ephx1	Down	No
Rgs1	Down	No
Prr7	Down	No
Ift27	Down	No
Gimap7	Down	No
Hist1h4i	Down	No
Galnt2	Down	No
Hist1h4k	Down	No
Fasl	Down	No
Nab1	Down	No
Prkch	Down	No
Hist1h2bf	Down	No
Ctsc	Down	No
Gpr65	Down	No
Glipr1	Down	No
Cd3d	Down	No
Adap1	Down	No
Sub1	Down	No
Hist1h2be	Down	No
Chn2	Down	No
Cxcr5	Down	No
Hist1h2br	Down	No

* In both datasets *Egr2* was knocked out, meaning that *Egr2* expression was reduced in KO cells in both datasets due to gene deletion rather than differential expression

Table 4.S4 – Buffers for ChIP-seq analysi

Buffer Name	Recipe
10X Formaldehyde Cross-Linking Buffer	50mM HEPES-KOH (pH 7.5) 100mM NaCl 1mM EDTA 11% Formaldehyde
Nuclear Extraction Buffer	20mM Tris-HCl (pH 8.0) 10mM NaCl 2mM EDTA 0.5% IGEPAL CA-630
ChIP Sonication Buffer	20mM Tris-HCl (pH 7.5) 150mM NaCl 2mM EDTA 1% IGEPAL CA-630 0.3% SDS
ChIP Dilution Buffer	20mM Tris-HCl pH 8.0 150mM NaCl 2mM EDTA 1% TritonX-100
ChIP IP Buffer	20mM Tris-HCl (pH 8.0) 150M NaCl 2mM EDTA 1% TritonX-100 0.15% SDS
ChIP Blocking Buffer	ChIP IP Buffer 0.1% BSA
ChIP Wash Buffer 1	20mM Tris-HCl pH 8.0 500mM NaCl 2mM EDTA 1% TritonX-100 0.1% SDS
ChIP Wash Buffer 2	20mM Tris-HCl pH 8.0 250mM LiCl 2mM EDTA 0.5% IGEPAL CA-630 0.1% SDS 0.5% Sodium Deoxycholate
Reverse Crosslinking Buffer	1% SDS 100mM $NaHCO_3$ 200mM NaCl

CHAPTER 5- FINAL DISCUSSION

5.1: Introduction

Molecular checkpoints responsible for limiting the activity of $CD8^+$ T cells are crucial in protecting the host from autoimmune disease and immunopathology. In comparison to effector-memory differentiation, the molecular pathways that regulate $CD8^+$ T cell tolerance and exhaustion are not as well characterised. Furthermore, despite the phenotypic similarities between tolerance and exhaustion, the extent of overlap between the molecular pathways driving these fates remains unclear. Understanding these molecular intricacies is increasingly crucial in the rapidly evolving landscape of cancer immunotherapy. While checkpoint blockade has shown remarkable clinical efficacy for cancer treatment (478), several autoimmune conditions arise as side effects of therapy due to the targeting of molecular regulators shared by both tolerance and exhaustion (479). As immunotherapy may proceed to becoming the first line of treatment for certain cancers (480), it is important to further characterise any potential novel molecular pathways that could be exclusively required for $CD8^+$ T cell exhaustion and not in self-tolerance processes. Exhaustion-specific pathways would represent better targets for more refined therapy approaches that reinvigorate exhausted tumour-specific T cells without triggering autoimmune disease. This thesis aimed to characterise the specific roles of the TFs FOXO3 and EGR2, and the ubiquitin ligase adaptor molecule NDFIP1, in $CD8^+$ T cell tolerance and exhaustion. The results from these studies have revealed several new insights into these differentiation states.

Chapter 2 explored the requirement of the TF FOXO3 in the induction of apoptosis in self-reactive $CD8^+$ T cells undergoing peripheral deletion. Despite its dephosphorylated and thus activated state during tolerance induction, FOXO3 was dispensable for inducing apoptosis in $CD8^+$ T cells undergoing deletional tolerance, in contrast to its role in effector and exhausted $CD8^+$ T cells. This result supports the concept that, at the level of cell survival pathways, cells undergoing tolerance and immunity are molecularly separable. Results from Chapter 3 further confirmed this concept, as loss of the ubiquitin ligase adaptor protein NDFIP1 did not affect $CD8^+$ T

cell effector differentiation during acute infection despite playing an indispensable role in the induction of $CD8^+$ T cell anergy. The reasons for these differences in the function of FOXO3 and Ndfip1 in tolerance versus immunity are discussed further in section 5.2.

Chapter 3 aimed to shed light on the unexplored role of ubiquitin ligases in $CD8^+$ T cell tolerance induction given their well-established role in the induction and maintenance of $CD4^+$ T cell anergy. The results of this study revealed a previously unappreciated antigen dose-dependent role of NDFIP1 in $CD8^+$ T cell tolerance induction. Collectively, these data provide the first evidence for the differential control of anergy versus deletion of $CD8^+$ T cells at the molecular level. Thus, NDFIP1 acts as a checkpoint that prevents responses against high levels of tolerogenic antigen in the periphery. As will be discussed later within this chapter, this finding could be utilised to create better experimental models to specifically test the contribution of anergy to peripheral self-tolerance.

Chapter 4 investigated the role of the TCR-induced TF EGR2, which is critically required for anergy induction, in $CD8^+$ T cell exhaustion. The results indicated that while EGR2 expression in exhaustion was driven by chronic antigen, possibly in a similar manner to anergy, the gene program regulated by EGR2 was distinct between exhaustion and anergy. EGR2 was repurposed to play a unique role in promoting terminal exhaustion, with these results bearing similarities to the repurposing of other effector-linked TFs during exhaustion. Surprisingly, this repurposing was not due to chromatin changes in the binding sites of anergy genes, indicating that other factors may contribute to altered EGR2 function in exhaustion versus tolerance. These results suggest that chronic antigen signals are differentially processed into transcriptional outputs in different contexts, even though the proximal factors downstream of chronic TCR signals may be shared. These distinctions may exist because tolerance and exhaustion likely evolved for fundamentally different purposes. We argue that these data collectively highlight important distinctions between tolerance and exhaustion, and suggest that these terms should not be used interchangeably. The importance of clarifying these definitions is discussed within this chapter, along with the implications of the thesis findings for immunotherapy.

5.2: Context-specific roles of molecular checkpoints in tolerance versus immunity

There is some evidence supporting the notion that tolerance and effector differentiation are unique differentiation states utilizing separate molecular pathways (234,268,481). Results from this thesis suggested that there are differential functions for FOXO3 and NDFIP1 in tolerance and effector differentiation. There are a number of potential underlying factors that could have led to these differences.

FOXO3 is differentially required for cell death in tolerance versus immunity despite being dephosphorylated and presumably transcriptionally active within tolerant OT-I cells (Fig. 2.1). Although it remains controversial whether FOXO3 binds to the *Bim* locus and directly controls apoptosis (137), another possibility for its lack of effect in tolerance versus immunity may be the presence of tolerance-specific cell death pathways that render FOXO3-dependent *Bim* induction redundant. Some candidate transcription factors that could directly induce *Bim* include HELIOS and NUR77. NUR77 is proposed to play a role in thymic tolerance of $CD8^+$ T cells (482) and both TFs are upregulated in $CD8^+$ T cells undergoing deletional tolerance (268). Although the involvement of these factors in inducing apoptosis is controversial (483–485), the presence of different factors could explain the redundant functions of FOXO3 in tolerance versus immunity. Conversely, perhaps specific co-factors or chromatin accessibility changes that are only induced during effector differentiation are required for FOXO3 to induce apoptotic cell death. Finally, we have not examined the levels of total FOXO3 protein during tolerance, so it is possible that there is less FOXO3 protein present during tolerance.

Results from Chapter 3 indicated that *Ndfip1* plays little role in restraining effector differentiation during acute LM-OVA and LCMV infections (Figure 3.S4 and 3.S5) despite its indispensable role in the maintenance of T cell anergy in response to high antigen doses. This difference is particularly surprising given that strong antigen signals will also be encountered by differentiating effector T cells in response to these systemic infections. One possibility is that NDFIP1 expression is dampened in an inflammatory environment. Previous *in vitro* experiments have indicated that

NDFIP1 expression is induced by CD3 and CD28 signaling (344), however it is possible that signaling from cytokine receptors such as IL-12R or IFN receptors could override these signals and shut down NDFIP1 expression in effector cells *in vivo*. While there are no reliable antibodies to detect NDFIP1 expression by flow cytometry, NDFIP1 reporter mice (344) could be used to address the above hypothesis. An alternative explanation may be that the function of NDFIP1 is irrelevant in immunity. In the peptide anergy model, lack of *Ndfip1* resulted in increased mTOR and pERK signaling. These pathways are normally impaired in anergic cells, and hence augmented signaling via these pathways results in a break in tolerance. In the context of effector differentiation, multiple pathways, including co-stimulatory and cytokine receptors, signal through and activate the mTOR pathway (82). As such, loss of NDFIP1 may not influence the magnitude of signalling by these pathways since they are already “maxed out” during infection.

Given the antigen-dose dependent role of *Ndfip1* in T cell tolerance, it will be important to discern whether NDFIP1 regulates $CD8^+$ T cell exhaustion. In the context of exhaustion, cells are exposed to sustained high levels of antigen relative to cells responding to an acute infection, meaning NDFIP1 may play an immunoregulatory role in this context. Furthermore, exhausted cells have deficiencies in mTOR signaling that contribute to the exhausted state(393,409), so it is possible that NDFIP1 deficiency could rescue mTOR signaling during exhaustion in a manner that could influence differentiation. The NDFIP1 deficient *krusty* mouse strain develops systemic inflammation (344) and this would confound any study of $CD8^+$ T cell exhaustion. However, *Ndfip1* could be conditionally deleted from effector $CD8^+$ T cells using *GranzymeB-Cre* (486) or *E8I-Cre* (93) (E8I-Cre mice specifically express Cre within peripheral $CD8^+$ T cells), and the response to chronic LCMV infection could be studied as in the LCMV Cl13 experiments performed in Chapter 4. In particular, it would be interesting to assess whether *Ndfip1*-deficient exhausted $CD8^+$ T cells would respond in a similar manner to the anergic counterparts through excessive expansion and potentially clearing the infection. Alternatively, NDFIP1 may regulate exhaustion in a differential manner to its role in tolerance. These future studies would help to further understand whether tolerance-specific factors are re-engaged during exhaustion.

5.3: The response to chronic antigen is plastic and context dependent

Chronic antigen engagement is a common feature of multiple states of negative regulation. Tolerant cells rely on persistent antigen encounter for durable tolerance induction. In particular, removal of cells from antigen results in a failure in peripheral deletion (270), although some studies have shown transcriptional and epigenetic commitment to a tolerant phenotype that is maintained even after withdrawal from antigen (474,481). Similarly, withdrawal from antigen can lead to a restoration of function within exhausted $CD8^+$ T cells early during the response, although the cells ultimately become committed to an exhausted fate at later time-points (423,453). Hence, chronic antigen is a crucial determining factor in the establishment of both tolerance and exhaustion. The link between chronic antigen and negative regulation is likely because chronic antigen is almost always a signal of a problem with the immune response. Chronic antigen will mainly be encountered in two situations. First, chronic antigen could arise because the immune response is unable to clear an infection. In this situation, maintaining the immune response against the infection could lead to fatal immunopathology. Thus, negative regulatory pathways would likely evolve in this context to temper the response, such that immunopathology was averted but the infection was still contained. Alternatively, chronic antigen encounter by the immune system could suggest that the antigen being targeted is either a self-antigen, or a harmless environmental antigen. In this context, maintaining a response against the antigen could lead to autoimmunity or chronic inflammation, and in this situation it would be preferable to completely inactivate the response. While it may be difficult to distinguish between these two possibilities during infection, any antigen chronically encountered during the steady state is almost certainly a self-antigen or harmless environmental antigen. We reason that this is why tolerance induction to steady-state antigens typically leads to complete inactivation of responding cells by either peripheral deletion or anergy. Thus, we would speculate that tolerance and exhaustion ultimately evolved for different reasons and thus have different end goals.

Our study of EGR2 function within exhaustion represented an opportunity to test whether the response to chronic antigen evolves depending on context. The results from Chapter 4 indicated that EGR2 expression was indeed sustained by chronic

antigen in exhausted virus-specific $CD8^+$ T cells, however its target genes were vastly different from those previously identified during anergy. The results from this chapter indicated that during exhaustion EGR2 fails to bind to the majority of direct EGR2 anergy targets, and even when EGR2 binding still occurs to anergy targets (eg. *Cblb*) it fails to influence gene expression (Figure 4.S6). Thus chronic antigen signals possibly engage different downstream pathways in different contexts and differentiation states.

The context-dependent role of *Egr2* makes sense given that the evolutionary purposes of tolerance versus exhaustion are likely different. *Egr2* promotes genes that drive terminal exhaustion in effector $CD8^+$ T cells. The exhaustion process, despite leading to diminished inflammatory function, still contributes to control of infections or tumours. On the other hand, *Egr2* actively inhibits T cell differentiation in anergy through the induction of negative regulators of T cell signaling, such as *Dgka* and *Cblb*. In contrast to exhaustion, this inactivation process prevents these cells from acquiring any effector function to prevent the likely self-reactive responding cells from causing autoimmunity. Hence, possibly as a result of these differential end goals, chronic antigen signals are processed in a context-dependent manner in tolerance and exhaustion as depicted in Figure 5.1. In exhaustion, EGR2 has been shown to bind to *Pdcd1, Tigit, Bach2* and *Bcl6* possibly resulting in its differential effect in exhaustion.

5.4: Building better mouse models to address unresolved questions in tolerance

The peripheral tolerance processes that control self-reactive $CD8^+$ T cells have thus far predominantly been explored using transgenic mouse models. While these models, where model antigens are expressed under the control of tissue-specific promoters, have helped us to understand the peripheral tolerance mechanisms that operate upon self-reactive transgenic $CD8^+$ T cell *in vivo* (233), it is unclear to what extent these mechanisms are responsible for controlling endogenous populations of

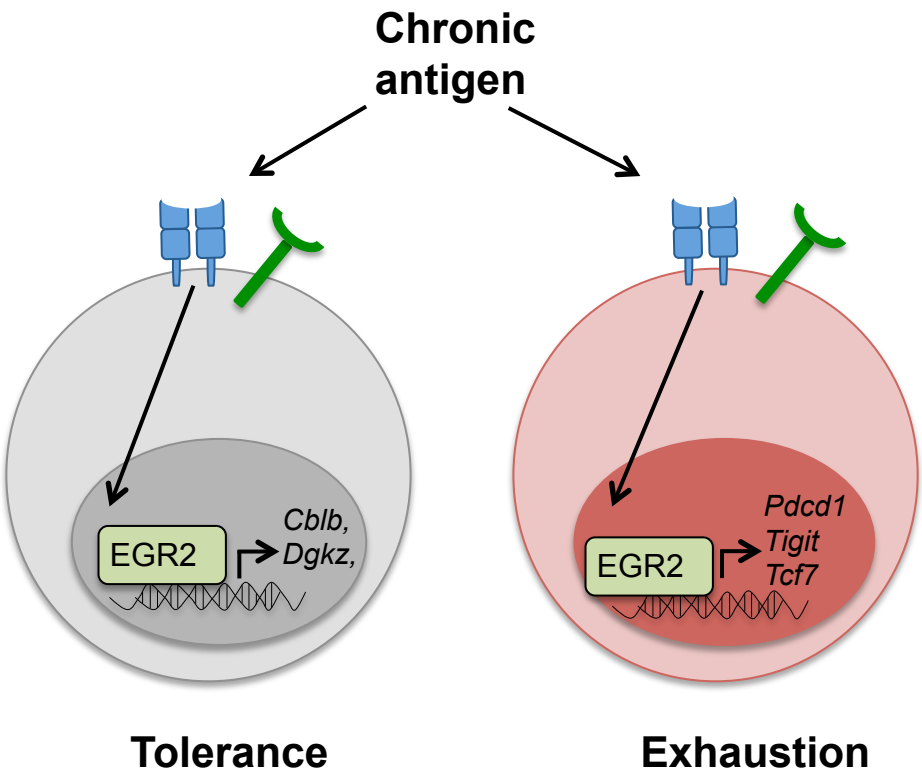

Figure 5.1. Differential downstream functions of transcription factor EGR2 in CD8⁺ T cell tolerance and exhaustion: EGR2 is induced downstream of chronic antigen signals in both CD8⁺ T cell tolerance and exhaustion. EGR2 is crucial in driving T cell tolerance by targeting genes such as *Cbl-b* and *Dgkz,* which limit TCR signaling. However, EGR2 is repurposed in exhaustion, and binds to different gene targets such as *Pdcd1, Tigit and Tcf7* which drive exhausted cells towards terminal differentiation.

polyclonal self-reactive T cells. Mouse models that have a genetic predisposition to autoimmunity, such as Non Obese Diabetic (NOD) mice (487), can help to identify the specific genetic pathways that might normally allow certain populations of self-reactive cells to escape tolerance and cause pathology. However, as these mouse models typically harbor multiple genetic lesions that disrupt both peripheral and central tolerance, it is difficult to use these models to assess the specific contribution of peripheral tolerance pathways to the prevention of autoimmune disease. The rapid inflammatory disease that ensues upon Treg depletion is arguably one of the few pieces of evidence that peripheral tolerance pathways constitutively prevent autoinflammatory disease, although it is unclear whether Tregs predominantly function in restraining existing effectors or enforcing peripheral tolerance in this context (316). While deficiency in cell intrinsic regulators of peripheral tolerance, such as PD-1 and CBL-B (294,488), also results in autoimmunity, it is again unclear in this model whether this affect is due to the influence of these factors on peripheral tolerance alone, or on peripheral and central tolerance (and/or other regulatory processes).

Due to the potential caveats of existing data, there are thus a number of key unanswered questions within the $CD8^+$ T cell peripheral tolerance field. First, what role (if any) do peripheral tolerance processes play in preventing autoimmune disease? Did peripheral tolerance mainly evolve to limit responses against harmless environmental antigens, or to only serve as a back-up pathway in the event that an inherited mutation caused thymic selection deficiencies? Second, what are the relative contributions of peripheral deletion and anergy to tolerance maintenance? Finally, what types of self-reactive cells (if any) are the main targets of peripheral tolerance pathways? Does peripheral tolerance mainly restrain low affinity self-reactive cells, or does it target high affinity cells specific for antigens not expressed in the thymus? Answering these questions requires experimental mouse models where the cell intrinsic pathways that regulate peripheral tolerance are selectively disrupted in peripheral $CD8^+$ T cells.

The results from Chapter 3 indicated that NDFIP1 is selectively required for $CD8^+$ T cell anergy to high dose self-antigens, while being largely dispensable for peripheral deletion. Thus, mice in which *Ndfip1* is conditionally deleted within peripheral $CD8^+$ T

cells (such as could be achieved with an *E8I-cre* transgene) should have a selective defect in peripheral anergy, at least as defined by the peptide anergy model. These mice could then be aged to examine whether a defect in peripheral anergy results in autoimmune disease, and/or expansion of self-reactive T cells clones (as assessed by TCR repertoire profiling). This proposed mouse model would provide, to our knowledge, the first opportunity to directly test how anergy contributes to $CD8^+$ T cell self-tolerance within an endogenous repertoire. If no autoimmune phenotype is observed in these mice, then further work could be done to determine whether anergy instead contributes to tolerance in other situations, such as tolerance to food or environmental antigens, or fetomaternal tolerance. We suggest that targeted models such as this are needed to determine the physiological contributions of peripheral tolerance processes to immune homeostasis.

5.5: A question of semantics: is there a need to develop better nomenclature around T cell exhaustion and tolerance?

There is currently a plethora of definitions used to describe the differentiation states that T cells adopt when they lose effector functions. These include terms such as hyporesponsive, dysfunctional, senescent and sub-optimal, in addition to existing terms used in this thesis such as tolerance, anergy and exhaustion. A major challenge for the field is that these terms are often poorly defined and/or have different meanings within the scientific community. The net result is that these terms are either used interchangeably, or the same terms are used to describe different states in different studies. The original papers describing the exhausted state (351,352), where the terms “exhaustion” and “anergy” were used interchangeably, perhaps best exemplify this problem. There is thus a need to develop a standardized system of classifying states of negative regulation. Part of the complication surrounding definitions is that even for established terms such as anergy and exhaustion, which have both existed for almost 30 years, their definitions have evolved over time. Exhaustion initially was used to describe the disappearance of virus-specific CTLs during chronic LCMV infection (351), but later evolved to describe the persistence of virus-specific T cells with diminished effector functions

during chronic LCMV infection (352). Similarly, classical *in vitro* "anergy" was subsequently extended to describe *in vivo* models of tolerance and tolerant human self-reactive T cells (273). Can these terms be extrapolated for use in other contexts of $CD8^+$ T cell restraint? There is now evidence that tumour-reactive cells display similar phenotypic features to exhausted cells during LCMV infection, with functionally and phenotypically similar "exhausted memory" and "terminally exhausted" subsets also evident within tumour-reactive T cells (377,461). Nevertheless, there are still clear differences between the transcriptional profile of exhausted cells and TILs (489,490), suggesting that there are at least some differences between these states. Thus, there needs to be a consensus on how these states can be defined and further extended to accommodate all scenarios where diminished $CD8^+$ T cell function may occur.

Any new system of nomenclature would have to first create new terminology with carefully constructed definitions to replace existing terms. Similar approaches to revise classification and nomenclature of cell subsets have been successful within the ILC and DC fields (50,491). As in these two examples, the creation of this nomenclature system would have to be a collaborative process, involving consensus from leaders within the field. New terminology is important, as simply redefining existing terms is unlikely to remove the ambiguity that would continue to be attached to them due to their long and complicated history (eg. anergy and exhaustion).

Second, the classification system would have to be carefully considered to avoid future ambiguity. For example, defining a state of negative regulation based on the specificity of the responding cells would be problematic given that self-reactive cells can be restrained by exhaustion (492) and that cells specific for foreign antigens (such as food and commensal antigens) can undergo peripheral tolerance (214,215). Molecular similarities and differences between states could be used as a starting point for reclassification, although as this is somewhat of a continuum, relying solely on molecular signatures may also ultimately cause problems. Perhaps the simplest classification system would be based on the point during the immune response at which responding T cells lose effector function (ie. the kinetics of negative regulation). For example, perhaps cells that fail to differentiate into effector cells and/or only minimally and transiently acquire effector functions early during

the immune response prior to being rapidly shutdown (such as occurs within peripheral tolerance models) would be classified as undergoing “Class I negative regulation” or a “Class I checkpoint”. In these situations, cells would also typically never acquire the capacity to infiltrate inflamed tissues. This checkpoint could be subdivided into cells that persist in an “anergic” state (Class Ia) or undergo apoptotic death (Class Ib). In contrast, cells that undergo negative regulation after initial relatively normal effector differentiation over the first 5-7 days of the response prior to a gradual and progressive loss of inflammatory function would be said to undergo a “Class II checkpoint”. This would encompass exhausted cells within tumours and during chronic viral infection. It may be possible to sub-divide this checkpoint into “Class IIa” and “Class IIb” based on phenotypic markers that distinguish exhausted cells in responses against chronic infections and tumours.

This classification system would largely align with both the published molecular profiles associated with these states, and the functional distinctions highlighted by this thesis (Figure 5.2). Nevertheless, ambiguities still exist even within this proposed system. Where is the dividing line between when something is classified as “Class I” and “Class II”, and will defining a specific point during the immune response ultimately cause further problems? Moreover, a recent study within a transfer tolerance model suggested that persistent anergic $CD8^+$ T cells adopt a gene signature with similarity to TILs (474). How would these cells be classified? Perhaps additional information on the epigenetic state of the cells would better help classify cells, given the strong similarities between TILs and exhausted cells from LCMV in this regard (467). Either way, overhauling the current nomenclature system is an important priority for the field.

5.6: Significance of thesis findings and implications in the clinic.

As mentioned earlier, targeting molecular checkpoints in exhaustion during cancer immunotherapy has led to remarkable efficacy against multiple cancer types (368). Many of these therapies are thought to work by releasing the “brakes” on exhausted

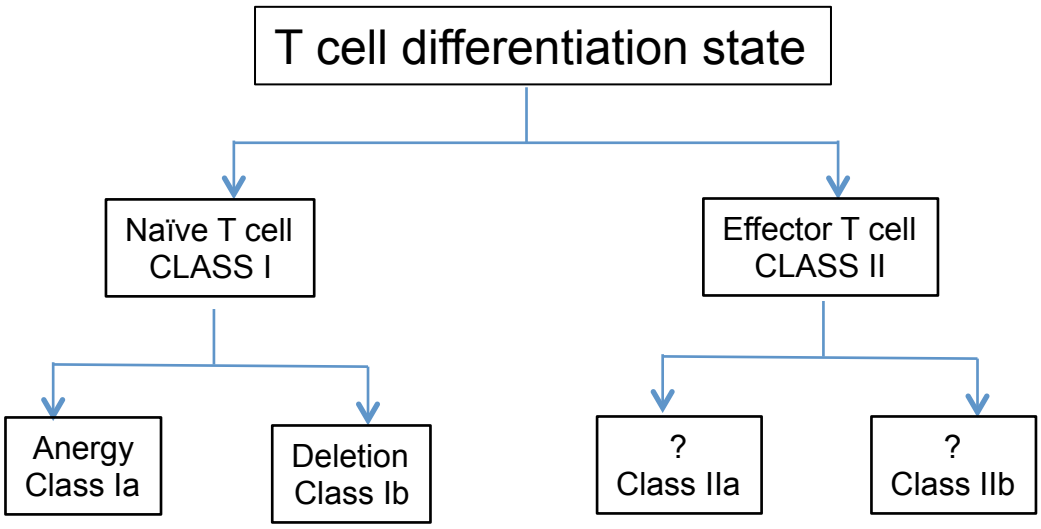

Figure 5.2. Proposed nomenclature system for negatively regulated CD8⁺ T cell differentiation states: The proposed system suggests that negatively regulated processes should initially be classified depending on the target T cell differentiation state. If the target CD8⁺ T cell population is a naïve cell, then it will be classified as Class I immunoregulation, while if the target population is an effector cell, the process will be classified as Class II immunoregulation. Both of these classes can be further categorised into a and b subdivisions based on the specifics of the cell phenotype. For example, anergy can be classified as Class Ia while peripheral deletion will be classified as Class Ib. Similar classification in Class II could also be based on phenotypic outcomes of the cells in the tumor environment or in chronic infections. However the current understanding of phenotypic variation between exhaustion responses to different viruses and tumor types is limited, although a classification based on phenotypic outcomes could be used in the future.

$CD8^+$ T cells and thereby “reinvigorating” the anti-tumour response. However to avoid autoimmune side effects downstream of therapy (479), it is important to find therapeutic targets that disrupt exhaustion within tumour-specific $CD8^+$ T cells while leaving self-tolerance processes intact. The data from this thesis indicates that tolerance is molecularly separable from effector differentiation as seen from the unique roles of FOXO3 and NDFIP1 in these states. Furthermore, results from Chapter 4 indicate that the manner in which negative regulatory pathways are “wired” during tolerance and exhaustion may be fundamentally different. Hence, given that there is evidence of molecular differences between these two states, future research on new molecular targets for immunotherapy should examine the feasibility and efficacy of targeting pathways that only operate in the exhaustion setting. Nevertheless, it is unclear whether this would prevent autoimmune disease. It has been shown that exhaustion likely acts as a “last resort” checkpoint to prevent autoimmune disease in some patients. It is thus possible that disrupting exhaustion rather than peripheral tolerance processes is the reason for the autoimmune side effects of therapy. In this scenario, autoimmune disease would only be triggered within patient subsets that already have peripheral tolerance defects that result in sub-clinical disease associated with an existing pool of self-reactive exhausted T cells.

Another potential problem with an exhaustion-targeted therapeutic approach is that disruption of peripheral tolerance to tumour antigens could contribute to the efficacy of current immunotherapy approaches. Clinical data identifying patients that respond to immunotherapy have suggested that exhausted $CD8^+$ T cell infiltration of the tumour is required for treatment efficacy (493,494). Given that tolerant cells often fail to infiltrate target tissues, this suggests that therapies are more likely to operate through disruption of exhaustion rather than tolerance. Nevertheless, peripheral tolerance to tumour antigens has been observed within the tumour draining lymph nodes in mouse models (494) raising the possibility that disrupting this pathway may amplify the response and contribute to efficacy. Furthermore, a recent case study indicated that the pathways that contribute to autoimmunity and anti-tumour responses may in fact be shared during checkpoint blockade. While most autoimmune adverse events are treated with a standard therapy of short-term immunosuppression, treating therapy-induced colitis in a colorectal cancer patient

with an anti-IL-17 monoclonal antibody resulted in relapse of the cancer (496). Thus, there is a need to further define the degree to which disrupting peripheral tolerance versus exhaustion contributes to treatment efficacy in the context of cancer immunotherapy. Models such as *Ndfip1* deletion within peripheral $CD8^+$ T cells could be used to examine whether peripheral anergy contributes to tumour control.

Apart from shedding light on the potential molecular overlap between tolerance and exhaustion, results from this thesis could be applied in the genetic engineering of immune adoptive cell therapy approaches for cancer treatment, such as the recently approved Chimeric Antigen Receptor (CAR)-T cells. CARs are engineered to be modified immune receptors that couple extracellular antibody-mediated recognition of an antigen to the intracellular signaling domain of both the TCR and co-stimulatory receptors (497). When cancer patients are treated with CAR T cells, cultured T cells from patients are transduced with plasmids containing a CAR that redirects the T cells towards a surface protein on the cancer (498). As these cells are already manipulated genetically during CAR insertion, there is scope for concurrently introducing other genetic manipulations (via, for example, CRISPR/Cas9 gene editing) that enhance CAR T cell function against the cancer. This is an area of active research, as while CAR T cells have demonstrated efficacy against blood cancers (498), they have not worked well against solid tumours (499).

While the reasons for this lack of efficacy are likely multifactorial, exhaustion of the T cell response likely contributes to lack of efficacy (499). A number of future questions relevant to CAR T cells are raised by the results within this thesis. First, would *Ndfip1* deletion in CAR T cells result in increased proliferation and improved efficacy against solid tumours? Could deletion of *Egr2* in CAR T cells boost the proportion of $TCF1^+$ cells, thereby augmenting the CAR T cell response to checkpoint blockade? On the other hand, it is also crucial to understanding immune tolerance mechanisms and how they affect treatment of autoimmune disease treatment. Is it really possible to restore tolerance in autoreactive T cells? These questions are becoming more relevant as the there is an increase in the incidence of autoimmune disease from immunotherapies. Answering these questions could reveal practical therapeutic applications for the results from this thesis.

CHAPTER 6- References

1. Janeway CA, Medzhitov R. Innate Immune Recognition. Annu Rev Immunol. 2002;20:197–216.
2. Blum JS, Wearsch PA, Cresswell P. Pathways of antigen processing. Annu Rev Immunol. 2013;31:443–73.
3. Thucydides, Warner R, Finley M. History of the Peloponnesian War. Penguin Books. 1972;
4. Burnet FM. A Modification of Jerne's Theory of Antibody Production using the Concept of Clonal Selection. Aust J Sci. 1957;20(3):67–9.
5. Moon JJ, Chu HH, Pepper M, McSorley SJ, Jameson SC, Kedl RM, et al. Naive CD4+ T Cell Frequency Varies for Different Epitopes and Predicts Repertoire Diversity and Response Magnitude. Immunity. 2007;27(2):203–13.
6. Blattman JN, Antia R, Sourdive DJD, Wang X, Kaech SM, Murali-Krishna K, et al. Estimating the precursor frequency of naive antigen-specific CD8 T cells. J Exp Med. 2002;195(5):657–64.
7. Cossu F. Genetics of SCID. Ital J Pediatr. 2010;36:1–17.
8. Davis MM, Boniface JJ, Reich Z, Lyons D, Hampl J, Arden B, et al. Ligand Recognition by αβ T Cell Receptors. Annu Rev Immunol. 1998;16:523–44.
9. Mian IS, Bradwell AR, Olson AJ. Structure, function and properties of antibody binding sites. J Mol Biol. 1991;217:133–51.
10. Brack C, Hirama M, Lenhard-Schuller R, Tonegawa S. A complete immunoglobulin gene is created by somatic recombination. Cell. 1978;15:1–14.
11. Walker LSK, Abbas AK. The enemy within: Keeping self-reactive T cells at bay in the periphery. Nat Rev Immunol. 2002;2:11–9.
12. Goodnow CC. Multistep Pathogenesis of Autoimmune Disease. Cell. 2007;130:25–35.
13. von Boehmer H, Melchers F. Checkpoints in lymphocyte development and autoimmune disease. Nat Immunol. 2010;11:14–20.
14. Zinkernagel RM, Doherty PC. Restriction of in vitro T cell-mediated cytotoxicity in lymphocytic chorio-meningitis within a syngeneic or semiallogeneic system. Nature. 1974;248:701–2.
15. Doyle C, Strominger JL. Interaction between CD4 and class II MHC molecules mediates cell adhesion. Nature. England; 1987;330:256–9.
16. Norment AM, Salter RD, Parham P, Engelhard VH, Littman DR. Cell-cell adhesion mediated by CD8 and MHC class I molecules. Nature. 1988;336:79–81.
17. Townsend ARM, Rothbard J, Gotch FM, Bahadur G, Wraith D, McMichael AJ. The epitopes of influenza nucleoprotein recognized by cytotoxic T lymphocytes can be defined with short synthetic peptides. Cell. 1986;44(6):959–68.
18. Williams MA, Bevan MJ. Effector and Memory CTL Differentiation. Annu Rev Immunol. 2007;25:171–92.
19. Liblau RS, Wong FS, Mars LT, Santamaria P. Autoreactive CD8 T cells in organ-specific autoimmunity: emerging targets for therapeutic intervention.

Immunity. 2002;17:1–6.
20. Barber DL, Wherry EJ, Masopust D, Zhu B, Allison JP, Sharpe AH, et al. Restoring function in exhausted CD8 T cells during chronic viral infection. Nature. 2006;439:682–7.
21. Frebel H, Nindl V, Schuepbach RA, Braunschweiler T, Richter K, Vogel J, et al. Programmed death 1 protects from fatal circulatory failure during systemic virus infection of mice. J Exp Med. 2012;209(13):2485–99.
22. Cornberg M, Kenney LL, Chen AT, Waggoner SN, Kim S-K, Dienes HP, et al. Clonal exhaustion as a mechanism to protect against severe immunopathology and death from an overwhelming CD8 T cell response. Front Immunol. 2013;4:475.
23. Arbor ML, Ord DC, Ley K, Ratech H, Maynard-curry C, Otten G, et al. Lymphocyte Homing and Leukocyte Rolling and Migration Are Impaired in L-Selectin-Deficient Mice. Immunity. 1994;1:247–60.
24. Goldrath AW. Maintaining the status quo: T-cell homeostasis. Microbes Infect. 2002;4(5):539–45.
25. Sprent J, Surh CD. Normal T cell homeostasis : the conversion of naive cells into memory-phenotype cells. Nat Rev Immunol. 2011;131(6):478–84.
26. Steinman R., Witmer M. Dendritic cells are the principal stimulators of the primary mixed leukocyte reaction in mice. J Exp Med. 1983;157(2):613–27.
27. Hildner K, Edelson BT, Purtha WE, Diamond M, Matsushita H, Kohyama M, et al. Batf3 Deficiency Reveals a Critical Role for CD8a+ Dendritic Cells in Cytotoxic T Cell Immunity. Science. 2008;322:1097–100.
28. Mashayekhi M, Sandau MM, Dunay IR, Frickel EM, Khan A, Goldszmid RS, et al. CD8a+ Dendritic Cells Are the Critical Source of Interleukin-12 that Controls Acute Infection by Toxoplasma gondii Tachyzoites. Immunity. 2011;35:249–59.
29. Jung S, Unutmaz D, Wong P, Sano G-I, De Los Santos K, Sparwasser T, et al. In vivo depletion of CD11c+ dendritic cells abrogates priming of CD8+ T cells by exogenous cell-associated antigens. Immunity. 2002;17:211–20.
30. Fukaya T, Murakami R, Takagi H, Sato K, Sato Y, Otsuka H, et al. Conditional ablation of CD205+ conventional dendritic cells impacts the regulation of T-cell immunity and homeostasis in vivo. Proc Natl Acad Sci. 2012;109(28):11288–93.
31. Swiecki M, Gilfillan S, Vermi W, Wang Y, Colonna M. Plasmacytoid Dendritic Cell Ablation Impacts Early Interferon Responses and Antiviral NK and CD8+ T Cell Accrual. Immunity. 2010;33:955–66.
32. Piva L, Tetlak P, Claser C, Karjalainen K, Renia L, Ruedl C, et al. Cutting Edge: Clec9A+ Dendritic Cells Mediate the Development of Experimental Cerebral Malaria. J Immunol. 2012;189:1128–32.
33. Shortman K, Naik SH. Steady-state and inflammatory dendritic-cell development. Nat Rev Immunol. 2007;7:19–30.
34. Sparwasser T, Vabulas RM, Villmow B, Lipford GB, Wagner H. Bacterial CpG-DNA activates dendritic cells in vivo : T helper cell-independent cytotoxic T cell responses to soluble proteins. Eur J Immunol. 2000;30:3591–7.

35. De Smedt T, Pajak B, Muraille E, Lespagnard L, Heinen E, De Baetselier P, et al. Regulation of Dendritic Cell Numbers and Maturation by Lipopolysaccharide In Vivo. J Exp Med. 1996;184:1413–24.
36. Inaba K, Witmer-Pack M, Inaba M, Hathcock KS, Sakuta H, Azuma M, et al. The tissue distribution of the B7-2 costimulator in mice: abundant expression on dendritic cells in situ and during maturation in vitro. J Exp Med. 1994;180(5):1849–60.
37. Caux C, Vanbervliet B, Massacrier C, Azuma M, Okumura K, Lanier LL, et al. B70/B7-2 is Identical to CD86 and Is the Major Functional Ligand for CD28 Expressed on Human Dendritic Cells. J Exp Med. 1994;180:1841–7.
38. Crouse J, Kalinke U, Oxenius A. Regulation of antiviral T cell responses by type i interferons. Nat Rev Immunol. 2015;15(4):231–42.
39. Koch F, Stanzl U, Jennewein P, Janke K, Heufler C, Eckhart K, et al. High Level IL-12 Production by Murine Dendritic Cells : Upregulation via MHC Class II and CD40 Molecules and Downregulation by IL-4 and IL-10. J Exp Med. 1996;(6):741–6.
40. Caetano R e S, Hieny S, Scharton-Kersten T, Jankovic D, Charest H, Germain RN, et al. In Vivo Microbial Stimulation Induces Rapid CD40 Ligand–independent Production of Interleukin 12 by Dendritic Cells and their Redistribution to T Cell Areas. J Exp Med. 1997;186(11):1819–29.
41. Dalod M, Salazar-mather TP, Malmgaard L, Lewis C, Asselin-paturel C, Brière F, et al. Interferon a/B and Interleukin 12 Responses to Viral Infections : Pathways Regulating Dendritic Cell Cytokine Expression In Vivo. J Exp Med. 2002;195(4):517–28.
42. Inaba BK, Turley S, Iyoda T, Yamaide F, Shimoyama S, Reis C, et al. The Formation of Immunogenic Major Histocompatibility Complex Class II – Peptide Ligands in Lysosomal Compartments of Dendritic Cells Is Regulated by Inflammatory Stimuli. J Exp Med. 2000;191(6):927–36.
43. West MA, Wallin RPA, Matthews SP, Svensson HG, Zaru R, Ljunggren H-G, et al. Enhanced dendritic cell antigen capture via toll-like receptor-induced actin remodeling. Science. 2004;305:1153–7.
44. Alloatti A, Kotsias F, Pauwels A-M, Carpier J-M, Jouve M, Timmerman E, et al. Toll-like Receptor 4 Engagement on Dendritic Cells Restrains Phago-Lysosome Fusion and Promotes Cross-Presentation of Antigens. Immunity. 2015;43:1087–100.
45. Heath WR, Carbone FR. Cross-presentation in viral immunity and self-tolerance. Nat Rev Immunol. 2001;1(2):126–34.
46. Belz GT, Smith CM, Eichner D, Shortman K, Karupiah G, Carbone FR, et al. Cutting Edge: Conventional CD8 + Dendritic Cells Are Generally Involved in Priming CTL Immunity to Viruses. J Immunol. 2004;172(4):1996–2000.
47. Belz GT, Shortman K, Bevan MJ, Heath WR. CD8 Dendritic Cells Selectively Present MHC Class I-Restricted Noncytolytic Viral and Intracellular Bacterial Antigens In Vivo. J Immunol. 2010;175(1):196–200.
48. Dorner BG, Dorner MB, Zhou X, Opitz C, Mora A, Guttler S, et al. Selective

Expression of the Chemokine Receptor XCR1 on Cross-presenting Dendritic Cells Determines Cooperation with CD8+ T Cells. Immunity. 2009;31:823–33.
49. Bachem A, Güttler S, Hartung E, Ebstein F, Schaefer M, Tannert A, et al. Superior antigen cross-presentation and XCR1 expression define human of mouse CD8+ dendritic cells. J Exp Med. 2010;207(6):1273–81.
50. Guilliams M, Ginhoux F, Jakubzick C, Naik SH, Onai N, Schraml BU, et al. Dendritic cells, monocytes and macrophages: a unified nomenclature based on ontogeny. Nat Rev Immunol. 2014;14(8):571–8.
51. Miller JC, Brown BD, Shay T, Gautier EL, Jojic V, Cohain A, et al. Deciphering the transcriptional network of the dendritic cell lineage. Nat Immunol. 2012;13(9):888–99.
52. Theisen DJ, Iv JTD, Briseño CG, Gargaro M, Lauron EJ, Wang Q, et al. WDFY4 is required for cross-presentation in response to viral and tumor antigens. Science. 2018;362:694–9.
53. Hugues S. Dynamics of dendritic cell – T cell interactions : a role in T cell outcome. Semin Immunopathol. 2010;32:227–38.
54. Grakoui A, Bromley SK, Sumen C, Davis MM, Shaw AS, Allen PM, et al. The immunological synapse: a molecular machine controlling T cell activation. Science. 1999;285:221–7.
55. Henrickson SE, Mempel TR, Mazo IB, Liu B, Artyomov MN, Zheng H, et al. T cell sensing of antigen dose governs interactive behavior with dendritic cells and sets a threshold for T cell activation. Nat Immunol. 2008;9(3):282–91.
56. Henrickson SE, von Andrian UH. Single-cell dynamics of T-cell priming. Curr Opin Immunol. 2007;19:249–58.
57. Scholer A, Hugues S, Boissonnas A, Fetler L, Amigorena S. Intercellular Adhesion Molecule-1-Dependent Stable Interactions between T Cells and Dendritic Cells Determine CD8 + T Cell Memory. Immunity. 2007;28:258–70.
58. Henrickson SE, Perro M, Loughhead SM, Senman B, Stutte S, Quigley M, et al. Antigen Availability Determines CD8 + T Cell-Dendritic Cell Interaction Kinetics and Memory Fate Decisions. Immunity. 2013;39(3):496–507.
59. Harding FA, McArthur JG, Gross JA, Raulet DH, Allison JP. CD28-mediated signalling co-stimulates murine T cells and prevents induction of anergy in T-cell clones. Nature. 1992;356:607–9.
60. Shahinian A, Pfeffer K, Lee KP, Kundig TM, Kishihara K, Wakman A, et al. Differential T cell co-stimulatory requirements in CD28 deficient mice. Science. 1993;261:609–12.
61. Tan JT, Whitmire JK, Ahmed R, Pearson TC, Larsen CP. 4-1BB ligand, a member of the TNF family, is important for the generation of antiviral CD8 T cell responses. J Immunol. 1999;163(9):4859–68.
62. Hendriks J, Gravestein LA, Tesselaar K, Van Lier RAW, Schumacher TNM, Borst J. CD27 is required for generation and long-term maintenance of T cell immunity. Nat Immunol. 2000;1(5):433–40.
63. Curtsinger JM, Schmidt CS, Mondino A, Lins DC, Kedl RM, Jenkins MK, et al. Inflammatory cytokines provide a third signal for activation of naive CD4+ and

CD8+ T cells. J Immunol. 1999;162(6):3256–62.
64. Curtsinger JM, Valenzuela JO, Agarwal P, Lins D, Mescher MF. Type I IFNs provide a third signal to CD8 T cells to stimulate clonal expansion and differentiation. J Immunol. 2005 Apr;174(8):4465–9.
65. Ross SH, Cantrell DA. Signaling and Function of Interleukin-2 in T Lymphocytes. Annu Rev Immunol. 2018;36:411–33.
66. Marchingo JM, Kan A, Sutherland RM, Duffy KR, Wellard CJ, Belz GT, et al. Antigen affinity, costimulation, and cytokine inputs sum linearly to amplify T cell expansion. Science. 2014;346:1123–7.
67. Nel AE. T-cell activation through the antigen receptor. Part 1: Signaling components, signaling pathways, and signal integration at the T-cell antigen receptor synapse. J Allergy Clin Immunol. 2002;109(5):758–70.
68. Oh-hora M, Rao A. Calcium signaling in lymphocytes. Curr Opin Immunol. 2008;20:250–8.
69. Shaw J, Utz PJ, Durand DB, Toole JJ, Emmel EA, Crabtree GR. Identification of a Putative Regulator of Early T Cell Activation Genes Actity. Science. 1988;241:202–5.
70. Jain J, McCaffery PG, Kerppola TK, Lambert JN, Verdine GL, Curran T, et al. The T cell transcription factor NFATp is a substrate for calcineurin and interacts with Fos and Jun. Nature. 1993;365:352–5.
71. Li W, Whaley CD, Mondino A, Mueller DL. Blocked Signal Transduction to the ERK and JNK Protein Kinases in Anergic CD4+ T cells. Science. 1996;271:1272–6.
72. Fields PE, Gajewski TF, Fitch FW. Blocked Ras Activation in Anergic CD4+ T cells. Science. 1996;271:1276–8.
73. Navarro MN, Cantrell DA. Serine-threonine kinases in TCR signaling. Nat Immunol. 2014;15(9):808–14.
74. Fischer AM, Katayama CD, Pagès G, Pouysségur J, Hedrick SM. The Role of Erk1 and Erk2 in Multiple Stages of T Cell Development. Immunity. 2005;23:431–43.
75. D'Souza WN, Chang C-F, Fischer AM, Li M, Hedrick SM. The Erk2 MAPK Regulates CD8 T Cell Proliferation and Survival. J Immunol. 2008;181(11):7617–29.
76. Gille H, Sharrocks AD, Shaw PE. Phosphorylation of transcription factor p62TCF by MAP kinase stimulates ternary complex formation of c-fos promoter. Nature. 1992;358:414–7.
77. Su B, Jacinto E, Hibi M, Kallunki T, Karin M, Ben-Neriah Y. JNK is involved in signal integration during costimulation of T lymphocytes. Cell. 1994;77(5):727–36.
78. Im S, Rao A. Activation and Deactivation of Gene Expression by Ca2+/Calcineurin-NFAT-mediated Signaling. Mol Cells. 2004;18:1–9.
79. Frauwirth KA, Riley JL, Harris MH, Parry RV, Rathmell JC et al. The CD28 signaling pathway regulates glucose metabolism. Immunity. 2002;16:769–77.
80. Salmond RJ, Emery J, Okkenhaug K, Zamoyska R. MAPK,

Phosphatidylinositol 3-Kinase, and Mammalian Target of Rapamycin Pathways Converge at the Level of Ribosomal Protein S6 Phosphorylation to Control Metabolic Signaling in CD8 T Cells. J Immunol. 2009;183(11):7388–97.
81. Hukelmann JL, Anderson KE, Sinclair L V., Grzes KM, Murillo AB, Hawkins PT, et al. The cytotoxic T cell proteome and its shaping by the kinase mTOR. Nat Immunol. 2016;17:104–12.
82. Delgoffe GM, Powell JD. Feeding an army: The metabolism of T cells in activation, anergy, and exhaustion. Mol Immunol. 2015;68(2):492–6.
83. Phan AT, Doedens AL, Palazon A, Tyrakis PA, Cheung KP, Johnson RS, et al. Constitutive Glycolytic Metabolism Supports CD8+T Cell Effector Memory Differentiation during Viral Infection. Immunity. 2016;45(5):1024–37.
84. Pollizzi KN, Powell JD. Integrating canonical and metabolic signalling programmes in the regulation of T cell responses. Nat Rev Immunol. 2014;14(7):435–46.
85. Buck MD, Sullivan DO, Pearce EL. T cell metabolism drives immunity. J Exp Med. 2015;212(9):1345–60.
86. Chang C, Pearce EL. Emerging concepts of T cell metabolism as a target of immunotherapy. Nat Immunol. 2016;17(4):364–8.
87. Finlay D, Cantrell DA. Metabolism, migration and memory in cytotoxic T cells. Nat Rev Immunol. 2011;11(2):109–17.
88. Chang CH, Curtis JD, Maggi LB, Faubert B, Villarino A V., O'Sullivan D, et al. Posttranscriptional control of T cell effector function by aerobic glycolysis. Cell. 2013;153(6):1239–51.
89. Mescher MF, Curtsinger JM, Casey KA, Hammerbeck CD. Signals required for programming effector and memory development by CD8 + T cells. Immunol Rev. 2006;211:81–92.
90. Joshi NS, Cui W, Chandele A, Lee HK, Urso DR, Hagman J, et al. Inflammation Directs Memory Precursor and Short-Lived Effector CD8+ T Cell Fates via the Graded Expression of T-bet Transcription Factor. Immunity. 2007;27(2):281–95.
91. Keppler SJ, Rosenits K, Koegl T, Vucikuja S, Aichele P. Signal 3 cytokines as modulators of primary immune responses during infections: the interplay of type I IFN and IL-12 in CD8 T cell responses. PLoS One. 2012;7(7):e40865.
92. Sullivan BM, Juedes A, Szabo SJ, Herrath M Von, Glimcher LH. Antigen-driven effector CD8 T cell function regulated by T-bet. Proc Natl Acad Sci. 2003;100(26):15818–23.
93. Maekawa Y, Minato Y, Ishifune C, Kurihara T, Kitamura A, Kojima H, et al. Notch2 integrates signaling by the transcription factors RBP-J and CREB1 to promote T cell cytotoxicity. Nat Immunol. 2008;9(10):1140–7.
94. Glimcher LH, Townsend MJ, Sullivan BM, Lord GM. Recent Developments in the Transcriptional Regulation of Cytolytic Effector Cells. Nat Rev Immunol. 2004;4:900–11.
95. Kaech SM, Tan JT, Wherry EJ, Konieczny BT, Surh CD, Ahmed R. Selective expression of the interleukin 7 receptor identifies effector CD8 T cells that give

rise to long-lived memory cells. Nat Immunol. 2003;4(12):1191–8.
96. Arsenio J, Kakaradov B, Metz PJ, Kim SH, Yeo GW, Chang JT. Early specification of CD8+ T lymphocyte fates during adaptive immunity revealed by single-cell gene-expression analyses. Nat Immunol. 2014;15(4):365–72.
97. Butz EA, Bevan MJ. Massive expansion of antigen-specific CD8+ T cells during an acute virus infection. Immunity. 1998;8(2):167–75.
98. Obar JJ, Khanna KM, Lefrancois L. Endogenous Naive CD8 + T Cell Precursor Frequency Regulates Primary and Memory Responses to Infection. Immunity. 2008;28:859–69.
99. Jenkins MK, Moon JJ. The role of naive T cell precursor frequency and recruitment in dictating immune response magnitude. J Immunol. 2012;188(9):4135–40.
100. Kaech SM, Cui W. Transcriptional control of effector and memory CD8+ T cell differentiation. Nat Rev Immunol. 2012;12(11):749–61.
101. Zehn D, Lee SY, Bevan MJ. Complete but curtailed T-cell response to very low-affinity antigen. Nature. 2009;458:211–4.
102. Ozga AJ, Moalli F, Abe J, Swoger J, Sharpe J, Zehn D, et al. pMHC affinity controls duration of CD8 $^{+}$ T cell–DC interactions and imprints timing of effector differentiation versus expansion. J Exp Med. 2016;213(12):2811–29.
103. Man K, Miasari M, Shi W, Xin A, Henstridge DC, Preston S, et al. The transcription factor IRF4 is essential for TCR affinity–mediated metabolic programming and clonal expansion of T cells. Nat Immunol. 2013;14(11):1155–65.
104. Kurachi M, Barnitz RA, Yosef N, Odorizzi PM, Diiorio MA, Lemieux ME, et al. The transcription factor BATF operates as an essential differentiation checkpoint in early effector CD8+ T cells. Nat Immunol. 2014;15(4):373–83.
105. von Andrian UH, Mackay CR. T cell function and migration: two sides of the same coin. N Engl J Med. 2000;343(14):1020–34.
106. Mora JR, Andrian UH Von. T-cell homing specificity and plasticity : new concepts and future challenges. Trends Immunol. 2006;27(5):235–43.
107. Venturi GM, Tu L, Kadono T, Khan AI, Fujimoto Y, Oshel P, et al. Leukocyte Migration is Regulated by L-Selectin Endoproteolytic Release. Immunity. 2003;19:713–24.
108. Ley K, Kansas GS. Selectins in T cell recruitment to non-lymphoid tissues and sites of inflammation. Nat Rev Immunol. 2004;4:1–11.
109. Sinclair L V, Finlay D, Feijoo C, Cornish GH, Gray A, Ager A, et al. Phosphatidylinositol-3-OH kinase and nutrient-sensing mTOR pathways control T lymphocyte trafficking. Nat Immunol. 2008;9(5):513–22.
110. Carlson CM, Endrizzi BT, Wu J, Ding X, Weinreich MA, Walsh ER, et al. Kruppel-like factor 2 regulates thymocyte and T-cell migration. Nature. 2006;442:299–302.
111. Bai A, Hu H, Yeung M, Chen J. Krüppel-Like Factor 2 Controls T Cell Trafficking by Activating L-Selectin (CD62L) and Sphingosine-1-Phosphate Receptor 1 Transcription. J Immunol. 2007;178:7632–9.

112. Sebzda E, Zou Z, Lee JS, Wang T, Kahn ML. Transcription factor KLF2 regulates the migration of naive T cells by restricting chemokine receptor expression patterns. Nat Immunol. 2008;9(3):292–300.
113. Scharer CD, Barwick BG, Benjamin A, Ahmed R, Boss JM. Global DNA Methylation Remodeling Accompanies CD8 T Cell Effector Function. J Immunol. 2013;191:3419–29.
114. Russ BE, Olshanksy M, Smallwood HS, Li J, Denton AE, Prier JE, et al. Distinct epigenetic signatures delineate transcriptional programs during virus-specific CD8+ T cell differentiation. Immunity. 2014;41(5):853–65.
115. Araki Y, Wang Z, Zang C, Wood WH, Schones D, Cui K, et al. Genome-wide Analysis of Histone Methylation Reveals Chromatin State-Based Regulation of Gene Transcription and Function of Memory CD8+ T Cells. Immunity. 2009;30(6):912–25.
116. Kakaradov B, Arsenio J, Widjaja CE, He Z, Aigner S, Metz PJ, et al. Early transcriptional and epigenetic regulation of CD8 + T cell differentiation revealed by single-cell RNA sequencing. Nat Immunol. 2017;18(4):422–32.
117. Scott-Browne JP, López-Moyado IF, Trifari S, Wong V, Chavez L, Rao A, et al. Dynamic Changes in Chromatin Accessibility Occur in CD8+T Cells Responding to Viral Infection. Immunity. 2016;45(6):1327–40.
118. Harty JT, Tvinnereim AR, White DW. CD8+ T Cell Effector Mechanisms in Resistance To Infection. Annu Rev Immunol. 2000;25:275–308.
119. Smyth MJ, Trapani JA. The Relative Role of Lymphocyte Granule Exocytosis versus Death Receptor-Mediated Cytotoxicity in Viral Pathophysiology. J Virol. 1998;72:1–9.
120. Trapani JA, Smyth MJ. Functional significance of the perforin/granzyme cell death pathway. Nat Rev Immunol. 2002;2(10):735–47.
121. Pearce EL, Mullen AC, Gislaine MA, Krawczyk CM, Hutchins AS, Zediak VP, et al. Control of Effector CD8+ T Cell Function by the Transcription Factor Eomesodermin. Science. 2003;302:1041–3.
122. Cruz-Guilloty F, Pipkin ME, Djuretic IM, Levanon D, Lotem J, Lichtenheld MG, et al. Runx3 and T-box proteins cooperate to establish the transcriptional program of effector CTLs. J Exp Med. 2009;206(1):51–9.
123. Dominguez CX, Amezquita RA, Guan T, Marshall HD, Joshi NS, Kleinstein SH, et al. The transcription factors ZEB2 and T-bet cooperate to program cytotoxic T cell terminal differentiation in response to LCMV viral infection. J Exp Med. 2015;212(12):2041–56.
124. Omilusik KD, Best JA, Yu B, Goossens S, Weidemann A, Nguyen J V., et al. Transcriptional repressor ZEB2 promotes terminal differentiation of CD8 $^{+}$ effector and memory T cell populations during infection. J Exp Med. 2015;212(12):2027–39.
125. Rutishauser RL, Martins GA, Kalachikov S, Chandele A, Parish IA, Meffre E, et al. Transcriptional Repressor Blimp-1 Promotes CD8+ T Cell Terminal Differentiation and Represses the Acquisition of Central Memory T Cell Properties. Immunity. 2009;31(2):296–308.

126. Ji Y, Pos Z, Rao M, Klebanoff CA, Yu Z, Sukumar M, et al. Repression of the DNA-binding inhibitor Id3 by Blimp-1 limits the formation of memory CD8+ T cells. Nat Immunol. 2011;12(12):1230–7.
127. Cannarile MA, Lind NA, Rivera R, Sheridan AD, Camfield KA, Wu BB, et al. Transcriptional regulator Id2 mediates CD8+ T cell immunity. Nat Immunol. 2006;7(12):1317–25.
128. Prlic M, Bevan MJ. Exploring regulatory mechanisms of CD8+ T cell contraction. Proc Natl Acad Sci. 2008;105(43):16689–94.
129. Pellegrini M, Belz G, Bouillet P, Strasser A. Shutdown of an acute T cell immune response to viral infection is mediated by the proapoptotic Bcl-2 homology 3-only protein Bim. Proc Natl Acad Sci. 2003;100(24):14175–80.
130. Fischer SF, Belz GT, Strasser A. BH3-only protein Puma contributes to death of antigen-specific T cells during shutdown of an immune response to acute viral infection. Proc Natl Acad Sci. 2008;105(8):3035–40.
131. Hedrick SM, Hess Michelini R, Doedens AL, Goldrath AW, Stone EL. FOXO transcription factors throughout T cell biology. Nat Rev Immunol. 2012;12(9):649–61.
132. Stahl M, Dijkers PF, Kops GJPL, Lens SMA, Coffer PJ, Burgering BMT, et al. The Forkhead Transcription Factor FoxO Regulates Transcription of p27Kip1 and Bim in Response to IL-2. J Immunol. 2002;168(10):5024–31.
133. Dijkers PF, Birkenkamp KU, Lam EW-F, Thomas NSB, Lammers J-WJ, Koenderman L, et al. FKHR-L1 can act as a critical effector of cell death induced by cytokine withdrawal: protein kinase B-enhanced cell survival through maintenance of mitochondrial integrity. J Cell Biol. 2002;156(3):531–42.
134. Dijkers PF, Medema RH, Lammers J-WJ, Koenderman L, Coffer PJ. Expression of the pro-apoptotic Bcl-2 family member Bim is regulated by the forkhead transcription factor FKHR-L1. Curr Biol. 2000;10(19):1201–4.
135. Sullivan JA, Kim EH, Plisch EH, Peng SL, Suresh M. FOXO3 regulates CD8 T cell memory by T cell-intrinsic mechanisms. PLoS Pathog. 2012;8(2):e1002533.
136. Tzelepis F, Joseph J, Haddad EK, Maclean S, Dudani R, Agenes F, et al. Intrinsic role of FoxO3a in the development of CD8+ T cell memory. J Immunol. 2013;190(3):1066–75.
137. Herold MJ, Rohrbeck L, Lang MJ, Grumont R, Gerondakis S, Tai L, et al. Foxo-mediated Bim transcription is dispensable for the apoptosis of hematopoietic cells that is mediated by this BH3-only protein. EMBO Rep. 2013;14(11):992–8.
138. Akiyama T, Bouillet P, Miyazaki T, Kadono Y, Chikuda H, Chung U, et al. Regulation of osteoclast apoptosis by ubiquitylation of proapoptotic BH3-only Bcl-2 family member Bim. EMBO J. 2003;22(24):6653–64.
139. Ley R, Balmanno K, Hadfield K, Weston C, Cook SJ. Activation of the ERK1 / 2 Signaling Pathway Promotes Phosphorylation and Proteasome-dependent Degradation of the BH3-only Protein , Bim. J Biol Chem. 2003;278(21):18811–

6.
140. Luciano F, Jacquel A, Colosetti P, Herrant M, Cagnol S, Pages G, et al. Phosphorylation of Bim-EL by Erk1 / 2 on serine 69 promotes its degradation via the proteasome pathway and regulates its proapoptotic function. Oncogene. 2003;22:6785–93.
141. Thimme R, Appay V, Koschella M, Roth E, Hislop AD, Rickinson AB, et al. Increased Expression of the NK Cell Receptor KLRG1 by Virus-Specific CD8 T Cells during Persistent Antigen Stimulation. J Virol. 2005;79(18):12112–6.
142. Robbins SH, Terrizzi SC, Sydora BC, Mikayama T, Brossay L. Differential Regulation of Killer Cell Lectin-Like Receptor G1 Expression on T Cells. J Immunol. 2003;170(12):5876–85.
143. Huster KM, Busch V, Schiemann M, Linkemann K, Kerksiek KM, Wagner H, et al. Selective expression of IL-7 receptor on memory T cells identifies early CD40L-dependent generation of distinct CD8+ memory T cell subsets. Proc Natl Acad Sci. 2004;101(15):5610–5.
144. Takemoto N, Intlekofer AM, Northrup JT, Wherry EJ, Reiner SL. Cutting Edge: IL-12 Inversely Regulates T-bet and Eomesodermin Expression during Pathogen-Induced CD8+ T Cell Differentiation. J Immunol. 2006;177(11):7515–9.
145. Yang CY, Best JA, Knell J, Yang E, Sheridan AD, Jesionek AK, et al. The transcriptional regulators Id2 and Id3 control the formation of distinct memory CD8+T cell subsets. Nat Immunol. 2011;12(12):1221–9.
146. Guan T, Dominguez CX, Amezquita RA, Laidlaw BJ, Cheng J, Henao-Mejia J, et al. ZEB1, ZEB2, and the miR-200 family form a counterregulatory network to regulate CD8 $^{+}$ T cell fates. J Exp Med. 2018;215(4):1153–68.
147. Intlekofer AM, Banerjee A, Takemoto N, Gordon SM, Dejong CS, Shin H, et al. Anomalous type 17 response to viral infection by CD8+ T cells lacking T-bet and Eomesodermin. Science. 2008;321:408–11.
148. Banerjee A, Gordon SM, Intlekofer AM, Paley MA, Mooney EC, Lindsten T, et al. Cutting Edge: The Transcription Factor Eomesodermin Enables CD8 + T Cells To Compete for the Memory Cell Niche. J Immunol. 2010;185:4988–92.
149. Intlekofer AM, Takemoto N, Wherry EJ, Longworth SA, Northrup JT, Palanivel VR, et al. Effector and memory CD8+ T cell fate coupled by T-bet and eomesodermin. Nat Immunol. 2005;6(12):1236–44.
150. Cui W, Liu Y, Weinstein JS, Craft J, Kaech SM. An interleukin-21- interleukin-10-STAT3 pathway is critical for functional maturation of memory CD8 + T cells. Immunity. 2011;35(5):792–805.
151. Nguyen KB, Watford WT, Salomon R, Hofmann SR, Pien GC, Morinobu A, et al. Critical Role for STAT4 Activation by Type I interferons in the Interferon-Gamma response to Viral Infection. Science. 2002;297:2063–6.
152. Siegel AM, Heimall J, Freeman AF, Hsu AP, Brittain E, Brenchley JM, et al. A Critical Role for STAT3 Transcription Factor Signaling in the Development and Maintenance of Human T Cell Memory. Immunity. 2011;35(5):806–18.
153. Kwon H, Thierry-mieg D, Thierry-mieg J, Kim H, Oh J, Tunyaplin C, et al.

Analysis of interleukin-21 induced Prdm1 gene regulation reveals functional cooperation of STAT3 and IRF4 transcription factors. Immunity. 2009;31(6):941–52.
154. Gong D, Malek TR. Cytokine-Dependent Blimp-1 Expression in Activated T Cells Inhibits IL-2 Production. J Immunol. 2007;178:242–52.
155. Kallies A, Xin A, Belz GT, Nutt SL. Blimp-1 Transcription Factor Is Required for the Differentiation of Effector CD8+ T Cells and Memory Responses. Immunity. 2009;31(2):283–95.
156. Ichii H, Sakamoto A, Hatano M, Okada S, Toyama H, Taki S, et al. Role for Bcl-6 in the generation and maintenance of memory CD8+ T cells. Nat Immunol. 2002;3(6):558–63.
157. Ichii H, Sakamoto A, Kuroda Y, Tokuhisa T, Alerts E. Bcl6 Acts as an Amplifier for the Generation and Proliferative Capacity of Central Memory CD8 + T Cells. J Immunol. 2004;173:883–91.
158. Gray SM, Amezquita RA, Guan T, Kleinstein SH, Kaech SM. Polycomb Repressive Complex 2-Mediated Chromatin Repression Guides Effector CD8+T Cell Terminal Differentiation and Loss of Multipotency. Immunity. 2017;46(4):596–608.
159. Henning AN, Roychoudhuri R, Restifo NP. Epigenetic control of CD8+ T cell differentiation. Nat Rev Immunol. 2018;18(5):340–56.
160. Murali-krishna K, Lau LL, Sambhara S. Persistence of Memory CD8 T Cells in MHC Class I – Deficient Mice. Science. 2012;1377:1377–82.
161. Schluns KS, Kieper WC, Jameson SC, Lefrançois L. Interleukin-7 mediates the homeostasis of naïve and memory CD8 T cells in vivo. Nat Immunol. 2000;1(5):426–32.
162. Becker TC, Wherry EJ, Boone D, Murali-Krishna K, Antia R, Ma A, et al. Interleukin 15 Is Required for Proliferative Renewal of Virus-specific Memory CD8 T Cells. J Exp Med. 2002;195(12):1541–8.
163. Sallusto F, Lenig D, Förster R, Lipp M, Lanzavecchia A. Two subsets of memory T lymphocytes with distinct homing potential and effector functions. Nature. 1999;401:708–12.
164. Fann M, Godlove JM, Catalfamo M, Iii WHW, Chrest FJ, Chun N, et al. Histone acetylation is associated with differential gene expression in the rapid and robust memory CD8+ T-cell response. Blood. 2006;108(10):3363–71.
165. Araki Y, Fann M, Wersto R, Weng N. Histone Acetylation Facilitates Rapid and Robust Memory CD8 T cell Response through Differential Expression of Effector Molecules (Eomesodermin and Its Targets: Perforin and Granzyme B). J Immunol. 2008;180:8102–8.
166. Masopust D, Vezys V, Marzo AL, Lefranc L. Preferential Localization of Effector Memory Cells in Nonlymphoid Tissue. Science. 2001;291:2413–7.
167. Wherry EJ, Teichgräber V, Becker TC, Masopust D, Kaech SM, Antia R, et al. Lineage relationship and protective immunity of memory CD8T cell subsets. Nat Immunol. 2003;4(3):225–34.
168. Marzo AL, Klonowski KD, Bon A Le, Borrow P, Tough DF, Lefrancois L. Initial

T cell frequency dictates memory CD8 + T cell lineage commitment. Nat Immunol. 2005;6(8):793–9.
169. Gebhardt T, Wakim LM, Eidsmo L, Reading PC, Heath WR, Carbone FR. Memory T cells in nonlymphoid tissue that provide enhanced local immunity during infection with herpes simplex virus. Nat Immunol. 2009;10(5):524–30.
170. Masopust D, Choo D, Vezys V, Wherry EJ, Duraiswamy J, Akondy R, et al. Dynamic T cell migration program provides resident memory within intestinal epithelium. J Exp Med. 2010;207(3):553–64.
171. Kim M V, Ouyang W, Liao W, Zhang MQ, Li MO. The Transcription Factor Foxo1 Controls Central-Memory CD8+ T Cell Responses to Infection. Immunity. 2013;39(2):286–97.
172. Michelini RH, Doedens AL, Goldrath AW, Hedrick SM. Differentiation of CD8 memory T cells depends on Foxo1. J Exp Med. 2013;210(6):1189–200.
173. Zhou X, Yu S, Zhao D, Harty JT, Badovinac VP, Xue H. Differentiation and Persistence of Memory CD8 + T Cells Depend on T Cell Factor 1. Immunity. 2010;33(2):229–40.
174. Mackay LK, Wynne-Jones E, Freestone D, Kallies A, Belz GT, Carbone FR, et al. T-box transcription factors combine with the cytokines TGF-B and IL-15 to control tissue-resident memory T cell fate. Immunity. 2015;43(6):1101–11.
175. Mackay LK, Minnich M, Kragten NAM, Liao Y, Freestone D, Braun A, et al. Hobit and Blimp1 instruct a universal transcriptional program of tissue residency in lymphocytes. Science. 2016;352:459–63.
176. Milner JJ, Toma C, Yu B, Zhang K, Omilusik K, Phan AT, et al. Runx3 programs CD8+ T cell residency in non-lymphoid tissues and tumours. Nature. 2017;552:254–7.
177. Mackay LK, Kallies A. Transcriptional Regulation of Tissue-Resident Lymphocytes. Trends Immunol. 2016;38(2):94–103.
178. Theofilopoulos AN, Kono DH, Baccala R. The multiple pathways to autoimmunity. Nat Immunol. 2017;18(7):716–24.
179. Davis MM, Bjorkman PJ. T-cell antigen receptor genes and T-cell recognition. Nature. 1988;334:395–402.
180. Arstila TP, Casrouge A, Baron V, Even J, Kanellopolous J, Kourilsky P. A direct estimate of the human αβT cell receptor diversity. Science. 1999;286:958–61.
181. Cheng M, Anderson MS. Thymic tolerance as a key brake on autoimmunity. Nat Immunol. 2018;19(7):659–64.
182. Xing Y, Hogquist K a. T-cell tolerance: central and peripheral. Cold Spring Harb Perspect Biol. 2012;4(6).
183. Kyewski B, Klein L. A Central Role for Central Tolerance. Annu Reveiw Immunol. 2006;24:571–606.
184. Gallegos AM, Bevan MJ. Central Tolerance to Tissue-specific Antigens Mediated by Direct and Indirect Antigen Presentation. J Exp Med. 2004;200(8):1039–49.
185. Wu L, Shortman K. Heterogeneity of thymic dendritic cells. Semin Immunol. 2005;17:304–12.

186. Daley SR, Hu DY, Goodnow CC. Helios marks strongly autoreactive CD4+ T cells in two major waves of thymic deletion distinguished by induction of PD-1 or NF- kB. J Exp Med. 2013;210(2):269–85.
187. Stritesky GL, Xing Y, Erickson JR, Kalekar LA, Wang X, Mueller DL, et al. Murine thymic selection quantified using a unique method to capture deleted T cells. Proc Natl Acad Sci. 2013;110(12):4679–84.
188. Kyewski B, Derbinski J. Self-Representation in the Thymus: An Extended View. Nat Rev Immunol. 2004;4:688–98.
189. Bonasio R, Scimone ML, Schaerli P, Grabie N, Lichtman AH, von Andrian UH. Clonal deletion of thymocytes by circulating dendritic cells homing to the thymus. Nat Immunol. 2006;7(10):1092–100.
190. Derbinski J, Schulte A, Kyewski B, Klein L. Promiscuous gene expression in medullary thymic epithelial cells mirrors the peripheral self. Nat Immunol. 2001;2(11):1032–9.
191. Gotter J, Brors B, Hergenhahn M, Kyewski B. Medullary Epithelial Cells of the Human Thymus Express a Highly Diverse Selection of Tissue-specific Genes Colocalized in Chromosomal Clusters. J Exp Med. 2004;199(2):155–66.
192. Derbinski J, Gäbler J, Brors B, Tierling S, Jonnakuty S, Hergenhahn M, et al. Promiscuous gene expression in thymic epithelial cells is regulated at multiple levels. J Exp Med. 2005;202(1):33–45.
193. Anderson MS, Venanzi ES, Klein L, Chen Z, Berzins SP, Turley SJ, et al. Projection of an Immunological Self Shadow Within the Thymus by the Aire Protein. Science. 2002;298:1395–401.
194. Anderson MS, Venanzi ES, Chen Z, Berzins SP, Benoist C, Mathis D. The Cellular Mechanism of Aire Control of T Cell Tolerance. Immunity. 2005;23:227–39.
195. Koble C, Kyewski B. The thymic medulla : a unique microenvironment for intercellular self-antigen transfer. J Exp Med. 2009;206(7):1505–13.
196. Takaba H, Morishita Y, Tomofuji Y, Danks L, Nitta T, Komatsu N. Fezf2 Orchestrates a Thymic Program of Self- Antigen Expression for Immune Tolerance. Cell. 2015;163(4):975–87.
197. Aaltonen J, Björses P, Perheentupa J, Horelli-Kuitunen N, Palotie A, Peltonen L, et al. An autoimmune disease, APECED, caused by mutations in a novel gene featuring two PHD-type zinc-finger domains. Nat Genet. 1997;17(4):399–403.
198. Nagamine K, Peterson P, Scott HS, Kudoh J, Minoshima S. Positional Cloning of the APECED gene. Nat Genet. 1997;17:393–8.
199. Liston A, Lesage S, Wilson J, Peltonen L, Goodnow CC. Aire regulates negative selection of organ-specific T cells. Nat Immunol. 2003;4(4):350–4.
200. Bouillet P, Purton JF, Godfrey DI, Zhang L-C, Coultas L, Puthalakath H, et al. BH3-only Bcl-2 family member Bim is required for apoptosis of autoreactive thymocytes. Nature. 2002;415:922–6.
201. Gray DHD, Kupresanin F, Berzins SP, Herold MJ, Reilly LAO, Bouillet P, et al. The BH3-Only Proteins Bim and Puma Cooperate to Impose Deletional

Tolerance of Organ-Specific Antigens. Immunity. 2012;37(3):451–62.
202. Ota K, Matsui M, Milford EL, Mackin GA, Weiner HL, Hafler DA. T-cell recognition of an immunodominant myelin basic protein epitope in multiple sclerosis. Nature. 1990;346:183–7.
203. Jingwu Z, Medaer R, Hashim GA, Chin Y, van den Berg-Loonen E, Raus JC. Myelin basic protein-specific T lymphocytes in multiple sclerosis and controls: precursor frequency, fine specificity, and cytotoxicity. Ann Neurol. 1992;32(3):330–8.
204. Lohmann T, Leslie RD, Londei M. T cell clones to epitopes of glutamic acid decarboxylase 65 raised from normal subjects and patients with insulin-dependent diabetes. J Autoimmun. 1996;9(3):385–9.
205. Maeda Y, Nishikawa H, Sugiyama D, Ha D, Hamaguchi M, Saito T, et al. Detection of self-reactive CD8 + T cells with an anergic phenotype in healthy individuals. Science. 2014;346:1536–41.
206. Culina S, Lalanne AI, Afonso G, Cerosaletti K, Pinto S, Sebastiani G, et al. Islet-reactive CD8 $^{+}$ T cell frequencies in the pancreas, but not in blood, distinguish type 1 diabetic patients from healthy donors. Sci Immunol. 2018;3(20):eaao4013.
207. Yu W, Jiang N, Ebert PJR, Kidd BA, Müller S, Lund PJ, et al. Clonal Deletion Prunes but Does Not Eliminate Self-Specific αβ CD8^{+} T Lymphocytes. Immunity. 2015;42(5):929–41.
208. Liu GY, Fairchild PJ, Smith RM, Prowle JR, Kioussis D, Wraith DC. Low avidity recognition of self-antigen by T cells permits escape from central tolerance. Immunity. 1995;3(4):407–15.
209. Bouneaud C, Kourilsky P, Bousso P. Impact of negative selection on the T cell repertoire reactive to a self-peptide: A large fraction of T cell clones escapes clonal deletion. Immunity. 2000;13(6):829–40.
210. Klein L, Kyewski B, Allen PM, Hogquist KA. Positive and negative selection of the T cell repertoire: what thymocytes see (and don't see). Nat Rev Immunol. 2014;14(6):377–91.
211. Allen S, Read S, DiPaolo R, McHugh RS, Shevach EM, Gleeson PA, et al. Promiscuous thymic expression of an autoantigen gene does not result in negative selection of pathogenic T cells. J Immunol. 2005;175(9):5759–64.
212. Heath WR, Belz GT, Behrens GMN, Smith CM, Forehan SP, Parish IA, et al. Cross-presentation, dendritic cell subsets, and the generation of immunity to cellular antigens. Immunol Rev. 2004;199:9–26.
213. Chatenoud L, Salomon B, Bluestone JA. Suppressor T cells – they're back and critical for regulation of autoimmunity! Immunol Rev. 2001;182:149–63.
214. Chinthrajah RS, Hernandez JD, Boyd SD, Galli SJ, Nadeau KC. Molecular and Cellular Mechanisms of Food Allergy and Food Tolerance. J Allergy Clin Immunol. 2016;137(4):984–97.
215. Belkaid Y, Harrison OJ. Homeostatic Immunity and the Microbiota. Immunity. 2017;46(4):562–76.
216. Erlebacher A. Mechanisms of T cell tolerance towards the allogeneic fetus. Nat

Rev Immunol. 2013;13(1):23–33.
217. Morgan DJ, Nugent CT, Raveney BJE, Sherman LA. In a transgenic model of spontaneous autoimmune diabetes, expression of a protective class II MHC molecule results in thymic deletion of diabetogenic CD8+ T cells. J Immunol. 2004;172(2):1000–8.
218. Adler BAJ, Marsh DW, Yochum GS, Guzzo JL, Nigam A, Nelson WG, et al. CD4+ T cell Tolerance to Parenchymal Self-Antigens Requires Presentation by Bone Marrow – derived Antigen-presenting Cells. J Exp Med. 1998;187(10):1555–64.
219. Ohashi PS, Oehen S, Buerki K, Pircher H, Ohashi CT, Odermatt B, et al. Ablation of “tolerance” and induction of diabetes by virus infection in viral antigen transgenic mice. Cell. 1991;65(2):305–17.
220. Kurts C, Heath WR, Carbone FR, Allison J, Miller JFAP, Kosaka H. Constitutive class I-restricted exogenous presentation of self antigens in vivo. J Exp Med. 1996;184(3):923–30.
221. Vezys V, Olson S, Lefrançois L. Expression of Intestine-Specific Antigen Reveals Novel Pathways of CD8 T Cell Tolerance Induction. Immunity. 2000;12(5):505–14.
222. Lohr J, Knoechel B, Nagabhushanam V, Abbas AK. T-cell tolerance and autoimmunity to systemic and tissue-restricted self-antigens. Immunol Rev. 2005;204:116–27.
223. Morgan DJ, Liblau R, Scott B, Fleck S, McDevitt HO, Sarvetnick N, et al. CD8(+) T cell-mediated spontaneous diabetes in neonatal mice. J Immunol. 1996;157(3):978–83.
224. Pircher H, Burki K, Lang R, Hengartner H, Zinkernagel RM. Tolerance induction in double specific T-cell receptor transgenic mice varies with antigen. Nature. 1989;342:559–61.
225. Hogquist KA, Jameson SC, Heath WR, Howard JL, Bevan MJ, Carbone FR. T cell receptor antagonist peptides induce positive selection. Cell. 1994;76:17–27.
226. Walker MD, Edlund T, Boulet AM, Rutter WJ. Cell-specific expression controlled by the 5’-flanking region of insulin and chymotrypsin genes. Nature. 1983;306:557–61.
227. Roman LM, Simons LF, Hammer RE, Sambrook JF, Gething M-JH. The expression of influenza virus hemagglutinin in the pancreatic β cells of transgenic mice results in autoimmune diabetes. Cell. 1990;61(3):383–96.
228. Heath WR, Kane KP, Mescher MF, Sherman LA. Alloreactive T cells discriminate among a diverse set of endogenous peptides. Proc Natl Acad Sci. 1991;88(12):5101–5.
229. Oldstone MBA, Nerenberg M, Southern P, Price J, Lewicki H. Virus infection triggers insulin-dependent diabetes mellitus in a transgenic model: Role of anti-self (virus) immune response. Cell. 1991;65(2):319–31.
230. Tsai S, Shameli A, Santamaria P. CD8+ T cells in type 1 diabetes. Adv Immunol. 2008;100:79–124.

231. Cao Y, Toben C, Na S, Stark K, Nitschke L, Peterson A, et al. Induction of experimental autoimmune encephalomyelitis in transgenic mice expressing ovalbumin in oligodendrocytes. Eur J Immunol. 2006;36:207–15.
232. Schildknecht A, Probst HC, McCoy KD, Miescher I, Brenner C, Leone DP, et al. Antigens expressed by myelinating glia cells induce peripheral cross-tolerance of endogenous CD8+ T cells. Eur J Immunol. 2009;39(6):1505–15.
233. Parish IA, Heath WR. Too dangerous to ignore: self-tolerance and the control of ignorant autoreactive T cells. Immunol Cell Biol. 2008;86(2):146–52.
234. Redmond WL, Sherman LA. Peripheral Tolerance of CD8 T Lymphocytes. Immunity. 2005;22(3):275–84.
235. Hawiger D, Inaba K, Dorsett Y, Guo M, Mahnke K, Rivera M, et al. Dendritic Cells Induce Peripheral T Cell Unresponsiveness under Steady State Conditions in Vivo. J Exp Med. 2001;194(6):769–80.
236. Liu K, Iyoda T, Saternus M, Kimura Y, Inaba K, Steinman RM. Immune Tolerance After Delivery of Dying Cells to Dendritic Cells In Situ. J Exp Med. 2002;196(8):1091–7.
237. Luckashenak N, Schroeder S, Endt K, Schmidt D, Mahnke K, Bachmann MF, et al. Constitutive crosspresentation of tissue antigens by dendritic cells controls CD8+ T cell tolerance in vivo. Immunity. 2008;28(4):521–32.
238. Belz GT, Behrens GMN, Smith CM, Miller JFAP, Jones C, Lejon K, et al. The CD8 + Dendritic Cell Is Responsible for Inducing Peripheral Self-Tolerance to Tissue-associated Antigens. J Exp Med. 2002;196(8):1099–104.
239. Probst HC, Lagnel J, Kollias G, van den Broek M. Inducible Transgenic Mice Reveal Resting Dendritic Cells as Potent Inducers of CD8+ T Cell Tolerance. Immunity. 2003;18(5):713–20.
240. Lo D, Freedman J, Hesse S, Palmiter RD, Brinster RL, Sherman LA. Peripheral tolerance to an islet cell-specific hemagglutinin transgene affects both CD4+ and CD8+ T cells. Eur J Immunol. 1992;22(4):1013–22.
241. Morgan DJ, Kurts C, Kreuwel HTC, Holst KL, Heath WR, Sherman LA. Ontogeny of T cell tolerance to peripherally expressed antigens. Proc Natl Acad Sci. 1999;96(7):3854–8.
242. Banchereau J, Steinman RM. Dendritic cells and the control of immunity. Nature. 1998;392:245–52.
243. Bonifaz L, Bonnyay D, Mahnke K, Rivera M, Nussenzweig MC, Steinman RM. Efficient targeting of protein antigen to the dendritic cell receptor DEC-205 in the steady state leads to antigen presentation on major histocompatibility complex class I products and peripheral CD8+ T cell tolerance. J Exp Med. 2002;196(12):1627–38.
244. Lutz MB, Schuler G. Immature, semi-mature and fully mature dendritic cells: which signals induce tolerance or immunity? Trends Immunol. 2002;23(9):445–9.
245. Albert ML, Jegathesan M, Darnell RB. Dendritic cell maturation is required for the cross-tolerization of CD8+ T cells. Nat Immunol. 2001;2(11):1010–7.
246. Jiang A, Bloom O, Ono S, Cui W, Unternaehrer J, Jiang S, et al. Disruption of

E-Cadherin-Mediated Adhesion Induces a Functionally Distinct Pathway of Dendritic Cell Maturation. Immunity. 2007;27:610–24.
247. Ardouin L, Chelbi R, Henri S, Dalod M, Malissen B, Chelbi R, et al. Broad and largely concordant molecular changes characterize tolerogenic and immunogenic Dendritic Cell maturation in thymus and periphery. Immunity. 2016;45:305–18.
248. Probst HC, McCoy K, Okazaki T, Honjo T, van den Broek M. Resting dendritic cells induce peripheral CD8+ T cell tolerance through PD-1 and CTLA-4. Nat Immunol. 2005;6(3):280–6.
249. Fife BT, Pauken KE, Eagar TN, Obu T, Wu J, Tang Q, et al. Interactions between PD-1 and PD-L1 promote tolerance by blocking the TCR – induced stop signal. Nat Immunol. 2009;10(11):1185–92.
250. Schneider H, Downey J, Smith A, Zinselmeyer BH, Rush C, Brewer JM, et al. Reversal of the TCR Stop signal by CTLA-4. Science. 2006;313:1972–5.
251. Odorizzi PM, Pauken KE, Paley M a, Sharpe A, Wherry EJ. Genetic absence of PD-1 promotes accumulation of terminally differentiated exhausted CD8+ T cells. J Exp Med. 2015;212(7):1125–37.
252. Ahn E, Araki K, Hashimoto M, Li W, Riley JL, Cheung J, et al. Role of PD-1 during effector CD8 T cell differentiation. Proc Natl Acad Sci. 2018;115(18):4749–54.
253. Shakhar G, Lindquist RL, Skokos D, Dudziak D, Huang JH, Nussenzweig MC, et al. Stable T cell-dendritic cell interactions precede the development of both tolerance and immunity in vivo. Nat Immunol. 2005;6(7):707–14.
254. Ono N, Murakami K, Chan O, Hall H, Elford AR, Yen P, et al. Exposure to sequestered self-antigens in vivo is not sufficient for the induction of autoimmune diabetes. PLoS One. 2017;12(3):e0173176.
255. Page N, Klimek B, De Roo M, Steinbach K, Soldati H, Lemeille S, et al. Expression of the DNA-Binding Factor TOX Promotes the Encephalitogenic Potential of Microbe-Induced Autoreactive CD8+T Cells. Immunity. 2018;48(5):937–950.e8.
256. Kurts C, Kosaka H, Carbone FR, Miller JF, Heath WR. Class I-restricted cross-presentation of exogenous self-antigens leads to deletion of autoreactive CD8(+) T cells. J Exp Med. 1997;186(2):239–45.
257. Förster I, Lieberam I. Peripheral tolerance of CD4 T cells following local activation in adolescent mice. Eur J Immunol. 1996;26(12):3194–202.
258. Kurts C, Miller JF, Subramaniam RM, Carbone FR, Heath WR. Major histocompatibility complex class I-restricted cross-presentation is biased towards high dose antigens and those released during cellular destruction. J Exp Med. 1998;188(2):409–14.
259. Kurts C, Sutherland RM, Davey G, Li M, Lew AM, Blanas E, et al. CD8 T cell ignorance or tolerance to islet antigens depends on antigen dose. Proc Natl Acad Sci. 1999;96(22):12703–7.
260. Enouz S, Carrie L, Merkler D, Bevan MJ, Zehn D, Carrié L, et al. Autoreactive T cells bypass negative selection and respond to self-antigen stimulation

during infection. J Exp Med. 2012;209(10):1769–79.
261. Rocha B, Grandien A, Freitas AA. Anergy and exhaustion are independent mechanisms of peripheral T cell tolerance. J Exp Med. 1995;181(3):993–1003.
262. Redmond WL, Marincek BC, Sherman LA. Distinct requirements for deletion versus anergy during CD8 T cell peripheral tolerance in vivo. J Immunol. 2005;174(4):2046–53.
263. Smith TRF, Verdeil G, Marquardt K, Sherman LA, Smith TRF, Verdeil G, et al. Contribution of TCR Signaling Strength to CD8+ T Cell Peripheral Tolerance Mechanisms. J Immunol. 2014;193:3409–16.
264. Steptoe RJ, Ritchie JM, Wilson NS, Villadangos JA, Lew AM, Harrison LC. Cognate CD4+ help elicited by resting dendritic cells does not impair the induction of peripheral tolerance in CD8+ T cells. J Immunol. 2007;178(4):2094–103.
265. Hernandez J, Aung S, Redmond WL, Sherman LA. Phenotypic and Functional Analysis of CD8+ T Cells Undergoing Peripheral Deletion in Response to Cross-Presentation of Self-Antigen. J Exp Med. 2001;194(6):707–18.
266. Adler AJ, Huang C, Yochum GS, Marsh DW, Pardoll DM. In Vivo CD4+ T Cell Tolerance Induction Versus Priming Is Independent of the Rate and Number of Cell Divisions. J Immunol. 2000;164:649–55.
267. Hernandez J, Aung S, Marquardt K, Sherman LA. Uncoupling of Proliferative Potential and Gain of Effector Function by CD8+ T Cells Responding to Self-Antigens. J Exp Med. 2002;196(3):323–33.
268. Parish IA, Rao S, Smyth GK, Juelich T, Denyer GS, Davey GM, et al. The molecular signature of CD8+ T cells undergoing deletional tolerance. Blood. 2009;113(19):4575–85.
269. Rocha B, Tanchot C, Von Boehmer H. Clonal anergy blocks in vivo growth of mature T cells and can be reversed in the absence of antigen. J Exp Med. 1993;177(5):1517–21.
270. Redmond WL, Hernandez J, Sherman LA. Deletion of naive CD8 T cells requires persistent antigen and is not programmed by an initial signal from the tolerogenic APC. J Immunol. 2003;171(12):6349–54.
271. Schwartz RH. Culture Model for Lymphocyte Clonal Anergy. Science. 1990;148:1349–56.
272. Desilva BDR, Feeser WS, Tancula EJ, Scherle PA. Anergic T Cells are Defective in Both Jun NH2-terminal Kinase and Mitogen-activated Protein Kinase Signaling Pathways. J Exp Med. 1996;183:2017–23.
273. Schwartz RH. T cell anergy. Annu Rev Immunol. 2003;21:305–34.
274. Aichele P, Brduscha-Riem K, Zinkernagel RM, Hengartner H, Pircher H. T cell priming versus T cell tolerance induced by synthetic peptides. J Exp Med. 1995;182(1):261–6.
275. Dubois PM, Pihlgren M, Tomkowiak M, Van Mechelen M, Marvel J. Tolerant CD8 T cells induced by multiple injections of peptide antigen show impaired TCR signaling and altered proliferative responses in vitro and in vivo. J Immunol. 1998;161(10):5260–7.

276. Heeg K, Wagner H. Induction of responsiveness in superantigen-induced anergic T cells. Role of ligand density and costimulatory signals. J Immunol. 1995;155(1):83–92.
277. Otten G, Germain R. Split anergy in a CD8+ T cell: receptor-dependent cytolysis in the absence of interleukin-2 production. Science. 1991;251:1228–31.
278. Davey GM, Kurts C, Miller JFAP, Bouillet P, Strasser A, Brooks AG, et al. Peripheral Deletion of Autoreactive CD8 T Cells by Cross Presentation of Self-Antigen Occurs by a Bcl-2-inhibitable Pathway Mediated by Bim. J Exp Med. 2002;196(7):947–55.
279. Keir ME, Freeman GJ, Sharpe AH. PD-1 regulates self-reactive CD8+ T cell responses to antigen in lymph nodes and tissues. J Immunol. 2007;179(8):5064–70.
280. Sharpe AH, Pauken KE. The diverse functions of the PD1 inhibitory pathway. Nat Rev Immunol. 2018;18:153–67.
281. Perez VL, Van Parijs L, Biuckians A, Zheng XX, Strom TB, Abbas AK. Induction of Peripheral T Cell Tolerance In Vivo Requires CTLA-4 Engagement. Immunity. 1997;6(4):411–7.
282. Grosso JF, Kelleher CC, Harris TJ, Maris CH, Hipkiss EL, Marzo A De, et al. LAG-3 regulates CD8 + T cell accumulation and effector function in murine self- and tumor- tolerance systems. J Clin Invest. 2007;117(11):3383–92.
283. Sánchez-fueyo A, Tian J, Picarella D, Domenig C, Zheng XX, Sabatos CA, et al. Tim-3 inhibits T helper type 1 – mediated auto- and alloimmune responses and promotes immunological tolerance. Nat Immunol. 2003;4(11):1093–101.
284. Sabatos CA, Chakravarti S, Cha E, Schubart A, Sánchez-fueyo A, Zheng XX, et al. Interaction of Tim-3 and Tim-3 ligand regulates T helper type 1 responses and induction of peripheral tolerance. Nat Immunol. 2003;4(11):1102–10.
285. Greenwald RJ, Freeman GJ, Sharpe AH. The B7 Family Revisited. Annu Reveiw Immunol. 2005;23:515–48.
286. Ishida Y, Agata Y, Shibahara K, Honjo T. Induced expression of PD-1, a novel member of the immunoglobulin gene superfamily , upon programmed cell death. EMBO J. 1992;11(11):3887–95.
287. Lindsten T, Lee KP, Harris ES, Petryniak B, Craighead N, Reynolds PJ, et al. Characterization of CTLA-4 structure and expression on human T cells. J Immunol. 1993;151(7):3489–99.
288. Brunner MC, Chambers CA, Ka-ming F, Hanke J, Winoto A, Allison JP, et al. CTLA-4-mediated inhibition of early events of T cell proliferation. J Immunol. 1999;162:5813–20.
289. Chen L. Co-inhibitory molecules of the B7-CD28 family in the control of T cell immunity. Nat Rev Immunol. 2004;4:336–47.
290. Freeman GJ, Long AJ, Iwai Y, Bourque K, Chernova T, Nishimura H, et al. Engagement of the PD-1 immunoinhibitory receptor by a novel B7 family member leads to negative regulation of lymphocyte activation. J Exp Med. 2000;192(7):1027–34.

291. Latchman Y, Wood CR, Chernova T, Chaudhary D, Chernova I, Iwai Y, et al. PD-L2 is a second ligand for PD-1 and inhibits T cell activation. Nat Immunol. 2001;2(3):261–8.
292. Okazaki T, Iwai Y, Honjo T. New regulatory co-receptors : inducible co-stimulator and PD-1. Curr Opin Immunol. 2002;14:779–82.
293. Nishimura H, Nose M, Hiai H, Minato N, Honjo T. Development of Lupus-like Autoimmune Diseases by Disruption of the PD-1 Gene Encoding an ITIM Motif-Carrying Immunoreceptor. Immunity. 1999;11:141–51.
294. Nishimura H, Okazaji T, Tanaka Y, Nakatani K, Hara M, Matsumori A, et al. Autoimmune Dilated Cardiomyopathy in PD-1 Receptor – Deficient Mice. Science. 2001;291:319–22.
295. Waterhouse P, Penninger JM, Timms E, Wakeham A, Shahinian A, Lee KP, et al. Lymphoproliferative Disorders with Early Lethality in Mice Deficient in Ctla-4. Science. 2016;270:985–8.
296. Pauken KE, Nelson CE, Martinov T, Spanier JA, Heffernan JR, Sahli NL, et al. Cutting Edge: Identification of Autoreactive CD4 + and CD8 + T Cell Subsets Resistant to PD-1 Pathway Blockade. J Immunol. 2015;(194):3551–5.
297. Walunas TL, Bluestone JA. CTLA-4 regulates tolerance induction and T cell differentiation in vivo. J Immunol. 1998;160(8):3855–60.
298. Eggena MP, Walker LSK, Nagabhushanam V, Barron L, Chodos A, Abbas AK. Cooperative Roles of CTLA-4 and Regulatory T Cells in Tolerance to an Islet Cell Antigen. J Exp Med. 2004;199(12):1725–30.
299. Wing K, Onishi Y, Prieto-martin P, Yamaguchi T, Miyara M, Fehervari Z, et al. CTLA-4 Control over Foxp3 + Regulatory T Cell Function. Science. 2008;322:271–5.
300. Frauwirth K a., Alegre M-L, Thompson CB. CTLA-4 Is Not Required for Induction of CD8+ T Cell Anergy In Vivo. J Immunol. 2001;167(9):4936–41.
301. Workman CJ, Rice DS, Dugger KJ, Kurschner C, Vignali DAA. Phenotypic analysis of the murine CD4-related glycoprotein , CD223 (LAG-3). Eur J Immunol. 2002;223:2255–63.
302. Workman CJ, Vignali DAA. The CD4-related molecule, LAG-3 (CD223) regulates the expansion of activated T cells. Eur J Immunol. 2003;33:970–9.
303. Zhu C, Anderson AC, Schubart A, Xiong H, Imitola J, Khoury SJ, et al. The Tim-3 ligand galectin-9 negatively regulates T helper type 1 immunity. Nat Immunol. 2005;6(12):1245–52.
304. Huang YH, Zhu C, Kondo Y, Anderson AC, Gandhi A, Russell A, et al. CEACAM1 regulates TIM-3-mediated tolerance and exhaustion. Nature. 2015;517:386–90.
305. Bennett SRM, Carbone FR, Karamalis F, Flavell RA, Miller JFAP, Heath WR. Help for cytotoxic-T-cell responses is mediated by CD40 signalling. Nature. 1998;393:478–80.
306. Schoenberger SP, Toes REM, van der Voort EIH, Offringa R, Melief CJM. T cell help for cytotoxic T lymphocytes is mediated by CD40-CD40L interactions. Nature. 1998;393:4–7.

307. Laidlaw BJ, Craft JE, Kaech SM. The multifaceted role of CD4+ T cells in CD8+ T cell memory. Nat Rev Immunol. 2016;16(2):102–11.
308. Caux C, Massacrier C, Vanbervliet B, Dubois B, Kooten C Van, Durand I, et al. Activation of Human Dendritic Cells through CD40 Cross-linking. J Exp Med. 1994;180(October):1263–72.
309. Celia BM, Scheidegger D, Palmer-lehmann K, Lane P, Lanzavecchia A, Alber G. Ligation of CD40 on Dendritic Cells Triggers Production of High Levels of Interleukin-12 and Enhances T cell Stimulatory Capacity: T-T Help via APC Activation. J Exp Med. 1996;184:747–52.
310. Behrens GMN, Li M, Davey GM, Allison J, Flavell R a, Carbone FR, et al. Helper requirements for generation of effector CTL to islet beta cell antigens. J Immunol. 2004;172(9):5420–6.
311. Vezys V, Alerts E. Cutting Edge: Inflammatory Signals Drive Organ-Specific Autoimmunity to Normally Cross-Tolerizing Endogenous Antigen. J Immunol. 2002;169:6677–80.
312. Sakaguchi S, Fukuma K, Kuribayashi K, Masuda T. Organ-specific autoimmune diseases induced in mice by elimination of T cell subset. J Exp Med. 1985;161:72–87.
313. Bluestone JA, Tang Q. How do CD4+ CD25+ regulatory T cells control autoimmunity ? Curr Opin Immunol. 2005;17:638–42.
314. Sakaguchi S, Yamaguchi T, Nomura T, Ono M. Regulatory T cells and immune tolerance. Cell. 2008;133:775–87.
315. McNally A, Hill GR, Sparwasser T, Thomas R, Steptoe RJ. CD4+ CD25+ regulatory T cells control CD8+ T cell effector differentiation by modulating IL-2 homeostasis. Proc Natl Acad Sci. 2011;108(18):7529–34.
316. Tang Q, Bluestone JA. Regulatory T-cell physiology and application to treat autoimmunity. Immunol Rev. 2006;212:217–37.
317. Green EA, Gorelik L, Mcgregor CM, Tran EH, Flavell RA. CD4+ CD25+ T regulatory cells control anti-islet CD8+ T cells through TGF-B – TGF-B receptor interactions in type 1 diabetes. Proc Natl Acad Sci. 2003;100(19):10878–83.
318. Rubtsov YP, Rasmussen JP, Chi EY, Fontenot J, Castelli L, Ye X, et al. Regulatory T cell-derived interleukin-10 limits inflammation at environmental interfaces. Immunity. 2008;28:546–58.
319. Von Boehmer H. Mechanisms of suppression by suppressor T cells. Nat Immunol. 2005;6(4):338–44.
320. Waithman J, Gebhardt T, Davey GM, Heath WR, Carbone FR. Cutting edge: Enhanced IL-2 signaling can convert self-specific T cell response from tolerance to autoimmunity. J Immunol. 2008;180(9):5789–93.
321. Powell JD, Lerner CG, Ewoldt GR, Schwartz RH. The -180 site of the IL-2 promoter is the target of CREB/CREM binding in T cell anergy. J Immunol. 1999;163(12):6631–9.
322. Zheng Y, Delgoffe GM, Meyer CF, Powell JD. Anergic T Cells Are Metabolically Anergic. J Immunol. 2009;183:6095–101.
323. Kimura M, Yamashita M, Kubo M, Iwashima M, Shimizu C, Tokoyoda K, et al.

Impaired Ca/calcineurin pathway in in vivo anergized CD4 T cells. Int Immunol. 2000;12(6):817–24.
324. Vanasek TL, Khoruts A, Zell T, Mueller DL. Antogonistic roles for CTLA-4 and the Mammalian Target of Rapamycin in the regulation of clonal anergy: enhanced cell cycle progression promotes recall antigen responsiveness. J Immunol. 2001;167:5636–44.
325. Zheng Y, Collins SL, Lutz MA, Amy N, Kole TP, Zarek PE, et al. A role for Mammalian Target of Rapamycin in regulating T cell activation versus anergy. J Immunol. 2007;178:2163–70.
326. Wiede F, Ziegler A, Zehn D, Tiganis T. PTPN2 restrains CD8+T cell responses after antigen cross-presentation for the maintenance of peripheral tolerance in mice. J Autoimmun. 2014;53:105–14.
327. Chuang E, Fisher TS, Morgan RW, Robbins MD, Duerr JM, Heiden MG Vander, et al. The CD28 and CTLA-4 receptors associate with the serine/threonine phosphatase PP2A. Immunity. 2000;13:313–22.
328. Sheppard K, Fitz LJ, Lee JM, Benander C, George JA, Wooters J, et al. PD-1 inhibits T-cell receptor induced phosphorylation of the ZAP70/CD3 zeta signalosome and downstream signaling to PKC-theta. FEBS Lett. 2004;574:37–41.
329. Parry R V, Chemnitz JM, Frauwirth KA, Lanfranco AR, Braunstein I, Kobayashi S V, et al. CTLA-4 and PD-1 Receptors Inhibit T-Cell Activation by Distinct Mechanisms. Mol Cell Biol. 2005;25(21):9543–53.
330. Yokosuka T, Takamatsu M, Kobayashi-imanishi W, Hashimoto-tane A, Azuma M, Saito T. Programmed cell death 1 forms negative costimulatory microclusters that directly inhibit T cell receptor signaling by recruiting phosphatase SHP2. J Exp Med. 2012;209(6):1201–17.
331. Zha Y, Marks R, Ho AW, Peterson AC, Janardhan S, Brown I, et al. T cell anergy is reversed by active Ras and is regulated by diacylglycerol kinase-alpha. Nat Immunol. 2006;7(11):1166–73.
332. Olenchock BA, Guo R, Carpenter JH, Jordan M, Topham MK, Koretzky GA, et al. Disruption of diacylglycerol metabolism impairs the induction of T cell anergy. Nat Immunol. 2006;7(11):1174–81.
333. Riese MJ, Grewal J, Das J, Zou T, Patil V, Chakraborty AK, et al. Decreased diacylglycerol metabolism enhances ERK activation and augments CD8+T cell functional responses. J Biol Chem. 2011;286(7):5254–65.
334. Zhou P, Shaffer DR, Arias DAA, Nakazaki Y, Pos W, Torres AJ, et al. In vivo discovery of immunotherapy targets in the tumour microenvironment. Nature. 2014;506:52–7.
335. Arumugam V, Bluemn T, Wesley E, Schmidt AM, Kambayashi T, Malarkannan S, et al. TCR signaling intensity controls CD8+ T cell responsiveness to TGF-b. J Leukoc Biol. 2015;98:703–12.
336. Varshavsky A. The Ubiquitin System, Autophagy, and Regulated Protein Degradation. Annu Rev Biochem. 2017;86:123–8.
337. Heissmeyer V, Macián F, Im S-H, Varma R, Feske S, Venuprasad K, et al.

Calcineurin imposes T cell unresponsiveness through targeted proteolysis of signaling proteins. Nat Immunol. 2004;5(3):255–65.
338. Gronski MA, Boulter JM, Moskophidis D, Nguyen LT, Holmberg K, Elford AR, et al. TCR affinity and negative regulation limit autoimmunity. Nat Med. 2004;10(11):1234–9.
339. Liu YC. The E3 ubiquitin ligase Itch in T cell activation, differentiation, and tolerance. Semin Immunol. 2007;19:197–205.
340. Anandasabapathy N, Ford GS, Bloom D, Holness C, Paragas V, Seroogy C, et al. GRAIL: An E3 Ubiquitin Ligase that Inhibits Cytokine Gene Transcription Is Expressed in Anergic CD4+ T Cells. Immunity. 2003;18(4):535–47.
341. Hsiao H-W, Liu W-H, Wang C-J, Lo Y-H, Wu Y-H, Jiang S-T, et al. Deltex1 Is a Target of the Transcription Factor NFAT that Promotes T Cell Anergy. Immunity. 2009;31(1):72–83.
342. Oliver PM, Cao X, Worthen GS, Shi P, Briones N, MacLeod M, et al. Ndfip1 protein promotes the function of itch ubiquitin ligase to prevent T cell activation and T helper 2 cell-mediated inflammation. Immunity. 2006;25(6):929–40.
343. Ramos-Hernández N, Ramon HE, Beal AM, Laroche A, Dekleva EA, Oliver PM. Ndfip1 enforces a requirement for CD28 costimulation by limiting IL-2 production. J Immunol. American Association of Immunologists; 2013;191(4):1536–46.
344. Altin JA, Daley SR, Howitt J, Rickards HJ, Batkin AK, Horikawa K, et al. Ndfip1 mediates peripheral tolerance to self and exogenous antigen by inducing cell cycle exit in responding CD4+ T cells. Proc Natl Acad Sci. 2014;111(6):2067–74.
345. Macián F, García-Cózar F, Im S-H, Horton HF, Byrne MC, Rao A. Transcriptional mechanisms underlying lymphocyte tolerance. Cell. 2002;109(6):719–31.
346. Schwartz RH. Models of T cell anergy: is there a common molecular mechanism? J Exp Med. 1996;184(1):1–8.
347. Martinez GJ, Pereira RM, Äijö T, Kim EY, Marangoni F, Pipkin ME, et al. The Transcription Factor NFAT Promotes Exhaustion of Activated CD8+ T Cells. Immunity. 2015;265–78.
348. Safford M, Collins S, Lutz MA, Allen A, Huang C-T, Kowalski J, et al. Egr-2 and Egr-3 are negative regulators of T cell activation. Nat Immunol. 2005;6(5):472–80.
349. Zheng Y, Zha Y, Driessens G, Locke F, Gajewski TF. Transcriptional regulator early growth response gene 2 (Egr2) is required for T cell anergy in vitro and in vivo. J Exp Med. 2012;209(12):2157–63.
350. Barron L, Knoechel B, Lohr J, Abbas AK. Cutting Edge: Contributions of Apoptosis and Anergy to Systemic T Cell Tolerance. J Immunol. 2008;180(5):2762–6.
351. Moskophidis D, Lechner F, Pircher H, Zinkernagel RM. Virus persistence in acutely infected immunocompetent mice by exhaustion of antiviral cytotoxic effector T cells. Nature. 1993;362:758–61.

352. Zajac AJ, Blattman JN, Murali-Krishna K, Sourdive DJD, Suresh M, Altman JD, et al. Viral Immune Evasion Due to Persistence of Activated T Cells Without Effector Function. J Exp Med. 1998;188(12):2205–13.
353. Wherry EJ, Blattman JN, Murali-Krishna K, van der Most R, Ahmed R. Viral persistence alters CD8 T-cell immunodominance and tissue distribution and results in distinct stages of functional impairment. J Virol. 2003;77(8):4911–27.
354. Goepfert PA, Bansal A, Edwards BH, Ritter GD, Tellez I, Pherson SAMC, et al. A Significant Number of Human Immunodeficiency Virus Epitope- Specific Cytotoxic T Lymphocytes Detected by Tetramer Binding Do Not Produce Gamma Interferon. J Virol. 2000;74(21):10249–55.
355. Khaitan A, Unutmaz D. Revisiting immune exhaustion during HIV infection. Curr HIV/AIDS Rep. 2011;8(1):4–11.
356. Ye B, Liu X, Li X, Kong H, Tian L, Chen Y. T-cell exhaustion in chronic hepatitis B infection: current knowledge and clinical significance. Cell Death Dis. 2015;6:e1694.
357. Gruener NH, Lechner F, Jung M, Diepolder H, Gerlach T, Lauer G, et al. Sustained Dysfunction of Antiviral CD8+ T Lymphocytes after Infection with Hepatitis C Virus. J Virol. 2001;75(12):5550–8.
358. Thimme R, Bukh J, Spangenberg HC, Wieland S, Pemberton J, Steiger C, et al. Viral and immunological determinants of hepatitis C virus clearance, persistence, and disease. Proc Natl Acad Sci. 2002;99(24):15661–8.
359. Lee PP, Yee C, Savage PA, Fong L, Brockstedt D, Weber JS, et al. Characterization of circulating T cells specific for tumor- associated antigens in melanoma patients. Nat Med. 1999;5(6):677–85.
360. Sade-Feldman M, Yizhak K, Bjorgaard SL, Ray JP, Boer CG De, Jenkins RW, et al. Defining T Cell States Associated with Response to Checkpoint Immunotherapy in Melanoma. Cell. 2018;175:998–1013.
361. Pauken KE, Wherry EJ. Overcoming T cell exhaustion in infection and cancer. Trends Immunol. 2015;36(4):265–76.
362. Leach DR, Krummel MF, Allison JP. Enhancement of Antitumor Immunity by CTLA-4 Blockade. Science. 1996;271:1734–6.
363. Velu V, Titanji K, Zhu B, Husain S, Pladevega A, Lai L, et al. Enhancing SIV-specific immunity in vivo by PD-1 blockade. Nature. 2009;457:206–10.
364. Palmer BE, Neff CP, Lecureux J, Ehler A, Dsouza M, Remling-mulder L, et al. In Vivo Blockade of the PD-1 Receptor Suppresses HIV-1 Viral Loads and Improves CD4 + T Cell Levels in Humanized Mice. J Immunol. 2013;190:211–9.
365. Seung E, Dudek TE, Allen TM, Freeman GJ, Luster AD, Tager AM. PD-1 Blockade in Chronically HIV-1-Infected Humanized Mice Suppresses Viral Loads. PLoS One. 2013;8(10):e77780.
366. Brahmer JR, Tykodi SS, Chow LQM, Hwu W, Topalian SL, Hwu P, et al. Safety and Activity of Anti–PD-L1 Antibody in Patients with Advanced Cancer. N Engl J Med. 2012;366(26):2455–65.
367. Wolchok JD, Kluger H, Callahan MK, Postow MA, Rizvi NA, Lesokhin AM, et

al. Nivolumab plus Ipilimumab in Advanced Melanoma. N Engl J Med. 2013;369(2):122–33.
368. Postow MA, Callahan MK, Wolchok JD. Immune Checkpoint Blockade in Cancer Therapy. J Clin Oncol. 2015;33(17):1974–82.
369. Kahan SM, Zajac AJ. Immune Exhaustion : Past Lessons and New Insights from Lymphocytic Choriomeningitis Virus. Viruses. 2019;11(156).
370. Ahmed R, Salmi A, Butler L, Chiller JM, Oldstone MBA. Selection of Genetic Variants of Lymphocytic Choriomeningitis Virus in Spleens of Persistently Infected Mice. J Exp Med. 1984;60:521–40.
371. Matloubian BM, Somasundaram T, Kolhekar SR, Selvakumar R, Ahmed R. Genetic Basis of Viral Persistence : Single Amino Acid Change in the Viral Glycoprotein Affects Ability of Lymphocytic Choriomeningitis Virus to Persist in Adult Mice. J Exp Med. 1990;172:1043–8.
372. Matloubian M, Kolhekar SR, Somasundaram T, Ahmed R. Molecular Determinants of Macrophage Tropism and Viral Persistence : Importance of Single Amino Acid Changes in the Polymerase and Glycoprotein of Lymphocytic Choriomeningitis Virus. J Virol. 1993;67(12):7340–9.
373. Sullivan BM, Emonet SF, Welch MJ, Lee AM, Campbell KP, De JC, et al. Point mutation in the glycoprotein of lymphocytic choriomeningitis virus is necessary for receptor binding , dendritic cell infection , and long-term persistence. Proc Natl Acad Sci. 2011;108(7):2969–74.
374. Wherry EJ, Ha S-J, Kaech SM, Haining WN, Sarkar S, Kalia V, et al. Molecular Signature of CD8+ T Cell Exhaustion during Chronic Viral Infection. Immunity. 2007;27(4):670–84.
375. Jin H-T, Anderson AC, Tan WG, West EE, Ha S-J, Araki K, et al. Cooperation of Tim-3 and PD-1 in CD8 T-cell exhaustion during chronic viral infection. Proc Natl Acad Sci U S A. 2010;107(33):14733–8.
376. Agnellini P, Wolint P, Rehr M, Cahenzli J, Karrer U, Oxenius A. Impaired NFAT nuclear translocation results in split exhaustion of virus-specific CD8+ T cell functions during chronic viral infection. Proc Natl Acad Sci. 2007;104(11):4565–70.
377. Miller BC, Sen DR, Abosy R Al, Bi K, Virkud Y V, Lafleur MW, et al. Subsets of exhausted CD8+ T cells differentially mediate tumour control and respond to checkpoint blockade. Nat Immunol. 2019;20:326–36.
378. Blackburn SD, Shin H, Haining WN, Zou T, Workman CJ, Polley A, et al. Coregulation of CD8+ T cell exhaustion by multiple inhibitory receptors during chronic viral infection. Nat Immunol. 2009;10(1):29–37.
379. Day CL, Kaufmann DE, Kiepiela P, Brown JA, Moodley ES, Reddy S, et al. PD-1 expression on HIV-specific T cells is associated with T-cell exhaustion and disease progression. Nature. 2006;443:350–4.
380. Fourcade J, Sun Z, Benallaoua M, Guillaume P, Luescher IF, Sander C, et al. Upregulation of Tim-3 and PD-1 expression is associated with tumor antigen – specific CD8+ T cell dysfunction in melanoma patients. J Exp Med. 2010;207(10):2175–86.

381. Sakuishi K, Apetoh L, Sullivan JM, Blazar BR, Kuchroo VK, Anderson AC. Targeting Tim-3 and PD-1 pathways to reverse T cell exhaustion and restore anti-tumor immunity. J Exp Med. 2010;207(10):2187–94.
382. Jones RB, Ndhlovu LC, Barbour JD, Sheth PM, Jha AR, Long BR, et al. Tim-3 expression defines a novel population of dysfunctional T cells with highly elevated frequencies in progressive HIV-1 infection. J Exp Med. 2008;205(12):2763–79.
383. Ferris RL, Lu B, Kane LP. Too Much of a Good Thing? Tim-3 and TCR Signaling in T Cell Exhaustion. J Immunol. 2014;193(4):1525–30.
384. Kaufmann DE, Kavanagh DG, Pereyra F, Zaunders JJ, Mackey EW, Miura T, et al. Upregulation of CTLA-4 by HIV-specific CD4+ T cells correlates with disease progression and defines a reversible immune dysfunction. Nat Immunol. 2007;8(11):1246–54.
385. Richter K, Agnellini P, Oxenius A. On the role of the inhibitory receptor LAG-3 in acute and chronic LCMV infection. Int Immunol. 2009;22(1):13–23.
386. Ye B, Li X, Dong Y, Wang Y, Tian L, Lin S, et al. Increasing LAG-3 expression suppresses T-cell function in chronic hepatitis B. Medicine (Baltimore). 2017;96(1):1–6.
387. West EE, Youngblood B, Tan WG, Jin H, Araki K, Alexe G, et al. Tight regulation of memory CD8+ T cells limits their effectiveness during sustained high viral load. Immunity. 2011;35:285–98.
388. Johnston RJ, Comps-agrar L, Hackney J, Yu X, Huseni M, Yang Y, et al. The Immunoreceptor TIGIT Regulates Antitumor and Antiviral CD8 + T Cell Effector Function. Cancer Cell. 2014;26:1–15.
389. Gupta PK, Godec J, Wolski D, Adland E, Yates K, Pauken KE, et al. CD39 Expression Identifies Terminally Exhausted CD8+ T Cells. PLOS Pathog. 2015;11(10):e1005177.
390. Boari JT, Bossio SN, Gorosito M. CD39 Expression Defines Cell Exhaustion in Tumor-Infiltrating CD8+ T Cells. Cancer Res. 2018;78(1):115–29.
391. Simoni Y, Becht E, Fehlings M, Loh CY, Koo S, Wei K, et al. Bystander CD8+ T cells are abundant and phenotypically distinct in human tumour infiltrates. Nature. 2018;557:575–9.
392. Quigley M, Pereyra F, Nilsson B, Porichis F, Fonseca C, Eichbaum Q, et al. Transcriptional analysis of HIV-specific CD8+ T cells shows that PD-1 inhibits T cell function by upregulating BATF. Nat Med. 2010;16(10):1147–51.
393. Staron MM, Gray SM, Marshall HD, Parish IA, Chen JH, Perry CJ, et al. The Transcription Factor FoxO1 Sustains Expression of the Inhibitory Receptor PD-1 and Survival of Antiviral CD8+ T Cells during Chronic Infection. Immunity. 2014;41(5):802–14.
394. Hui E, Cheung J, Zhu J, Su X, Taylor MJ, Wallweber HA, et al. T cell costimulatory receptor CD28 is a primary target for PD-1 – mediated inhibition. Science. 2017;4:1428–33.
395. Kamphorst AO, Kamphorst AO, Wieland A, Nasti T, Yang S, Zhang R, et al. Rescue of exhausted CD8 T cells by PD-1 – targeted therapies is CD28-

dependent. Science. 2017;355:1423–7.
396. Man K, Gabriel SS, Liao Y, Febbraio MA, Shi W, Kallies A, et al. Transcription Factor IRF4 Promotes CD8 + T Cell Exhaustion and Limits the Development of Memory- like T Cells during Chronic Infection. Immunity. 2017;47(6):1129–41.
397. Youngblood B, Oestreich KJ, Ha S, Duraiswamy J, Akondy RS, West EE, et al. Chronic Virus Infection Enforces Demethylation of the Locus that Encodes PD-1 in Antigen-Specific CD8+ T cells. Immunity. 2011;35(3):400–12.
398. Sen DR, Kaminski J, Barnitz RA, Kurachi M, Gerdemann U, Yates KB, et al. The epigenetic landscape of T cell exhaustion. Science. 2016;354:1165–9.
399. Li J, He Y, Ling N, Dong C. High Levels of Eomes Promote Exhaustion of Anti-tumor CD8 + T Cells. Front Immunol. 2018;9:1–13.
400. Wu T, Ji Y, Moseman EA, Xu HC, Manglani M, Kirby M, et al. The TCF1-Bcl6 axis counteracts type I interferon to repress exhaustion and maintain T cell stemness. Sci Immunol. 2016;1(6):eaai8593.
401. Riley JL. PD-1 signaling in primary T cells. Immunol Rev. 2009;229:114–25.
402. Blackburn SD, Crawford A, Shin H, Polley A, Freeman GJ, Wherry EJ. Tissue-specific differences in PD-1 and PD-L1 expression during chronic viral infection: implications for CD8 T-cell exhaustion. J Virol. 2010;84(4):2078–89.
403. Mueller SN, Sharpe AH, Ahmed R, Mueller SN, Vanguri VK, Ha S, et al. PD-L1 has distinct functions in hematopoietic and nonhematopoietic cells in regulating T cell responses during chronic infection in mice. J Clin Invest. 2010;120(7):2508–15.
404. Blank C, Brown I, Peterson AC, Spiotto M, Iwai Y, Honjo T, et al. PD-L1 / B7H-1 Inhibits the Effector Phase of Tumor Rejection by T Cell Receptor. Cancer Res. 2004;64:1140–5.
405. Petrovas C, Casazza JP, Brenchley JM, Price DA, Gostick E, Adams WC, et al. PD-1 is a regulator of virus-specific CD8 + T cell survival in HIV infection. J Exp Med. 2006;203(10):2281–92.
406. Trautmann L, Janbazian L, Chomont N, Said EA, Gimmig S, Bessette B, et al. Upregulation of PD-1 expression on HIV-specific CD8 + T cells leads to reversible immune dysfunction. Nat Med. 2006;12(10):1198–202.
407. Vezys V, Penaloza-MacMaster P, Barber DL, Ha S-J, Konieczny B, Freeman GJ, et al. 4-1BB signaling synergizes with programmed death ligand 1 blockade to augment CD8 T cell responses during chronic viral infection. J Immunol. 2011;187(4):1634–42.
408. Larkin J, Chiarion-Sileni V, Gonzalez R, Grob JJ, Cowey CL, Lao CD, et al. Combined Nivolumab and Ipilimumab or Monotherapy in Untreated Melanoma. N Engl J Med. 2015;373(1):23–34.
409. Bengsch B, Johnson AL, Kurachi M, Paley MA, Delgoffe GM, Wherry EJ, et al. Bioenergetic insufficiencies due to metabolic alterations regulated by the inhibitory receptor PD-1 are an early driver of CD8+ T cell exhaustion. Immunity. 2016;45(2):358–73.
410. Bengsch B, Ohtani T, Khan O, Setty M, Manne S, O'Brien S, et al. Epigenomic-Guided Mass Cytometry Profiling Reveals Disease-Specific Features of

Exhausted CD8 T Cells. Immunity. 2018;48(5):1029–1045.e5.
411. Wei SC, Levine JH, Wargo JA, Pe D, Allison JP, Wei SC, et al. Distinct Cellular Mechanisms Underlie Anti-CTLA-4 and Anti-PD-1 Checkpoint Blockade. Cell. 2017;170(6):1120–5.
412. Finlay DK, Rosenzweig E, Sinclair L V, Feijoo-carnero C, Hukelmann JL, Rolf J, et al. PDK1 regulation of mTOR and hypoxia-inducible factor 1 integrate metabolism and migration of CD8+ T cells. J Exp Med. 2012;209(13):2441–53.
413. Doedens AL, Phan AT, Stradner MH, Fujimoto JK, Nguyen J V, Yang E, et al. Hypoxia-inducible factors enhance the effector responses of CD8(+) T cells to persistent antigen. Nat Immunol. 2013;14(11):1173–82.
414. Shin H, Blackburn SD, Blattman JN, Wherry EJ. Viral antigen and extensive division maintain virus-specific CD8 T cells during chronic infection. J Exp Med. 2007;204(4):941–9.
415. Pellegrini M, Calzascia T, Toe JG, Preston SP, Lin AE, Elford AR, et al. IL-7 engages multiple mechanisms to overcome chronic viral infection and limit organ pathology. Cell. 2011;144(4):601–13.
416. Wherry EJ, Barber DL, Kaech SM, Blattman JN, Ahmed R. Antigen-independent memory CD8 T cells do not develop during chronic viral infection. Proc Natl Acad Sci. 2004;101(45):16004–9.
417. Utzschneider DT, Alfei F, Roelli P, Barras D, Chennupati V, Darbre S, et al. High antigen levels induce an exhausted phenotype in a chronic infection without impairing T cell expansion and survival. J Exp Med. 2016;213(9):1819–34.
418. Blattman JN, Wherry EJ, Ha S-J, van der Most RG, Ahmed R. Impact of epitope escape on PD-1 expression and CD8 T-cell exhaustion during chronic infection. J Virol. 2009;83(9):4386–94.
419. Puglielli MT, Zajac AJ, Most R, Dzuris JL, Sette A, Altman JD, et al. In Vivo Selection of a Lymphocytic Choriomeningitis Virus Variant That Affects Recognition of the GP33-43 Epitope by H-2D b but Not H-2K b. J Virol. 2001;75(11):5099–107.
420. Schmitz JE, Kuroda MJ, Santra S, Sasseville VG, Simon MA, Lifton MA, et al. Control of Viremia in Simian Immunodeficiency Virus Infection by CD8+ Lymphocytes. Science. 1999;283(5403):857–60.
421. Jin X, Bauer DE, Tuttleton SE, Lewin S, Gettie A, Blanchard J, et al. Dramatic rise in plasma viremia after CD8+ T cell Depletion in simian immunodeficiency virus-infected macaques. J Exp Med. 1999;189(6):991–8.
422. Wherry EJ, Blattman JN, Ahmed R. Low CD8 T-Cell Proliferative Potential and High Viral Load Limit the Effectiveness of Therapeutic Vaccination. J Virol. 2005;79(14):8960–8.
423. Brooks DG, Mcgavern DB, Oldstone MBA. Reprogramming of antiviral T cells prevents inactivation and restores T cell activity during persistent viral infection. J Clin Invest. 2006;116(6):1675–85.
424. Mueller SN, Ahmed R. High antigen levels are the cause of T cell exhaustion during chronic viral infection. Proc Natl Acad Sci. 2009;106:6–11.

425. Bucks CM, Norton JA, Boesteanu AC, Mueller YM, Katsikis PD. Chronic Antigen Stimulation Alone Is Sufficient to Drive CD8 + T Cell Exhaustion. J Immunol. 2009;182:6697–708.
426. Waggoner SN, Cornberg M, Selin LK, Welsh RM. Natural killer cells act as rheostats modulating antiviral T cells. Nature. 2012;481:394–8.
427. Mueller SN, Matloubian M, Clemens DM, Sharpe AH, Freeman GJ, Gangappa S, et al. Viral targeting of fibroblastic reticular cells contributes to immunosuppression and persistence during chronic infection. Proc Natl Acad Sci. 2007;104(39):15430–5.
428. Ng CT, Snell LM, Brooks DG, Oldstone MBA. Networking at the Level of Host Immunity : Immune Cell Interactions during Persistent Viral Infections. Cell Host Microbe. 2013;13(6):652–64.
429. Ma X, Bi E, Lu Y, Su P, Huang C, Liu L, et al. Cholesterol Induces CD8+ T Cell Exhaustion in the Tumor Microenvironment. Cell Metab. 2019;30:1–14.
430. Vodnala SK, Eil R, Kishton RJ, Sukumar M, Yamamoto TN, Ha N, et al. T cell stemness and dysfunction in tumors are triggered by a common mechanism. Science. 2019;363:eaau0135.
431. Ng CT, Oldstone MBA. Infected CD8α− dendritic cells are the predominant source of IL-10 during establishment of persistent viral infection. Proc Natl Acad Sci. 2012;109(35):14116–21.
432. Zuniga EI, Liou L, Mack L, Mendoza M, Oldstone MBA. Persistent virus infection inhibits type I interferon production by plasmacytoid dendritic cells to facilitate opportunistic infections. Cell Host Microbe. 2008;4:374–86.
433. Wilson EB, Kidani Y, Elsaesser H, Barnard J, Raff L, Karp CL, et al. Emergence of Distinct Multiarmed Immunoregulatory Antigen-Presenting Cells during Persistent Viral Infection. Cell Host Microbe. 2012;11(5):481–91.
434. Brooks DG, Trifilo MJ, Edelmann KH, Teyton L, Mcgavern DB, Oldstone MBA. Interleukin-10 determines viral clearance or persistence in vivo. Nat Med. 2006;12(11):1301–9.
435. Ejrnaes M, Filippi CM, Martinic MM, Ling EM, Togher LM, Crotty S, et al. Resolution of a chronic viral infection after interleukin-10 receptor blockade. J Exp Med. 2006;203(11):2641–2472.
436. Teijaro JR, Ng C, Lee AM, Sullivan BM, Sheehan KCF, Welch M, et al. Persistent LCMV Infection is Controlled by Blockade of Type I Interferon Signaling. Science. 2013;340:207–11.
437. Wilson EB, Yamada DH, Elsaesser H, Herskovitz J, Deng J, Cheng G, et al. Blockade of Chronic Type I Interferon Signaling to Control Persistent LCMV Infection. Science. 2013;340:202–7.
438. Ng CT, Sullivan BM, Schreiber RD, Oldstone MBA, Ng CT, Sullivan BM, et al. Blockade of Interferon Beta , but Not Interferon Alpha , Signaling Controls Persistent Viral Infection. Cell Host Microbe. 2015;17(5):653–61.
439. Snell LM, Brooks DG. New insights into type I interferon and the immunopathogenesis of persistent viral infections. Curr Opin Immunol. 2015;34:91–8.

440. Norris BA, Uebelhoer LS, Nakaya HI, Price AA, Grakoui A, Pulendran B. Chronic but not acute virus infection induces sustained expansion of myeloid suppressor cell numbers that inhibit viral-specific T cell immunity. Immunity. 2013;38(2):309–21.
441. Richter K, Perriard G, Behrendt R, Schwendener RA, Sexl V, Dunn R, et al. Macrophage and T Cell Produced IL-10 Promotes Viral Chronicity. PLOS Pathog. 2013;9(11).
442. Chen JH, Perry CJ, Tsui Y-C, Staron MM, Parish IA, Dominguez CX, et al. Prostaglandin E2 and programmed cell death 1 signaling coordinately impair CTL function and survival during chronic viral infection. Nat Med. 2015;21(4):327–34.
443. Matloubian M, Concepcion RJ, Ahmed R. CD4+ T Cells Are Required To Sustain CD8+ Cytotoxic T-Cell Responses during Chronic Viral Infection. J Virol. 1994;68(12):8056–63.
444. Elsaesser H, Sauer K, Brooks DG. IL-21 Is Required to Control Chronic Viral Infection. Science. 2010;324:1569–72.
445. Fröhlich A, Kisielow J, Schmitz I, Freigang S, Shamshiev AT, Weber J, et al. IL-21R on T Cells Is Critical for Sustained Functionality and Control of Chronic Viral Infection. Science. 2009;324:1576–80.
446. Yi JS, Du M, Zajac AJ. A Vital Role for Interleukin-21 in the Control of a Chronic Viral Infection. Science. 2009;324:1572–6.
447. Bachmann MF, Wolint P, Walton S, Schwarz K, Oxenius A. Differential role of IL-2R signaling for CD8 + T cell responses in acute and chronic viral infections. Eur J Immunol. 2007;37:1502–12.
448. Blattman JN, Grayson JM, Wherry EJ, Kaech SM, Smith KA, Ahmed R. Therapeutic use of IL-2 to enhance antiviral T-cell responses in vivo. Nat Med. 2003;9(5):540–7.
449. Parish IA, Marshall HD, Staron MM, Lang PA, Brüstle A, Chen JH, et al. Chronic viral infection promotes sustained Th1-derived immunoregulatory IL-10 via BLIMP-1. J Clin Invest. 2014;124(8):3455–68.
450. Penaloza-MacMaster P, Kamphorst a. O, Wieland A, Araki K, Iyer SS, West EE, et al. Interplay between regulatory T cells and PD-1 in modulating T cell exhaustion and viral control during chronic LCMV infection. J Exp Med. 2014;211(9):1905–18.
451. Tinoco R, Alcalde V, Yang Y, Sauer K, Zuniga EI. Cell-Intrinsic Transforming Growth Factor- b Signaling Mediates Virus-Specific CD8+ T Cell Deletion and Viral Persistence In Vivo. Immunity. 2009;31(1):145–57.
452. Sawant D V, Yano H, Chikina M, Zhang Q, Liao M, Liu C, et al. Adaptive plasticity of IL-10+ and IL-35+ Treg cells cooperatively promotes tumor T cell exhaustion. Nat Immunol. 2019;20(6):724–35.
453. Angelosanto JM, Blackburn SD, Crawford A, Wherry EJ. Progressive loss of memory T cell potential and commitment to exhaustion during chronic viral infection. J Virol. 2012;86(15):8161–70.
454. Blackburn SD, Shin H, Freeman GJ, Wherry EJ. Selective expansion of a

subset of exhausted CD8 T cells by alphaPD-L1 blockade. Proc Natl Acad Sci. 2008;105(39):15016–21.
455. Paley M a, Kroy DC, Odorizzi PM, Johnnidis JB, Dolfi D V, Barnett BE, et al. Progenitor and terminal subsets of CD8+ T cells cooperate to contain chronic viral infection. Science. 2012;338:1220–5.
456. Im SJ, Hashimoto M, Gerner MY, Lee J, Kissick HT, Burger MC, et al. Defining CD8+ T cells that provide the proliferative burst after PD-1 therapy. Nature. 2016;537:417–21.
457. Leong YA, Chen Y, Ong HS, Wu D, Man K, Deleage C, et al. CXCR5 + follicular cytotoxic T cells control viral infection in B cell follicles. Nat Immunol. 2016;17(10):1187–96.
458. He R, Hou S, Liu C, Zhang A, Bai Q, Han M, et al. Follicular CXCR5-expressing CD8+ T cells curtail chronic viral infection. Nature. 2016;537:412–6.
459. Utzschneider DT, Charmoy M, Chennupati V, Pousse L, Ferreira DP, Calderon-Copete S, et al. T Cell Factor 1-Expressing Memory-like CD8+ T Cells Sustain the Immune Response to Chronic Viral Infections. Immunity. 2016;45(2):415–27.
460. Siddiqui I, Schaeuble K, Chennupati V, Marraco SAF, Calderon-copete S, Ferreira DP, et al. Intratumoral Tcf1+ PD-1+ CD8+ T cells with Stem-like Properties Promote Tumor Control in Response to Vaccination and Checkpoint Blockade Immunotherapy. Immunity. 2019;50(1):195–211.
461. Kurtulus S, Madi A, Escobar G, Klapholz M, Nyman J, Christian E, et al. Checkpoint Blockade Immunotherapy Induces Dynamic Changes in PD-1-CD8+ tumour infiltrating T cells. Immunity. 2019;50:1–14.
462. Doering TA, Crawford A, Angelosanto JM, Paley MA, Ziegler CG, Wherry EJ. Network Analysis Reveals Centrally Connected Genes and Pathways Involved in CD8+ T Cell Exhaustion versus Memory. Immunity. 2012;37(6):1130–44.
463. Kao C, Oestreich KJ, Paley MA, Crawford A, Angelosanto JM, Ali M-AA, et al. Transcription factor T-bet represses expression of the inhibitory receptor PD-1 and sustains virus-specific CD8+ T cell responses during chronic infection. Nat Immunol. 2011;12(7):663–71.
464. Shin H, Blackburn SD, Intlekofer AM, Kao C, Angelosanto JM, Reiner SL, et al. A Role for the Transcriptional Repressor Blimp-1 in CD8+ T Cell Exhaustion during Chronic Viral Infection. Immunity. 2009;31(2):309–20.
465. Liu X, Wang Y, Lu H, Li J, Yan X, Xiao M, et al. Genome-wide analysis identifies NR4A1 as a key mediator of T cell dysfunction. Nature. 2019;567:525–9.
466. Chen J, Lopez-Moyado IF, Seo H, Lio C-WJ, Hempleman LJ, Sekiya T, et al. NR4A transcription factors limit CAR T cell function in solid tumours. Nature. 2019;567:530–4.
467. Philip M, Fairchild L, Sun L, Horste EL, Camara S, Shakiba M, et al. Chromatin states define tumour-specific T cell dysfunction and reprogramming. Nature. 2017;545:452–6.
468. Ghoneim HE, Fan Y, Moustaki A, Abdelsamed HA, Dash P, Dogra P, et al. De

Novo Epigenetic Programs Inhibit PD-1 Blockade-Mediated T Cell Rejuvenation. Cell. 2017;170(1):142–57.
469. Pauken KE, Sammons MA, Odorizzi PM, Manne S, Godec J, Khan O, et al. Epigenetic stability of exhausted T cells limits durability of reinvigoration by PD-1 blockade. Science. 2016;354:1160–5.
470. Mclane LM, Abdel-hakeem MS, Wherry EJ. CD8 T Cell Exhaustion During Chronic Viral Infection and Cancer. Annu Rev Immunol. 2019;37:457–95.
471. McKinney EF, Lee JC, Jayne DRW, Lyons P a., Smith KGC. T-cell exhaustion, co-stimulation and clinical outcome in autoimmunity and infection. Nature. 2015;523:612–6.
472. Mackerness KJ, Cox MA, Lilly LM, Weaver CT, Harrington LE, Zajac AJ. Pronounced virus-dependent activation drives exhaustion but sustains IFN-γ transcript levels. J Immunol. 2010;185(6):3643–51.
473. Ou R, Zhang M, Huang L, Moskophidis D. Control of virus-specific CD8+ T-cell exhaustion and immune-mediated pathology by E3 ubiquitin ligase Cbl-b during chronic viral infection. J Virol. 2008;82(7):3353–68.
474. Nelson CE, Mills LJ, Mccurtain JL, Thompson EA, Seelig DM, Bhela S, et al. Reprogramming responsiveness to checkpoint blockade in dysfunctional CD8 T cells. Proc Natl Acad Sci. 2019;116(7):2640–5.
475. Crawford A, Angelosanto JM, Kao C, Doering TA, Odorizzi PM, Barnett BE, et al. Molecular and Transcriptional Basis of CD4+ T Cell Dysfunction during Chronic Infection. Immunity. 2014;40(2):289–302.
476. Weant AE, Michalek RD, Crump KE, Liu C, Konopitski AP, Grayson JM. Defects in apoptosis increase memory CD8+ T cells following infection of Bim-/-Faslpr/lpr mice. Cell Immunol. 2011;271(2):256–66.
477. Sullivan JA, Kim EH, Plisch EH, Suresh M. FOXO3 regulates the CD8 T cell response to a chronic viral infection. J Virol. 2012;86(17):9025–34.
478. Sharma P, Allison JP. The future of immune checkpoint therapy. Science. 2015;348:56–61.
479. Postow MA, Sidlow R, Hellmann MD. Immune-Related Adverse Events Associated with Immune Checkpoint Blockade. N Engl J Med. 2018;378(2):158–68.
480. Ramamurthy C, Godwin JL, Borghaei H. Immune Checkpoint Inhibitor Therapy : What Line of Therapy and How to Choose? Curr Treat Options Oncol. Current Treatment Options in Oncology; 2017;18(33).
481. Schietinger A, Delrow JJ, Basom RS, Blattman JN, Greenberg PD. Rescued Tolerant CD8 T Cells Are Preprogrammed to Reestablish the Tolerant State. Science. 2012;335:723–7.
482. Hu QN, Suen AYW, Henao Caviedes LM, Baldwin TA. Nur77 Regulates Nondeletional Mechanisms of Tolerance in T Cells. J Immunol. 2017;199(9):3147–57.
483. Woronicz JD, Calnan B, Ngo V, Winoto A. Requirement for the orphan steroid receptor Nur77 in apoptosis of T-cell hybridomas. Nature. 1994;367:277–81.
484. Lee SL, Wesselschmidt RL, Linette GP, Kanagawa O, Russell JH, Milbrandt J.

Unimpaired thymic and peripheral T cell death in mice lacking the nuclear receptor NGFI-B (Nur77). Science. 1995;269:532–5.
485. Cai Q, Dierich A, Oulad-Abdelghani M, Chan S, Kastner P. Helios deficiency has minimal impact on T cell development and function. J Immunol. 2009;183(4):2303–11.
486. Jacob J, Baltimore D. Modelling T-cell memory by genetic marking of memory Tcells in vivo. Nature. 1999;399:593–7.
487. Anderson MS, Bluestone JA. The NOD Mouse : A Model of Immune Dysregulation. Annu Reveiw Immunol. 2005;23:447–85.
488. Bachmaier K, Krawczyk C, Kozieradzki I, Kong YY, Sasaki T, Oliveira-dos-Santos A, et al. Negative regulation of lymphocyte activation and autoimmunity by the molecular adaptor Cbl-b. Nature. 2000;403:211–6.
489. Schietinger A, Philip M, Krisnawan VE, Chiu EY, Delrow JJ, Basom RS, et al. Tumor-Specific T Cell Dysfunction Is a Dynamic Antigen-Driven Differentiation Program Initiated Early during Tumorigenesis. Immunity. 2016;45(2):389–401.
490. Waugh KA, Leach SM, Slansky JE. Tolerance of tumor-specific T cells in melanoma metastases. J Clin Cell Immunol. 2016;7(2):1–8.
491. Spits H, Artis D, Colonna M, Diefenbach A, Santo JP Di, Eberl G, et al. Innate lymphoid cells- a proposal for uniform nomenclature. Nat Rev Immunol. 2013;13(2):1–5.
492. McKinney EF, Lyons PA, Carr EJ, Hollis JL, Jayne DRW, Willcocks LC, et al. A CD8+ T cell transcription signature predicts prognosis in autoimmune disease. Nat Med. 2010;16(5):586–91.
493. Huang AC, Postow MA, Orlowski RJ, Mick R, Bengsch B, Manne S, et al. T-cell invigoration to tumour burden ratio associated with anti-PD-1 response. Nature. 2017;545:60–5.
494. Jiang P, Gu S, Pan D, Fu J, Sahu A, Hu X, et al. Signatures of T cell dysfunction and exclusion predict cancer immunotherapy response. Nat Med. 2018;24(10):1550–8.
495. Lyman MA, Aung S, Biggs JA, Sherman LA. A Spontaneously Arising Pancreatic Tumor Does Not Promote the Differentiation of Naive CD8+ T Lymphocytes into Effector CTL. J Immunol. 2004;172(11):6558–67.
496. Esfahani K, Miller WH. Reversal of Autoimmune Toxicity and Loss of Tumor Response by Interleukin-17 Blockade. N Engl J Med. 2017;276(20):1989–91.
497. Eshhar Z, Waks T, Grosst G, Schindler DG. Specific activation and targeting of cytotoxic lymphocytes through chimeric single chains consisting of antibody-binding domains and the gamma or zeta subunits of the immunoglobulin and T-cell receptors. Proc Natl Acad Sci. 1993;90:720–4.
498. Maude SL, Frey N, Shaw P, Aplenc R, Barrett DM, Bunin NJ, et al. Chimeric Antigen Receptor T Cells for Sustained Remissions in Leukemia. N Engl J Med. 2014;371(16):1507–17.
499. Yong CSM, Dardalhon V, Devaud C, Taylor N, Darcy PK, Kershaw MH. CAR T-cell therapy of solid tumors. Immunol Cell Biol. 2017;95:356–63.